Hyaluronic acid based Bioinks for Biofabrication of Mesenchymal Stem Cells

Hyaluronsäure basierte Biotinten zur Biofabrikation von Mesenchymalen Stromazellen

Dissertation to obtain the doctoral degree in natural sciences
(Dr. rer. nat.)
from the Graduate School of Life Sciences,
Julius-Maximilians-University Würzburg,
Section Biomedicine

presented by

Leonard Forster

from Würzburg

Würzburg 2022

This work was carried out from February 2018 until December 2021 at the Department for Functional Materials in Medicine and Dentistry of the University of Würzburg under the supervision of Dr. habil. Jörg Teßmar.

Submission of thesis application:

Date of examination:

Examination board:	Chairman:	Prof. U. Gbureck
	1. Expert:	Dr. habil. J. Teßmar
	2. Expert:	Prof. Dr. T. Blunk
	3. Expert:	Dr. R. Detsch

I would like to leave the world a better place than when I entered it. I would hope that by the end of my time on earth I could have learned from the years of living and hand something down.

“Do more than just exist” - Dawn C. Parson, MareBlu

Affidavit

I hereby confirm that my thesis entitled “Hyaluronic acid based Bioinks for Biofabrication of Mesenchymal Stem Cells” is the result of my own work. I did not receive any help or support from commercial consultants. All sources and / or materials applied are listed and specified in the thesis.

Furthermore, I confirm that this thesis has not yet been submitted as part of another examination process neither in identical nor in similar form.

Würzburg, 09.11.22

Place, Date Signature

Eidesstattliche Erklärung

Hiermit erkläre ich an Eides statt, die Dissertation “Hyaluronsäure basierte Biotinten zur Biofabrikation von Mesenchymalen Stromazellen” eigenständig, d.h. insbesondere selbständig und ohne Hilfe eines kommerziellen Promotionsberaters, angefertigt und keine anderen als die von mir angegebenen Quellen und Hilfsmittel verwendet zu haben.

Ich erkläre außerdem, dass die Dissertation weder in gleicher noch in ähnlicher Form bereits in einem anderen Prüfungsverfahren vorgelegen hat.

Würzburg, 09.11.22

Ort, Datum Unterschrift

Table of content

Abbreviations

2D	Two-dimensional
3D	Three-dimensional
AA	Acrylic anhydride
ACAN	Aggrecan
AcCl	Acetyl chloride
ACN	Acetonitrile
AcSH	Thioacetic acid
AG	Working group
Ala	L-Alanine
Alloc-Cl	Allyl chloroformate
Ar	Argon
Boc	*tert*-Butoxycarbonyl
C6-HASH	C6-thiolated hyaluronic acid
CD44	Cluster of differentiation 44
$CDCl_3$	Deutero-chloroform
CEA	2-Carboxyethyl acrylate
$CHCl_3$	Chloroform
CO_2	Carbon dioxide
COL	Collagen
Đ	Dispersity
D_2O	Deuterium oxide
d^6-DMSO	Deutero-dimethyl sulfoxide
DBU	1,8-Diazabicyclo[5.4.0]undec-7-ene
DCC	*N*,*N* -Dicyclohexyl carbodiimide
DCM	Dichloromethane
DE	Diethyl ether
DIAD	Diisopropyl azodicarboxylate
DIPEA	*N*,*N* -Diisopropylethylamine
DMAP	4-Dimethylaminopyridine
DMF	*N*,*N*-Dimethylformamide

DMSO	Dimethyl sulfoxide
DS	Degree of substitution
DTPH	3,3'-Dithiobis(propanoic dihydrazide)
DTP-OMe	Dimethyl 3,3'-dithiobispropionate
DTT	1,4-Dithiothreitol
ECM	Extracellular matrix
EDC	1-(3-Dimethylaminopropyl)-3-ethylcarbodiimide hydrochloride
eq.	Equivalent
EtOAc	Ethyl acetate
EtOH	Ethanol
FG	Functional group
GAG	Glycosaminoglycan
Gly	Glycine
HA	Hyaluronic acid
HAA	Hyaluronic acrylate
HAPA	Hyaluronic pentenoate
HASH	Thiolated hyaluronic acid
HCl	Hydrochloric acid
HEPES	4-(2-Hydroxyethyl)-1-piperazineethanesulfonic acid
HEMA	Hydroxyethyl methacrylate
hMSC	Human mesenchymal stem cells
HOAt	1-Hydroxy-7-azabenzotriazole
HOBt	1-Hydroxybenzotriazole
HPLC	High performance liquid chromatography
HRMS	High-resolution mass spectrometry
HV	High vacuum
I2959	2-Hydroxy-4’-(2-hydroxyethoxy)-2-methylpropiophenone
*i*PrOH	*iso*-Propanol
K_2HPO_4	Di-potassium hydrogen phosphate
KH_2PO_4	Potassium dihydrogen phosphate
LAP	Lithium phenyl-2,4,6-trimethylbenzoylphosphinate
Leu	L-Leucine

APGL	Leucine-glycine-proline-alanine tetrapeptide
MALS	Multi-angle light scattering
MEHQ	4-Methoxyphenol
MeOH	Methanol
MesCl	Methanesulfonyl chloride
$MgSO_4$	Magnesium sulfate
MilliQ	Ultrapure water
MMP	Matrix metalloproteinases
M_n	Number average molecular weight
M_w	Weight average molecular weight
MWCO	Molecular weight cut-off
Na_2HPO_4	Di-sodium hydrogen phosphate
$Na_2S_2O_3$	Sodium thiosulfate
$Na_2S_2O_4$	Sodium dithionite
$Na_2S_2O_5$	Sodium metabisulfite
$NaHSO_3$	Sodium bisulfite
NaN_3	Sodium azide
$NaNO_3$	Sodium nitrate
NaOH	Sodium hydroxide
NH_3	Ammonia
NHS	*N*-Hydroxysuccinimide
NMR	Nuclear magnetic resonance
PA	Pentenoic anhydride
P(AGE)	Poly(allyl glycidyl ether-*co*-glycidol)
PBS	Phosphate buffered saline
PEG	Polyethylene glycol
pHEMA	Poly(hydroxyethyl methacrylate)
Pro	L-Proline
Pyr	Pyridine
RC	Regenerated cellulose
roti	rotary evaporator
rpm	Revolutions per minute

rt	Room temperature
SDS	Sodium dodecyl sulfate
SFB TRR225	Collaborative research center “Transregio 225”
TBA	Tetra-*n*-butylammonium
TBA-OH	Tetra-*n*-butylammonium hydroxide
TCEP	Tris(carboxyethyl)phosphine HCl
TEA	Triethylamine
TFA	Trifluoroacetic acid
TFAA	Trifluoroacetic anhydride
TFF	Tangential flow filtration
TGF-β1	Transforming growth factor β1
THF	Tetrahydrofuran
UV	Ultraviolet

List of figures and tables

1 Introduction

1.1 Theoretical background

Today's medicine is able to cure or to palliate the symptoms of a large part of diseases of exogenous causes such as bacteria, viruses or poisoning by the application of active pharmaceutical ingredients. The product range of these natural and synthetic drugs is being expanded every year through research of new drugs for the treatment of previously untreatable diseases or as an addition to or replacement for already existing drugs. Normally, the applied drug is assimilated, metabolized and excreted by the body over time; hence it must be regularly administered for a certain period of time according to the disease and the course of the disease, and is discontinued after it is cured. Chronic incurable diseases on the other hand mostly require the permanent intake of drugs to palliate the symptoms and extend the patient's lifetime, whereby a permanent cure is always part of ongoing research. The treatment of endogenous causes of disease is proving more difficult, since they are caused by the body itself and, depending on the cause, can be contained completely or not at all. For example, many types of cancer can already be treated while degenerative diseases such as Parkinson's, Alzheimer's or Huntington's disease cannot be cured at present, at most they can be delayed.

Contrarily, therapy of the loss of life-sustaining tissues or entire organs that cannot be regenerated or transplanted is similarly complicated as no drugs but entire functional tissue structures are required. The cultivation of these tissues in a living organism and their subsequent extraction are not only very complicated from a scientific point of view, but also quickly reach ethical limits, so that a generation outside the body under laboratory conditions is targeted. A very young and theoretically promising method is biofabrication, which aims at such tissue structures by combining cells and biomaterials in casting and 3D printing processes. The latter is, among biomedical applications, the latest novelty and comprises the fabrication of living tissue constructs via layer by layer deposition of bioinks, a mixture of both, cells and biomaterials[1]. The overall aim is the integration of the patient's own cells into the bioink and the generation of a tailored tissue to counter implant rejection reaction which is the current major issue of trans- and implantations. In addition, tissue models for research are highly desirable especially on endogenously caused diseases, as they allow research to be conducted in a uniform framework without the need for living patients, each of whom is different from the others. In the following, the current 3D printing techniques are presented together with the most commonly used bioinks consisting of hydrogels made from polymers or polymer precursors. In addition, the different crosslinking strategies for the generation of these bioinks and hydrogels will be introduced, and in particular the two polymers used in this work, polyethylene glycol and hyaluronic acid, as well as their modifications.

3D bioprinting

In the actual state of the art, 3D bioprinting of fully functional organs or large tissues is not possible due to several barriers e.g. lack of vascularization methods, which is subject of current research, and hence, the focus is on the biofabrication of small tissue parts and tissue models for transplantation and study purposes[2-4].Different printing techniques have been evolved so far to enable the biofabrication of a broad bioink spectrum featuring each specific advantages and can be classified according to their operating principle: laser-based, droplet-based and extrusion-based[1,5,6].Laser-based bioprinting operates with defined light triggered curing or transfer processes, that allow for high resolved 3D constructs while demanding translucent bioink materials and photoinitiators. Despite the great advantage of high resolution, the major disadvantages are the limit of compatible bioinks and

photoinitiators and the required low complexity of constructs since it is a single material process[3,5,6]. Droplet-based bioprinting is based on physical phenomena that generate droplets continuously or on demand, enabling high-resolution 3D printing via e.g. vapor bubble formation, pulsed material deformation or utilization of Rayleigh-Plateau instabilities. In contrast to the laser-based method, multiple materials can be printed simultaneously enabling the generation of high complexity structures whereas the disadvantage of this method lays in the necessity of low-viscosity, homogeneous inks to prevent nozzle clogging, and thus mainly non-porous constructs of low structural and mechanical integrity can be produced[4,5,7]. Extrusion-based bioprinting consists of the continuous deposition of cylindrical bioink filament in air or media, driven by mechanical, pneumatic or solenoidal forces, that features rapid fabrication and subsequently enables 3D bioprinting of large scale structures. Its disadvantages are basing upon the shear-stress related limitations of nozzle diameter and consequently reduced resolution and low complexity of the constructs as well as upon the high requirement for the bioinks, however, it represents the most convenient and predominantly used 3D bioprinting technique[1,3-5].

The bioinks used for this purpose have to meet certain criteria with regard to their physical, chemical and biological properties while in addition to those, non-essential but beneficial attributes can be implemented for the improvement of 3D bioprinting outcome. The imperative characteristics comprise general printability plus controlled, rapid crosslinking to ensure structural and mechanical integrity, while the biodegradable components and their degradation fragments must possess cytocompatibility in terms of toxicity and immunogenicity. Finally, the structure requires interconnected mesh to allow for nutrient and waste transport via diffusion as well as for cell proliferation[8]. The biological performance can be boosted by not only the choice of cell promotional ink component but also by integration of biodegradation and cell adhesion motifs, cell stimulants e.g. growth factors and mitogens as well as by the integration of cells into the bioink as single cells or cell clusters. Cell viability and printability can simultaneously be improved by induction of shear-thinning bioink behavior via pre-crosslinking or addition of lubricants, whereas the final mechanical features can be tuned by the crosslinking type and density, implementation of additional post-printing crosslinking, termed multi-stage crosslinking approaches or by simultaneous generation of additional networks, so-called interpenetrating network approaches[5,8-11].

However, there is yet, and most likely will be, no universal single bioink that meets all requirements at once and hence, today's researchers spec into bioinks engineered and optimized accordingly to the desired application while trading various characteristics due to paradigms such as the biofabrication window[1,12]. The iterative process of variation of ink component subsequently properties is called bioink development and is highly dependent on the developer's perspective and the sighted application[8].

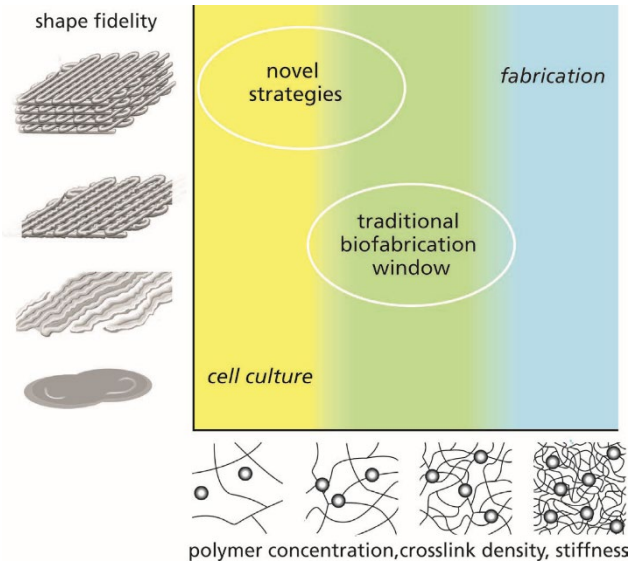

Figure 1: Illustrated biofabrication window depending on the polymer content of the bioink and the shape fidelity of the printed constructs with permission from Malda *et al.*[12].

Hydrogels

In nature, hydrogels, which by definition are 3D polymer networks that can absorb many times their dry weight in water and possess a porous structure[13], are found in a variety of plants and in the bodies of a large proportion of living organisms, for example, brown algae make use of the mechanical properties of a hydrogel based on alginate, a polysaccharide, to improve the flexibility of their leaves to grow even in areas with rough seas while succulents take advantage of the water binding properties of hydrogels from various polysaccharides in their water storage organs. Hence, mimicking natural occurring hydrogels is often used for the design of artificial hydrogels for biomedical or pharmaceutical applications, especially in bioinks for 3D bioprinting approaches[14].The basis of bioinks are hydrogels formed from hydrophilic polymer components linked by chemical bonds or physical interactions, e.g. ionic forces or hydrophobic interactions. Its properties depend on several factors, such as the type and concentration of the polymer component, the crosslinking type and density, and others, and can be specifically tailored by these. Hydrogels can be formed in two different ways, by crosslinking already existing polymers or by *in situ* polymerization and crosslinking of monomers. The latter offers the advantage of low initial viscosity of the precursor solution whereas the polymerization outcome and consequently the hydrogel properties can be only controlled to a limited extend when cells are included and hence, is mostly applied for preparation of biomaterials instead of bioinks. For the preparation of bioinks, the crosslinking reaction must be biocompatible and should not interfere with biological processes in cells, i.e. it should be bioorthogonal, and at the same time should be as controllable as possible. A variety of approaches are available for this, of which the most prominent are pH-, temperature- or light-induced or occur chemically spontaneous within a short period of time.

pH- and temperature-controlled gelation occurs mainly in protein-based formulations containing gelatin, collagen and their modifications, and less frequently in formulations comprising polysaccharides such as agarose. Although gelatin is hydrolyzed collagen, the gelation temperature ranges of the two proteins are different at neutral pH, so that gelatin is liquid at 37 °C and gels at room temperature, while collagen gels at both temperatures. However, the gelation of collagen is pH sensitive and is impeded in acidic media.

Crosslinking via light exposure with the appropriate wavelength is used for crosslinking by means of free-radical polymerization (FRP) of α,β-unsaturated carbonyl functions or thiol-ene reaction between thiols and alkenes/alkynes (Figure 2). The reaction rate, the required wavelength and light intensity can be adjusted by the choice of photoinitiators[15] such as I2959, LAP or Ru/SPS[16], which each have their advantages and disadvantages with regard to water solubility, absorption range and coloration. FRP is a chain-growth polymerization type[17] in which an α,β-unsaturated carbonyl radical is formed that reacts with other α,β-unsaturated carbonyls until reactant depletion or termination, forming random polymer chains or 3D networks with aliphatic backbone, if multivalent reactants are present, thus, the polymerization outcome cannot be controlled while the reaction kinetics can be tuned by the choice of α,β-unsaturated carbonyl moiety. In contrast, the thiol-ene reaction is a free-radical addition reaction of a thiyl radical to an alkene/alkyne with no further chain growth at the intermediately formed carbon centered alkyl radical, depending on the choice of thiol and alkene/alkyne, and by this yields rather defined products[18,19]. Both feature specific back draws, such as the α,β-unsaturated carbonyls for FRP are light sensitive and may undergo polymerization already during storage, especially in solutions, if exposed to UV-light, whereas thiols are sensitive to oxidation and cannot be stored in solutions for long periods. Their stock solutions have to be prepared freshly prior to application.

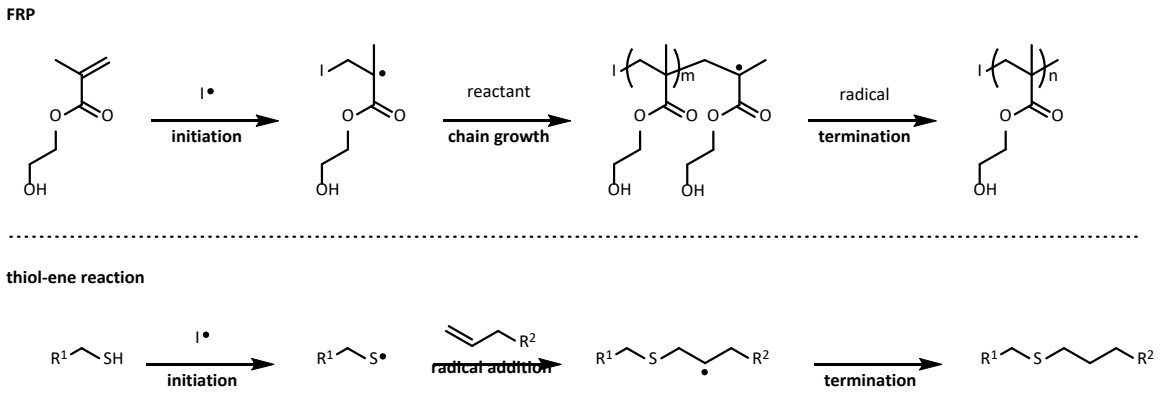

Figure 2: Schematic reaction mechanism of FRP at the example of 2-hydroxyethyl methylacrylate (top) and the thiol-ene reaction between a terminal thiol and an alkene (bottom).

Chemical spontaneous crosslinking reactions are mainly based on Huisgen and Diels-Alder cycloaddition or on Michael-addition, all of which exhibit high chemical selectivity and excellent cell compatibility. The use of the Huisgen reaction of azides and alkynes is less common among hydrogel/bioink formulations due to the involved reaction conditions, as either strained alkynes (SPAAC), typically complex hydrophobic molecules, or transition metal catalysts (CuAAC) are required for the reaction under normal conditions, limiting its applicability. In contrast, the Diels-Alder cycloaddition between electron-rich dienes and electron-deficient dienophiles is simpler to implement[20,21] and the reaction partners furan and maleimide are frequently used[22]. The latter is also predominantly used in another crosslinking type, Michael-addition consisting of nucleophilic addition of thiyl anion (Michael donor) to α,β-unsaturated carbonyl functions (Michael acceptor). The reaction occurs spontaneous and is strongly dependent on the applied pH and the choice of the donor-acceptor combination as their reactivity increases with decreasing pK_a of the thiol and decreasing electron-density of the terminal $H_2C=$[23] or by addition of organic catalysts. Deployment of the latter in hydrogel and bioink compositions is mostly avoided as these catalyst exhibit low cell compatibility in the required concentrations and due to high reaction rates even without additives.

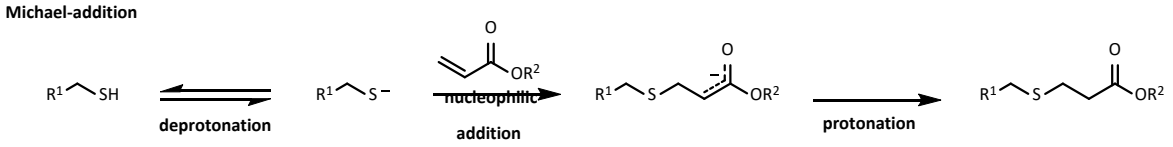

Figure 3: Schematic reaction mechanism of the Michael-addition at the example of a aliphatic thiol and an acrylate.

The high chemical and regioselectivity of the Michael-addition even in aqueous systems is the reason for its wide application, especially biological systems, for coating, labeling, conjugation and crosslinking[23]. Disadvantages of the reaction include possible side reactions with other free thiols of deployed components or cell media and the low storage stability of the reactants due to their sensitivity to oxidation in solution or polymerization upon exposure to daylight (UV).

Polymers

Polymers are macromolecules composed of smaller repetitive building blocks and can be classified, by their origin, into natural and synthetical polymers. Their properties are determined not only by the chemical structure of the individual building blocks, but also by the type of chemical linkage and interactions between them, i.e. intramolecular, and also by intermolecular interactions among the macromolecules. This diversity of factors is the basis for what is, in theory, a gigantic range of possible products, some of which have arisen in nature as a result of evolution, so called biopolymers. The three main classes are polynucleotides, -saccharides and -peptides whose macromolecular backbone comprises heteroatomic linkages, namely full acetals, phosphodiesters and amides, making them comparably facile to biodegrade by most organisms while, in addition to these main classes, also a few highly specialized polymers are existing with primarily C-C bonds in their backbones, e.g. natural rubber, cutin, lignin, which in contrast can only be biodegraded by a small number of organisms.

Natural polymers, especially those without a defined repetition unit, have a higher dispersity and a more frequent batch-to-batch variation than synthetic polymers, depending on their biological origin[14]. While proteins and polynucleotides, e.g. hemoglobin or DNA, have a dispersity of 1 and all macromolecules are therefore an exact copy of each other, the most commonly used proteins, collagen and gelatin, do not possess a defined repetition unit but only a rough amino acid composition ratio. The same applies to alginate, whose ratio of glucuronic and mannuronic acid determines the resulting hydrogel properties and may differ depending on the type of extracted alga. Hence, it may occur that the properties of several batches of natural polymers differ slightly to strongly, even if they are of the same origin. Nevertheless, the diversity of properties of biopolymers enables very broad biomedical and pharmaceutical applications, focusing on the mimicry of the body's chemical environment and functions to compensate for a defect or malfunction, and are thus used in drug delivery, regenerative medicine and tissue engineering.

Next to biopolymers, synthetic polymers have been discovered and are by now a substantial constituent of the human life as for example packaging, fabrics and electrotechnology. Through controlled synthesis conditions, not only very uniform polymers with low dispersity can be obtained, but also specific functional groups can be integrated and thus ultimately the material properties can be controlled which is next to processability and the resistance to environmental stresses, i.e. non-biodegradability the reason for this wide range of applications. The polymer backbone consists of chemically very stable C-C bonds such as polyolefins or C-heteroatom bonds like polyethers, -amides, -urethanes, -siloxanes and -esters. The latter are potentially cleavable under

environmental conditions but are biodegraded very slowly due to their high hydrophobicity and associated steep contact angles[24].

For 3D bioprinting, however, biological properties are huge importance, since an ink with perfect printing properties but with no or negative biological cues is only of value for 3D bioprinting itself, but not for the implementation and cultivation of cells. On the other hand, most biopolymers have to be modified to form hydrogels and furthermore to match the requirements of a bioink which commonly is not achieved by pure biopolymer compositions and hence a mixture of natural and synthetic polymers is used instead[14]. These hybrid bioink system comprise the desired biological properties via the biopolymer and a synthetic polymer as defined crosslinker or additive for improvement of the mechanical properties. Since each cell type and application demands different properties, no universally perfect composition exist or will exist, and the clue of current ink composition is to find and subsequently fine tune a suitable polymer formulation with the desired biological outcome.

Hyaluronic acid

Hyaluronic acid (HA) is composed of a well-defined repetition unit consisting of D-glucuronic acid and D-*N*-acetylglucosamine alternatingly linked via β-1,4 and β-1,3 glycosidic bonds (Figure 4) and occurs as salt under physiological conditions leading to the term hyaluronan[25]. It is ubiquitously present in the human body, namely in the extracellular matrix (ECM), but also intracellular and in high concentration in e.g. vitreous body, synovial fluid and soft connective tissues[26-28] with molecular weights ranging from several kDa up to MDa. Its structural composition enables intermolecular interaction such as hydrogen bonding, which are largely responsible for the huge water binding capacity, pseudoplasticity as well as lubricating properties and viscosity of HA solutions[25,29]. The latter increases very strongly with rising molecular weight and associated increase in polymer chain entanglement[28] while the critical mass for this phenomenon remains to be discovered but is presumably between 100-200 kDa.

Originally extracted from vertebrate sources e.g. vitreous humor, umbilical cord and rooster comb, today's commercial HA derives from biotechnologically developed bacteria[29], mainly *streptococcus* and *staphylococcus* allowing obtainment of high molecular weight HA in large quantities[30,31]. As ubiquitous as its occurrence in the human body is, the involvement of HA in biological processes is equally diverse, making it a highly valuable component for biomedical and pharmaceutical applications[24]. However, pure HA alone can easily be washed off any surface over time or is degraded within days thus is administered once such as postoperative antiadhesive or shielding agent in drug delivery systems or otherwise has to be applied frequently e.g. as lubrication of irritated eyes or in osteoarthritic joints[25,32]. Further applications are rendered possible by crosslinking hyaluronic acid to form a 3D network respectively hydrogel, which not only improves the viscoelastic properties but also slows down the degradation of HA[32]. Particularly in tissue engineering and regenerative medicine, HA hydrogels are of great interest, especially in the field of 3D bioprinting.

The chemical modifications required for this can be introduced at two locations of the HA backbone, at the carboxylic acid function and the primary and secondary alcohols. The most common methods are the nucleophilic modification of the carboxylic acid after carbodiimide-mediated activation by electron-rich heteroatomic groups such as alcohols, amines or hydrazine derivatives, and the electrophilic modification of the primary and secondary alcohols in alkaline milieu by, for example, epoxides, lactones and activated carboxylic acid derivatives (Figure 4). The predominantly modifications used for hydrogel or bioink formulations are (meth-)acrylated HA, thiolated HA, and alkene-functionalized HA that are crosslinked via FRP, thiol-ene reaction or Michael-addition[17,33-37].

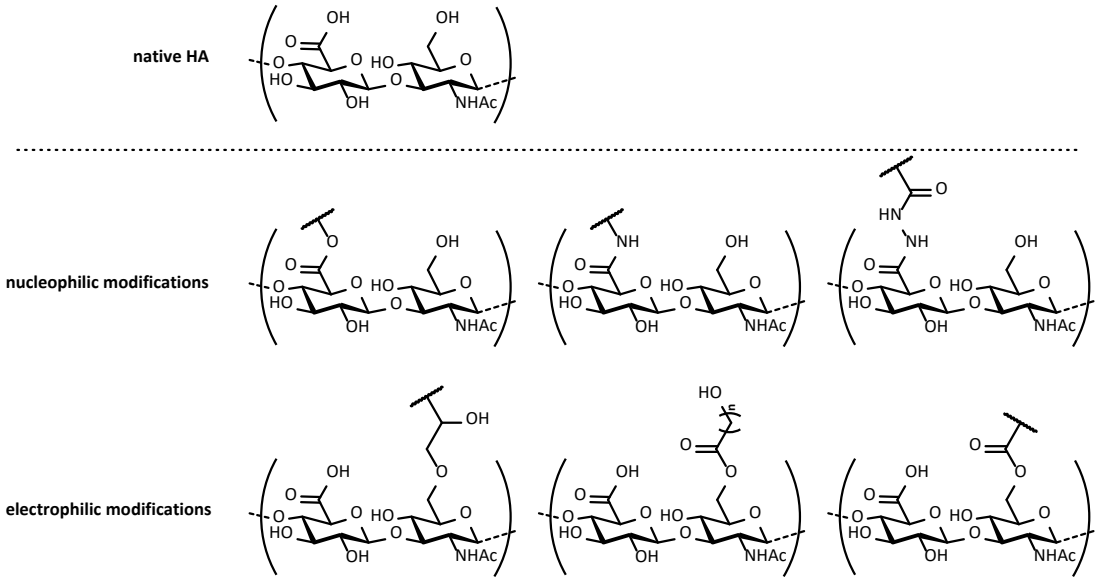

Figure 4: Chemical structure of HA's repetition unit (top) and its most prominent nucleophilic (middle) and electrophilic modifications (bottom).

Polyethylene glycol

Polyethylene glycol (PEG), also known as polyethylene oxide (PEO), is a polyether obtained by polymerization of ethylene oxide and, compared to many synthetic polymers, exhibits a very high hydrophilicity and dissolves spontaneously in water and almost all organic solvents, except linear ethers and alkanes[38]. In addition to linear PEGs, multivalent derivatives can be obtained, and their end groups can be modified depending on choice of initiator and the work-up of the polymerization reaction. The solubility of PEG decreases with increasing molecular weight, while the melting point steadily increases, such that linear PEG-OH is present as a colorless, amorphous solid from approx. >1000 Da, and as a clear liquid below that molecular weight.

From a chemical perspective, PEG is mostly inert under biological conditions due to its chemically very stable ether backbone and only decomposes under extreme conditions, e.g. temperature (>130 °C), strong acidic or strong oxidative environment. The sum of its physical and chemical properties make PEG an interesting component with wide-ranging applications[39] in the commercial, industrial and healthcare sectors in unmodified or esterified form as for example non-ionic surfactant, dispersant or moisture regulator. Especially in pharmaceuticals and other medical products, PEG is used e.g. as an excipient, laxative or stabilizer of emulsions, as well as hydrophilic polymer in hydrogels for biomedical applications[38,39]. A newly developed market niche is the use of modified PEGs in bioinks for bioprinting due to its biological stealth character, its transparency in solution and the relatively low-cost production of crosslinkable derivatives.

Chemically, PEG's terminal groups can be modified in multiple ways to meet the requirements for different applications e.g. via esterification, oxidation and subsequent carboxylic acid activation with auxiliaries, or transformation of the alcohols into amines or thiols[17,40-43]. For coatings and PEGylation processes, PEG modified with maleimide, vinyl sulfone, succinimide esters or amino functionalities are deployed whereas in bioinks predominantly peptide, thiol, vinyl or acrylate carrying PEG derivatives are used for the implementation of biological cues and motifs into the ink or as multivalent crosslinker for the formation 3D polymer networks in single- or multistage crosslinking approaches.

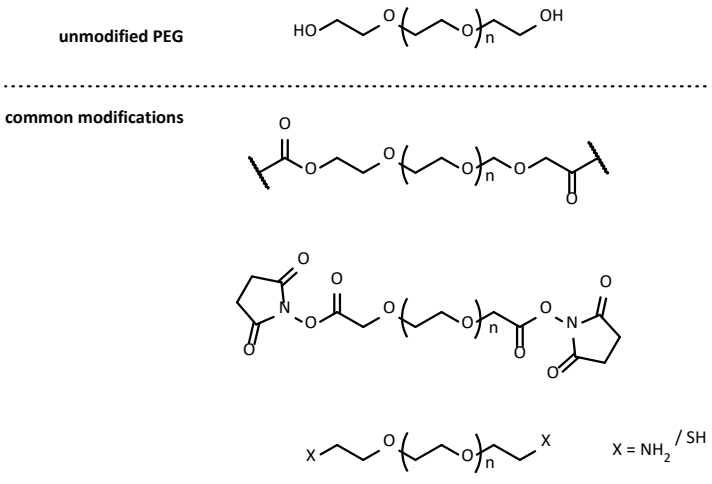

Figure 5: Chemical structure of linear unmodified PEG and the most common modifications.

1.2 Objective of thesis

HA, one major component of the natural human ECM, represents a favorable hydrogel forming material and consequently a suitable bioink material for regenerative medicine as well as tissue engineering approaches. It is already used in combination with hMSCs and was accordingly considered a promising candidate for 3D bioprinting of human cartilage for cartilage regeneration due to the structural and mechanical support of HA paired with its involvement in signaling processes via specific surface receptors.

However, so far only a few biofabrication approaches are based on HA as the main bioink component since it requires chemical modification to ensure sufficient long-term stability in cell culture. Therefore, this thesis aimed for the development and characterization of a very flexible material platform featuring high initial shape fidelity after the printing process while keeping the material content at the lowest possible to enable biologically favorable conditions in terms of cell viability, differentiation of MSC and ECM distribution which are currently lacking. Systematic variation of different properties of the HA material such as molecular weight, type and amount of functionalization combined with low molecular weight, multifunctional PEG crosslinkers was intended to yield hydrogels and bioinks with high initial mechanical stability and shape fidelity. Incorporation of enzymatically cleavable peptide sequences and growth factors were targeted to enhance the biological performance of the developed formulations whereas the comprehensive biological evaluations were part of the theses of Julia Hauptstein, J. and Schmidt, S. of the team of Prof. Blunk, T..

The underlying idea for the bioink development was a controlled one-pot dual-stage crosslinking approach consisting of two biocompatible and independent reactions: a Michael-addition as a first step and a secondary thiol-ene reaction, based on three ink components: HASH, PEG-acrylate and PEG-allyl carbonate. In the first stage, the Michael-addition between parts of the thiols of HASH and PEG-acrylates should result in a weakly pre-crosslinked, shear thinning bioink which is further crosslinked in the second stage, after 3D printing, via thiol-ene reaction between the remaining thiols and PEG-diallyl carbonate, triggered by UV exposure to give the final biofabricate. The development strategy was to vary the molar ratios of the components in such a way that the initial low viscosity facilitated cell dispersion and transformed after the first stage into an easily printable cell suspension, which subsequently can be converted into *in vitro* cultivatable cell-loaded hydrogels/constructs.

Rheological evaluation of both crosslinking reactions of the developed formulations should provide proof of their applicability. Controlled modifications of the required HA and PEG materials in large scales were of great importance in order to overcome one of the most prominent issues in 3D (bio-)printing, batch-to-batch variations, while focusing on their reproducibility.

1.3 Project position within SFB TRR225

As part of the A section (material development projects) of the SFB TRR225 the subproject A02 represented a material supplier for numerous subprojects and hence was strongly interconnected in the consortium. Within the A section, the A02 materials should be provided to three cooperation partners focusing on bioink development, microgels for various biofabrication approaches such as microfluidic gel formation, cell encapsulation, or comprehensive rheological investigations. Further cooperation in section B (processing and method development projects) in total seven subprojects dealing with ultra-soft matrix composites, micro-vascularization, bioreactor application, in-gel printing of vascular structures, glycocalyx engineering, reporter cell lines, bulk- and nanogels were supplied with materials and hydrogel as well as bioink formulations. In section C (modelling and biofabricate development projects) two partners investigating 3D printed tumor models of breast cancer as well as

tumor dormancy should be provided with materials and bioink formulations[44]. Supply of these in total 13 cooperating subprojects resulted in a high material demand and hence appropriate provision of high-quality materials was of paramount importance for this PhD project.

2 Results and Discussion

The following results were obtained by investigations largely performed in parallel. Obtained findings could therefore not always be transferred to other reactions that would have benefited from them and discussions are arranged in such way to promote understanding. Hence, chronological orders are only partially given and discussions of similar issues in different subchapters may occur but are prevented by cross-referencing where possible, unless explicitly necessary for explanation or to ensure a good flow of reading. Ideas for applications apart from those of the A02 project proposal came up most often during or after characterization of the materials for the main hypothesis and may therefore appear spontaneous and unplanned, but always improved understanding and the development of the ink platform. Development of the materials for specific applications was performed in cooperation with the applicants to enable tailoring of the product towards their laboratory infrastructure and experimental requirements. Final 3D bioprinting and consecutive cell biological investigations using the developed materials were, in many cases, still in progress by the end of this PhD thesis and are therefore in the state of further development.

2.1 Modification and characterization of hyaluronic acid (HA) derivates

2.1.1 Thiolated hyaluronic acid (HASH & C6-HASH)

The thiolation of hyaluronic acid was described first by Shu *et al*.[45] in 2002 using thiol-carrying dihydrazides and EDC chemistry addressing the carboxylic acid of the HA repetition unit and has since often been used as a template for HASH synthesis[35,46-49] even though the protocol yields a product with several disadvantages that are discussed below. Yet, no updated literature with optimized protocol was published. Since 2006, HASH is commercially available under the name of "Glycosil®" in 10 mg and 50 mg package size with variable molecular weights and thiol contents and is often used in 3D cell culture studies[50-52]. It contains buffering salts (PBS) for the maintenance of a neutral pH specially designed for proprietary hydrogel kits impeding the use of alternative buffer systems and its price per gram HASH is in the range of 3600-4800 €, which exceeds by far the budget of biofabrication projects typically consuming large quantities of ink components and being very sensitive to batch-to-batch variabilities. Alternative to the thiolation at the carboxylic acid, the alcohols, in particular the primary alcohol, of the sugar backbone can be modified according to Zhang *et al*.[53] by epoxides containing protected thiol moieties representing the only literature for C6-thiolated HA so far and no commercial product for this type of HASH exists. Both modification routes were investigated, improved in terms of product quality as well as scalability and are extensively described in the following. Polymer concentrations are stated as % throughout this thesis and imply percent by weight unless a differentiation is necessary for better understanding whereas % in the case of the degree of substitution (DS) regarding the HA modifications imply the amount of modification at the carboxylic acid or primary alcohol (C6) per disaccharide repetition unit but does not necessarily equal the thiol content which is defined as the amount of thiol-carrying modifications per disaccharide repetition unit. The remaining unmodified repetition units still possess their native form and could therefore interact with cell receptors as signaling molecule. If the repetition unit is only modified with thiol-carriers, the DS and the thiol content are identical. All batches of HA were purchased from Biosynth Carbosynth and are named in the following pursuant to the range of molar mass stated by the manufacturer's information (Table 1). Each batch was analyzed by size-exclusion chromatography (SEC MALS) whereas repeated measurements showed slight fluctuation of the results, a typical occurrence for polymers of natural origin. The manufacturer determined the molecular weight range by an Ubbelohde viscometer, which is considered to provide only rough values but seems to be prone to errors as the SEC MALS measurements showed only a M_w of 60.5 kDa and 1.33 MDa lying both outside of the stated range of 80-100 kDa, respectively2.0-2.5 MDa batch and 1.09 MDa at the edge

of the range for the 1.0-2.0 MDa batch. The measured values of the remaining batches were in accordance with the supplier's specifications.

Table 1: Specifications of all available HA batches and the results of their SEC MALS analyses.

Specifications		SEC MALS analysis		
8-15	kDa	15.3	kDa	Đ 2.48
80-100	kDa	60.5	kDa	Đ 2.49
0.2-0.5	MDa	0.395	MDa	Đ 2.16
0.6-1.0	MDa	0.765	MDa	Đ 1.61
1.0-2.0	MDa	1.09	MDa	Đ 1.31
2.0-2.5	MDa	1.33	MDa	Đ 1.07

HASH

The investigation plan was composed of three consecutive objectives containing in the first place the analysis of requirements for all synthesis steps, such as reaction, purification, isolation and characterization. Based on this, reproducibility and process optimization were thoroughly examined, and the gained insight transferred on the final part, production of large batches according to requirements of hydrogels and bioinks. HASH produced pursuant to literature references[45,54] was characterized and used as (negative) reference. Herein utilized HA was of low molecular weight (<150 kDa) with certainly very low viscosity in the deployed concentrations (≤1.5 %) and resulted in M_w <50 kDa with a thiol content of 30-40 % and the formation of an undesirable by-product (Figure 7)

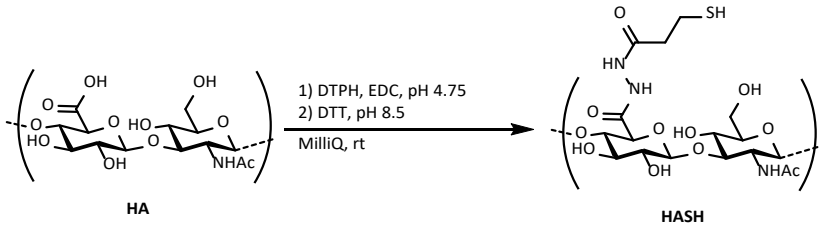

Figure 6: Reaction scheme of the HASH synthesis according to the literature[45,54].

According to one of the authors, the products characteristics uncontrollably varied, and the synthesis was repeated until the desired product was obtained, which strongly indicates unsteady reaction conditions for a reproducible product. A straight transfer of the existing protocols to HA with up to 1.0-2.0 MDa failed completely due to its high viscosity at concentrations above 1 % and a synthesis protocol for such high molecular weight starting materials had to be developed from scratch. Directly using HA 1.0-2.0 MDa, the reaction parameters were systematically investigated and adapted to render properly controlled reaction characteristics. As a first step, an incubator instead of a flask with stir bar was utilized to ensure homogeneous mixing of the highly viscous reaction solutions and a concentration series of pure HA in MilliQ was examined to determine the largest possible concentration at which the reaction could be performed. Despite 0.75 % was found to be the optimal compromise, the concentration had to be further reduced to 0.5 % as the other reactants increased the viscosity by withdrawing solvent for their dissolution. Next, a suitable buffer system was implemented to maintain a constant pH during the reaction without further additions of HCl over time. Buffers from carbonic and sulfuric acids were considered inapplicable as they would be also activated by the carbodiimide and not only form DTPH consuming by-products but also could yield undesirable esterification and sulfonation[55] of the sugar backbone. Such modifications would alter the polymer characteristics, which may have severe impact on the biological response to the material and their hydrolysis is either impossible or requires harsh reaction conditions. Consequently, a phosphate-based buffer was chosen that could still react with carbodiimides[56], but such by-products would be cleaved

from the backbone during the alkaline reduction step. Moreover, the product quality was considerably enhanced by adding the auxiliary reagent *N*-hydroxysuccinimide (NHS). Without NHS addition, a by-product was formed by *O*-*N*-acylurea rearrangement during the carboxylic acid activation with EDC (Figure 7), independent of the reaction parameters, and yielded an *N*-acylureate that not only resonates in the same range as the thiol-bearing modification impeding accurate determination of the DS respectively thiol content via NMR (Figure 8), but also carries a terminal dimethylamine group that changes the polarity of the carboxylic acid from anionic to cationic and hence has an unknown effect on hydrogel formation and cellular behavior[57]. The added NHS accordingly prevented the *O*-*N*-acylurea rearrangement and thus the formation of the undesirable by-product.

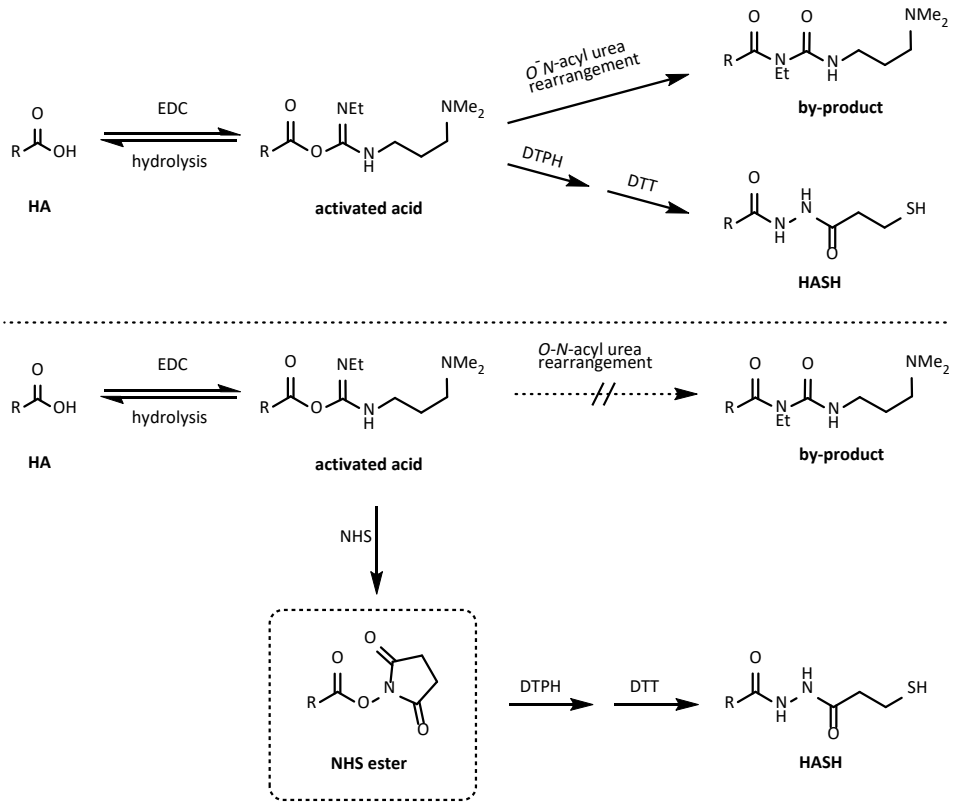

Figure 7: Schematic mechanism of the HASH synthesis without NHS (top) and with NHS (bottom).

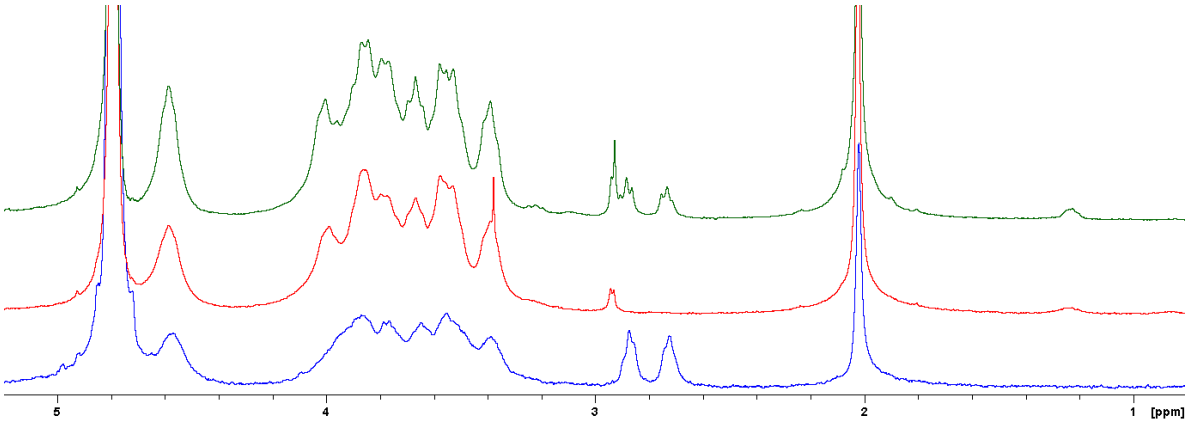

Figure 8: ^{1}H NMR overlay plot of HASH and HASH by-product in D_2O. Top to bottom: with by-product, only by-product, no by-product.

Based on that, the requirements for the dialysis were investigated such as the pH of the dialysis media, dialysis duration and the MWCO of dialysis tubes (1.0, 3.5, 12-14 kDa). In a series of experiments, product solutions were dialyzed under identical condition except for using dialysis media with different

pHs in the range of 3-7 and the purity of the resultant products was analyzed by ^{1}H NMR (Figure 9). Reactants, especially cationic ones like DTPH and waste EDC, remained in the product solutions dialyzed against pH 4-7 buffers after 7 d whereas dialysis against pH 3 media resulted in nearly quantitative removal of all impurities and thereby implies the necessity of acidic dialysis media with a pH of at least pH 3. In subsequently performed experiments, increasing the media exchange rate from initially 2 to 4 per day using pH 3 media was found to remove all reactants independent of the MWCO of the dialysis tube.

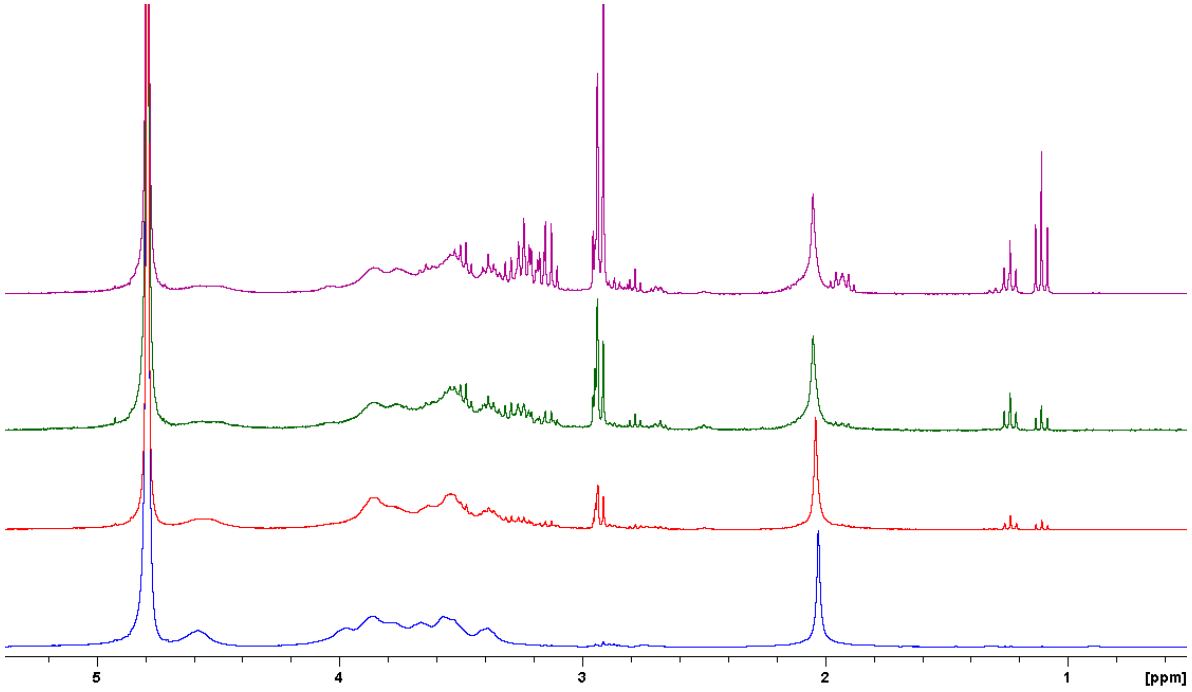

Figure 9: ^{1}H NMR overlay plot of HASH dialyzed for 7 days against media with different pH in D_2O. Top to bottom: pH 7, 5, 4, 3.

During all these investigations, the molecular weight of the polymer was significantly reduced, and a stability test was conducted in which pure HA was incubated over 35 days in different acidic buffering solutions it is exposed during the synthesis and dialysis with an additional 10-fold stronger buffer to simultaneously check the correlation between buffer concentration and HA stability. The molecular weight was monitored over time (Figure 10) by SEC MALS. For this, the HA was dissolved in MilliQ at rt and then mixed in a 1:1 ratio with each buffer to prevent exposure of HA to acidic media already during the dissolution process while the used buffer solutions were twice as concentrated to yield the respective molarities.

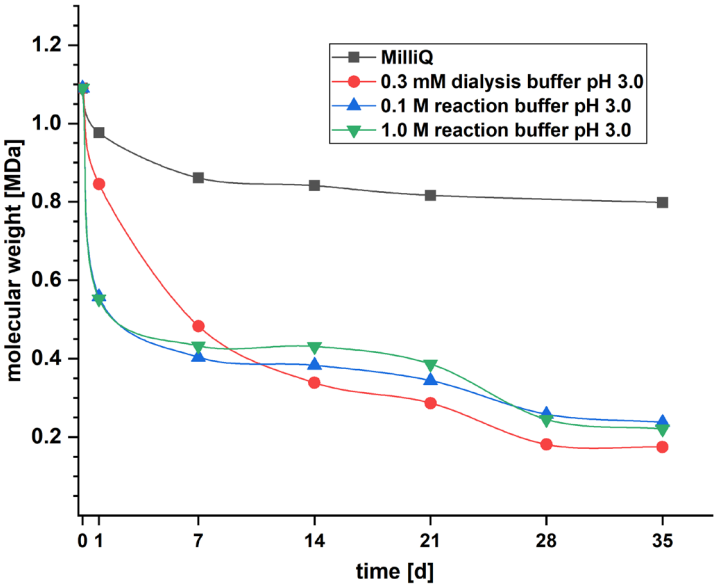

Figure 10: Degradation of pure HA (1.0-2.0 MDa) in different acidic buffers used during the thiolation process (day 28 of the MilliQ series was omitted due to a measurement failure).

HA degraded in all media over time by 27-84 % depending on the conditions. In MilliQ the least degradation with 27 % was observed and incubation in all buffers yielded a reduction of the initial molecular weight by 79-84 %. Within the buffers, degradation progression was closely identical for the reaction buffers with an intermediate plateau between day 7 and 21 independent of the buffer concentration, while the dialysis buffer caused an almost constant degradation following an exponential decay. Initially surprising, the degradation of HA even in MilliQ can ultimately be explained by the slight acidic pH of the utilized MilliQ water exposed to air forming bicarbonate by absorbing carbon dioxide that causes a drop of the pH to 5.6 similarly as observed for rain and snow[58]. pH measurements of pure MilliQ, the HA-MilliQ solution after day 35 and freshly prepared HA-MilliQ solutions exhibited in all cases values of 5.5-5.6 due to the inevitable equilibrium between gases in the solutions and the surrounding air. The insignificant effect of sodium hyaluronate on the pH was expected as 0.5 % HA comprises less than the 12.5 µM of sodium carboxylates, which is easily buffered by the media with more than 20-fold the concentration.

Indicated by the convergence of the molecular weight to around 0.2 MDa after day 35 and the availability of different batches of HA, a follow-up stability experiment was conducted with all starting materials above 0.2 MDa to identify the most stable one, which will then be chosen for the synthesis of high molecular weight HA (Figure 11). The setup was identical to the previous stability test except for only using dialysis buffer as HA is exposed to it for the longest time during the whole synthesis and purification procedure. The experiment also revealed the common trend for every HA, in which the degradation occurred stronger the higher the initial molecular weight ranging between 43 % for 0.2-0.5 MDa HA and 73 % for 2.0-2.5 MDa HA.

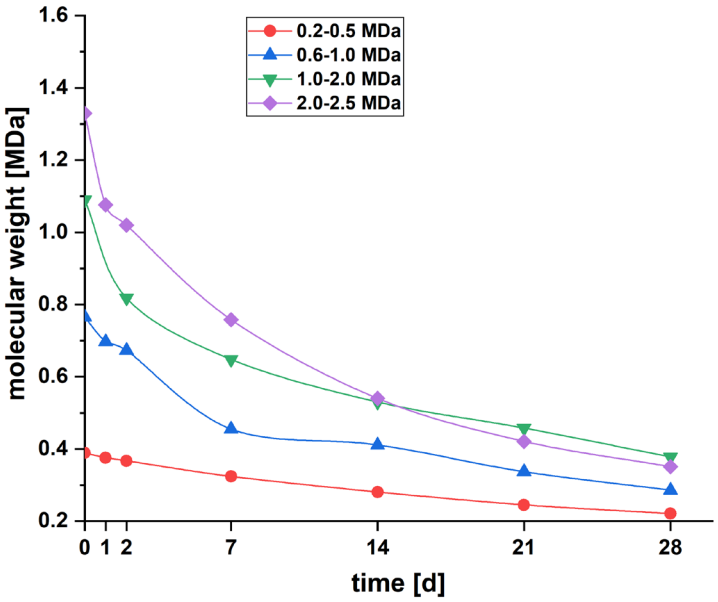

Figure 11: Degradation of pure HA with different molar masses in 0.3 mM pH 3.0 dialysis media over 28 days (day 1 of the HA 1.0-2.0 MDa series was omitted due to a measurement failure).

Considering that the thiolation process takes up to 12 days, starting materials with larger molecular weights yielded larger product M_w and thus 2.0-2.5 MDa HA should be chosen, but due to supply shortages for this specific molecular weight and an only minor difference to the 1.0-2.0 MDa batch the latter was ordered in 1.5 kg stock and used for all further experiments.

Comparing the curve progression of this batch in both degradation studies (Figure 10: red, Figure 11: green) yielding different molecular weights after day 28, the hydrolysis of the polymer seemed to occur randomly following a certain trend of larger molecules to quickly degrade forming more and more stable smaller polymer chains, which results in the exponential decay curve. This observation was underpinned by product analysis of three identically and simultaneously performed HASH syntheses yielding molar masses in the range of 144-210 kDa and DS of 22-25 % representing the effectiveness of constant reaction conditions, such as temperature, mixing and pH, by the above-mentioned improvements and hence represents the replicability of the synthesis meaning that synthesis results are replicable by one person using identical protocols, chemicals and equipment in the same laboratory[59]. As the HASH synthesis is of paramount importance for the SFB it must also be performable for future successors independent of their working place and a reproducibility[59] study was performed with the help of three scientific staff members. The study consisted of the provision of synthesis protocol (SOP), chemicals and equipment to the test persons, hereinafter referred to as person A, B, C, without preliminary instruction of A and B, while person C was shown the synthesis once beforehand. All students used the same chemicals and A and C performed the synthesis with the same equipment whereat B was sent to another laboratory with different equipment (glassware, scale, pH electrode, incubator, dialysis tubes) and the obtained results were analyzed identically by the author of the protocols. With this, all parameters were varied that have been identical in the replicability setup namely operator, knowledge, location and equipment with the exception of chemicals as different HA batches with the same molar mass were not available at this time point and were examined separately upon arrival of the shipment.

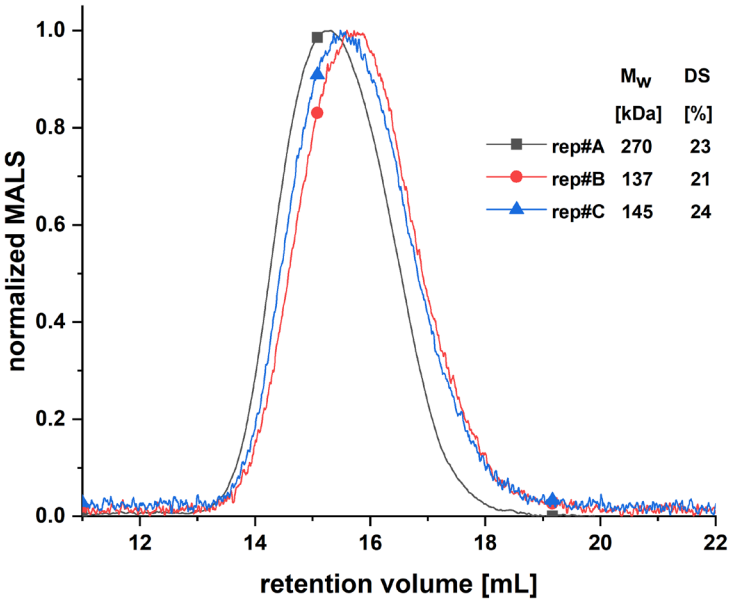

Figure 12: Normalized MALS overlay plot of resulting HASH batches of a reproducibility study and their characteristics.

Analysis of the three obtained HASH batches showed molar mass between 137-270 kDa and thiol contents of 21-24 % both lying in a very close range like for the HASH from the replicability study. With the molar mass being uncontrollable due to random hydrolytical breakdown and regarding the resultant DS, no noteworthy differences existed between A and C as well as A/C and B and thus the altered factors did not affect the synthesis outcome proving the rigidity of the synthesis protocol and its reproducibility.

All HASH batches produced so far were applied in a follow-up gelation experiment to determine the required DS for hydrogel formation using P(AGE-*co*-G), an allyl-modified polyglycidol, Irgacure I2959 as photoinitiator, 365 nm UV handlamp as light source and 90 µL borosilicate glass cylinders as molds according to the protocol of Stichler *et al*.[54]. The concentrations of polyglycidol and I2959 were fixed at 5 % and 0.05 % the and the HASH content was stepwise increased from 1.0 to 5 % whereas HASH batches with a DS of 5, 16 and 25 % were applied. As a reference, a HASH batch from *PolyVation*, an industry cooperation partner, with 27.4 kDa and 43 % DS was utilized that was produced using the articles protocol[54]. The hydrogels from the literature were reproducible with the HASH reference and kept their cylindrical shape while HASH with 25 % only formed very weak hydrogels after UV exposure (10 min, 365 nm) and gelation experiments with all other HASH batches failed. Neither an increase of allyl-crosslinker or initiator nor an extension of UV irradiation led to inherently stable hydrogels even though the utilized HASH batch had four times the molar mass of the reference batch.

The only difference between these batches consisted in a DS of 25 % versus 43 % and consequently, the impact of several reaction parameters on the thiol DS were systematically examined such as temperature, pH of the reaction solution and EDC equivalents. As a first step, the role of the reaction temperature was investigated since two reactions simultaneously take place during the substitution process with unknown kinetics, the reaction of coupling reagent (EDC) with carboxylic acids and with water, each consuming the applied amount of EDC and thus affecting the achievable thiol content. Despite the possibility of hydrolysis of the activated carboxylate by water, the activated intermediate is thought to react almost completely with NHS and DTPH since both are highly potent nucleophiles due to the α-effect[60,61] and H_2O is only a weak nucleophile.

Conducting identical syntheses at three different temperatures, 5, 25 and 37 °C, and the analysis of the resultant DS revealed an increased values with increasing temperature whereas cooling of the

reaction solution led to prevention of thiolation. This observation indicates different kinetics for the two competitive reactions with EDC slowly reacting with water but not with carboxylic acids at 5 °C while carboxylic acid activation is enhanced by factor 1.4 at 37 °C compared to 25 °C. Reactions at higher temperatures were not conducted to keep the rate of hydrolytical degradation as low as possible and all further syntheses were accordingly performed at 37 °C.

Secondly, the influence of the amount of coupling reagent and the pH of the reaction solution on the DS were simultaneously investigated by a synthesis screening consisting of identical syntheses at pH values of 4.0 to 6.0 in 0.5 steps, each with 5.0, 7.5, 10 and 12.5 eq. EDC. The obtained DS ranged from 5 % to a maximum of 70 % and followed a clear trend of increasing DS with increased amount of coupling reagent and with decreased pH value (Figure 13). The value at pH 4.5 and 7.5 eq. EDC was inconclusive due to reoxidation of the HASH during dialysis. Regarding the reaction series with 12.5 eq. EDC, the DS strongly increases from pH 6.0 towards 4.5 and reaching a plateau between 4.5 and 4.0 similar to the 5.0 eq. EDC reaction series that is consistent with EDC reactivity literature[62]. This converging progression resembled a saturation curve and raised the question of an already reached maximum which led to additional syntheses with more acidic pH values of 3.5 and 3.0 confirming the existence of a maximum for 12.5 eq. EDC at around 70-77 %. A follow-up experiment with pH 3.0 and 15 eq. EDC yielded no increased DS and was deemed to be caused by enhanced hydration kinetics of EDC in acidic media[62,63].

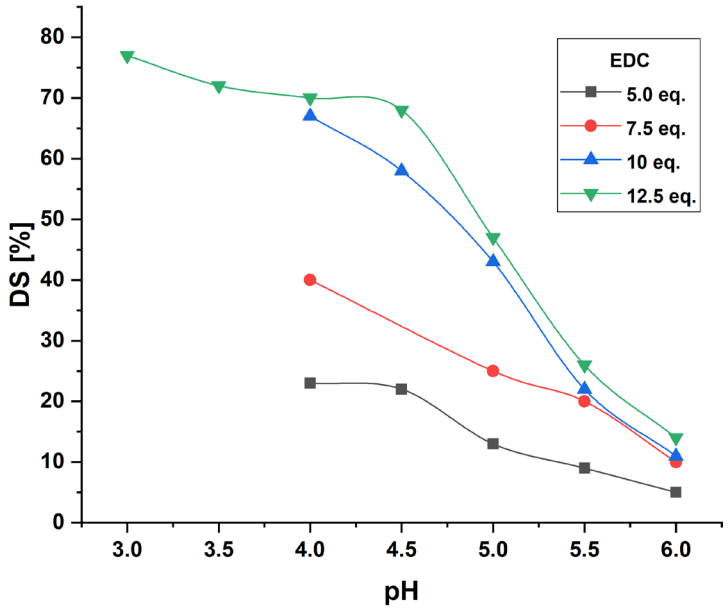

Figure 13: Impact of amount of coupling reagent (EDC) and pH of reaction solution on the degree of substitution

The consumption of the available commercial DTPH stock (Arké Organics, IT) and the long, unclear delivery times of this crucial reagent due to the corona pandemic led to the in-house synthesis of DTPH (see chapter 2.3.1, p. 54) according to Vercruysse *et al.*[64] and yielded the desired product in unexpected appearance. The obtained snow-white, shiny, and odorless crystals differed strongly from the commercial product, a pale-yellow, amorphous powder with pungent amine odor. This new educt resulted in an almost quantitative thiolation of HA at pH 4.0 and 12.5 eq. EDC. The odor of the commercial product was most likely caused by hydrazine impurities from improper purification during the production process, a competitive and very potent nucleophile that not only reacts with the activated intermediate but also changes the polarity of the modified carboxylic acid from neutral to cationic. Consequently, following experiments were conducted at pH 4.0 using the in-house produced

DTPH and the obtained DS equaled the thiol content and was adjusted by the amount of coupling reagent.

In parallel to the investigation of the relevant factors for an increased DS in aqueous reaction media, a method to enable HASH synthesis under water-free conditions in organic media was also examined. Therefore, the sodium hyaluronate was transformed into a DMF soluble Tetra-*n*-butylammonium salt (TBA) according to Oh *et al*.[65] by loading cationic ion exchange resin with Tetra-*n*-butylammonium hydroxide (TBA-OH) following the addition of sodium HA solution to the TBA-loaded resin. The obtained TBA-HA was freeze dried before dissolution in dry DMF and the subsequent reaction with identical chemicals as in the aqueous HASH synthesis but with reduced amount of EDC. A DS range of 75-85 % were achieved at already 3.0 equivalents. EDC as the coupling reagent proved to be long-term stable in the absence of water, while a considerable amount of by-product was formed (10-15 %) during the substitution. Together with an enormous decrease in molecular weight from initial 1.09 MDa to 60-70 kDa due to the inevitable strong alkaline conditions during the TBA-HA preparation, the TBA method was not pursued further as alternative method for thiolation.

After investigation and optimization of the substitution step, the reduction and dialysis steps were examined in more detail to determine the requirements and the scope for possible improvements. According to the protocols, Dithiothreitol (DTT), a telechelic dithiol was deployed under alkaline conditions following acidification and dialysis against acidic media. The mechanism of the reduction by DTT consists of two sequential thiol-disulfide exchange reactions including an initial nucleophilic attack of deprotonated DTT-thiol on the DTPH disulfide, generating a new mixed disulfide which is ultimately cleaved by a second nucleophilic attack of the remaining free thiol of DTT (Figure 14). The chemical equilibrium of the thiol-disulfide exchange is shifted towards the oxidation of DTT as the six-membered ring is thermodynamically favored.

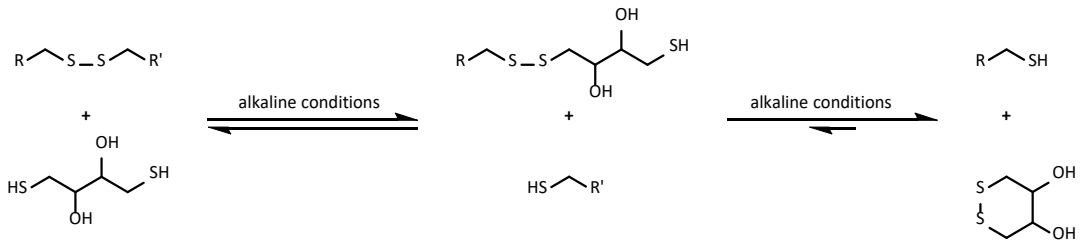

Figure 14: Schematic reaction mechanism of a disulfide reduction via DTT under alkaline conditions.

In a screening experiment, the required pH value for proper reduction overnight was determined and the pH was checked before and after the reaction. For this purpose, identical reactions were performed, and the pH was adjusted after the substitution to different values starting from 7.0 to 10.0 in 0.5 steps. Since DTT oxidizes when exposed to oxygen, the reaction was performed in a sealed environment. The pH turned out to drop overnight by approx. 0.5 independent of the starting pH and incompletely reduced mixtures were obtained for reactions with initial pH 7.0-8.0, indicated by remaining gel parts in the mixture while all other applied pH values led to homogenous solutions. In order to prevent two possibilities, the incomplete reduction by too low pH and HA degradation by too alkaline conditions, a pH value of 8.5-9.0 was chosen. Despite dialysis over even 10 days, the product still kept a DTT odor and thus indicated residual DTT which was not detectable by ^{1}H-NMR but might have potential influence on biological experiments. One possible explanation could be incomplete DTT cleavage from the intermediate with DTT covalently bound to the modified polymer. This intermediate can also be formed by reaction of reduced HASH with oxidized DTT, a thermodynamically unfavored reaction whose probability depends on the reaction conditions. As the reduction is an equilibrium, it must therefore be assumed that this intermediate exists to a certain extent at the time of acidification for dialysis. Once protonated, DTT is unable to undergo intramolecular cyclisation and remains bound

to the polymer. The addition of TCEP to the dialysis media within the first days of dialysis was found to be beneficial in three ways. First, it is a non-covalently binding and pH independent reducing agent which reduces all disulfides present during acidic dialysis including the DTT intermediate and does not form intermediates itself. Secondly led to accelerated elimination of the thiol-containing reactants (reduced DTPH, DTT) which, together with the pH gradient, shortened the duration of dialysis from initially 7 days to 5 days. This reduction in the residence time of the hyaluronan-based product in an acidic environment also led to a reduction in acid-catalyzed hydrolysis of the sugar backbone and thus to larger molar masses of the product. The third advantage of TCEP in the dialysis media was complete prevention of reoxidation due to sulfide or metal contaminants in the dialysis tube material. Purchased so called "pre-wetted" tubes were treated by the manufacturer using their individual pre-treatment protocol and led to nearly no oxidation during dialysis without TCEP addition, while dry dialysis tubes were untreated and may contain disulfide and transition metal traces from the manufacturing process oxidizing the product during the dialysis in a noteworthy number of cases when TCEP was not applied. Washing of the dry dialysis tubes according to the pre-treatment protocol with MilliQ, $NaHCO_3$ and EDTA sodium at higher temperatures prior to the dialysis reduced the probability of HASH reoxidation while reoxidation was completely prevented when TCEP was present in dialysis media. From an economical point of view, the dry tubes including the treatment steps were three times as cost-efficient as the "pre-wetted" alternatives independent of the MWCO which is negligible when dialyzing only small volumes but must be considered when upscaling the material production to liters of reaction solutions and with a limited yearly budget. Other alternative reducing agents such as sulfites ($NaHSO_3$, $Na_2S_2O_5$), dithionite ($Na_2S_2O_4$) and thiosulfate ($Na_2S_2O_3$) were tested for application during the reduction and the dialysis step as DTT and TCEP are both pricy chemicals. In the case of both sulfites and the thiosulfate, the reduction was incomplete even after 3 days of incubation whereas sodium dithionite with a higher redox potential (-0.66 V)[66] than DTT (-0.44 V)[67] generated nearly homogeneous solutions with only slight gel residues after 3 days and was deemed to reduce disulfides under proper conditions within the same time as DTT but due to the limitation by the products chemical stability in terms of pH and temperature the dithionite was inapplicable. As none of the tested alternatives quantitatively reduced the HA-disulfide intermediate, their application in dialysis media was redundant.

All HASH batches, obtained by the above-mentioned screening experiments with 1-2 MDa HA, summed up in a huge variety of materials all differing in molar mass as well as thiol content and were used in a repetition of the gelation experiment (see p. 17) to determine the required thiol content for gelation. The applied materials possessed molar masses >140 kDa and a DS of 25, 30, 36, 40, 52, 60, 78 and 100 %. All solutions with 1 % HASH and 5 % P(AGE-*co*-G) and 0.05 % I2959 formed hydrogels after 10 min UV exposure, whereas solutions of HASH with a DS of 78 and 100 % contained gel parts from HASH oxidized during the dissolution process. A general trend was observed that stiffer hydrogels with higher shape fidelity were obtained with increasing DS for HASH with 25-60 % thiol content while no difference between hydrogels from HASH with 60-100 % DS was observed. A thiol content of 25-36 % only yielded very weak hydrogels that were not suitable for application in bioinks as they would deliquesce when layers are stacked and hence, a DS of 40-60 % was deemed appropriate for the following ink development. The solubility of HASH depending on the DS was subsequently investigated due to the gel parts formed during dissolution of HASH with high thiol contents. The setup was adapted from the SEC MALS preparation and consisted of the dissolution of different HASH batches with varying DS ranging from 1-100 % in MilliQ at rt using a vortexer and the solutions were filtered by 0.2 µm (RC) syringe filters. Solutions were labeled homogeneous when no filter clogging occurred by gel parts and experiments were repeated twice more when solutions were inhomogeneous to prevent false-negative results. In the range of 1-60 %, all HASH batches yielded homogeneous solutions after 10 min vortexing while a DS of 66-77 % was not soluble in 1 or 2 out of 3 trials. Above 77 % thiol content,

filtration was impeded in all trials indicating a higher probability of reoxidation during dissolution in aqueous media with increasing thiol content. The use of degassed solvents and media might circumvent this issue but is inapplicable for cell experiments and was therefore not implemented. Based on the observations from the gelation experiment and the HASH solubility test, HASH batches with 40-60 % thiol content were used in hydrogels (2.4.1, p. 63 ff.) and ink development (2.5, p. 72 ff.). Supplying cooperation projects with materials with consistent characteristics was a major objective of this thesis and was non-trivial for HASH as the molar mass varies uncontrollable from batch to batch due to random hydrolytical breakdown. However, the reproducibility of the thiol content was proven which was considered crucial for hydrogels and bioinks since the amount of reactive groups remains constant at a given weight (e.g., 100 mg) independent of the molar mass of the polymer while the latter above 200 kDa, within the achievable range of up to 550 kDa, solely influences the initial viscosity of the precursor solution (2.5.1, p. 72).

Since chemical reactions are bound to probability and the surety of identical DS of two consecutive batches is not given, slight changes of material behavior may occur impeding at worst the replicability of printing or biological experiments. To eliminate any eventualities, exclusive 3 g HASH batches were produced for each cooperation project which is by far sufficient for any project type. Upscaling of HASH synthesis from 0.25 g to 3.0 g at pH 4.0 and with 12.5 eq. EDC was almost straight forward and did not require changes in the quantity ratio of reactants or reaction procedure only necessitating adjustment of the equipment. The volume of the reaction vessel, a Schott bottle, was increased from 100 mL to 1 L and the viscous reaction solution had to be mixed manually before incubation due to the sheer volume (600 mL) and the fast reaction speed. The resulting DS dropped from 70 % to 60 % mainly due to the reduction of the probability that a reactant encounters a reaction partner within the first minute of mixing as during this time a weak hydrogel was formed by DTPH crosslinked HA progressively impeding the effect of further mixing. Diffusion of reactants inside the hydrogel is possible but deemed negligible when comparing diffusion range (mm) and spatial dimensions of the reaction volume (cm). Ultimately, the reaction volume was increased from 600 to 700 mL (4.4.1, p. 103) to facilitate proper mixing and the dialysis of the viscous reaction solution. As a DS of 40-45 % was found suitable for bioink application during the bioink development (2.5.1, p. 72), the reaction conditions were adapted using the larger reaction volume of 700 mL at which pH 4.0 and 7.5 eq. EDC yielded the targeted thiol content. In addition, dialysis was optimized by setting the pH of the product solution to 3.0 and using a weakly buffering media with pH 5 which initially generated an acidic environment and gradually converged to pH 5.0 over the duration of the dialysis. This temporal pH gradient removed the amine-containing reactants (DTP, EDC) particularly quickly within 5 days while reducing the speed of hydrolytic degradation.

Simultaneously, a different and faster purification method as dialysis was investigated to lower residence time of HA in acidic aqueous media and consequently minor hydrolytical breakdown and to reduce the current production time of 12 days. Two ways of ultrafiltration were tested, driven by centrifugation (VivaSpin, Sartorius) and by peristaltic pumping (VivaFlow, Sartorius). The VivaSpin system was made of a bipartite falcon with a reservoir on the top and a waste container on the bottom. The membrane was implemented in the lower part of the top section pointing downward at an acute angle to prevent filter pressing effects known from dead-end filtration systems and for filtration, the reservoir was filled with product solution, centrifuged for 30-60 min at 3000-4000 G, resuspended with dialysis media and the procedure repeated several times. Each filtration had a capacity of 20 mL and eight units were operated at once summing up to 160 mL per run. The VivaFlow system is based on tangential flow (TFF) meaning the flow direction is perpendicular to the filter membrane and consisted of a filter cassette with inflow, backflow and waste outlet. The tubing for in- and backflow were placed in the sample solution creating a circular flow driven by the peristaltic pump and fed with fresh dialysis media to compensate the volume of filtrate leaving the system. A flow restrictor at the backflow outlet

generated the required pressure of 3.0 bar and was controlled by the pump rotation speed and a built-in pressure gauge. The principle is based on constant filtration until all low molecular weight reactants traversed through the membrane with only the polymer product remaining inside the system. Both systems were tested with different membrane materials (PES, Hydrosart) and MWCOs (2, 3, 5 kDa) and the filtration progress monitored by ^{1}H NMR. Unfortunately, the filtration failed in each system due to membrane cloggage. During the first centrifugation step, a wet layer remained on the membrane and complete filtration was inhibited in the second run independent of the duration or speed of centrifugation indicating the product sticking to or in the membrane. The TFF system showed within the first 2 h initial good filtration progress, visible by the amount of waste volume (200 mL) per hour which then steadily decreased until only single drops per minute ran out the drain after 5 h of filtration. Neither increasing the pressure via higher flow rate nor flushing the system with reductive, alkaline media for several hours removed the cloggage. Identical problems appeared for all applied MWCOs and the ultrafiltration was considered inapplicable for HASH. According to the manufacturer, the filtration system is meant to purify protein samples with ease whereat, compared to the folded proteins, HA and its derivatives described in this thesis do not form tertiary structures and are present as linear chains, which only clogged the rigid, solid membranes of the ultrafiltration setup but not the flexible soft membranes of dialysis tubes. Consequently, dialysis remained the purification method of choice.

Alternative thiol carriers, such as cysteamine and cystamine, were tested under reaction conditions of Kafedjiiski *et al*.[68] and the optimized protocol using DTPH. The idea was to compare the HASHs with different thiol carriers in terms of the reactivity in gelation experiments and the solubility of the product. The thiolation under both conditions was only marginally successful and yielded thiol contents of less than 10 %. Generating NHS-activated HA at pH 5.5 with subsequent addition of cysteamine and pH adjustment to pH 6.0 as described by the literature led the formation of the HA by-product via *O*-*N*-acylurea rearrangement and a very low thiol content of 5 % while the use of cystamine under DTPH reaction conditions at pH 5.5 yielded no by-product and a DS of 10 %. The pH of both reactions had to be less acidic to enable nucleophilic attack of the amines or the thiol and contrasted with the reactivity of EDC, reacting faster under more acidic conditions[62]. This susceptible balance between these two pH-dependent reactivities led to the discontinuation of the first attempts. Another hydrazide-based alternative is described by Fu *et al.*[69] consisting of EDC-mediated coupling of an adipic dihydrazide-linker to HA prior to addition of DTP-NHS diester and subsequent DTT reduction but was deemed inapplicable. The modification of HA with a non-cleavable bivalent dihydrazide linker not only is prone to yield covalently bound HA oligomers but also represents an additional synthesis step exposing HA to acidic media and thus was not pursued. As the supply of the SFB was very urgent and suitable HASH, synthesized with in-house DTPH, had already been produced no further alternatives were searched for or investigated. The optimized protocol for the HASH synthesis was ultimately transferred on all HA starting materials available and led to different molecular weights of HASH ranging from 8-577 kDa (Figure 16) with closely the same thiol contents (40-45 %). These results nicely demonstrate the rigidity, reproducibility, and universal transferability of the established HASH synthesis protocol (Figure 15).

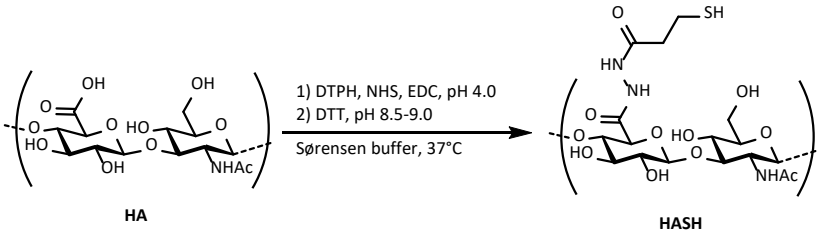

Figure 15: Reaction scheme of the optimized HASH synthesis.

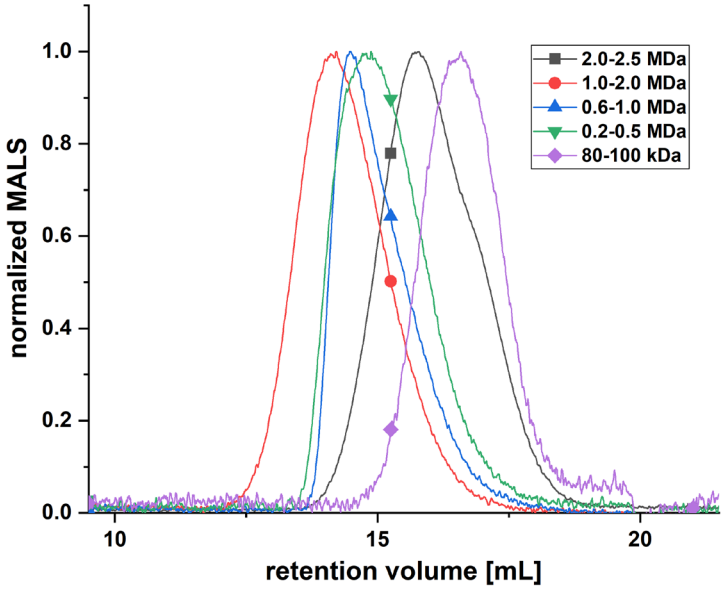

Figure 16: Normalized MALS overlay plot of HASH from all HA starting materials except 8-15 kDa requiring different SEC columns due to too small M_w.

Regarding the characterization of the HASH, thiol contents were determined by comparison of the integrals of the thiol-bearing modification and an internal reference, a combination of the *N*-Acetyl group (3H) at 2.05 ppm and the anomeric protons (2H) around 4.60 ppm. The reference peaks were integrated in such way to yield integrals with the ratio 3:2 while the *N*-Acetyl peak was used for integral calibration following the integration of both CH_2 signals of the 3-mercaptopropionic hydrazide between 2.65-2.95 ppm. Division of the latter by the maximal possible integral (DS 100 % = 4 protons) led to the respective thiol content since only one thiol-carrier can be introduced per HA repetition unit. The satellite signals of the *N*-Acetyl peak (± 0.22 ppm) were excluded from integration to not falsify the results and the sugar backbone signals between 3.2-4.2 ppm were not integrated or used as reference due to superimposition with sodium ascorbate signals, present in traces (~0.7 mg/mL) in the dialysis media. NMR samples were prepared in concentrations of 4-5 mg per 0.6 mL D_2O and dissolved within 10 min on a vortexer. Inhomogeneous sample solutions or higher concentrations of polymer led to higher viscosity and subsequently to peak broadening[70] which above a certain level compromised exact determination of the DS and thus had to be avoided.

For SEC MALS measurements, a screening was performed with different HA batches for the determination of the most suitable sample concentration by preparation of 2 mg/mL sample solutions and injection of each sample with 100, 50, 25 µL injection volume whereas 100 µL represented the default injection volume and injecting only 50 µL is equal to the amount of polymer that would be injected with default settings and half the sample concentration (1.0 mg/mL), respectively 25 µL equals 0.5 mg/mL. The results were compared within each sample injection row and results with values shifted towards lower molecular weight were considered to arise from a column overload and were rejected. HA below 0.6-1.0 MDa showed no differences between 50 µL and 25 µL injections and for HA above 0.6-1.0 MDa only 25 µL injection volume showed no indications of column overload. Consequently, all HASH samples were prepared to yield a concentration of 0.5 mg/mL. For this, the samples were dissolved over 6 h in MilliQ and diluted to a concentration of 1.0 mg/mL, which was then mixed in a 1:1 ratio with 0.5 mg/mL TCEP solution in MilliQ to ensure the absence of disulfide aggregates and hence more accurately mirrors the actual molar mass distribution of the obtained product. MilliQ as solvent was chosen since the eluent contains sodium nitrate, an oxidative reagent, that causes disulfide formation during dissolution.

C6-HASH

The synthesis of thiolated hyaluronic acid with the thiol-carrier at the C6-alcohol (C6-HASH) according to Zhan *et al*.[53] was not pursued due to several synthetical concerns as follows. The achieved thiol content was only negligible with 3.5 % and is definitively insufficient for application in bioinks since a minimum of 35 % is required according to the HASH gelation experiments. Furthermore, the described modification is based on the reaction of C6-hydroxyl group and the epoxide moiety of the thiol-carrier which is eventually undergoing ROP chain polymerization leading to local high thiol content along the formed glycidol chain(s) instead of a thiolation along the HA backbone. The synthesis of the thiol-carrier consists of six steps with an overall yield of only 13 % including several purifications via column chromatography, an inapplicable purification method for upscaled processes, and is considered too laborious for ultimately minor and uncontrollable thiolation of HA. Another concern is the hydrolytical degradation during the final Boc-deprotection under highly acidic condition for 4 hours by addition of neat TFA with a pK_a of 0.23[71]. In contrast to the expected degradation, the stated SEC measurements showed an increase in molar mass compared to the starting material that can in no way be attributed to the added molar mass of the modification with only 3.5 % DS. This discrepancy in the values casted strong doubt on the credibility of the literature source. Instead of using epoxide chemistry for C6-thiolation, two possible strategies were devised based on the reaction of the primary alcohol with an anhydride, pentenoic anhydride (HAPA) or acrylic anhydride (HAA), following the conjugation of thioacetic acid (AcSH) and the cleavage of the thioester. By this time point, the modification of both intermediates, the HAPA and HAA, were already established and are described in the chapters 2.1.2 (p. 27) and 2.1.3 (p. 31) respectively, while the conjugation of AcSH and the thioester cleavage had to be investigated from scratch. Thiolation of the C=C bond of the pentenoate can be achieved by thiol-ene reaction yielding a 5-thiopentanoate whereas the acrylate can be thiolated via Michael-addition initiated solely by deprotonation of AcSH forming a 3-thiopropionate. In accordance with Nair *et al*.[23], the pK_a of aliphatic thiols increases with increasing aliphatic chain length and thus the reactivity of 3-thiopropionate is higher in Michael-addition reactions at pH 7.6, the pH of the aimed bioink. Together with the reduced solubility of HAPA with DS >50 % and the thiolation via Michael-addition being considered simpler, C6-HASH modification via the HAA route was chosen (Figure 17).

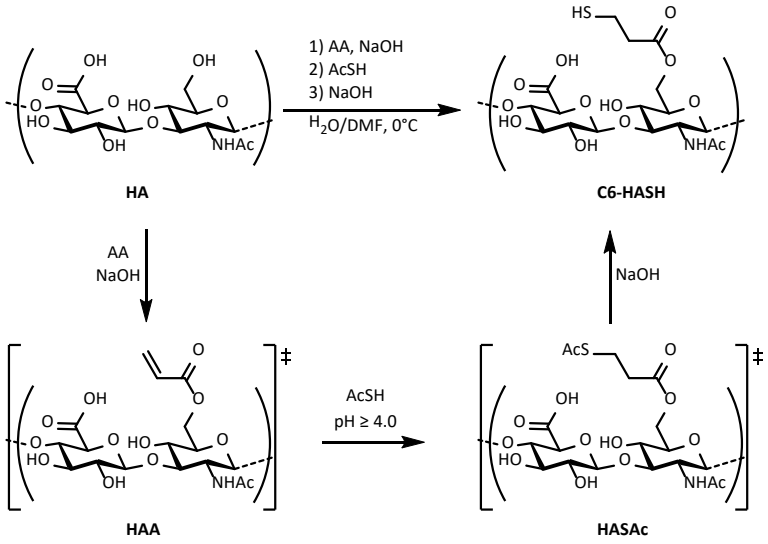

Figure 17: Reaction scheme of the C6-HASH synthesis via HAA intermediate.

First, each step was qualitatively investigated by means of 8-15 kDa HA in 200 mg scale and the success of transformation monitored by ^{1}H NMR after which the synthesis was transferred onto 200-500 kDa HA and optimized in terms of production times, and upscaling. Starting with the acrylation of the

C6-alcohol, identical reaction conditions as for the synthesis of HAA, were successfully applied. In brief, the acrylation was performed in complete darkness in MilliQ/DMF (3:2) at 0 °C using acrylic anhydride (AA) and NaOH, added in 10 portions every 2.5 min. The reaction was stirred overnight, and the product purified by dialysis against MilliQ for 5 days. For the Michael-addition of AcSH to HAA, the reaction was carried out at 0 °C to prevent major decomposition of AcSH in the aqueous media forming hydrogen sulfide, a highly potent and bivalent Michael-donor with the ability to crosslink HAA covalently. Acidification of the reaction solution was considered a second precautionary measure as hydrogen sulfide with a pK_a of 7.0 requires neutral to alkaline conditions to undergo Michael-addition[72], but was found unnecessary due to the acidity of AcSH with a pK_a of 3.33[73], already lowering the pH to 4.0 when added to MilliQ. Via this, the majority of AcSH exists in the deprotonated and thus reactive form. The quantitative transformation of HAA to HASAc was proven by the disappearance of acrylate proton signals in the ^1H NMR spectra in the range of 5.9-6.7 ppm whereas the S-acetyl peak appeared at 2.4 ppm together with the two CH_2-groups of the propionic acid between 2.7-3.3 ppm (Figure 18). Cleavage of the thioester under mild conditions was subject of the last synthesis step and hydroxide anions were deemed suitable for quantitative removal of the acetyl protection group whereas to alkaline conditions would lead to polymer degradation and possible *N*-acetyl cleavage. Based on the experience from the HASH reduction step, a mixture of K_2HPO_4 and DTT was utilized to buffer the slight alkaline pH of 8.5-9.0 and concurrently prevent disulfide formation. Dialysis identical to the HASH synthesis yielded a clean product with superimposed CH_2-group signals at 2.7-3.0 ppm whereas the S-acetyl peak vanished (Figure 18). Despite the unexpected multiplicity of the CH_2-group peaks, an indefinable multiplet with singlet character, the product formed hydrogels within 10 min when mixed with 8-15 kDa HAA (5 % / 5 %) in HEPES buffer pH 7.6, confirming the success of thiolation.

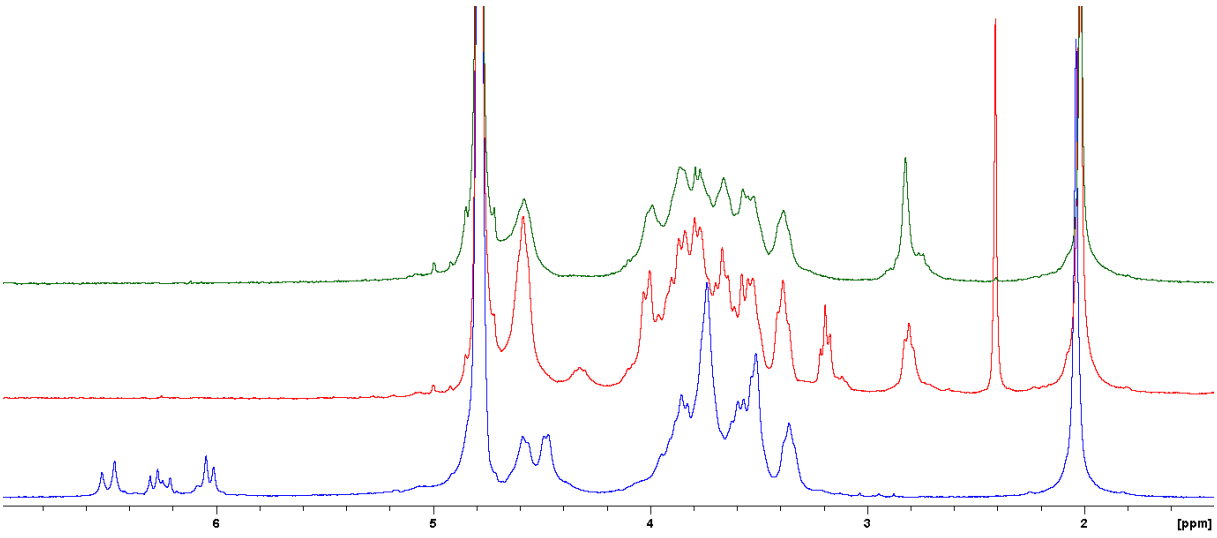

Figure 18: ^1H NMR overlay plot of each C6-HASH synthesis step in D_2O. Top to bottom: C6-HASH, HASAc, HAA.

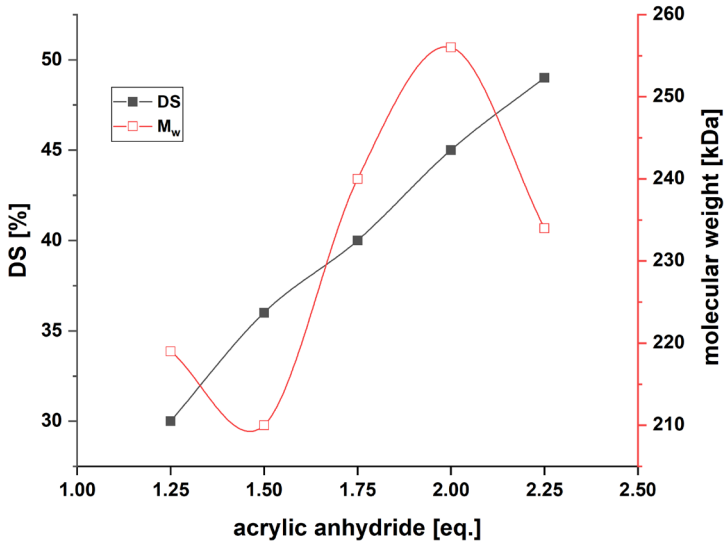

Figure 19: Impact of acrylic anhydride amount on the thiol content and molar mass of C6-HASH.

The reaction conditions were then transferred on HA 200-500 kDa in 1.0 g scale, while the modification was combined in a one-pot synthesis to reduce the production times and the optimization of reaction parameters was investigated to establish a tunable and reproducible protocol. The one-pot approach was realized by adjustment of the pH and usage of slight consecutive excess of reactants at each reaction step and one final dialysis against acidic reductive media. Regarding the tunability of the DS, the relation between the applied equivalents of acrylic anhydride and the thiol content of the product was investigated within the range of 1.25-2.25 eq. in 0.25 eq. steps and the results characterized by ^{1}H NMR and SEC MALS. A clear trend of steadily increasing DS with increasing eq. acrylic anhydride was revealed while the molar mass varied trendless around 233 kDa ± 23 kDa. Starting with 30 % DS at 1.25 eq. anhydride, every additional 0.25 eq. yielded an average increase of 5 % with a maximum at 49 % at 2.25 eq. (Figure 19), lying mostly in the optimal DS range for hydrogel formation of HASH. Successful thiolation was confirmed by the formation of hydrogels with HAA 8-15 kDa in HEPES pH 7.6 concentrations of 1 % / 1 % and the obtained products were examined for their applicability in bioink development according to an in-house established evaluation protocol with 6k-PEG-diacryl, further described in chapter 2.5.1 (p. 72), and sent to the respective cooperation partner for CD44 interaction experiments which were still in progress by the end of this thesis.

Simultaneously, different nucleophiles for the deacetylation of HASAc in step three were tested in parallel for the determination of the most suitable approach. For this, nucleophiles based on oxygen and nitrogen were used, operating under slight acidic conditions (NHS, $AcHNNH_2$) or alkaline conditions (NH_4OH, K_2HPO_4) whereas DTT was added to all reactions with imperative alkaline conditions and TCEP to those with acidic pH to maintain reductive conditions. Unexpectedly, the reaction with the nitrogen-based nucleophiles and NHS did not quantitatively cleave the thioester independent of the reaction time or molarity of the nucleophiles while the addition of K_2HPO_4 yielded the same result as the anhydride screening. As C6-HASH was already produced at this stage with a suitable DS for hydrogel formation and the CD44 interaction tests were still in preparation, further investigations of alternative nucleophiles such as *N*,*N*-dimethyl hydrazine were omitted.

2.1.2 Hyaluronic acid pentenoate (HAPA)

4-pentenoic acid, hereinafter referred to as pentenoic acid, is next to 3-butenoic acid the second smallest carboxylic acid with a terminal alkene that is not in conjugation with the carbonyl group like acrylic acid and therefore represents a highly useful functional group for thiol-ene crosslinking of polymers. Due to the low availability and high price of 3-butenoic acid deriving electrophiles like 3-butenoyl chloride or 3-butenoic anhydride the interest was focused on pentenoic electrophiles to modify polymers of which pentenoic anhydride (PA) has the best availability and lowest price on the market. The introduction of pentenoate esters to hyaluronic acid was target of interest, as the modified polymer represents a multi-arm thiol-ene crosslinker with a biodegradable polymer backbone in comparison to commonly used multi-arm PG or POx derivatives [35,52,54] or PEG. The idea was to increase the pool of thiol-ene crosslinkers for the development of dual-stage crosslinking bioinks and thus enhance the tunability of the inks towards any desired application of in-house projects and external cooperation partners. The synthesis of HAPA was first described in 2012 by Mergy *et al*.[74] using pentenoic anhydride (PA) as electrophile and sodium hydroxide for maintenance of aqueous basic conditions, named Schotten-Baumann reaction[75,76] and was utilized without modifications in literature[77,78]. In-house, the synthesis of HAPA was investigated for the development of two-component bioinks based on thiol-ene chemistry and the esterification was compared under different conditions, Schotten-Baumann and Steglich[79].

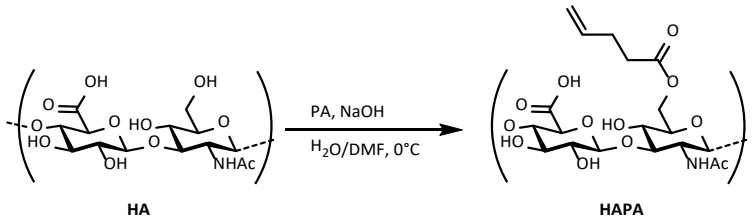

Figure 20: Reaction scheme of the HAPA synthesis.

In the resulting thesis of Oberst, K.[80], crucial reaction parameters for the control and reproducibility of the synthesis were described (Figure 20) and a highly reliable analysis method was developed for the degree of substitution. In summary, the reaction was carried out at 4 °C to prevent hydrolysis of the electrophile, an endothermic process, a mixture of water/DMF was used to enable dissolution of the hydrophobic anhydride and step wise addition of NaOH was found to be more advantageous compared to the addition on demand, when the pH dropped. In direct comparison, the Schotten-Baumann method was favored over the Steglich esterification since both methods resulted in closely same degrees of substitution while purification of Schotten-Baumann was simpler as only an anionic chemical, pentenoic acid, had to be removed after the reaction whereas the Steglich esterification yielded also cationic residues, protonated DMAP and TEA, necessitating additional NaCl in the dialysis media for their separation from the anionic product. Next to increased equivalents of anhydride also lower molecular weights of HA and hence lower viscosity at the same HA concentration led to higher DS values. Ultimately, a range of 1-85 % were achieved which corresponds to less than one pentenoate per repetition unit indicating that only the least sterically hindered alcohol at C6 reacts with the anhydride. With increasing DS, the product becomes steadily more hydrophobic and less soluble in aqueous media impeding gradually two analytical methods, NMR and SEC MALS. Increasing hydrophobicity causes higher viscosities of product solutions that result in longer spin-spin relaxation times and low signal-to-noise ratio[70] during NMR measurements that can only be counteracted to a limited extend with higher magnetic field strength and operating temperatures. In SEC MALS measurements, a high hydrophobicity causes aggregation and different coiling behaviors which changes the hydrodynamic radius of the polymer and thereby falsifies results despite the addition of detergent, SDS, to the eluent. Compared to the HASH synthesis, the esterification did not alter the

initial molecular weight of the starting material which has the advantage of selectable polymer characteristics such as viscosity and HAPA batches are named in the following according to the molar mass range of the starting material. To enable the quantification of pentenoates per repetition units, a reverse-phase HPLC analysis of dextran methacrylates was adapted from Stenekes *et al.*[81] to hyaluronic pentenoate, a method in which the esters were hydrolyzed by NaOH treatment and the amount of pentenoic acid was analyzed via integration of its UV signal calibrated according to DIN 32645[82]. Finally, HAPA with DS <50 % were found to be homogeneously soluble in aqueous media and most of the produced batches ranged between 25-50 % DS and consisted of 300 mg each.

As batch-to-batch variations should be reduced by all means possible to ensure replicable ink properties and the A02 project is an important material provider within the SFB TRR225, the investigations were continued in cooperation with Oberst, K. with respect to key reaction parameters for upscaling the modification process and the transfer of the reaction conditions to all available starting materials to extend the material pool. First, the reaction conditions were applied without modifications to the identical starting materials but in 1.0 g and 3.0 g scales and a DS of approx. 30 % was aimed at. Therefore, the extrapolated plot of the underlying literature was used to roughly estimate the required equivalents of pentenoic anhydride to be 3.3 (Figure 21). The upscaling from 300 mg to 3.0 g was successful even though mixing of > 250 mL viscous reaction solution via stir bar had been a major concern. HPLC analysis of the products' DS revealed a slight decrease of the pentenoate content with increasing batch size compared to the expected results from the 300 mg test reactions, which correlates well with the findings of upscaling the HASH synthesis (chapter 2.1.1, p. 11). The obtained average DS were 28.6 % (1.0 g) and 28.2 % (3.0 g), meaning that the average difference between expectation and result lies within 1.5-6.3 % (1.0 g) and 2.7-7.5 % (3.0 g) in terms of the lower and upper limit of the expect DS (Figure 22).

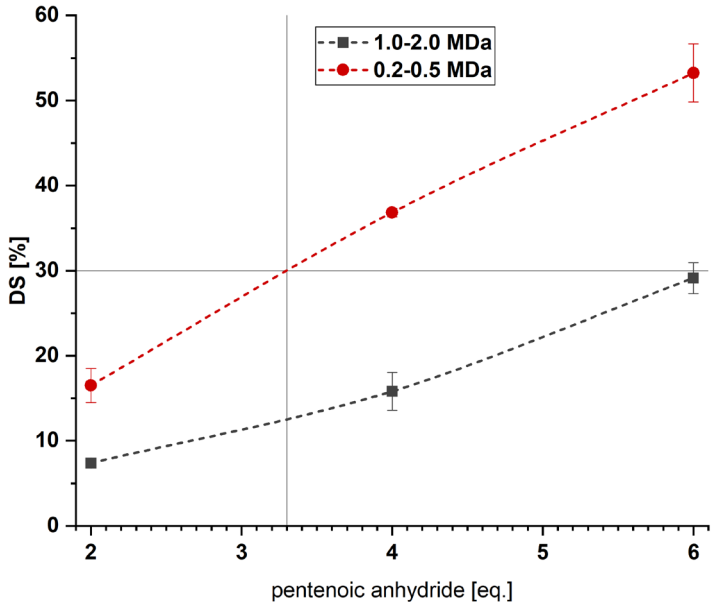

Figure 21: Correlation of pentenoic anhydride and resultant DS for different starting materials according to Oberst[80], modified, with guidance lines and zoomed in.

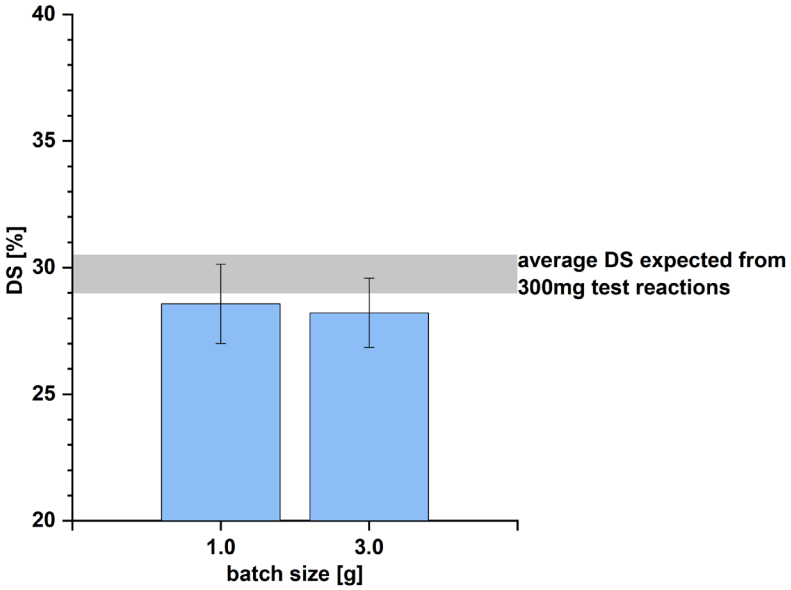

Figure 22: DS analysis by HPLC of upscaled HAPA (200-500 kDa) with 1.0 and 3.0 g batch size.

As indicated by the literature the influence of the viscosity of the reaction solution on the esterification is significantly high as it is shown in Figure 21 and was another target of interest while continuing Oberst's investigations. The viscosity of the solution depends on two variables, the molecular weight of the HA and the applied HA concentration, offering two possible strategies. One strategy is to create HA solutions of each available molecular weight with identical viscosities by adjusting the HA concentration to compare the outcome of the modification or using the identical HA concentration for each molar mass while applying identical amounts of reactants. Strategy one requires regular viscosity measurements and is highly dependent on batch-to-batch variations and thus was considered not feasible for future modification. Hence, strategy two was chosen. The HA concentration was kept constant at 1 % and the reactions were driven simultaneously under identical conditions and stoichiometries. The HPLC analyses of the products underline the hypothesis based on the literatures' data and observations that a higher viscosity leads to lower degree of substitution (Figure 23). With increasing molecular weight, the viscosity of the reaction solution raises visibly from unchanged, water-like (8-15 kDa) to sirup-like (2.0-2.5 MDa) while the DS drops roughly from 33 % to 19 % within this range of viscosity with a steep decrease by one fifth between 200-500 kDa and 0.6-1.0 MDa. The latter is thought to be caused by passing the critical molecular weight of HA at which entanglement of the polymer chains is enabled, strongly reducing the degrees of freedom of molecules in solution and culminating in higher viscosity. At lower molecular weights, entanglement is not possible or to a small extent as only few polymer chains are large enough whereas at higher molecular weights all chains are beyond the critical mass and a further increase in molecular weight has minor effects on the already high viscosity of the polymer solution. By number, the critical mass is unknown but estimated to lie between 200-300 kDa according to observations during HA modifications (HASH, HAPA, HAA).

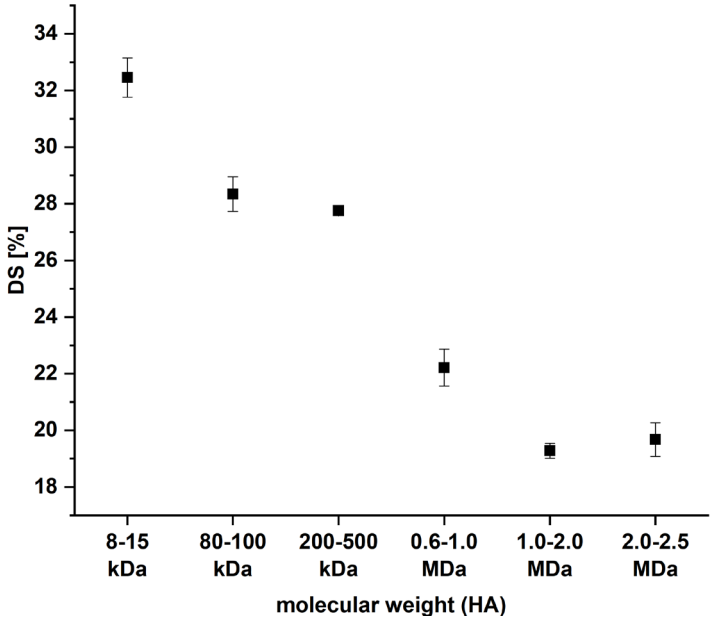

Figure 23: Correlation of the molecular weight on the degree of substitution (DS) at identical reaction conditions and stoichiometries.

In the following, the impact of the amount of NaOH on the DS was investigated closely as the literatures' data partially shows a monotonically non-decreasing correlation while theoretically a maximum should exist after which the DS decreases again due to higher probability of hydrolysis by the NaOH excess. Therefore, a row of reactions was conducted under identical conditions and constant equivalents of pentenoic anhydride but different amounts of NaOH that was added in 6 portions every 5 min. The optimum was expected to be within the range of 1.0 and 2.5 eq. NaOH based on the literature using 1.0-1.5 eq. and the theory that two hydroxide anions are consumed during the reaction for deprotonation of the oxonium intermediate and the neutralization of subsequently formed pentenoic acid. First, the range of 1.0-2.0 eq was simultaneously investigated in 0.25 eq. steps and the results analyzed, with the option of further experiments if the maximum is not reached, as the technical effort would be too large for simultaneous reactions and analyses. The obtained results (Figure 24) showed the expected optimum already at 1.75 eq. with a monotonically increasing behavior starting from 1.0 as indicated by the literature and a decrease from 1.75 towards 2.0 confirming the theoretical supposition. Based on this, the correlation of DS and NaOH excess under constant conditions can be seen as graph of a function of second order. No further reactions with more than 2.0 eq. NaOH were conducted as the maximum was yet revealed and the following syntheses were carried out with a 1:1.75 ratio of anhydride to NaOH to reduce the required excess of pricy pentenoic anhydride.

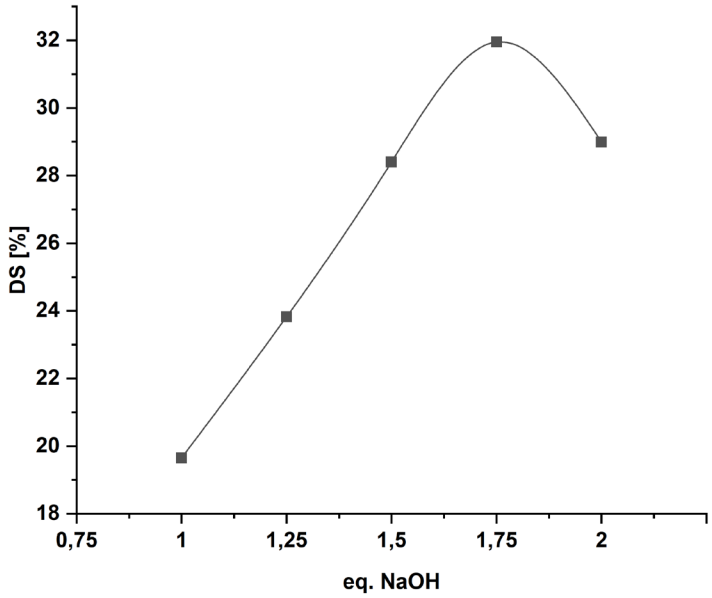

Figure 24: Relation between equivalents of NaOH and resultant amount of pentenoates per HA repetition unit at constant equivalents of pentenoic anhydride.

2.1.3 Hyaluronic acid acrylate (HAA)

With the established HAPA synthesis, the idea was born to transfer the reaction conditions onto HA 8-15 kDa while using acrylic anhydride to generate HAA, a multi-arm crosslinker. Background of the HAA synthesis were the development of hydrogel or bioink alternatives for two side-projects with different biological applications, the fixation of trypanosomes and the biofabrication of metastatic melanoma cells which are discussed in detail in chapter 2.4.5, p. 69 and 2.5.3, p 81. Compared to the broad application of HASH, HAA was meant for very specific applications and the foundation of its synthesis was built on the experience from the HAPA modification. Consequently, the HAA modification had to be investigated less extensive and the focus was placed on the replicability and upscaling of the synthesis (Figure 25).

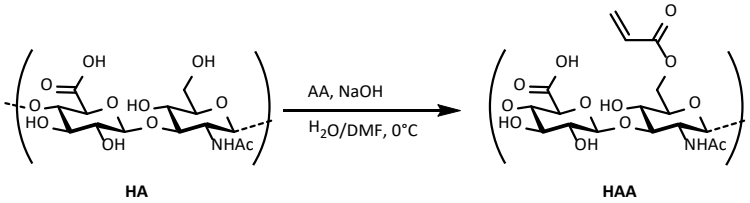

Figure 25: Reaction scheme of the HAA synthesis.

Acrylated HA was estimated to have similar properties to HAPA such as increased hydrophobicity with increasing ester content and consequently, the lowest molecular weight of HA was chosen as starting material for the first attempts which's excellent solubility should overcompensate every possible ester content. As no specific DS was aimed for, the reaction conditions of low molecular weight HAPA were applied with acrylic anhydride instead of pentenoic anhydride and the first trial was conducted with 1.8 eq. acrylic anhydride / NaOH in a 3 g and 6 g scale which led to a DS of 75 % (3 g) and 43 % (6 g) exhibiting two relations. First, the reactivity of acrylic anhydride in this reaction setup is much higher compared to pentenoic anhydride (Figure 23, p. 28) as nearly twice as much pentenoic anhydride (3.3 eq.) resulted in less than half the DS (33 %). Aside of different electron densities at the carbonyl function due to different molecular constitutions, the decreased hydrophobicity of acrylic anhydride

enhances its solubility in the reaction media and consequently the probability of ester formation is increased. This theory is underpinned by the observation that added pentenoic anhydride forms oily drops on the reaction media surface defying the vortex of the stir bar for several minutes while acrylic anhydride is instantly dissolved. Second, the upscaling had a severe impact on the DS and is not comparable to the upscaling of the HAPA modification. The unexpected reactivity raised the question of the acrylation of not only the C6-alcohol but also the secondary alcohols of the sugar backbone and a closer look at the NMR spectra further raised concerns. By overlaying both spectra, 3 g and 6 g batch, additional weak peaks in the range of 4.0-4.2 ppm were revealed only in the 3 g batch with 75 % DS (Figure 26) indicating also an acrylation of secondary alcohols as the C6 ester CH_2 signal only resonates at around 3.75 ppm.

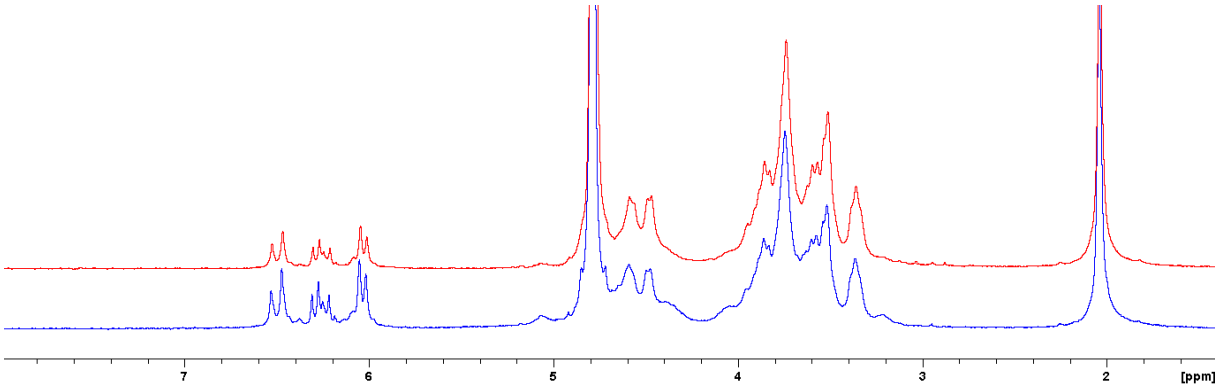

Figure 26: ^{1}H NMR overlay plot of two HAA batches with different sizes in D_2O. Top to bottom: 6 g batch, 3 g batch.

In a follow-up 6 g scale reaction, a much higher probability of acrylating secondary alcohols was further created by using half the solvent and thus doubling the reactant concentration. NMR analysis showed a DS of 98 % and now much more pronounced peaks in the identical range as in the 3 g batch NMR, confirming the ester formation also at the secondary alcohols of HA. The achieved high acryl content was the foundation for the fixation of trypanosomes and the biofabrication of metastatic melanoma cells, which are discussed in detail in chapter 2.4.5, p. 69 and 2.5.3, p 81. For both applications, a high polymer content of 5-10 % was tested suitable and increased the demand of HAA in larger batch sizes. Hence, reactions with up to 25 g were performed under the same conditions that led to 98 % DS and as alternative purification method, precipitation in acetone was tested as dialysis of such reaction volume would exceed the limits of the freeze dryer. The precipitation in ice cold acetone was successful and the product was obtained as fine crude solid. Despite several washings with pure acetone, remaining reactants were present that were ultimately removed quantitatively by the addition of 10 % MilliQ to the washing media.

As part of a bioink composed of HAA and pure HA as thickener (2.5.3, p. 81), it was of interest to transfer the reaction conditions to HA of larger molecular weights with the potential benefit of higher initial viscosity and consequently reduction of polymer content. The reaction using 0.6-1.0 MDa HA was straight forward according to the HAPA and previous HAA syntheses and the final solution was split into two parts, one for purification via dialysis and the other one for precipitation in acetone. The latter led to the formation of cocoon like solids that encased the reactants independent of the precipitation approach as well as speed of drop wise addition and impeded the effect of further washing steps which was identically described by Oberst for HAPA with molecular weights above 100 kDa[80]. Simultaneously, dialysis against MilliQ in absolute darkness resulted in a highly viscous, inhomogeneous solution which, after freeze drying, formed insoluble, gel parts impeding NMR and SEC MALS analysis. A repetition with 0.2-0.5 MDa HA yielded in the same observations and reminded of similar issues during the in-house master thesis of T. Zorn when preparing polyglycidol acrylate with

different acryl contents[83]. In this setup, the acrylated polymer of low molecular weight (< 5 kDa) was dialyzed against organic solvents and subsequently dried *in vacuo* yielding a honey-like viscous liquid that was highly prone to polymerization even during storage at -20 °C in complete darkness. Here, the liquid state of the product and the relatively high proximity of the acrylates along the polymer backbone were held to be reason for the susceptibility to polymerization. Consequently, the HAA batches were labeled according to the molar mass ranges of the respective starting material. Regarding high molecular weight HAA, acrylation of primary and secondary alcohols and thus close proximity of acryl groups is considered to promote the probability of partial polymerization during the dialysis leading to higher viscosity and the formation of insoluble parts. As the dialysis was already performed in complete darkness, only oxygen or a Lewis acid (proton) could have initiated the polymerization, which can be prevented by raising the pH to neutral or slight alkaline level and the usage of degassed media or the addition of a reducing agent to the dialysis media, likewise to dialysis of HASH, which then has to be removed within the last media exchanges before freeze drying. Further attempts were not made due to the lack of demand for high molecular weight HAA within the SFB and the focus was shifted towards the production and supply of low molecular weight HAA. The impact of the amount of acrylic anhydride on the degree of substitution was investigated during the C6-HASH synthesis and is explicitly described in chapter 2.1.1..

2.1.4 Upscaling of HA derivatization processes

A key challenge in this thesis was the upscaling of the HA modification reactions since these materials represent the basis of all formulation developments, hydrogels and bioinks. Preliminary HA based syntheses were performed in large beakers with a stir bar on a heating plate or at rt and purified via dialysis in diluted HCl which led to the desired product but was accompanied with several suboptimal features such as inhomogeneity, large batch-to-batch variations, side reactions and was certainly limited to low molecular weight, accordingly low viscous starting materials. All these factors of variability were consecutively investigated and eliminated. The switch from a stirrer to an incubator enabled not only homogeneous mixing of highly viscous reaction solutions but also precise temperature control and was successfully implemented in the HASH synthesis. Independent of the molecular weight of the starting material, simultaneous production of eight single 3 g batches was rendered possible which in total is equal to 2.4-4.8 L hydrogel/bioink formulation, depending on the used HASH concentration. Combining these single batches after dialysis before freeze drying would yield a homogenous 24 g batch sufficient for even the largest experiment series or comparative round-robin experiments within the SFB but necessitates prior quality check of each product. Utilization of an incubator reached its limits in reactions requiring low temperatures due to the specifications of the current instrument. Although the incubator can cool 15 °C below surrounding temperatures meaning a minimum of 5 °C in air-conditioned laboratories, reactions at 0 °C were rather performed in ice baths using stir bars and Schott bottles as reaction vessels. Providing homogeneous mixing in these reactions necessitated for reduced viscous reaction solutions as well as large vessels to keep low fluid levels and was achieved by adjustment of the starting material concentration in the case of high molecular weight C6-HASH and HAPA, all currently being producible in 3g batches, equal to 150-600 mL of formulation. Further upscaling of these reaction was not conducted since this batch size was rated sufficient for the present demand of in-house, SFB and external cooperation and larger batches can be generated by the same method as for HASH batches, blending after quality control prior to freeze drying. Synthesis of high molecular weight HAA is possible using this strategy but was omitted due to the lack of demand for this material plus its high sensitivity towards polymerization and consequently difficult storage and handling. Low molecular weight C6-HASH and HAPA were only partially synthesized in batches of maximal 1 g due the lack of demand but can be upscaled analog low

molecular weight HAA which was produced in up to 30 g batches by reduction of the solvent volume and purification via precipitation with a yield loss of 10-20 %. Generally, all HA derivatives were purified via dialysis despite its long duration and potential decrease in reaction yield since alternative methods such as tangential flow filtration and precipitation were found inapplicable after intensive investigations. However, the decrease in yield can be reduced to < 10 % by the selection of appropriate MWCO, meaning 1 kDa for products from 8-15 kDa and 80-100 kDa starting materials and 3.5 kDa in the case of all higher molecular weights.

2.2 Modification and characterization of polyethylene glycol (PEG) derivates

2.2.1 PEG-acrylates

PEG-acrylate presents a crucial component for the intended bioink and its synthesis as well as upscaling was of great importance for the SFB. Many synthesis protocols, starting from 1994 by Bignotti *et al*.[84] until today[85], have been published using different solvents, reaction conditions and purification methods without a clear favorite emerging, which was quite unexpected for an exceedingly used material after more than 25 years of application. Even within one working group, the acrylation was performed differently each year[41,86,87] and thereby raised strong doubts on the credibility of the protocols. In the following, the acrylation reaction was extensively investigated by means of 6k-PEG-diol and the resulting reaction conditions were meant to be subsequently transferred onto all available starting materials with different molecular weights and geometries. Contrary to the HA modifications, the degree of substitution of all PEG-modifications implies the percentage of modified end groups such as alcohols or amines.

Acrylation of alcohols generally can be achieved by several strategies, such as acid catalysis, alcoholysis of acryl electrophiles, nucleophilic substitution and chemical as well as enzymatic transesterification, each offering different advantages in terms of quantitative conversion, sensitivity, reaction duration, scalability and purification (Figure 27).

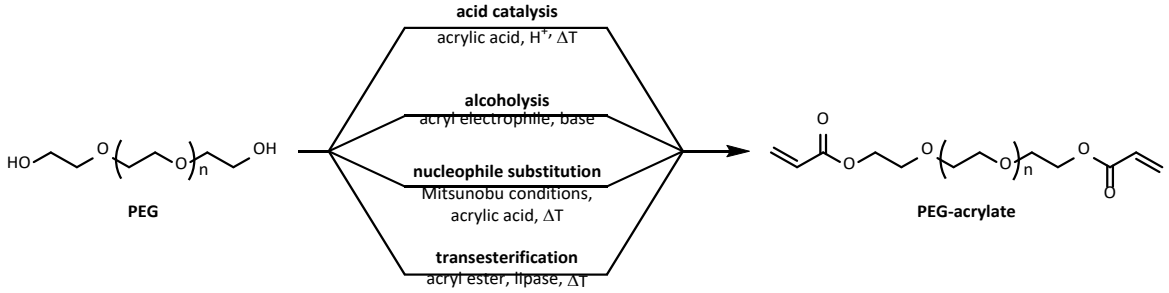

Figure 27: Schematic overview of possible synthesis routes for PEG-acrylate by means of linear PEG.

The acid catalysis provides the huge advantage of simplified purification due to the low number of reactants and can be upscaled without major limitations, in theory. The driving force of this reaction, next to strong inorganic catalytic acids, is dehydration and can be improved by either large excess of alcohol or water removal with molecular sieves or by distillation. In the case of PEG modification, the focus laid on the quantitative esterification of the alcohol (PEG) instead of the applied acid and since acrylic acid is prone to polymerize in acidic conditions at raised temperatures, only molecular sieves are suitable for shifting the chemical equilibrium towards the ester formation. The limitation in applicable temperature, was considered a major inhibiting factor causing either long reaction times or impediment of acrylation and hence, reactions via this strategy were not conducted in the first instance. Transesterification is based on identical reaction mechanism as acid catalysis with the difference of the generation of an alcohol, instead of water, that must be withdrawn from the equilibrium using the same methods as described above. Despite the fact, that alcohols such as MeOH or EtOH, formed during the reaction when using their respective acryl ester, have a lower boiling point (65 °C, 78 °C) than water and can thereby be removed easier from the reaction solution, their boiling points in combination with the required acidic conditions were still deemed an inhibiting factor and the strategy not pursued. Contrary, transformation of the alcohol via Mitsunobu conditions into an oxyphosphonium ion following nucleophilic substitution by acrylic acid has the advantage of very mild reaction conditions at rt and can be upscaled to the limit of laboratory glassware. The major disadvantages (2.2.4, p. 45) are the high sensitivity of the reaction towards residual water and oxygen,

the long reaction times and the lack of literature proving quantitative conversion paired with only minor possibilities for improvement. Alcoholysis of acrylic electrophiles, such as acryloyl chloride or acrylic anhydride, are performed under very mild reaction conditions below rt without any risk of polymerization and can be boosted by an excess of the electrophile. Similar to the Schotten-Baumann reaction of the HAPA synthesis (2.1.2, p. 27), the reaction of PEG-OH and acrylic electrophiles generates HCl or acrylic acid, depending on the applied electrophile, which necessitates the addition of non-nucleophilic auxiliary bases to maintain alkaline reaction conditions. In the end, the product must be separated from several reactants with different physical and chemicals properties that requires a multi-step purification.

Short production times, quantitative conversion and prevention of polymerization was the main objective for the provision of material supply for the SFB and accordingly alcoholysis of acryloyl chloride was tested first in 1.0 g scale according to Cruise *et al*.[87] with toluene as solvent instead of benzene and TEA as auxiliary base. The water of crystallization of the commercial PEG product was removed by azeotropic distillation with toluene and the reaction was carried out at rt after addition of the reactants. Despite the stated purification by filtration following repeated precipitation in cold diethyl ether (DE), ^{1}H NMR analysis showed remaining impurities in considerable amounts and dialysis against MilliQ was tested for purification but led to only minor changes in the resulting NMR spectra. Nevertheless, an NMR assay using TFAA for complete esterification showed a complete acrylation of PEG and a shift of the signals of impurities, reinforcing the suspicion that TEA salts of HCl or acrylic acid were not sufficiently removed by precipitation and neutral dialysis. Hence, the product was dialyzed once more against acidic media at pH 3, originating from the HASH synthesis yielding major reduction of impurities but not complete removal and additionally ended up in an 80 % loss of yield over both dialysis steps even though an MWCO of 1 kDa was used. To exclude the possibility of inseparable impurities deriving from already expired chemicals, the reaction was repeated with newly purchased chemicals and dry toluene but resulted in the identical purification challenge, which could be reproduced by mixing PEG with deliberately produced TEA salts in toluene. PEG-diacrylate extraction with DCM from aqueous solution pursuant to Elbert *et al*.[88] was tested incapable to remove the TEA salts regardless of any additive such as NaCl or $NaHCO_3$ or the applied pH of the aqueous layer. Additionally, the product generated a very stable emulsion and thereby prevented the separation of the different solvent layers. Since TEA salts were inseparable by all yet tested purification methods, dry pyridine was applied in the following and dry DCM was used as solvent to enable reaction at 0 °C as PEG precipitates in toluene nearly quantitative at this temperature. For this, the PEG was dried solvent-free under high vacuum at 110 °C until end of steam bubble formation. The scale was raised to 5.0 g and the final reaction solution was aliquoted for testing each of the above-mentioned purification methods. ^{1}H NMR analysis, likewise to the reaction with TEA, showed quantitative acrylation of PEG but also remaining auxiliary base salts independent of the purification method: precipitation, dialysis, extraction.

On the basis of experiences from earlier purification challenges of non-polymeric substances[89] and the observed differences in solubility of PEG in toluene and DCM, recrystallization of PEG-diacrylate in several low boiling organic solvents was investigated in a solubility screening. Consequently, the reaction was upscaled to 100 g using DCM and TEA at 0 °C, the resulting product solution was dried *in vacuo* to give an orangish solid which was aliquoted, dissolved at 40 °C in acetone, ACN, EtOAc, THF, toluene, MeOH, EtOH and *i*PrOH and cooled to 5 °C and -20 °C. The solubility was evaluated by means of PEG precipitate after centrifugation and the following solubility rows were obtained:

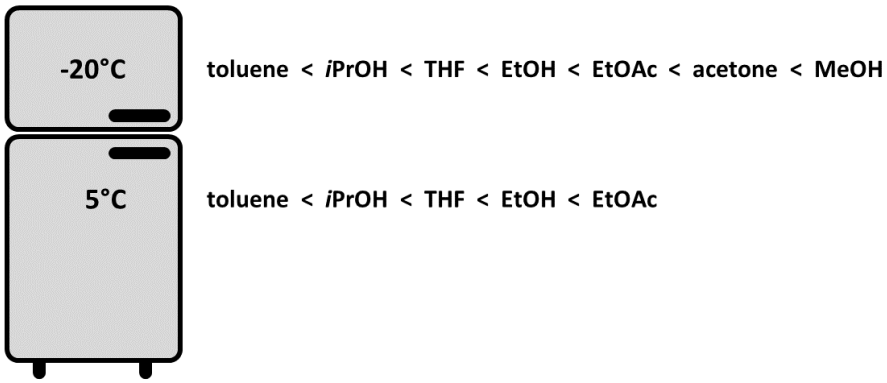

Figure 28: Solubility of 6k-PEG-diacrylate in different organic solvents at -20°C and 5°C measured by the quantity of obtained precipitate.

At 5 °C PEG-diacrylate only precipitated in the mentioned solvents whereas at -20 °C it precipitated in all solvents except ACN. Quantitative precipitation was observed at 5 °C until EtOH and at -20 °C until EtOAc. Since the solubility of the TEA salts is of the same importance as the one of PEG, the coloration of the supernatant was simultaneously monitored. The orangish color of these salts was pronounced more in the supernatant the more polar the solvent and the precipitate was colorized stronger the less polar the solvent. Based on this, two solvents were found to be suitable for recrystallization, EtOH and EtOAc, and EtOH was used in the following experiment due to its better availability in current laboratory stocks and quantitative precipitation at already 5 °C. The synthesis was replicated, the obtained product dissolved in 1.5 L EtOH in a 2 L Schott bottle at 40 °C and placed in the fridge overnight. The precipitate color was paler than the initial crude product and in contrast, the supernatant had a strong orange coloration, confirming the effect of the purification method. The process of dilution and precipitation required in total eight repetitions until almost complete discoloration of the product. An additional, nineth repetition led to no color change of the bulky precipitate with a slight tinge of remaining orangish color, indicating adsorption of impurities to PEG to a small extend which cannot be separated by the recrystallization process. However, only product signals were present in the ^{1}H NMR spectra and the product subsequently tested in first gelation experiments with HASH in direct comparison with PEG-diacrylate product from acidic aqueous dialysis.

For this, HASH (465 kDa, 60 %) and PEG-diacrylate solutions (1.5 %/2.0 %) were prepared using a self-made pH 7.6 154 mM phosphate buffer to maintain the required pH<7.0 for the Michael-addition. The solutions were then incubated at 37 C and tested every 10 min for their gelation status. After 50 min both mixtures resulted in hydrogel formation whereas the solution with recrystallized PEG-diacrylate already gelled after 10 min and yielded an extrudable hydrogel (400 µm, 0.25 “, steel) with high shape fidelity (see chapter 2.4, p. 63). In contrast, the dialyzed PEG product yielded a very weak extrudable hydrogel that deliquesced after placement on a flat surface. The impurities therefore clearly have a negative influence on the hydrogel formation, both the gelation rate and the final hydrogel properties, and must be separated from the product by all means. The observations of the manual gelation experiment were then proven by rheological measurements (time sweep), applying identical conditions (0.2 %, 10 rad/s, 37 °C) to the two precursor solutions (Figure 29). Impurities containing an acrylate moiety were thought to interfere during Michael-addition by consumption of free thiols without crosslinking the polymer strands and a series of combinations of the deployed reactants in DCM was conducted to identify the exact disruptive impurities. The dark-orange color was reproducible when mixing TEA with acryloyl chloride but not with acrylic acid or water-free HCl which only led to clear yellow coloration of the DCM solution and indicated a reaction of the tertiary amine with the acyl chloride. Mixing TEA with acrylic anhydride at 0 °C as well as raised temperatures did not yield the same dark-orange coloration and a reaction between them could be excluded. Instead, the

stabilizing agent of acryloyl chloride, phenothiazine, was shown to cause the respective coloration. When mixing TEA with acryloyl chloride, stabilized with 4-methoxyphenol (MEHQ) or a freshly distilled one, the DCM solution only turned slightly yellow whereas addition of phenothiazine powder resulted in orange coloration (Figure 30). Since acrylic acid and its anhydride are both stabilized with MEHQ, the orange coloration was absent and only the yellow coloration of organic TEA salts occurred, which were completely removable by recrystallization while the colored product of phenothiazine was not removed at all. Consequently, all following experiments were conducted using freshly distilled acryloyl chloride and the reaction conditions were transferred onto all other PEG raw materials to give a pool of crosslinkers for the extension of the bioink platform.

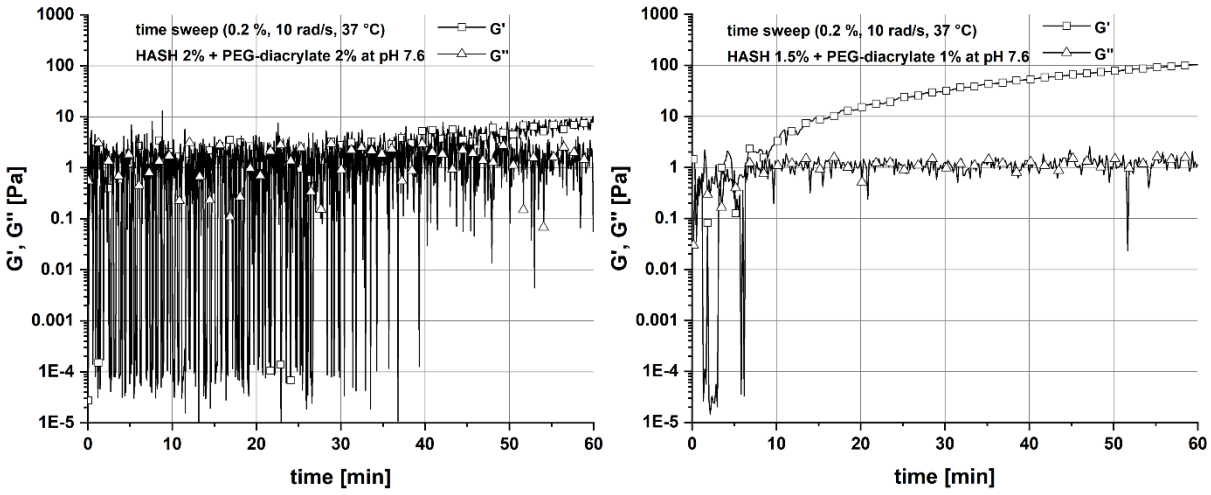

Figure 29: Time sweep of the gelation of HASH and PEG-diacrylate formulations with impure (left) and purified (right) 6k-PEG-diacrylate in PBS.

Figure 30: Photography of mixtures of different acryloyl chlorides and TEA in DCM at rt. Left to right: Commercial phenothiazine stabilized, distilled, distilled with added phenothiazine.

Simultaneously, the transesterification of vinyl methacrylate via an enzymatic pathway was investigated (2.2.2, p. 42) and the reaction conditions were directly transferred on linear 6k-PEG and 8arm-10k-PEG with the use of vinyl acrylate, a pricy chemical, to potentially enable a simplified production of clean PEG-acrylate. In a 1.0 g scale test reaction, the acrylation turned out to be straightforward according to the protocol and PEG was converted quantitatively. On top, purification by precipitation in diethyl ether (DE) and washing of the white bulky sediment with DE yielded in both cases clean products (Figure 31) and seemed a promising alternative for PEG-acrylate synthesis. A subsequent upscaling of the reaction with linear 6k-PEG to 25 g resulted in a very clean product with only 55 % acrylation regardless of the excess of vinyl acrylate, whereas upscaling to 5.0 g in the case of 8arm-10k-PEG led to a suitable acryl content of 95 % and was sent to the respective cooperators (Prof. Blunk) for their experiments on the TGF-β incorporation into hydrogels and bioinks and consequently, no other multi-arm PEGs were acrylated. Identically to the enzymatic methacrylation of

linear PEGs with longer chain lengths (10 kDa and 20 kDa), complete enzymatic acrylation was not possible for neither of these independent of the applied amount of acryl donor. Since the possible parameters of the synthesis had already been depleted without providing a suitable result for linear PEGs this synthesis route was not pursued further for starting materials of linear nature.

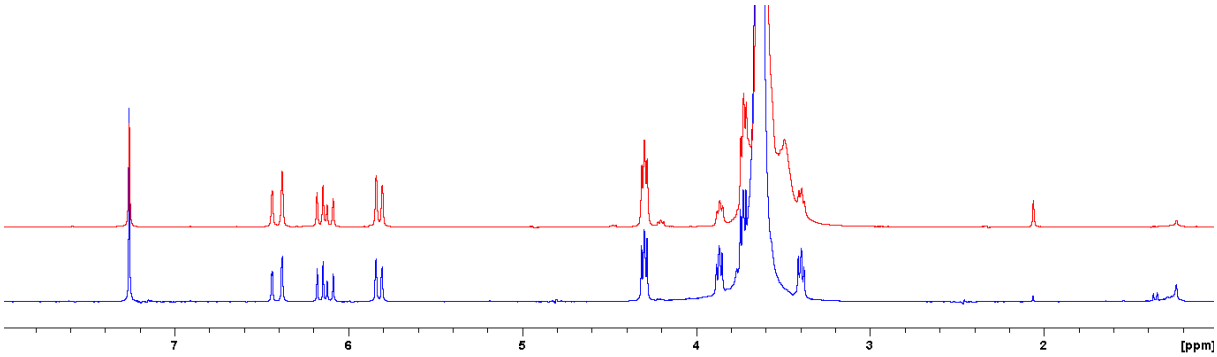

Figure 31: ^{1}H NMR overlay plot of PEG-acrylates produced by enzymatic transesterification. Top to bottom: 8arm-10kDa-PEG-acrylate, 6k-PEG-diacrylate in $CDCl_3$.

Refocusing on the synthesis route using acryloyl chloride, the reaction conditions were applied to linear 10k- and 20k-PEG in toluene as it is used for azeotropic water removal and freshly distilled acryloyl chloride and TEA were added. After the reaction at rt, the products were precipitated by cooling of the product solutions and addition of cold DE and the resultant sediments recrystallized in EtOH until discoloration of both, PEG products and supernatants. Compared to linear 6k-PEG, the solubility of the 10k and 20k variant in toluene and EtOH was significantly lower and the process had to be adapted by increased reaction solvent usage in both cases and downscaling of the synthesis from 100 g to 50 g in the case of the 20k variant. Characterization of the pure products revealed 100 % acryl content for 10k-PEG-diacrylate and approx. 95 % DS for 20k-PEG-diacrylate, which was considered suitable for hydrogel and bioink development. With increasing chain length, the NMR signals were less distinct due to the lower number of functional groups per milligram product and the concentration had to be increased for NMR spectroscopy from initially 20 mg (6 kDa) to 30 mg (10 kDa) and 40 mg (20 kDa), which in turn gradually caused peak broadening and complicated the analysis. SEC MALS measurements of the products showed in all cases a high molecular weight shoulder due to partial polymerization (Figure 32), even though the reactions were all conducted in absence of light, whereas the dissolution process during recrystallization was partially performed at day light. The combination of heat, removal of all stabilizers and presence of UV light therefore was regarded as the only potential reason for the slight polymerization.

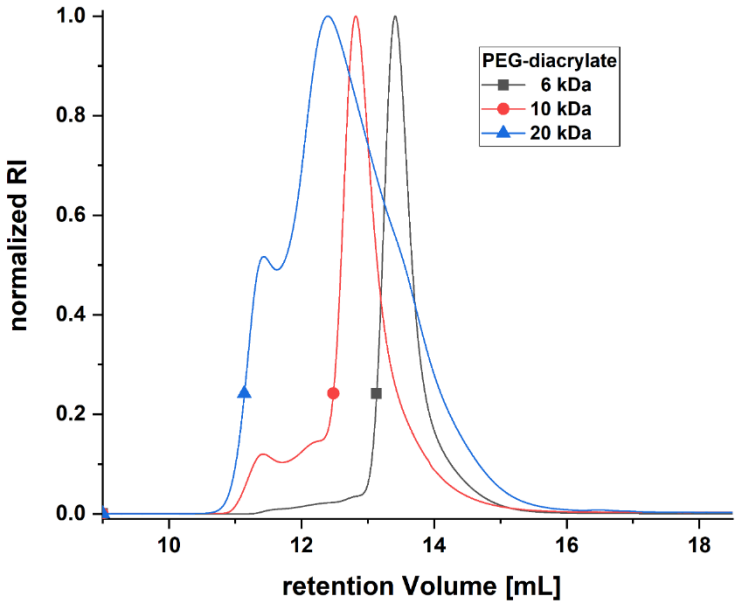

Figure 32: SEC MALS overlay plot of all linear PEG-diacrylates after recrystallization in EtOH.

As complete light exclusion during recrystallization is not feasible, adsorption of the impurities onto polystyrene resins was tested as heat-free alternative in analogy to former studies on the hydrophobic product extraction from aqueous solutions[90]. The adsorption to the macroporous resin is based on π-π and van der Waals interactions between the adsorbate and the highly hydrophobic polystyrene surface while both interactions are stronger the more hydrophobic and π-electron-poor the adsorbate is. TEA hydrochloride, from reactions using TEA and acryloyl chloride, represents a hydrophobic but not aromatic adsorbate and only weakly interacts with the resin. Hence, the reaction was adapted by the utilization of pyridine and acrylic anhydride to generate not only an aromatic, electron-deficient organic salt but also the more hydrophobic pyridinium acrylate variant compared to pyridinium chloride formed when applying acryloyl chloride instead of the anhydride. Two resins were purchased, composed of polydivinylbenzene (PAD600) and divinylbenzene crosslinked polystyrene (MN202) and were tested in direct comparison with a natural adsorbent, activated charcoal. Accordingly, linear 6k-PEG was acrylated in a 50 g scale using pyridine and acrylic anhydride in DCM and after the reaction overnight at rt the solvent was evaporated. The obtained crude product was redissolved in water, remaining volatile residues were removed *in vacuo* over 30 min and the product solution was aliquoted in three portions, one per adsorbent. After addition of adsorbents and incubation overnight at rt in complete darkness, the solutions were filtered, freeze dried and the purity of the product was analyzed by ^{1}H NMR. Unfortunately, both resins not only adsorbed all reactants but also the PEG-diacrylate in nearly quantitative manner, which was thought to be caused by the nature of acrylated PEG to act as a detergent, settling at the interface of aqueous solution and hydrophobic resin surface. Contrary to this and highly unexpected, activated charcoal adsorbed most of the reactants while not retaining the acrylated PEG and yielded a clean product after a repetition of the adsorption step following filtration of the solution (Figure 33). With this, polystyrene resins were proven unsuitable for the purification of PEG whereas activated charcoal was found to be a promising heat-free alternative purification method to the recrystallization in organic solvents.

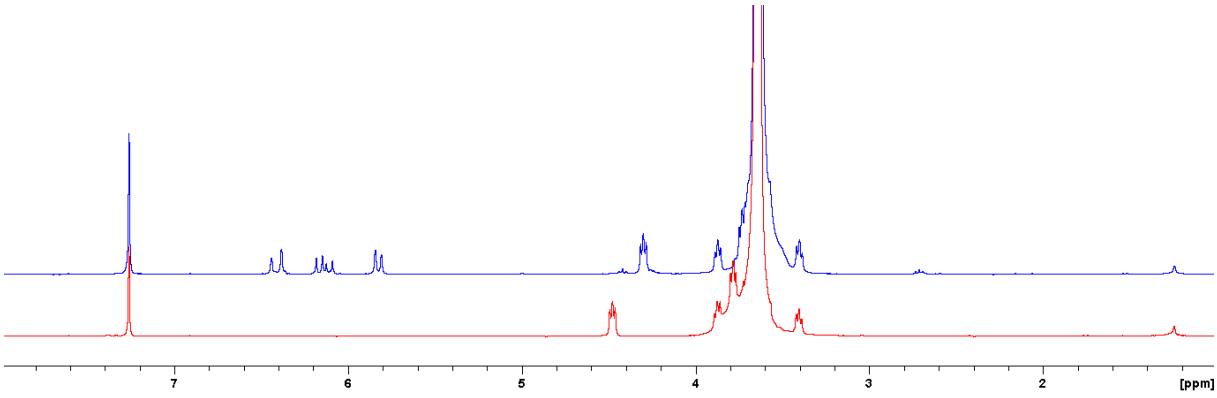

Figure 33: ^{1}H NMR overlay plot of 6k-PEG-diacrylate (top) purified by activated charcoal and 6k-PEG-TFA diester (bottom) as reference in $CDCl_3$.

At the same time, other synthesis routes were tested concurrently for their applicability with the aim to select the most reliable one with regards to simpler purification and prevention of polymerization. According to the PEG-amine synthesis via the Mitsunobu route (2.2.4, p. 45), the reaction conditions were adapted to generate PEG-acrylate by using acrylic acid as nucleophile. Acid catalysis in heated ACN using only acrylic acid was also conducted next to acrylation via Schotten-Baumann reaction conditions using acrylic anhydride and aqueous NaOH identical to the HAA synthesis (2.1.3, p. 31). ^{1}H NMR analysis revealed only minor acryl contents <30 % for all the products obtained by these syntheses and was in all cases unexpected low. While the Mitsunobu route led to an acryl content of 30 %, the Schotten-Baumann reaction did only produce PEG-acrylate with a DS of 15 %. In the well-known case of the Mitsunobu reaction the applied nucleophile is more reactive the higher its nucleophilicity and if carboxylic acids are used, the higher the basicity of the respective carboxylate. Despite a lower pk_a of acrylic acid (4.3)[91] than acetic acid (4.75), the observations indicate less nucleophilicity of its carboxylate than initially anticipated and raised doubts about the possibility of quantitative conversion. In addition, acrylation by acid catalysis was surprisingly fully absent after 3 d at 70 °C.

Together with the observations during the Mitsunobu reaction, the assumption that acrylic acid is not behaving like a common carboxylic acid was further manifested. Due to this, a reaction based on Brandl *et al.*[92] with modifications was performed using 2-carboxyethyl acrylate and DCC in DCM to generate the respective anhydride, which was then conjugated to linear 6k-PEG. Identical to the protocol, DIPEA was used as auxiliary base and after stirring 3 h at rt, the obtained product was precipitated and washed with DE. The resultant DS was far too low (30 %) for application and a follow-up experiment with the use of DMAP in equimolar amount was performed whereas the reaction time stirred overnight and purification by activated charcoal was tested. The deployment of the Steglich catalyst and the extended reaction times led to an increased but still insufficient acryl content of 90 % while even more impurities remained after purification compared to the use of DIPEA and DE washing. An increase of the reaction temperature to 50 °C by the use of ACN instead of DCM, resulted in a lower DS of 20 %. Contrary to 6k-PEG-OH, the reaction of 6k-PEG-diamine with DCC, CEA and DIPEA yielded quantitative acrylation of the polymer showing the large difference in reactivity between PEG-OH and PEG-amine.

2.2.2 PEG-methacrylates

The synthesis of PEG-methacrylates was deemed a pragmatic, while not perfectly fitting, alternative to PEG-acrylates due to the urge for material and the, at this time point, progressing purification challenges of acrylated PEGs. The reactivity of methacrylates towards Michael-addition with HASH at pH 7.6 of the aimed bioink is considerably lower than the one of acrylates[23] due to the additional α-methyl group with +I-effect, reducing the electron deficiency of the β-carbon, the terminal $=CH_2$ group. Therefore, the pre-crosslinking of the bioink with PEG-methacrylates may be retarded for several minutes and not applicable for the final bioink but would render possible first gelation experiments and printing trials for the bioink development. The methacrylation can be performed via two strategies, chemical reaction with methacryloyl chloride / methacrylic anhydride or enzymatic transfer on PEG-OH from an methacryl donor. Chemical methacrylation would require identical reaction conditions that caused the current purification difficulty of PEG-acrylates and was omitted whereas the enzymatic synthesis route would only require the separation of the polymeric product from the methacryl donor and the respective leaving alcohol, both highly soluble in DE. Regarding this, the enzymatic pathway was chosen and first trials were conducted on the basis of a modified protocol from Warwel *et al*.[90,93] with the use of linear 6k-PEG (1 g), immobilized lipase from *candida antarctica* (Novozyme 435), vinyl methacrylate as methacryl donor and toluene as solvent (Figure 34).

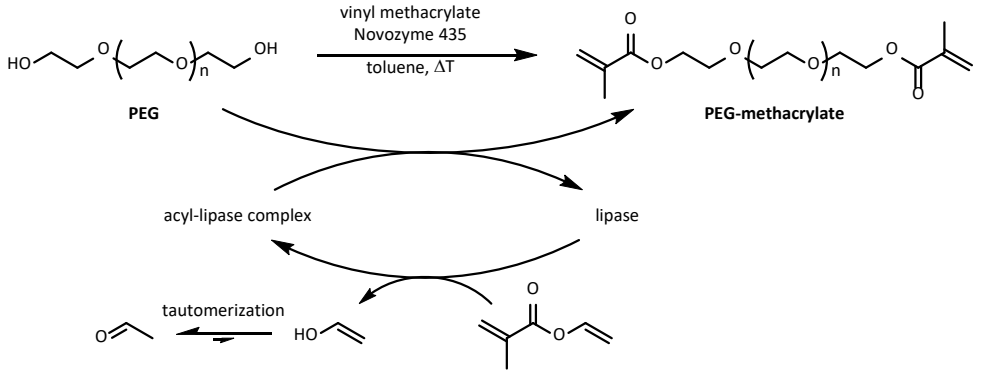

Figure 34: Reaction scheme and schematic reaction mechanism of the enzymatic PEG-methacrylate synthesis by means of linear PEG.

The advantage of vinyl methacrylate over other methacryl esters deriving from alkyl alcohols (MeOH, EtOH…) is the direct tautomerization of the vinyl alcohol leaving group into acetaldehyde and thus shifting the chemical equilibrium towards the methacrylate product. After 48 h of incubation at 37 °C, the crude product was obtained by precipitation and washing with DE yielding quantitative methacrylation, confirmed by the TFAA ^{1}H NMR assay. Several impurities were detected originating from toluene soluble constituents of the used Falcon Tube plastics and the reaction was subsequently repeated in a borosilicate Schott bottle leading to pure product with DS 100 %. The reaction conditions were then transferred on all in-house available linear (1.5, 10 , 20 kDa) and branched PEGs (4-arm 5 kDa, 4-arm 10 kDa, 8-arm 10 kDa) to generate a pool of crosslinkers for gelation experiments. Quantitative conversion was obtained only for linear 1.5k-PEG and the DS decreased with increasing chain length of the linear PEGs to 50 % for 20k-PEG, respectively 65 % for 10k-PEG, both inapplicable for gelation experiments, whereas for the branched starting materials, the methacryl content increased with decreasing individual PEG chain length and the reaction yielded products with 85, 90 and 95 % methacryl content for 4-arm 10kDa, 8-arm 10kDa and 4-arm 5kDa. A DS >50 % for 4-arm PEGs and >25 % for 8-arm PEGs are theoretically sufficient for crosslinking as in average two methacrylates per crosslinker molecule are present but is considered a concern due to possible existence of non- and mono-methacrylated PEGs, each incapable to crosslink. To ensure sufficient

reactive groups for proper gelation, DS values above 75 % for all branched PEGs and >95 % for linear PEGs were intended. Batches with insufficient methacryl content were discarded.

Increasing the equivalents of methacryl donor from 3.0 to 5.0 in reactions with linear 10k-PEG and 20k-PEG only led to slight increase of the methacryl content instead of the desired quantitative conversion and further attempts were omitted. Simultaneously, upscaling of the process by means of linear 6k-PEG in a 25 g scale under identical conditions as the test reaction but with prolonged reaction time (72 h) yielded only methacryl contents of 55 % and increased methacryl donor amount of 5.0 eq. was applied. Similar to the methacrylation attempts of longer PEG molecules, this increase only resulted in an insignificant higher DS value of 65 %. Since all PEGs were dried in HV at 110 °C and dry solvent as well as augmented amount of enzyme was deployed, consumption of the methacryl donor by water residues and enzymatic fatigue can be excluded. Due to this, no further attempts were conducted to quantitatively methacrylate linear PEGs and the findings were used for enzymatic acrylation of 8arm-10k-PEG (2.2.1, p. 35) for the immobilization of growth factors (TGF-β) in the bioink.

2.2.3 PEG-allyl carbonates

PEG-allyl carbonates rank among the unsatured, asymmetric carbonates and are unique within the class of organic carbonates due to the polymeric substituent[94]. Organic carbonates can be prepared by various methods including phosgenation, (trans-) metal catalysis, carbonate interchange and activated formates. In both, phosgenation and carbonate interchange reactions, a carbonyl (+IV) compound reacts with alcohol solvent, while metal catalysts convert carbonyl (+III) and (+IV) compounds and alcohols to organic carbonates. All of these methods use an excess of alcohols, mostly applied as solvents, and produce nearly exclusively symmetric carbonates. Although a production of asymmetric carbonates via these reactions is surely possible when applying two different alcohols, the resulting mixture of symmetric and asymmetric carbonates must be separated. A transfer to PEG-OH, a bivalent alcohol, would imply a separation of the desired PEG-allyl carbonate from diallyl carbonate and multi-PEG carbonates and is inapplicable for the required large-scale production.

Solely, conversions of actived allyl formates lead to exclusively asymmetric organic carbonates whereas different reactants are currently commercially available: allyl chloroformate, allyl NHS carbonate, allyl HOBt carbonate, allyl HOAt carbonate and diallyl pyrocarbonate. No literature exists yet for the synthesis of polymeric allyl carbonates with either of these reactants and the synthesis had to be investigated extensively from scratch. While a reaction of PEG-OH with activated carbonates, based on *N*-hydroxy auxiliaries, was deemed to be unsuitable in view of the stability of these active esters towards alcoholysis[95] and their high costs, diallyl pyrocarbonate is hardly used in literature and not applicable for a reaction with alcohols due to the generation of a competing alcohol, allyl alcohol, during the reaction.

According to protection group chemistry[96-98], an approach was pursued to transfer the alloc protecting group from amines to PEG-OH using allyl chloroformate by adjustments of the reaction conditions. The reaction of allyl chloroformate with the alcohol produces HCl, which must be captured by means of an auxiliary base to maintain basic reaction conditions, while the alcohol can be deprotonated before or after the nucleophilic attack (Figure 35).

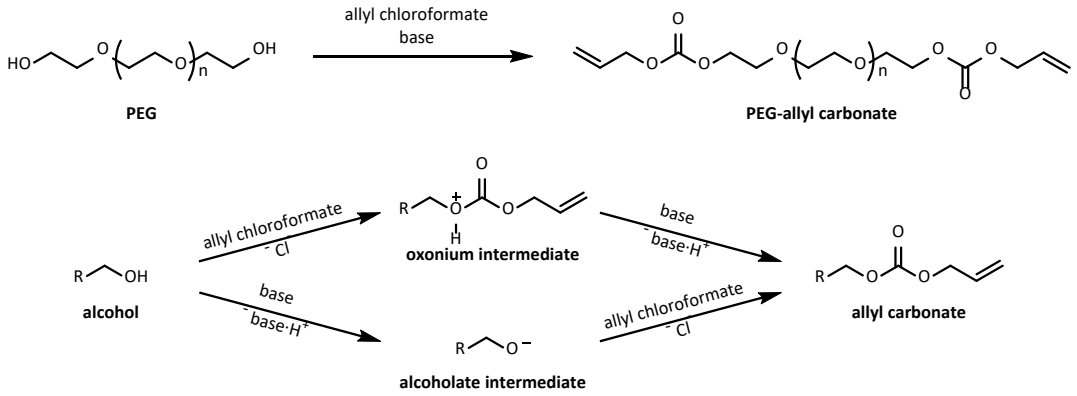

Figure 35: Reaction scheme of the PEG-allyl carbonate synthesis by means of linear PEG (top) and schematic reaction mechanism of the alcoholysis of allyl chloroformate (bottom).

For deprotonation before the nucleophilic attack, only a few non-nucleophilic bases have a sufficiently high pk_a value for primary alcohols (>16), such as KHMDS (potassium bis(trimethylsilyl)amide, 26), LDA (lithium diisopropylamide, 36) or metal hydrides. However, the latter react with the chloroformate, requiring the synthesis to be divided into two steps, deprotonation with subsequent isolation of the metal PEG-alcoholate and substitution. Even though the generated metal alcoholates would react with the chloroformate regardless of the underlying mechanism, the great disadvantage of these strongly basic metal salts is their sensitivity to water, which occurs in considerable amounts as water of crystallization of crystallization in commercially available PEGs and requires preliminary quantitative drying of the reactant. Even slight residues of water can impede complete conversion into PEG-allyl. In the presence of water molecules metal hydroxides will be formed, that yield in chloroformate decomposition into metal chloride, carbon dioxide and allyl alcohol, creating an alcoholate equilibrium between PEG-OH and allyl alcohol. In the following, diallyl carbonate and re-protonated PEG-OH will be formed consuming the deployed base and chloroformate. Competing this side reaction by sheer excess of reactants, chloroformate and metal base, would complicate the purification process and excludes the use of metal hydrides. In contrast, much weaker bases (pk_a >9) e.g., TEA, DIPEA, DBU, which are not water-sensitive, are sufficient for the deprotonation of the oxonium ion, an intermediate by nucleophilic attack of the alcohol on the chloroformate without prior deprotonation. Due to the potential difficulties of metal base reactions, the first PEG-allyl carbonate synthesis attempts were made using non-nucleophilic tertiary amine bases and allyl chloroformate as reactants.

As a starting point, TEA was tested as auxiliary base and toluene was used as solvent to remove the water of crystallization by azeotropic distillation and the reaction subsequently was conducted in an ice bath. However, the reaction had to be carried out at room temperature due to the crystallization of linear 6k-PEG in toluene at 0 °C. The resulting degree of substitution was, though, only very low (<10 %) in several experiments and the product thus unsuitable for applications. Increasing the reaction temperature to 60 °C remained unsuccessful and extreme bubble formation was observed, indicating thermal decomposition of chloroformate, which was confirmed by injection of alloc-chloride into dry toluene at 60 °C. To realize a reaction at 0 °C, dry DCM was used as solvent in the following and PEG was dried solvent-free under high vacuum at 110 °C. Due to lack of synthesis success with the use of TEA, a screening with different auxiliary bases was carried out in which, in addition to non-nucleophilic tertiary amines (TEA, DIPEA, DBU), catalytically acting amine bases (pyridine, DMAP) were tested. Analogous to the reaction with TEA, the use of DIPEA was ineffective while the use of pyridine with a resulting DS of 90 % represented an enormous progress. A quantitative conversion was ultimately obtained by deployment of DMAP and DBU (Figure 36), although purification proved difficult as isolation of pure product was only possible by dialysis against acidic aqueous media, regardless of the auxiliary bases, since neither precipitation nor dialysis against MilliQ could remove

the amine salts quantitatively. Unfortunately, dialysis resulted in a partial reduction of the DS by roughly 20 %. Due to thermal decomposition of the reactant, recrystallization in ethanol was considered a concern as temperatures above 50 °C are imperative and the product was found to be moderately stable in acidic aqueous media. Consequently, since the product could not be isolated via any purification procedure with guaranteed constant DS, no follow-up experiments or upscaling were pursued and synthesis of the surely stable PEG-allyl carbamate via PEG-amine was aimed at.

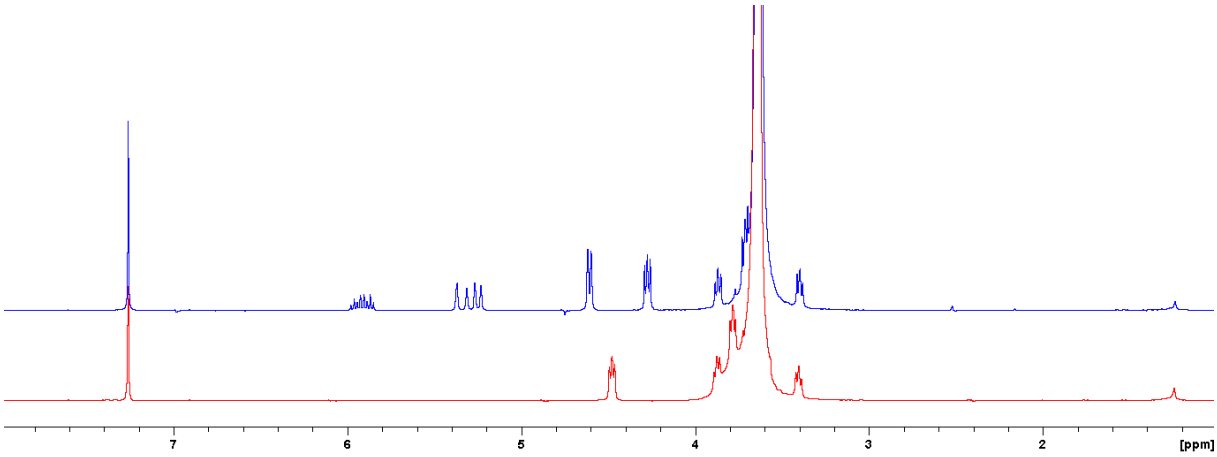

Figure 36: ^{1}H NMR overlay of 6k-PEG-diallyl carbonate (top) and 6k-PEG-TFA diester (bottom) in $CDCl_3$.

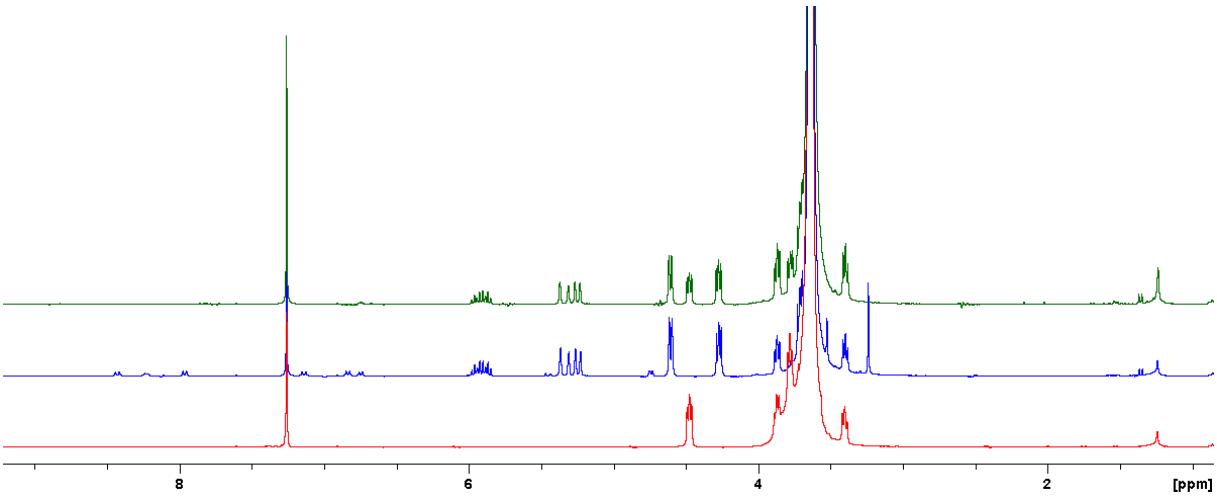

Figure 37: ^{1}H NMR overlay of 6k-PEG-diallyl carbonate after dialysis (top), before dialysis (middle) and 6k-PEG-TFA diester (bottom) in $CDCl_3$.

2.2.4 PEG-amines

The synthesis of PEG-amine was of great importance and the demand for large quantities was very high as it represents a precursor for PEG-allyl carbamate and peptide-modified PEG-crosslinkers, carrying acryl and allyl end groups. The overall aim was the establishment of a highly reproducible synthesis procedure leading to complete conversion to PEG-amine based on readily available linear geometry and subsequently transfer the reaction conditions to starting materials with different geometries and molecular weights depending on the demand. The desired amino group can generally be introduced by two strategies, addition of amine carrying moieties, strategy 1, or substitution of the alcohol, strategy 2, offering together an immense variety of possible reactions whereat all of them comprise multi-step procedures (Figure 38). The introduction of amine carrying functionalities can be achieved by two types of reactions that are composed of either addition of *N*-protected electrophiles

that generate esters or ethers and final removal of the protection group (e.g., *N*-boc-glycine anhydride, *N*-boc-chloroethyl carbamate) or addition of C=C double bonds and thiol-ene reaction with mercapto amines (e.g., allyl bromide + cysteamine)[99] while substitution of a leaving group (sulfonates, oxyphosphonium ions), preliminary produced by conversion of the alcohol, with nitrogen-based nucleophiles (ammonia, azide, phthalimide) does not increase the molecular weight of the polymer or introduce additional functionalities, possibly changing its properties. As the maintenance of the polymer size and properties was considered to be more advantageous, strategy 2 was chosen to synthesize PEG-amines and a more detailed selection process, sorting according to quantitative conversion and potential problems like side reactions and complex purifications, was necessitated due to the sheer number of possible reactions. Within this strategy, the most abundant leaving groups are mesylates and tosylates, both sulfonates, and oxyphosphonium ions deriving from the reaction of alcohols with triphenylphosphine and azodicarboxylates, named Mitsunobu reaction[100,101]. The mesylate and tosylate are hardly different in their reactivity towards alcohols, their quality as leaving groups and solubility in organic and aqueous media and therefore no preference for one of them exists in current literatures. From a spectroscopic analysis point of view the tosylate's aromatic structure is beneficial in methods using UV-Detection, as well as for NMR or TLC, while the mesyl-chloride with an average of 7.6 €/mol is nearly twice as cost-efficient as the tosyl-chloride, a by-product of the Remsen-Fahlberg process for saccharin production. Both sulfonates can be substituted by nitrogen-based nucleophiles that are subsequently converted into amines in quantitative yields. For example, sodium azide[102] can be used and reduced in a Staudinger reaction by addition of triphenylphosphine[103,104]. An alternative is phthalimide and its salts[105], often used in Gabriel reactions, requiring higher temperatures for quantitative substitution and hydrazinolysis[106], and is often inapplicable due to its harsh reaction conditions[107]. Using the same nucleophiles and work-up processes, the Mitsunobu reaction differs solely in the generation of an alternative leaving group, the oxyphosphonium ion and thus offers no advantage compared to the sulfonate route. Substitution with ammonium hydroxide is also often employed and represents an additional alternative for the sulfonate route[108]. The absence of a clear favorite in literatures and the timely high material demand of cooperative SFB projects led to the simultaneous conduct of two reactions, the mesyl route using ammonia as nucleophile[109] and the Mitsunobu variant with phthalimide and hydrazine[42] to identify the most suitable method.

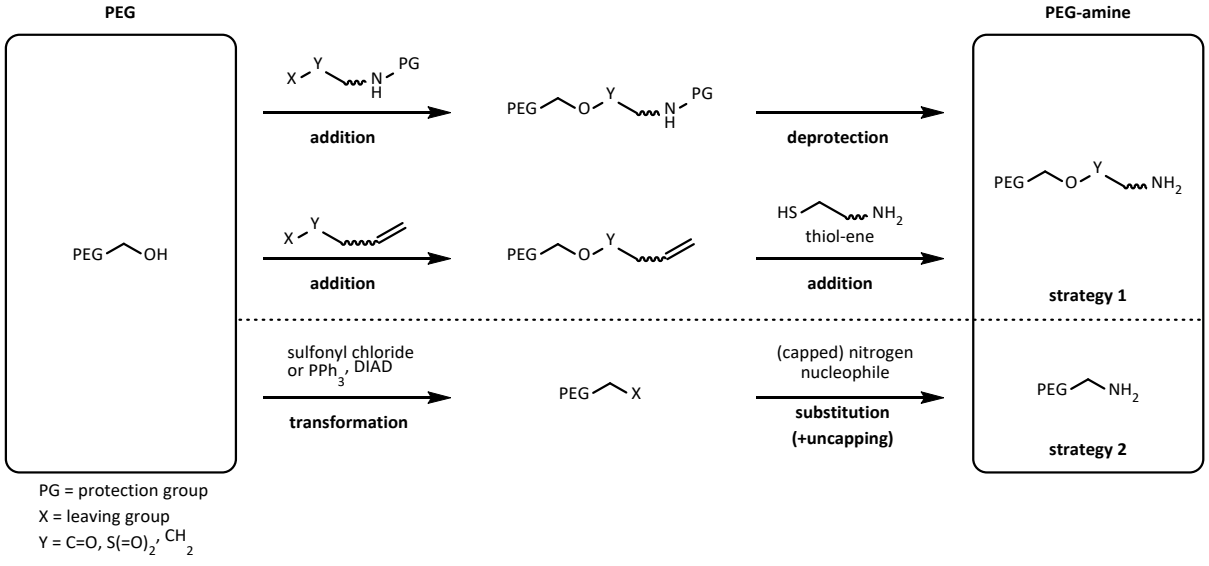

Figure 38: Schematic strategy overview for the PEG-amine synthesis.

Regarding the application of Mitsunobu conditions, the procedure described by Mongondry *et al*.[42] and Brandl *et al*.[110] were initially transferred onto linear 6k-PEG-OH, keeping the reactant excess at

1.5 equivalents with regards to the functional groups. The only exception was the use of dry THF and air-free technique to prevent inhibition of the reaction by residues of water or air in the reaction solution. Since no coloration was mentioned, the reaction progress lacked a visual control and yielded in a clear, brown solution from which a white solid was obtained after the described purification procedure and freeze drying. ^{1}H NMR analysis showed a small but broad peak at 7.8-8.2 ppm in the range of aromatic proton signals and compared with an additional measurement after dialysis of the product as proof of PEG-bound phthalimide, while the addition of TFAA revealed incomplete conversion with a DS of <50%. The water of crystallization of the employed PEG-OH was considered a possible inhibitor of the conversion and a follow-up experiment under air-free conditions with dried PEG-OH, dry THF, a guard funnel filled with anhydrous $CaCl_2$ and a reduced reactant excess of 1.2 was performed yielding in a different colored solution as in the previous experiment, namely yellow greenish. The quantitative transformation, shown by NMR using the TFAA assay, confirmed this hypothesis. Hydrazinolysis of the intermediate product was found to be straightforward yielding in the desired PEG-amine. From the start of synthesis to the final PEG-amine, this route takes about 8-10 days, composed of 2 d substitution, 1 d PEG-phthalimide purification, 3-5 d freeze drying, 2 d hydrazinolysis and product isolation. Several shortcuts were deemed to reduce the production duration but have not been investigated such as minimizing the reaction time of substitution and hydrazinolysis to the least necessary duration, testing the water tolerance of hydrazinolysis in order to possibly skip freeze drying or performing this reaction in aqueous media with alternative nucleophiles like metal hydroxides. A transfer of the reaction conditions on linear PEG-OH with 10 kDa and 20 kDa was successful but was accompanied by a required downscaling of the synthesis since PEG's solubility in THF decreases strongly with increasing molecular weight and dissolution after the drying process took 10 h at elevated temperature in the case of the 20 kDa material presenting the near limit of solubility with approx. 0.05 g/mL compared to 6k-PEG with approx. 0.4 g/mL. The production of PEG-amine is limited by PEG's solubility in THF, the freeze dryer capacity and ultimately by the necessity of air-free technique and thus laboratory glass ware with NS joints. Though, productions in 50-100 g scales were achieved for all linear starting materials. Other PEG geometries were not used as no demand for branched PEG-amine existed by then.

The mesylate route first mentioned by Yoshimoto *et al*.[108] and later described by Iijima *et al*.[109] was applied to previously dried linear 6k-PEG-OH analogously to the Mitsunobu conditions. The synthesis consisted of two steps, mesylation in THF using mesyl chloride and TEA as auxiliary base following a substitution in aqueous ammonium hydroxide (30 %). Despite the very brief description of the reaction procedure the individual steps were quite feasible and led to near quantitative conversion into PEG-amine with the drawback of partial hydrolysis of the mesylates caused by the alkaline aqueous media and of huge impurities in the intermediate and final product due to the large excess of reactants during mesylation. Purification of the product by precipitation in diethyl ether was not successful and dialysis (MWCO 1 kDa) against acidic aqueous media was tested suitable but also led to major yield loss since PEG, a highly flexible polymer on a molecular level, can easily diffuse through the membrane. Because of these challenges, crucial reaction parameters and several procedural modifications were investigated to optimize the yield and product quality.

First, the solvent was changed to DCM for better dissolution of PEGs with higher molecular weight and the equivalent excess of the reactants were reduced, namely mesyl chloride 3.0 (6.0) and TEA 3.0 (10.0). A decrease of the reaction temperature from rt to 0 °C was found beneficial for preventing reactant quenching by residual water and resulted in a highly reproducible and quantitative conversion into PEG-mesylate while washing of the crude product solution at the end of the synthesis by dilute HCl, MilliQ and brine removed all impurities, and the product could be isolated via precipitation in DE. Trials to shorten the production time by skipping the purification and isolation processes after mesylation were successful underlining the vast tolerance of the substitution reaction. As dialysis led

to a huge loss in yield, alternative purification methods were of great interest and according to the Mitsunobu route, extraction with DCM at pH 9-10 was tested. An extraction without prior removal of ammonia, remaining in the aqueous layer, caused poor long-term layer separation in every iteration which was also found when the pH was below 9 or above 11. Even though the pk_a of PEG-amine is unknown, it can be estimated quite precisely with the help of ethanolamine (9.50)[111] which represents a fictive PEG-monoamine with only one repetition unit and explains the above mentioned issue as at the borders of this pk_a range, the polymer remains charged and therefore features worse partition coefficients. Quantitative removal of ammonia was realized over 48 h by evaporation in the fume hood using a crystallization dish and maintaining the pH >10 with 2 N NaOH, crucial to counter the formation of ammonium carbonate. The nucleophile competition between ammonia and hydroxide during the substitution reaction was subject of another investigation as the conversion of PEG-mesylate varied from 95 to 100 % (Figure 39). To understand the correlation between reaction temperature and resultant amine content a temperature screening was conducted to determine the conditions with the least hydrolysis, revealing an optimum at rt with 95-100 % amines while cooling (-20 °C) and boiling (+40 °C) promoted hydrolysis gradually. Regarding the percentage of amination within the temperature range, this finding indicates different reactivity-temperature profiles for the two nucleophiles since identical trends would have led to always the same amine content and commonly reactivities don't decrease with increasing temperature. At -20 °C an amine content of 30 % was obtained meaning that the reactivity of ammonia was lower than that of hydroxide anions but equals at 5 °C with resulting 50 % amines. At rt a near quantitative conversion indicates a huge gap in reactivity which declined until 40 °C yielding in 85 % amines. Analysis of the products via SEC MALS revealed slight peak broadening towards higher molecular weights caused by the substitution of PEG-mesylates by already formed PEG-amine and thus creating PEG-oligomers with increased molecular weights (Figure 40). Unfortunately, the probability of this reaction can only be minimized by increasing the excess of ammonium hydroxide but not prevented completely which represents a great disadvantage compared to the employment of blocked nitrogen-based nucleophiles as in the Mitsunobu reaction. The shift of the product peaks in the elugrams compared to the starting material were reproducible for all PEG-diamine batches and can be attributed to analyst-column interactions due to its occurrence in the ionic state during the elution in aqueous media.

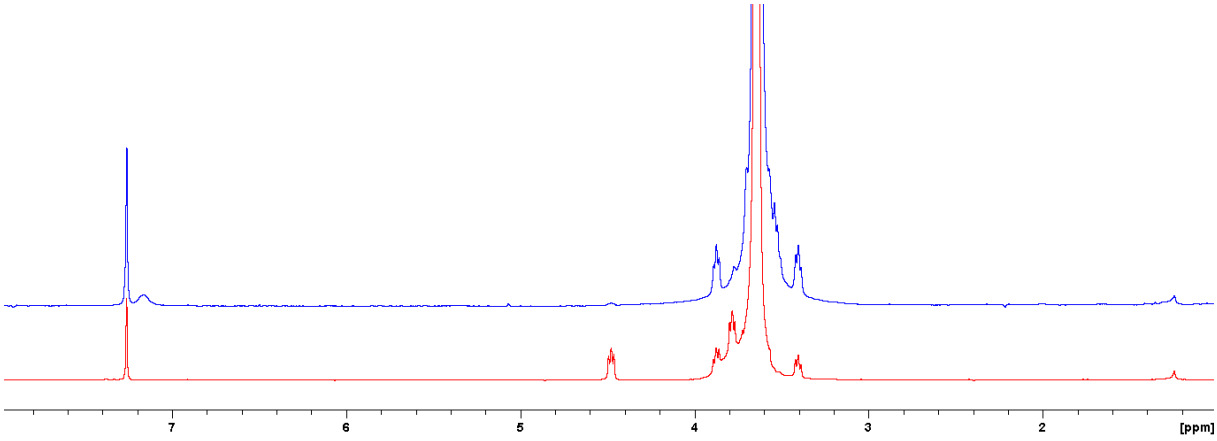

Figure 39: ^{1}H NMR overlay of 6k-PEG-TFA diamide (top) and 6k-PEG-TFA diester (bottom) in $CDCl_3$.

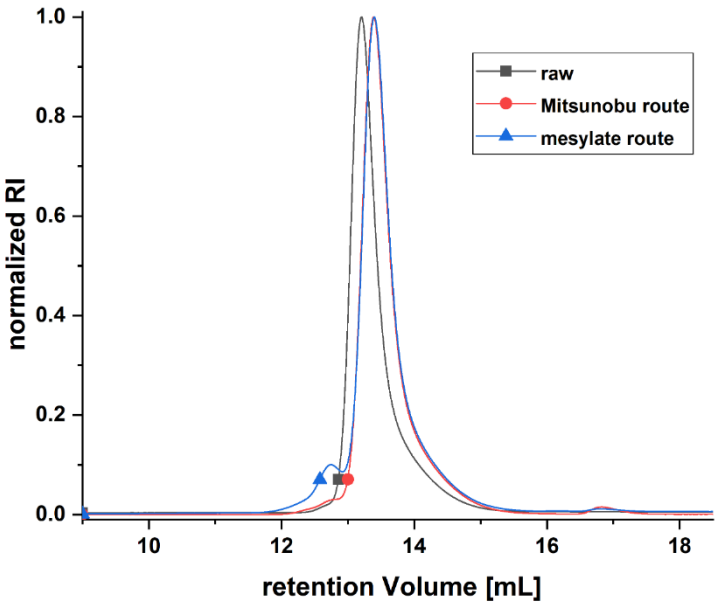

Figure 40: SEC MALS overlay plot of 6k-PEG-diamine, synthesized via Mitsunobu and mesylate route.

In summary, the most beneficial reaction conditions are for step 1, mesylation, reduced reactants (3.0 eq.) in DCM at 0 °C, conversion of the crude product in ammonium hydroxide at rt and product extraction with DCM at pH 9-10. In the following, these conditions were successfully transferred on other PEG starting materials with different geometries (4- / 8-armed) and molecular weights (5 / 10 kDa) with the disbenefit that branched PEGs have worse partition coefficients causing long-term layer separation and subsequent loss in yield. With regards to the conversion into PEG-amine, no significant difference exists between the two synthesis routes, yielding both amine contents of >95 %, whereas only the Mitsunobu reaction does not affect the molecular weight of the product and consequently was favored over the mesylate route despite the adverse production time and volume.

2.2.5 PEG-allyl carbamates

PEG-allyl carbamate represents, regarding its chemical structure, nothing less than a *N*-alloc protected terminal amino group and the synthesis was designed accordingly. Based on the literature of PEG-allyl carbonate synthesis (2.2.3, p. 43), the introduction of the allyl carbamate was attempted using allyl chloroformate and TEA in comparison with pyridine as auxiliary base in a first trial (Figure 41).

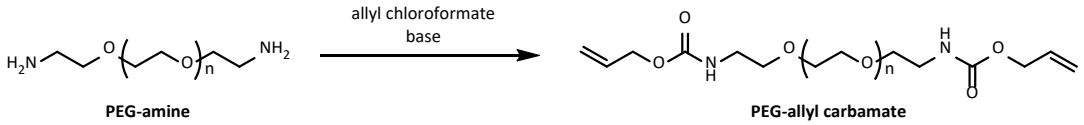

Figure 41: Reaction scheme of the PEG-allyl carbamate synthesis by means of PEG-amine and allyl chloroformate.

Due to high delivery pressure and the lack of PEG-amine, commercial 5k-PEG-diamine was used first and the established synthesis conditions were then transferred to the self-produced material as soon as it was available in sufficient quality and quantity. Since the thermal stability of PEG-amine was unknown, it was refrained from drying the polymer by azeotropic distillation in toluene or in high vacuum at 100 °C prior to the reaction and the synthesis was performed in DCM at 0 °C to prevent reactant quenching by water residues. The use of each auxiliary bases led to a quantitative formation

of PEG-allyl carbamate that had to be dialyzed against acidic aqueous media to remove the poorly soluble amine-based impurities as it was required for PEG-allyl carbonate. In contrast to the carbonate form, the carbamate was stable under these conditions and was isolated in pure form after freeze drying, shown by NMR but went along with a yield loss of 60-80 %. Upscaling of this synthesis route is theoretically possible for the reaction part whereas the purification by dialysis has its limits, and the inevitable yield loss was considered not to be economical worthwhile. An alternative synthesis route had to be established that tackles the major drawback of the current method, nearly inseparable impurities and the necessity for dialysis. Within polymer chemistry, literatures either claim to separate TEA- or pyridine hydrochlorides by precipitation in ether which is deemed to be an intentional false statement to preserve an advantage over competitors as TEA and pyridine salts are as insoluble in ether as the polymer itself and thus both precipitate simultaneously. Literature research for synthesis of small peptide building blocks with just a few Daltons (<1000 Da) led to a promising synthesis route using aqueous alkaline conditions ending up in the formation of the desired product and hydrolysis of the remaining reactant allyl chloroformate. This synthesis was described by Barthel *et al*.[112] and based on D-alanine as amino carrier with near quantitative yield and was transferred with a slight modification on 6k-PEG-diamine, produced in-house with 95 % amines. The one-pot synthesis was simply stirred at rt for 3 h, washed with diethyl ether and then extracted with DCM and added saline. Drying over anhydrous magnesium sulfate and precipitation in diethyl ether resulted in a pure product and quantitative conversion of the amino groups, shown by the absence of TFA amide signal at 7.18 ppm while traces of diethyl ether were detectable at 1.22 ppm (Figure 42).

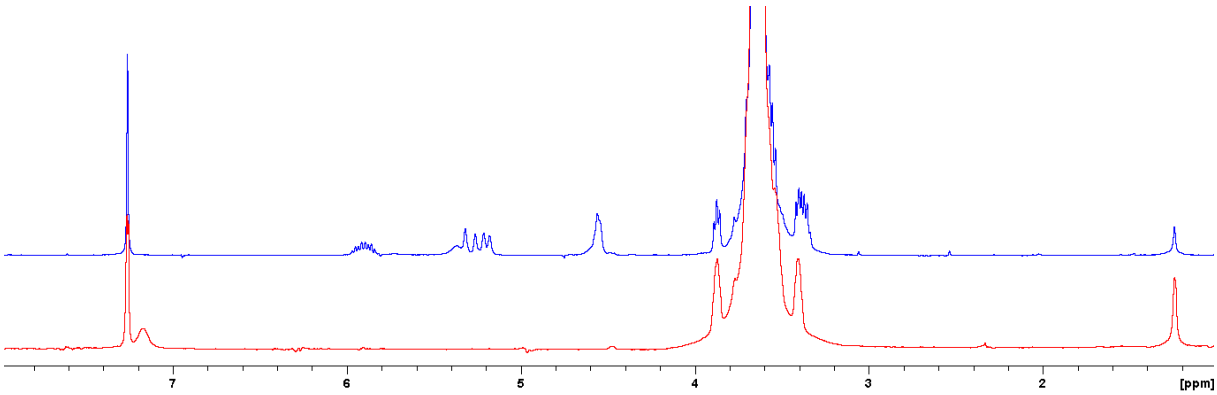

Figure 42: ^{1}H NMR overlay of PEG-diallyl carbamate 6 kDa (top) and PEG-TFA diamide (bottom) in $CDCl_3$.

However, SEC MALS analysis of the product revealed a high molecular weight shoulder originating from the formation of PEG-urea oligomers during the synthesis and in a 15 g scale repetition of the reaction the reaction solution heated up by the exothermic reaction to such an extent that the obtained product showed an even more pronounced oligomer formation (Figure 43). Performance of the reaction in an ice bath and portion wise addition of NaOH was found to prevent the undesired oligomerization and yielded the desired product.

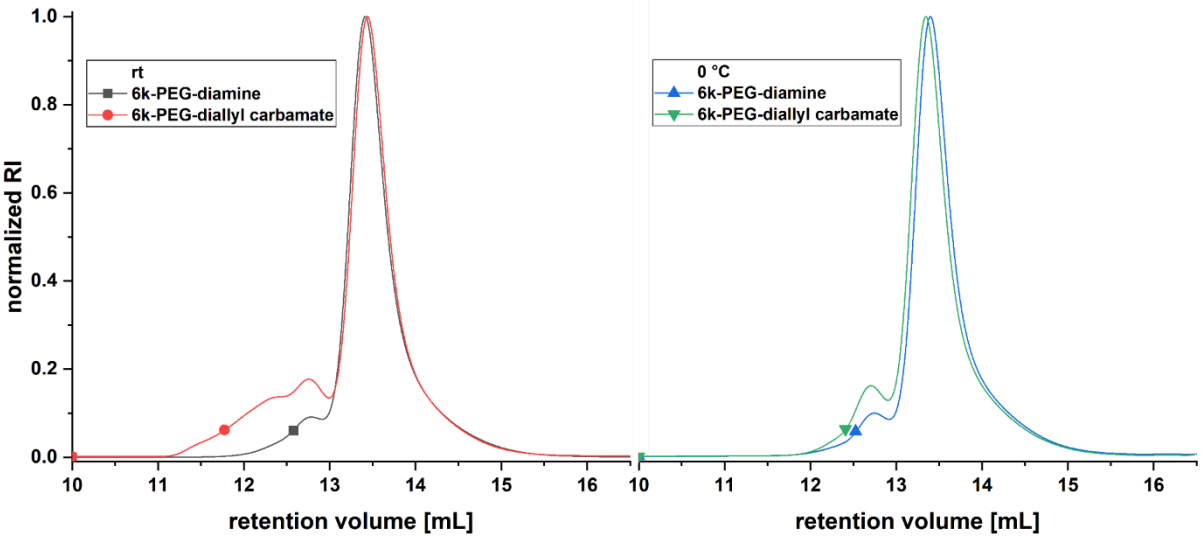

Figure 43: SEC MALS overlay plot of PEG-diallyl carbamate, synthesized at rt (left) and at 0 °C (right), and the respective PEG-diamine starting material

2.2.6 PEG-maleimides

The reactivity of maleimides towards Michael-addition is even higher than the one of acrylates[23] and originates from the reduction of electron density at the β-carbon by the -I-effect of the adjacent carboxy group. Implementation of such more reactive crosslinker in the bioink was thought to reduce the pre-crosslinking time and consequently widens the bioinks' processing window. With the experience from the PEG-amine synthesis (2.2.4, p. 45) and the potential benefit for the bioink, the synthesis of PEG-maleimide was of interest and both possible modification routes were tested in parallel, mesylate and Mitsunobu. In order to reduce the amount of simultaneous experiments, in each route a different PEG was used: linear PEG for mesylate and branched PEG for Mitsunobu (Figure 44).

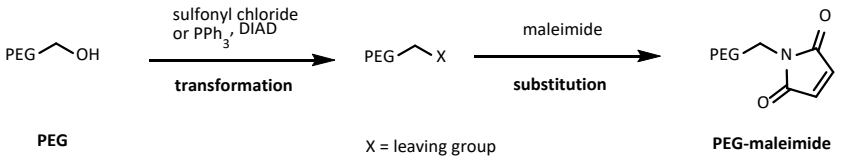

Figure 44: Schematic strategy overview for the PEG-maleimide synthesis.

Regarding the mesylate route, the mesyl-intermediate was synthesized and purified as described before and solely maleimide was added as nucleophile. The reaction was performed in two different solvents, DCM and DMF, as DCM offers the best solubility for PEG while DMF is predominantly used for substitution reactions and enables reactions at higher temperatures than DCM with a boiling point of 40 °C. Both reactions yielded no substitution independent of reaction times with up to 3 days and temperatures of 60 °C, shown by the presence of only PEG-mesylate signals in the ^{1}H NMR spectra. Even the addition of a non-nucleophilic auxiliary base (TEA) and augmented temperatures remained ineffective and the mesylate route was not pursued further. For the Mitsunobu route, reaction conditions of the PEG-amino synthesis were directly transferred onto 8arm-10k-PEG and maleimide used as nucleophilic instead of phthalimide. The reaction was straight forward compared to PEG-amine with only a different color gradient during the reaction from orange to dark red-brown and yielded a greyish solid with a DS of 75 %, meaning an average modification of 6 of the 8 arms and is sufficient for gelation experiments as well as growth factor incorporation. Nevertheless, the non-quantitative conversion, with regards to linear PEGs, was considered a concern as DS values of >95 % were aimed

at. Optimization of the reaction conditions and handling to potentially yield sufficient maleimide content were deemed non-rewarding in terms of time and applicability as the product is highly prone to polymerize due to the reactivity of the maleimides and was not pursued further.

2.2.7 Upscaling of PEG derivatization processes

One major crux of PEG modifications is the water of crystallization when it comes to upscaling those processes. In test reactions most often one-digit gram scales were used and application of HV at higher temperatures of >100 °C adequately removed the water residues as the surface-to-volume ratio of the melt is very high, even inside round-bottom flasks. Via this, steam bubbles, predominantly formed on the flask bottom where the temperature is the highest, can easily pass through the molten PEG to the surface and can be withdrawn by the vacuum. The surface-to-volume ratio can be tuned when using small scales by the choice of flask size but it is compromised when passing a certain scale since laboratory equipment is limited in size. With increasing scale, the ratio constantly decreases, and the steam bubbles have to pass a longer distance to be removed. This can be circumvented by continual rotation of the flask around a tilted axis similar to a rotatory evaporator but requires special equipment that is not available in most laboratories. A rotatory evaporator is a basic part of laboratory infrastructure and can be used for this purpose but requires the exchange of the heating medium as the required temperature is higher than waters' boiling point and water steam from the outside can be sucked into the flask through the glass joints. All possible medias are based on mineral or silicone oils and frequent exchanges of the heating medium are therefore associated with greater efforts in terms of time, material costs, waste removal and are avoided where possible. Raising the temperature results in augmented gas expansion and accelerates steam bubble passage but should not exceed 130 °C, to prevent possible thermal degradation of the polymer. Azeotropic distillation with toluene, however, is a possible but slow alternative and due to the pressure-dependent azeotrope the distillation has to be performed at ambient pressure and requires 110 °C to evaporate toluene and the azeotrope. In the final stage of this drying method, toluene must be removed from the concentrated PEG slurry and requires the same conditions and time as the solvent-free drying method. The only advantage of the azeotropic distillation is the water removal from high molecular weight PEGs, which in the molten state possess very high viscosities and by this trap steam bubbles at a certain molecular weight. In several experiments using linear 20k-PEG the viscosity of the melt was nearly too high for steam bubble passage and led to downscaling of the process to ensure proper water removal and subsequently successful syntheses. Regarding these observations, it is recommended for linear 20k-PEG, if downscaling to <50 g is no possibility, to either freeze dry the starting material prior to solvent-free drying or freeze dry prior to azeotropic distillation using toluene. All other PEGs with lower molecular weights can be effortlessly dried using the solvent-free method in scales up to 100 g within 2 h.

Besides the limitations by the drying methods and the physical properties PEG, the solubility of PEGs in different solvents is an important factor in terms of upscaling. Depending on the required solvent for the aimed synthesis, the scale possibly must be reduced to 25 g per synthesis due to the limited size of laboratory glassware which comes into play if reflux, vacuum, drying funnels, temperatures above 100 °C, reaction overnight at raised temperatures, protection gas technique or overhead stirrers are part of the synthesis. In all other cases borosilicate Schott-bottles with up to 10 L can be used. By the example of linear 6k-PEG at rt, the solubility in alcohols decreases the larger the alkyl moiety and the less polar the organic solvent is. The best solubility was observed for DCM and $CHCl_3$ with more than 50 g per 100 mL whereat THF and toluene dissolve less than 15 g per 100 mL at rt. For reactions at 0 °C, the latter and all alcohols, except MeOH, are inapplicable as PEG precipitates nearly quantitative while it remains dissolved in DCM and $CHCl_3$. This trend is even more pronounced for PEGs

with larger molecular weights and culminates in the very poor solubility of 20k-PEG in toluene with less than approx. 3 g per 100 mL already at rt. More specifically, the only moderate solubility of PEG in THF limits the scale of Mitsunobu reactions to less than 25-60 g per 1000 mL reaction volume whereas mesylation of PEG in DCM delivers more than 100-250 g product per 1000 mL.

The strongly temperature dependent solubility of PEG in alcohols can be utilized for its purification to a certain extend if the impurities are better soluble in alcohols than the polymer and such solubility discrepancy was present during the PEG-acryl synthesis using phenothiazine stabilized acryloyl chloride (2.2.1, p. 35). In this case, extensive recrystallization in EtOH led to the removal of the great majority of the stabilizer, which was inseparable from the polymer by all other purification methods such as dialysis and precipitation, except adsorption to activated charcoal which was investigated afterwards. Dialysis of PEG derivates, independent of the molecular weight and geometry, did not quantitatively remove organic impurities from the polymer and on top resulted in huge yield losses of 60-95 % even with the use of MWCO 0.5 kDa dialysis tubes. Additionally, PEG acted as a detergent and the impurities were adsorbed to the polymer independent of dialysis conditions and hence, dialysis was omitted completely. Furthermore, precipitation of the polymer was for none of the above discussed modifications an alternative purification method as the impurities, especially organic salts, were not soluble at all in diethyl ether and precipitated together with the PEG-product. Respective literature stating purification of their PEG-derivates via precipitation were consequently either considered to be intentionally stated false or their subsequent applications were tolerant enough towards impurities from the PEG modification reaction. Extraction with DCM from aqueous solution was only partially possible for the modified PEGs such as PEG-amine (at alkaline pH), PEG-mesylate and PEG-diallyl carbamate whereat PEG-(meth)acrylates and PEG-maleimides were inseparable and acted as strong detergents, completely impeding layer separation even with addition of saturated NaCl solution. Adsorption of the reactants to strongly hydrophobic and macroporous polystyrene resins was tested possible although inapplicable due to concurrent adsorption of PEG to the resin in near quantitative extent. A separation of reactants and PEG by elution with ethanol-water mixtures from the resin is possible by theory but was deemed to be a long-term process without assured success and thus was omitted. Instead purification by adsorption to activated charcoal was found a simple and heat-free alternative to recrystallization as the PEG product was not bound by the adsorbent, in contrast to the polystyrene resins. The remaining small amount of reactants were removed in a subsequent repetition of the purification step and the fine powdered activated charcoal separated from the cleaned product solution via decanting and vacuum filtration (0.2 µm, CE). The great advantage of this purification method are its very mild conditions without the necessity for heat combined with the scalability. Prevention of light passage by the suspended activated charcoal is an additional, beneficial side-effect for purifying light-sensitive PEG-acrylates.

2.3 Synthesis of non-polymeric products

2.3.1 3,3'-Dithiobis(propanoic dihydrazide) (DTPH)

The in-house synthesis of DPTH was not intended though became necessary as the commercial product was analyzed by curiosity when facing limits of the thiol content during HASH synthesis (2.1.1, p. 11). Briefly, the relation pH of the reaction solution and the thiol content was investigated and showed a clear trend of higher DS with lower pH, converging to a limit of 80 %. Systematic exclusion of reaction parameters raised concerns of impurities in the deployed chemicals, which were then analyzed by ^{1}H NMR without showing suspicious clues. Syntheses of NHS and EDC were considered complicated in terms of separation of product and by-products and DTPH was tested based on a published protocol of Vercruysse *et al*.[64] in a 10 g scale with slight modifications (Figure 45).

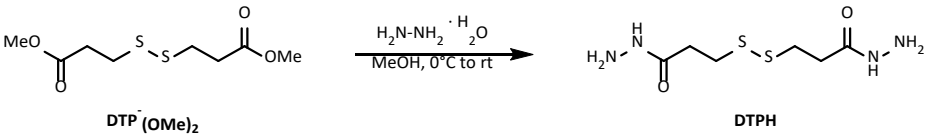

Figure 45: Reaction scheme of the DTPH synthesis

The reaction was performed using DTP-$(OMe)_2$ and hydrazine in MeOH at rt overnight yielding a yellowish suspension and product precipitation was enhanced by cooling to 0 °C. Centrifugation, washing with cold MeOH and DE led to discoloration of the supernatant and the obtained snow-white, odorless powder was analyzed by ^{1}H NMR (Figure 46). Quantitative conversion was proven by the absence of the methyl ester signals at 3.65 ppm whereas no difference in the spectra was observable compared to the commercial off-white DTPH with strong amine odor. Application of the self-made DTPH in the HASH synthesis yielded effortless a DS of 100 % and further deployment of the commercial DTPH was rejected. The difference in coloration and odor were regarded to originate from hydrazine residues due to only partial purification, that subsequently competed with DTPH for the activated carboxylic acids and thus limited the DS to 80 %. The reaction was refined in the following with regards to required amount of hydrazine, upscaling and simplified purification. The equivalents of hydrazine per methyl ester group were varied from 3-5 eq. in 0.5 eq. steps and obtained products were analyzed via ^{1}H NMR. An excess of 4.0 eq. hydrazine and higher was found to yield quantitative conversion of DTP-$(OMe)_2$ into DTPH while <3.5 eq. showed remaining starting material signals when using d_6-DMSO as sample solvent, capable of dissolving both, the dimethyl ester and the dihydrazide. Upscaling of the reaction to 100 g was possible using 2 L Schott bottles as reaction vessel without necessities for changes of the procedure whereas the reaction volume of >1000 mL exceeded the centrifuge capacity and purification had to be adapted. Repetition of sedimentation over 1 h, withdrawal of the supernatant by suction and resuspension was tested suitable but time consuming and suspension and dead-end filtration using liquid chromatography columns was tested. The crude product suspension was filled into the column with POR4 frit, the liquids were pressed out by application of air pressure at the columns top end and the drain was closed for resuspension of the filter cake in MeOH and DE. After several repetitions, the filter cake was washed with DE to replace MeOH with the low boiling non-solvent for accelerated drying of the product *in vacuo*. Both methods yielded the sighted white, odorless product whereas washing of the product inside the column required far less organic solvent, compared to the sedimentation method, and was used in the following. Occasionally, ether residues were enclosed inside larger solids of the product, inseparable by vacuum and thus appeared in the NMR spectra, and the product was dissolved in hot MilliQ (60 °C) and freeze dried.

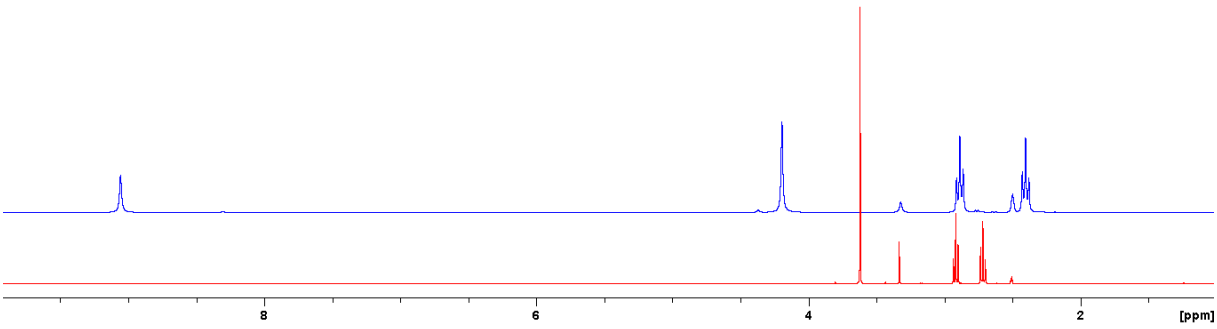

Figure 46: ^{1}H NMR overlay plot of DTPH (top) and DTP-$(OMe)_2$ (bottom) in d_6-DMSO.

2.3.2 Ala-Pro-Gly-Leu peptide sequence

The incorporation of a protease cleavable peptide sequence into the PEG-crosslinkers of the bioink was subject of the bioink optimization to enhance the biodegradability of the final printed 3D constructs. Based on the publication of Brandl *et al.*[92], the tetrapeptide APGL was chosen for this purpose as it represents not only a non-specific peptide sequence that can be cleaved by most of the MMPs, secreted by the incorporated hMSCs used in subproject A02, but also offers the possibility of implementation in other hydrogel/bioink systems and utilization of different cell types, which was of great interest to the SFB. The proposed idea was to insert the tetrapeptide between the PEG and the telechelic crosslinking moiety by polymer-analog synthesis based on the respective PEG but was considered disadvantageous as ^{1}H NMR analysis of linear PEG-acrylate showed strong peak broadening with increasing chain length (2.2.1, p. 35), gradually impeding the analyses, and the evidence of correct peptide synthesis can potentially not be provided. A proper troubleshooting might be impossible whereas modification of commercial APGL in the required double-digit gram scale for material supply and subsequent addition to PEG does not feature this potential disadvantage. However, the strategy was compromised by the price of 1000-1600 € per gram tetrapeptide, exceeding by far the budget of the project. Hence, phase-independent synthesis of the tetrapeptide was chosen and strategically divided into a side-by-side synthesis of two dipeptides, GL and AP, while the latter carries the crosslinking functionality. This offers the benefit of simultaneous and thus time efficient syntheses of building blocks with simplified analysis via ^{1}H NMR and high-resolution mass spectrometry (HRMS) due to their low molecular nature. HRMS analysis was performed for all di- and tetrapeptides as the intermediates, the NHS esters, are less stable during HRMS and would show also decomposed fragments instead of solely the product signal. The obtained spectra were added to the appendix (p. 119) for spatial reasons. In the following, discussions of the individual reaction steps were pooled in terms of the reaction type and all compounds were stated without designators but imply the natural L-configuration for the flow of reading.

NHS ester synthesis

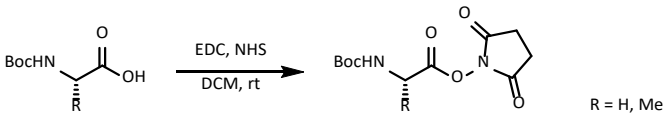

Figure 47: Reaction scheme of the NHS ester synthesis of Boc-glycine and Boc-alanine.

The synthesis of NHS esters of the boc-protected amino acids, glycine and alanine, was investigated by means of glycine in a small gram scale and the reaction conditions then refined in terms of upscaling,

product isolation and purity which were subsequently transferred to alanine (Figure 47). Starting with a 5 g scale, the reaction was performed as a one-pot synthesis in DCM using 1.2 eq. NHS and 1.6 eq. EDC at rt and the initial white suspension of Boc-glycine and NHS was dissolved within 2 min after EDC addition, indicating a high reaction rate of carboxylic acid and EDC under these conditions. The clear, yellowish solution was stirred overnight forming a turbid yellowish suspension, which became clear when heated to 40 °C, the boiling point of DCM. Washing of the product solution with 4x MilliQ resulted in almost complete discoloration of the organic layer and a yellowish solid was obtained after drying over anhydrous $MgSO_4$ and removal of the solvent *in vacuo*. ^{1}H NMR analysis confirmed the reaction success but also revealed remaining reactants in considerable amounts, which was thought to cause the products' yellowish coloration and a more intense washing of the product solution was pursued. Simultaneously, the reaction was upscaled to the limit of the laboratory glassware using 50 g starting material in 1000 mL DCM with identical reactant excess and the resulting DCM solution was washed several times with dilute HCl and MilliQ. While the washing removed the reactants almost completely with only traces of NHS remaining in the product, the formation of the *N*-acyl urea byproduct in larger amounts was detected, identical to the HASH synthesis (2.1.1, p. 11), which was inseparable with the applied purification method. Due to the lack of alternative methods, the prevention of the byproduct was considered key for the product quality in upscaled reactions and the excess of reactants and the reaction procedure were adapted. Increasing the amount of NHS to 1.6 eq. and the reduction of EDC to 1.2 eq. combined with a portion wise addition of the coupling reagent over 30 min was found to prevent the formation of the inseparable byproduct und yielded a clean product (Figure 48) with slight residues of water (3.33 ppm) and DCM (5.75 ppm). Due to the equilibrium between the cis and trans conformers by rotation round the amide bond[113,114], the N-H and the adjacent α-proton signals appeared split in 80:20 ratio (trans:cis) in the case of glycine. The reaction conditions were then directly transferred onto Boc-alanine and Boc-ala-proline which was straightforward apart from the necessity for twice the solvent as the solubility of these NHS esters was significantly lower compared to the glycine variant and resulted in product precipitation during the synthesis and purification. The success of the syntheses and the product purities were proven by ^{1}H NMR, whereas the methyl group superimposed with the Boc groups signals (1.41 ppm) (Figure 48) in the case Boc-alanine while coupling of proline led to their separation. Occasionally, residues of NHS remained in the product but were found to not interfere in the following coupling reactions.

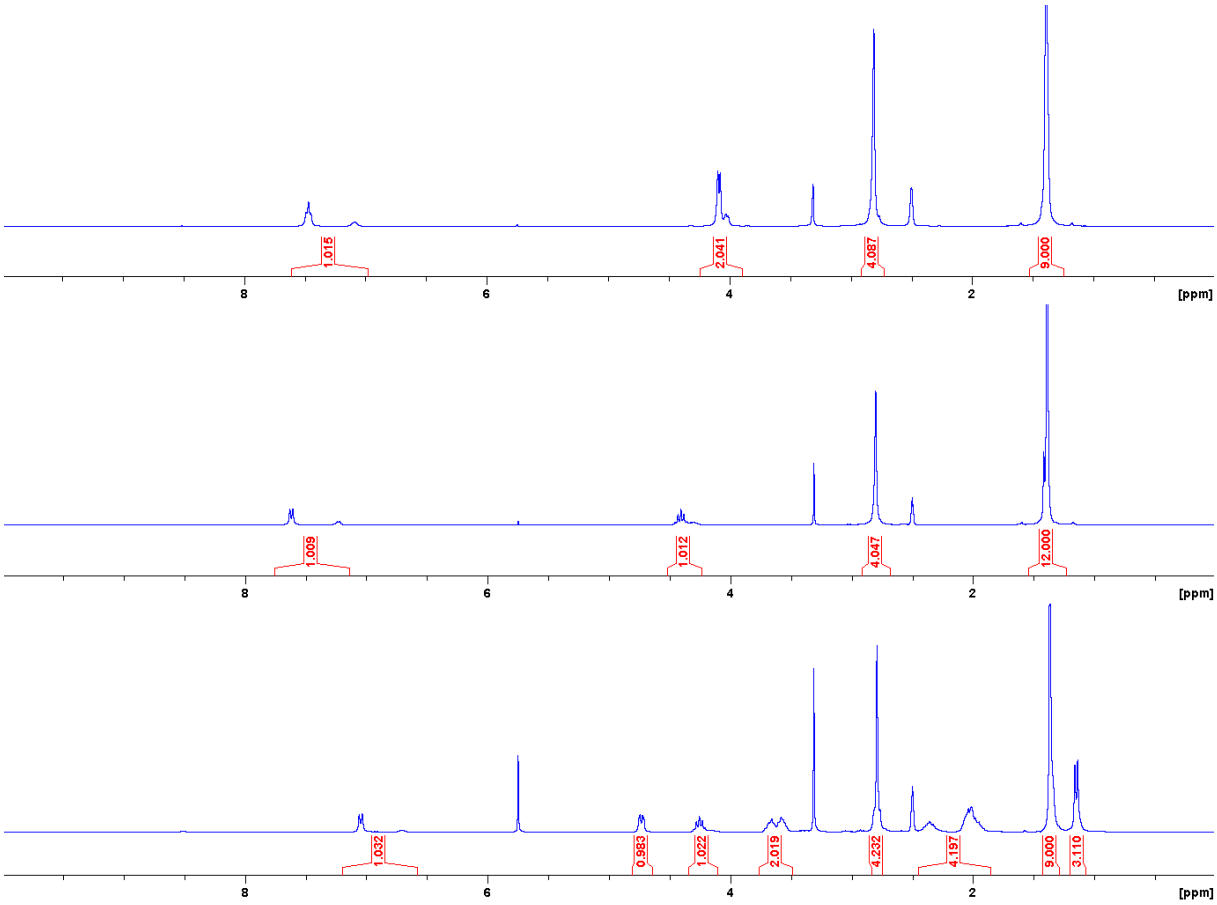

Figure 48: ^{1}H NMR of NHS esters of Boc-glycine (top), Boc-alanine (middle) and Boc-ala-proline (bottom) in d_6-DMSO.

Coupling reactions

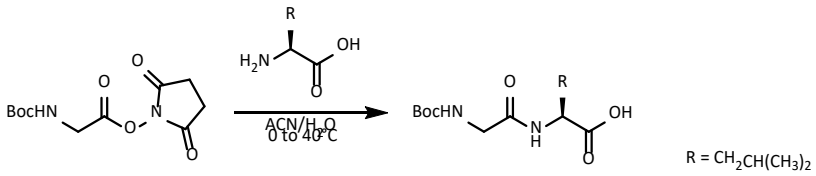

Figure 49: Reaction scheme of the peptide synthesis at the example of Boc-glycine NHS ester and leucine.

The optimal reaction conditions for the syntheses of di- and tetrapeptides were investigated by means of the synthesis of the dipeptide Boc-gly-leu and were transferred with slight adaptation onto the other amide coupling reactions. First, the solubility of Leucine in DMF and ACN, prominent for peptide modifications, was tested to identify the most suitable solvent for this reaction whereas the amino acid was poorly soluble in ACN and mediocre in DMF. Hence, the reaction was conducted in DMF at rt using aqueous NaOH for two purposes, as solvent for leucine and as auxiliary base for the reaction. The absence of hydrophile sidechains and the N-terminal, hydrophobic Boc-group were thought to increase the solubility of the resulting dipeptide in organic solvents and extraction of the product from the product solution was tested using DE, DCM and $CHCl_3$ at different pH values. While extraction with both halogenated solvents was ineffective at all, acidification to pH <1 with HCl and subsequent extraction with DE was found suitable and yielded a clean product after washing with acidified MilliQ. The utilization of NaOH in the reaction came along with high yield loss (<70 %) as the NHS ester was

cleaved by the hydroxyl anions to a major extend and was replaced by the non-nucleophilic auxiliary base TEA. As the combination of leucine and TEA was only poorly soluble in water and impeded the separate dissolution of NHS ester and reactants with subsequent intermixture, the reaction was transformed into a one-pot synthesis and MilliQ was added to the resulting DMF suspension until it became clear (2:1, DMF:H_2O). Despite the deployment of a non-nucleophilic base, the obtained yield loss was only marginally reduced (<60 %) and the reaction temperature was regarded to promote ester hydrolysis in the alkaline aqueous media. In a 30 g upscale, two parameters were investigated simultaneously, the effect of reduced temperature on the ester hydrolysis and the yield loss during washing of the organic layers after the extraction. Drawing of aliquots from the combined organic layer before and after washing and from the combined washing suds following the removal of the solvents *in vacuo* and by freeze-drying revealed near quantitative conversion of the NHS ester whereat approx. 50 % of the product was washed out from the organic layer during its purification. As DMF residues were only found in the washing suds, it was deemed to entrain the product into the aqueous layers and ACN, the less potent solvent, was tested as reaction solvent. Although, its different solubility, the reaction suspension in ACN:H_2O (2:1) cleared up after 30 min at 0 °C, indicating the consumption and thus dissolution of the reactants over time yielded a clean product with less yield loss (<30 %).

Compared to the reactions in DMF, acidification of the product solution in ACN/MilliQ led to the formation of a white suspension which was dissolved by extraction with DE and raised the idea of precipitation as purification method. In the 80 g follow-up experiment, ACN, with a lower boiling point of 82 °C than DMF, was removed *in vacuo* after the reaction and the obtained clear, aqueous solution was slowly acidified with 10 % HCl until quantitative precipitation at once at pH<3. Via centrifugation, the white precipitate was separated from the yellowish supernatant and the precipitation step was repeated three times by dissolution of the sediment at pH>8 using NaOH and re-acidification with HCl. Resuspension of the final precipitate in MilliQ and freeze drying yielded a clean product with an overall yield of 74 %. The purity of the dipeptide was confirmed by HRMS (Figure 96, p. 120) and ^{1}H NMR (Figure 50), showing residual water (3.33 ppm) and slight NHS traces (2.54 ppm). The proton signals the leucine side chain appear in the upfield range while the β-CH_2 and the γ-CH groups superimpose with the Boc group around 1.5 ppm and the two methyl groups resonate at 0.85 ppm whereby the α- and amide proton appear in the downfield at 4.20 ppm and 7.95 ppm The transfer of the reaction conditions on the Boc-ala-proline synthesis in a 10 g scale was straightforward without the requirement for modifications and was subsequently upscaled to 80 g, generating a clean product in 56 % yield (Figure 50). In the upfield range, proton signals appeared for the alanine methyl group (1.15 ppm), the Boc moiety (1.35 ppm), the β- and γ-CH_2 groups (1.7-2.2 ppm) and the δ-CH_2 group (3.75 ppm) while the α-protons superimpose at 4.25 ppm and the amide signal of alanine splits into three between 6.3-7.0 ppm.

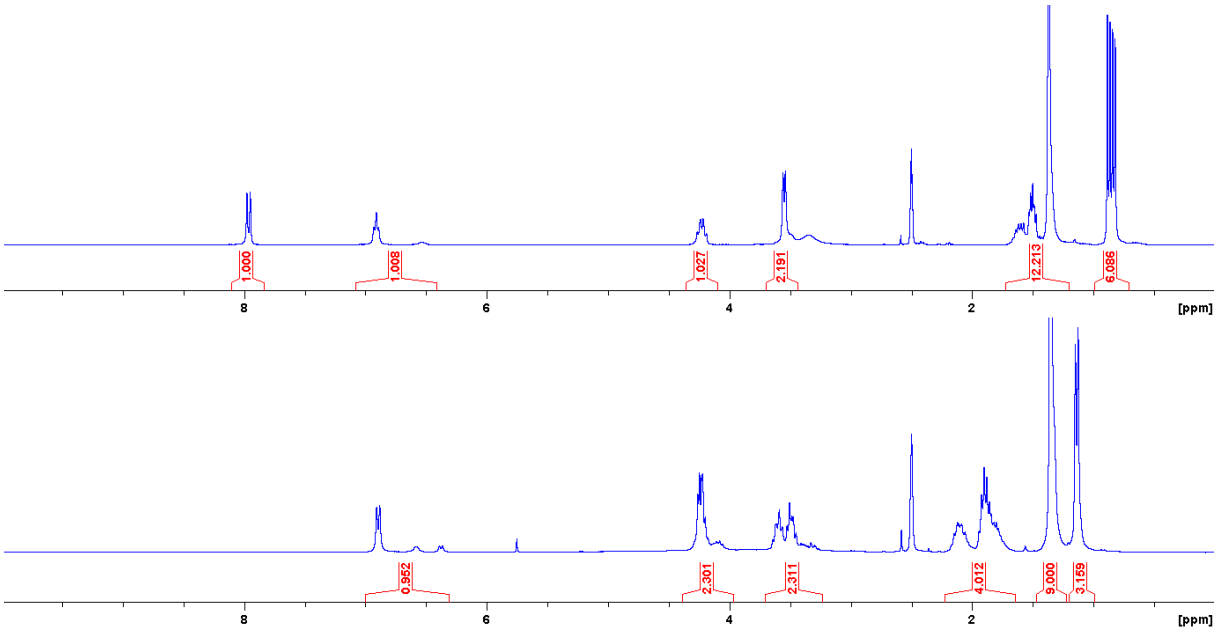

Figure 50: ^{1}H NMR of Boc-gly-leucine (top) and Boc-ala-proline (bottom) in d_6-DMSO.

The synthesis of the Boc-APGL tetrapeptide from Boc-ala-proline and gly-leu dipeptide, which's deprotection is discussed in the following subchapter, was performed in ACN:H_2O (2:1) under the same conditions as both Boc-dipeptides but yielded a mixture of product and Boc-ala-proline since they possessed very close properties such as pK_a and solubility in organic solvents. Hence, extraction with DE and precipitation remained ineffective, independent of the applied pH of the aqueous layer. HPLC using a semi-prep RP column and an ACN:H_2O:TFA gradient, was found to separate the two peptides due to their different hydrophobic side chains but can only purify 20 mg per run and thus was inapplicable for the production of tetrapeptide in gram scale. To circumvent this, the gly-leu dipeptide was deployed as methyl ester to generate a neutral product, offering the enormous advantage of dipeptide removal by extraction and washing with acidic and alkaline MilliQ. In a 5 g test reaction in ACN:H_2O (7:3), the reactants were combined at 0 °C, stirred for 1 h and then heated to 50 °C for 3 h to produce a mixture of four components, the neutral product methyl ester, anionic Boc-ala-proline, cationic gly-leucine methyl ester and TEA. After removal of ACN from the product solution *in vacuo*, extraction of the product with DE was tested inefficient while DCM was applicable and washing of the organic layer with HCl and NaOH yielded a clean product. The reaction then was upscaled to 25 g using the same procedure with a final yield of 77 % and synthesis success was proven by HRMS (Figure 99, p. 123) and ^{1}H NMR (Figure 51). In the upfield range the methyl groups of the leucine, alanine and boc-moiety resonated as sharp separate signals at 0.86, 1.15 and 1.36 ppm. Additionally, superimposed signals of the β-/γ-protons of leucine and proline between 1.45-2.15 ppm and of the methyl ester, α-glycine and δ-proline protons between 3.39-3.84 ppm were detected. The remaining α-protons appeared in the downfield between 4.0-4.45 ppm and the amide proton signals were in the range of 6.64-8.36 ppm with residual water at 3.33 ppm.

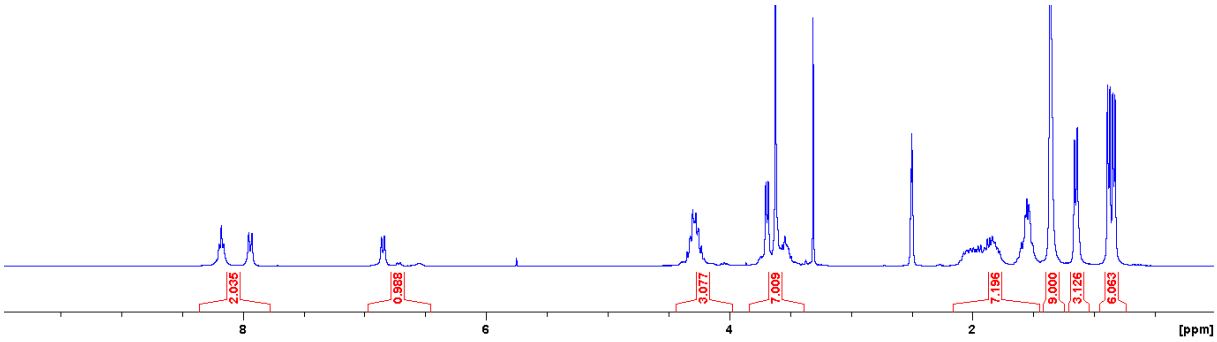

Figure 51: ^{1}H NMR of Boc-APGL methyl ester in d_6-DMSO.

Boc deprotection

The removal of the Boc-protection group from Boc-gly-leucine was crucial for the subsequent synthesis of the Boc-APGL tetrapeptide and was performed in accordance with Santos *et al*.[115] in neat TFA at rt. In a 2 g test reaction, the Boc-dipeptide was dissolved in 10 eq. neat TFA, stirred for 30min, generating heat and intense bubble formation, indicating progressing deprotection. The excess TFA was removed by precipitation in cold DE and washing of the brownish powder several times with DE at rt. ^{1}H NMR analysis confirmed the success of the synthesis but showed indefinable residues and remaining TFA. The brownish coloration of the reaction solution raised suspicions about the purity of the TFA batch and the reaction was repeated in a 9 g scale with fresh TFA yielding a clear, yellowish solution and after purification, a clean white powder. Due to the heat formation and the highly reactive TFA, the reaction was conducted at 0 °C with 5.0 eq. TFA in the following experiments. The separation issue of Boc-APGL and Boc-ala-proline led to the synthesis becoming redundant. Instead, simultaneous deprotection and esterification was required for the desired synthesis of Boc-APGL methyl ester and a transformation with methanol HCl was investigated. Consequently, a 5 g scale reaction was performed, pursuant to Brandl *et al*.[92], generating first methanolic HCl by addition of acetyl chloride to dry MeOH at 0 °C and subsequent addition of Boc-dipeptide (Figure 52). The turbid suspension was allowed to warm up to rt and the solvent was removed *in vacuo* at 50 °C during which intense bubbling was observed indicating the necessity of heat for deprotection. NMR analysis of the obtained white powder confirmed quantitative deprotection and concurrent methyl ester formation. Upscaling of the reaction to 60 g was straightforward, the excess of HCl was neutralized using NaOH and the resulting suspension was freeze-dried to give an off-white powder. Analysis via HRMS (Figure 98, p. 122) and ^{1}H NMR verified the formation and purity of the product (Figure 53). The protons of the leucine side chain resonated between 0.75-1.79 ppm while the α-protons of glycine overlapped with the methyl ester signals in the range of 3.42-3.70 ppm and the α-leucine proton appeared at 4.33 ppm. The amide proton and the protonated deprotected amino moiety were detected between 8.05-9.18 ppm. Traces of methyl acetate were found at 3.72 ppm.

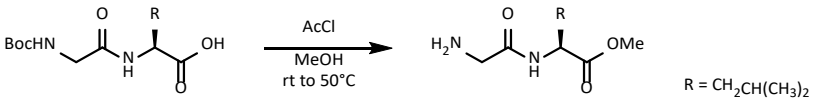

Figure 52: Reaction scheme of the Boc deprotection using methanolic HCl at the example of Boc-gly-leucine.

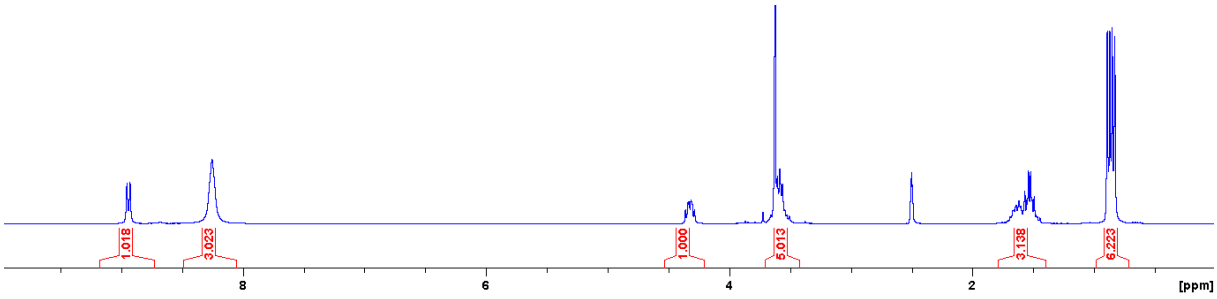

Figure 53: ^{1}H NMR of gly-leucine methyl ester in d_6-DMSO.

Methyl ester cleavage

The final step of the Boc-tetrapeptide synthesis was the saponification of its methyl ester derivative and was performed pursuant to Revelou *et al*.[116] using NaOH in MeOH (Figure 54). In a 2 g scale, the Boc-APGL methyl ester was dissolved in MeOH, 2.2 eq. 2N NaOH added and the clear solution stirred for 1h at rt. After neutralization with HCl and removal of the organic solvent *in vacuo*, the product was precipitated by acidification of the aqueous solution to pH<3. Resuspension in MilliQ and freeze-drying led to a pure product and the reaction was upscaled to 20 g without modifications. HRMS (Figure **100**, p. 124) and ^{1}H NMR (Figure 55) confirmed the formation of the desired product. Compared to the methyl ester NMR spectra. the product proton signals appeared at identical ranges with exception of a shift of the leucine α-proton from 7.94 to 7.80 ppm and the disappearance of the methyl ester signal at 3.62 ppm.

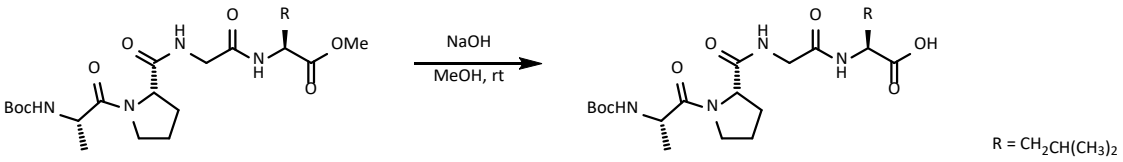

Figure 54: Reaction scheme of the ester cleavage of the Boc-APGL tetrapeptide methyl ester.

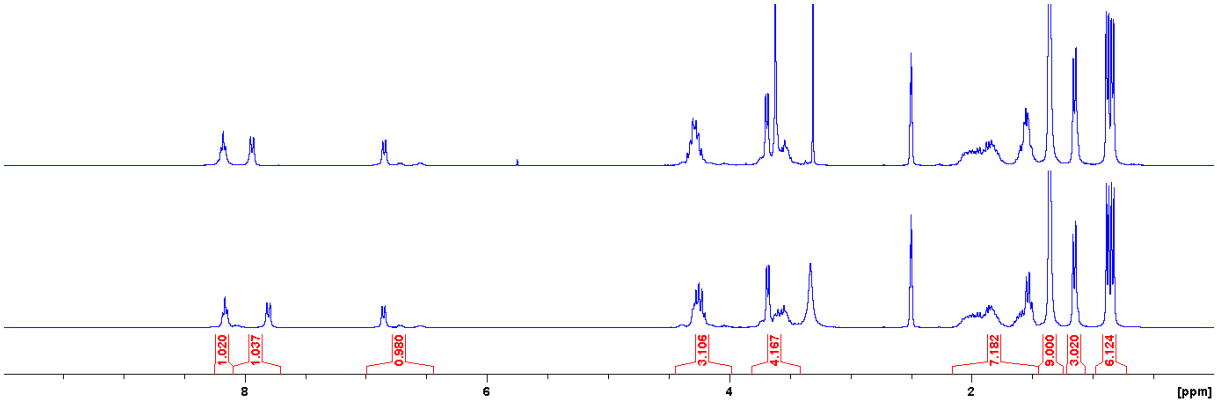

Figure 55: ^{1}H NMR of Boc-APGL methyl ester (top) and Boc-APGL-OH (bottom) in d_6-DMSO.

2.3.3 Upscaling of non-polymeric syntheses

For material supply with polymeric products, syntheses of the required non-polymeric building blocks in large quantities were crucial and, in all cases, conducted at the limits of the laboratory equipment. The DTPH synthesis was performed in 100 g scale in a 2 L Schott bottle and required solvent and hydrazine excess to prevent oligomerization during the synthesis. Therefore, a reduction of solvent was counterproductive and further increase of batch size would require not only larger vessels for the reaction but also larger columns for purification via washing. The current production limit was found sufficient for the present material demand as 100 g DTPH can generate 42 g of HASH suitable for 84-8.4 L of hydrogel/bioink with 5.0-0.5 % HASH content, depending on the application and formulation. Similar to DTPH, the upscaling of the peptide synthesis was mainly limited by the solubility of the reactants or products and thus by the reaction vessel size. This was clearly demonstrated during the NHS ester synthesis of Boc-alanine, in which the product was only moderately soluble in the solvent (DCM) at 30g/L at 35°C. Utilization of different, non-water-miscible solvents was tested less effective and the synthesis was repeated on demand since purification was limited by the volume of the separation funnel (1.4 L). Upscaling of the coupling reactions was straightforward to the test reactions and reached its limits at a scale of 80 g due to the size of the reaction vessel. Additionally, isolation and purification via extraction had to be substituted with precipitation in acidic aqueous conditions to render such large scales possible. Boc deprotection and ester cleavage were both performed at the limits of the current stocks of reactants with 60 g and 20 g but possess a theoretical production limit of 250 g (deprotection) and 150 g (ester cleavage) when using 2 L reaction vessels.

2.4 Hydrogel formulation and characterization

2.4.1 HASH + PEG-acrylate

The formation of hydrogels with thiolated hyaluronic acid and PEG-acrylate was the first step towards the desired dual-stage crosslinking bioinks and was investigated thoroughly in terms of the requirements and tunability of the gelation. The obtained observations were utilized in the bioink development. During the establishment of the HASH synthesis, several batches HASH with different thiol contents were produced and deployed in two consecutive gelation experiments for the determination of required thiol content for proper gelation. In the first screening, using P(AGE) and HASH with varying thiol contents of 5-25 %, only HASH with a DS of 25 % after 10 min at 365 nm gelled when mixed in 5:5:0.05 % ratio (HASH:P(AGE):I2959) while the second screening including HASH with 25-100 % thiol content revealed proper gelation starting with 40 % DS and no difference in stiffness above 60 % DS in concentrations of 1:5:0.05 % (HASH:P(AGE):I2959). Hence, a 40-60 % thiol content was regarded sufficient for hydrogel formation. The gained insight was then transferred onto the gelation of HASH and PEG-acrylates whereas a large pool of each component was produced with different contents of reactive groups, molecular weights and geometries (Table 2).

Table 2: List of all produced HASH and PEG-acrylate batches at the beginning of the hydrogel screening. Suitable HASH batches are encased with dashed lines.

HASH				PEG-acrylate	
M_w [kDa]	DS [%]	M_w [kDa]	DS [%]	geometry	M_n [kDa]
335	77	80	40	linear	1.5
192	70	105	26	linear	6
149	68	54	25	linear	10
415	67	144	24	linear	20
240	67	161	23	4-arm	5
269	63	164	22	4-arm	10
465	60	137	21	8-arm	10
363	58	76	20		
107	47	264	18		
404	43	68	14		

Due to the sheer number of possible combinations, a screening was conducted using one HASH batch (425 kDa, DS 60 %), all available PEG-acrylates and commercial PBS as solvent. The idea was to find a starting point in terms of necessary component concentrations from which the relations between formulation and hydrogel properties such as stiffness, extrudability and shape fidelity were about to be examined. Based on the findings of the first gelation experiments with P(AGE), the HASH concentration was set to 2 % and the PEG-acrylates were added in slight excess with 3 % to ensure gelation while the PBS buffer with a pH of 7.4 was thought to maintain a suitable pH of <7 for the desired Michael-addition. pH measurements of the stocks showed unaltered values for the PEG-acrylates but the pH dropped to 6 in case of HASH-solutions due to the acidic dialysis of this compound and only 9 % buffering salts in the solvent. Manual pH adjustments with NaOH were possible but filigree and diluted the stocks. Hence, a self-made, isotone (=154 mM) PBS with 150 mM buffering phosphate salts and 4 mM NaCl was produced with an initial pH of 7.8 to yield a pH of ≥7.4 after HASH dissolution, which was confirmed in a follow-up test. With the now obtained, suitable buffer, the stocks for the screening experiment were reproduced, the aimed formulations generated and incubated at 37 °C in a closed environment (Eppi) to prevent water evaporation. After 2 h, the hydrogel stiffness was examined manually by careful poking with a 1 mL syringe plunger. Formulations based on PEG-diacrylate below 1.5 kDa were liquid to extremely weak and the formed hydrogel was

considered a result of rather HASH oxidation than Michael-addition, whereas no significant difference between the formulation including 4-arm 10 kDa and 8-arm 10 kDa crosslinkers and only minor differences between deployment of linear 6 kDa- and 4-arm 10 kDa PEG-acrylate was noticed. Contrary to that, with increasing chain length of the linear PEG variants the hydrogels were less stiff due to the decreasing number of functional groups present at same PEG concentration. In the following, utilization of the branched PEG-acrylates was put on ice and the focus was placed on formulations based on linear crosslinkers in molecular weights of 6-20 kDa to study the achievable range of stiffness. For this, the HASH concentration was fixed to 1 %, the amount of acrylate crosslinkers varied between 0-4.0 % in 0.25 % steps and the formulations examined manually after 1 h of incubation at 37 °C. An overall trend of increased stiffness with increasing crosslinker concentration was observed for all chain length, while the 6 kDa variant yielded weak hydrogels already at 0.5 % compared to the 10 kDa and 20 kDa variants, requiring a minimum crosslinker concentration of 1.0 %, respectively 2.25 %, for gelation.

Objective characterization of these hydrogels' stiffness was the subsequent target of interest and could be performed by different measurement devices, available at this time in the laboratory infrastructure: dynamic mechanical analysis (DMA) for determination of the Young's Modulus and rheological analysis for determination of storage and loss modulus. In view of the number of samples from the actual screening of future hydrogel and bioink developments, both methods were found less applicable for the desired purpose. While DMA offers a high throughput of preincubated samples, it lacks the ability to analyze very weak hydrogels with poor shape fidelity as the methods' mathematics are based on defined, static hydrogel dimensions. Rheological characterization instead is independent of the dimensions but requires the sample to be incubated on the measuring plate to prevent errors from wall slipping as well as to ensure appropriate sample trimming and thus represents a time-consuming method, suitable for in-depth characterization hydrogel formulations, though, not for large sample screenings. Therefore, a new method was established by adaptation of a mechanical extrudability setup for cement pastes from Weichhold, J. (copyright) in which the formulations were mounted in syringes and pressed through a steel needle with a constant crosshead displacement (Figure 56).

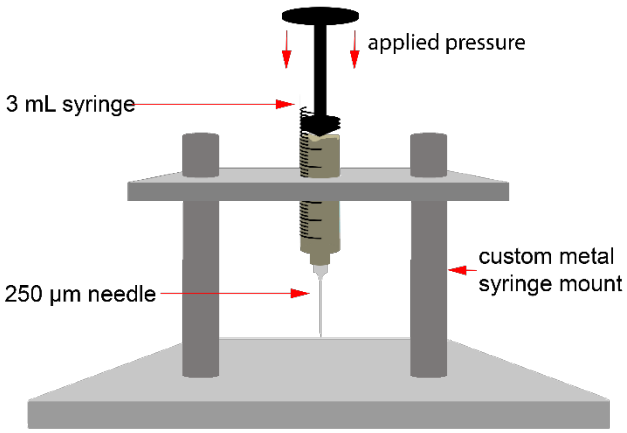

Figure 56: Scheme of custom-made extrudability test setup for dimension-less hydrogel stiffness characterization adapted with permission of Weichhold, J.

The idea was to shear the hydrogel through 3D printer needle (410 µm, steel) and to monitor the required force, which was expected to increase proportional to the hydrogel stiffness/viscosity, while standardized testing conditions render possible comparison of different formulations. This theoretical concept was confirmed by extrusion of the hydrogels used for the manual screening experiment and yielded clear force-distance curves for each formulation after adjustments of the displacement rate to a sufficiently high level (10 mm/s) to raise the required force to distinguishable values. The curves

showed an initial force peak, assigned to the inertia of the rubber plug, followed by a characteristic plateau, that was used as sample attribute, and a final steep increase in one case (0.4 %) when the plug reached the dead-end and the measurement was stopped (Figure 57).

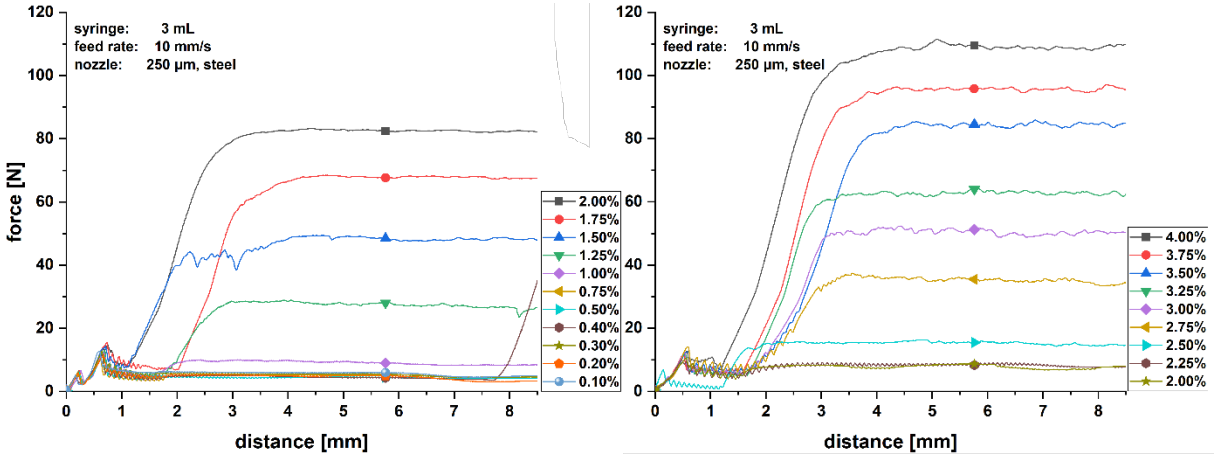

Figure 57: Force-distance diagram for mechanical extrusion of formulations with 1 % HASH (425 kDa, 60 %) and different PEG-diacrylates (6 kDa left, 10 kDa right) contents after incubation (1 h, 37 °C).

With this, the results of the subjective, manual experiments were underpinned by objective data and became comparable with future formulation screenings as subjective impression might fade over time while the objective data remained. Nevertheless, this method came along with a certain threshold in which extrusion of very weak, almost liquid hydrogels and of pure HASH solutions yielded identical curves albeit these formulations were not intended for applications and thus the method represented a quick, though, solely rough dimension-less characterization technique for the hydrogel stiffness with a certain threshold, suitable for weak to strong hydrogels. Utilization of these formulations in combination with the self-made PBS buffer in 3D cell culture experiments with hMSCs showed very poor cell survival compared to identical formulations with commercial PBS and the high phosphate content in the self-made PBS was found to be the reason. An exchange of the buffering phosphates by HEPES, an organic buffering salt, did not affect the gelation speed and hydrogel properties and its biocompatibility was confirmed in subsequent repetition of the 3D cell culture. With this, self-made HEPES (pH 7.6) was used for HASH stock preparation and commercial PBS for PEG stock preparation for optimal cell compatibility and maintenance of an appropriate pH for the Michael-addition. Expectedly, incomplete saturation of the available thiols by acrylate groups within a formulation led to hydrogel shrinkage within the first days of cell culture but was found negligible in most applications using a 1:1 ratio of the polymers. Which in consequence results in a thiol saturation of around 25-40 %, depending on the respective DS of the HASH and by means of used 6k-PEG-diacrylate. For oxidation of the remaining free thiols a close proximity within 3D network is required as the hydrogel network is only flexible to a certain extend after gelation and therefore not all free thiols will yield secondary crosslinking via an oxidative disulfide formation, which subsequently results in hydrogel shrinkage and strengthening. The introduction of a quenching molecule, unable to crosslink while saturating the remaining free thiols was considered highly difficult and inapplicable for several reasons. Next to the unknown effect of this thiol-saturation on the hydrogel properties and cells, the mechanism of the saturation, the introduction into the hydrogel and the chemical composition of the quencher had to be investigated as yet no literature existed regarding this strategy. For the saturation of the thiols Michael-addition and thiol-ene reaction could be used, both reactions have different contrary disadvantages. For a subsequent Michael-addition, no initiator is required and the quencher has to be an efficient Michael-acceptor, which might as well be taken up by cells and there interferes with thiol-based natural pathways as well as the hydrogel formation, while the UV-mediated

thiol-saturation does not affect the gelation but requires an additional initiator or irradiation, that in combination with the remaining acrylates after gelation might yield FRP and hence a secondary hydrogel network. Deployment of the quencher after the hydrogel formation necessitates a highly diffusible hydrogel network and a small and simultaneously highly water-soluble quencher molecule that reaches the whole volume of the hydrogel, whereas larger quenchers, such as PEG-monoacrylate, are better applied before gelation but might alter the hydrogel properties in terms of stiffness, osmolarity and accessible mesh volumes. The probability of shrinkage via disulfide formation was forwarded to all cooperators using this hydrogel composition. Enzymatic degradation of the hydrogels is theoretically possible as the acrylate moiety, an ester, can be hydrolyzed, resulting in crosslinker cleavage, but was not explicitly examined. Additionally degradability of the crosslinked HASH/PEG hydrogels could be attributed to the action of hyaluronidases similar to HASH-P(AGE) hydrogels, which were investigated by in-house bachelor student Züge, A[117]. In his thesis, he incubated photo-crosslinked HASH-P(AGE) hydrogels in different concentrated solutions of hyaluronidase from bovine testes and analyzed the degradation by weight. In summary, crosslinked HASH was degradable to only insignificant extent on the hydrogel surface over days while non-crosslinked HASH and pure HA were both degraded by >50 % in terms of chain length within a few hours. A comparison of the latter revealed a reduced degradation rate of non-crosslinked HASH due to the thiol-modification at the carboxylate group. Enabling enzymatic degradation by integration of a protease-cleavable APGL peptide sequence into the PEG-crosslinkers was still in progress by end of this thesis.

In the following, several formulations screenings using different fixed HASH concentrations and 6k-PEG-diacrylate where conducted, as the overall concept was to decrease the polymer content of the hydrogels as far as possible for enhanced biological output, which resulted in a variety of different hydrogels with different characteristics and cooperating subprojects were offered the materials for their applications. After the material supply, the interested subprojects were introduced in the handling and the formulations were tailored towards the customers' demand in feedback-loops. A promising application for the non-printable HASH-PEG-diacrylate hydrogels was their combination with MEW fibers from PCL for the formation of three dimensional neuronal network investigated by subproject C05 (former B01) in the AG Villmann of the Institute for clinical Neurobiology in Würzburg. The overall idea was to establish a 3D model based on MEW supported ultra-soft matrices for in-depth investigation of neuronal networks and glioblastoma cell migration using commercially available hydrogel kits and evaluating them with hydrogel systems, developed by the TRR225. As no clear requirements except for low stiffness existed, the cooperation partners tailored the formulation themselves in consecutive cell experiments, leading to a final composition of 0.75 % of each, HASH (264 kDa, 44 %) and 6k-PEG-diacrylate in HEPES (154 mM, pH 7.6) and commercial PBS. Comparison of the commercial HASH, Glycosil, and the provided HASH showed significantly increased cell migration in hydrogels from self-made HASH and thus encouraging first results for the desired 3D model and led to an expanded study. The obtained results are content of a published manuscript[118].

Another application was the 3D cultivation of human umbilical vein endothelial cells (HUVEC) in HASH-PEG-diacrylate hydrogels for the analysis of the cell behavior in hyaluronan based hydrogels with regards to the planned investigation of embedding pre- and post-endothelialized networks in tissue-specific hydrogels by the subproject B02 in AG Cicha of the University Hospital Erlangen, Section of experimental Oncology and Nanomedicine. For their project purposes, different hydrogels, produced by the TRR225, were tested for their response on the embedded HUVECs and the results of using HASH-PEG-diacrylate formulation was found promising at first instance. The application consisted of casting the cell-loaded gels in borosilicate glass rings (ID 6 mm) with the aim for well distributed cells. In feedback-loops with the partners, a formulation of 1 %/1 % was tested to yield a soft hydrogel that not only featured high shape fidelity but also gelled after only 20 min, preventing cell sedimentation during incubation. As additional refinement, HEPES with slightly more alkaline pH

of 7.8 was prepared and provided an accelerated gelation of the precursor solution, with gelation times of <10 min at 37 °C without affecting the cell biology. Since crosslinked HASH is not degradable by hyaluronidase[117] and the PEG chains only contain inert polyethers, the hydrogel is yet non-degradable by a bioorthogonal enzymatic approach and the cells were solely extractable by mechanical homogenization (TissueLyser, Quiagen)[119]. Deployment of protease-cleavable APGL-modified PEG-crosslinkers was initially anticipated to enable a mild extraction alternative but was postponed as their synthesis was still in progress by the end of this thesis. However, application of the non-degradable formulation was continued on expanded scope and resulted in the preparation of a manuscript.

2.4.2 HASH + PEG-vinyl sulfone

PEG-vinyl sulfone represents a commercially available and highly reactive Michael-acceptor for Michael-addition crosslinking of thiolated polymers and yet was used in many applications[120-123]. The terminal vinyl group in conjugation with the sulfone S=O double bond generates a reactivity even higher than acrylates[23] due to the included heteroatom and thus offers high crosslinking rates. When mixed with a thiolated polymer under physiological conditions, this fast gelation time can be used as advantage in applications with small operating windows such as the fixation of intrinsically fast-moving flagellates for live-cell imaging[124]. In this publication of Glogger *et al*., the successfully utilized hydrogel system was composed of low molecular weight HASH und P(AGE) and crosslinked on demand via thiol-ene reaction with 365 nm UV light over 5 min in the presence of I2959 for cell immobilization on glass cover slips and consecutive imaging within 60 min. Hydrogels with 15 % polymer content were found to yield a sufficient strong network for quantitative suppression of flagellar motion with a Young's Modulus of 150 kPa. As an alternative to the UV-mediated crosslinking approach, cell fixation via Michael-addition was investigated by means of PEG-vinyl sulfone and HASH as this combination offers the tunability of the crosslinking rate by the pH of the media. This investigation was launched by Glogger, M. and first results using 10 % polymer content showed very fast gel formation within less than 60 s already at 4 °C at pH 8.3 and rendered cell immobilization possible in close proximity to the glass support by gel formation during the centrifugation process which was beneficial for the following imaging procedure[125]. After the graduation of Glogger M., investigations of this promising hydrogel system were taken over by Schwebs, M. for motion studies of surface glycoprotein coats on living trypanosomes and required material supply with suitable HASH. As the preliminary HASH batch was of low molecular weight nature (<30 kDa) with a DS of approx. 50 %, two different HAs, 8-15 kDa and 80-100 kDa, were thiolated according to the optimized HASH protocol (2.1.1, p. 11) resulting in HASH with 12 kDa, 40 % and 53 kDa, 48 % that were tested for their applicability. Quantitative immobilization according to the preliminary hydrogel composition was not possible with both batches and the formulation was adapted, resulting in 15 % polymer content. Thereupon, HASH (53 kDa, 48 %) turned inapplicable for reasons of solubility in the required stock concentration (25 %) and HASH (12 kDa, 40 %) was chosen for further use. The Young's Modulus of hydrogels from the final formulation was determined in triplicates following the procedure of Oberst, K[80], revealing a value of 105 ± 29 kPa. A manuscript of the performed biological studies was in preparation by end of this thesis.

2.4.3 HASH + HAA

The idea for crosslinking HASH and HAA appeared during the C6-HASH synthesis when thiolating the acrylates with the acetyl-protected and hence monovalent thiol, thioacetic acid. The reaction was performed at 0 °C to prevent the *in-situ* generation of hydrogen sulfide, a bivalent thiol, by decomposition of thioacetic acid, and subsequent crosslinking of two acrylates/polymer strands. Intentional crosslinking via the underlying mechanism, Michael-addition, using high molecular weight HASH and low molecular weight HAA was considered to yield fast gelling hydrogels at physiological conditions with tunable properties based on the characteristics of the deployed polymers, which are both of natural origin and thus biodegradable. In first casting experiments, formulations of HASH (222 kDa, 38 %) and HAA (8-15 kDa, 75 %) with a 1:1 ratio and polymer contents of 1-5 % in 1 % steps were prepared using HEPES-buffer (154 mM, pH 7.6), incubated at 37 °C and examined manually in terms of gelation rate and hydrogel stiffness. All formulations formed transparent hydrogels within 15 min with a high shape fidelity, whereas gelation was faster and stiffness was higher the higher the polymer content of the precursor solution was. The high hydrogel stiffness of the 5 % formulation was similar to PEG- and HEMA-based hydrogels, used in-house for dual-setting cements[126-128], and in combination with the very fast hydrogel formation within <2 min, the idea for a dual-setting cement HA polymer network for bone defects was raised. The concept was to investigate the tunability of the hydrogel properties by its composition and the pH of the precursor solution to enable cement paste preparation and subsequent paste spreading in the bone defect of a patient. The gelation was meant to occur within 10-20 min, on the one hand to not interfere with paste preparation and application and on the other hand to avoid long-term wound exposure of the patient in the surgical room. With the use of a HA polymer network and α-TCP, resulting in hydroxyl apatite cement at physiological pH, the whole composition is biocompatible and biodegradable in the human body[129]. Unfortunately, the project was put on ice due to long-term reproducibility issues with the α-TCP synthesis until the end of this thesis and no preliminary studies of the hydrogel system were conducted.

2.4.4 HASH + HAPA

In recent literature, HAPA was used in combination with a bivalent thiol-crosslinker, DTT, for various applications such as 3D bioprinting[78] or microgel production[130] by various techniques and the synthesis was investigated by Oberst, K. during her master thesis and optimized in the final year of this thesis in cooperation with her as described in chapter 2.1.2, p. 27. In all these studies, the pentenoate modified HA was regarded as main polymer that is crosslinked with small thiol carrying molecules, leading to short distances between two crosslinked polymer strands and thus more likely to smaller mesh sizes, whereas its utilization as multi-arm UV-crosslinker for high molecular weight HASH was considered advantageous in term of larger mesh sizes and consequently improve biological performance. This combination of side-chain functionalized HAs provides not only biocompatibility but also potentially improved biodegradability of the network and the possibility of biological response to the HA matrix. The distance between crosslinking points along the polymer strands was regarded inhomogeneous, due to the random and non-quantitative modification occurring during each polymer synthesis. Though, variation of the polymer's DS might offer a huge flexibility of possible mesh sizes as well as broad stiffness range. As a starting point, HAPA 200-500 kDa with two different vinyl contents, 6 % und 34 %, were mixed in concentrations of 0.5-2.0 % in 0.5 % steps with 1 % HASH (385 kDa, 40 %) to investigate the effect of thiol under- and oversaturation on the shape fidelity and hydrogel stiffness, evaluated manually by poking with a rubber plunger and by its response to snipping against the underlying petri dish. For the preparation of the precursor solutions HEPES (154 mM, pH 7.6) with 0.05 % LAP was used, the mixture filled in borosilicate rings and irradiated with a 405 nm flashlight for 60 s. The resulting transparent hydrogels possessed a good shape fidelity, meaning minimal straddling

of the cylinder bottom, independent of the vinyl content while the stiffness increased with increasing vinyl content and increasing HAPA content even when the thiols were oversaturated with vinyl groups. Surprisingly, the formulation of 0.5 % HAPA (DS 6 %) yielded a very soft hydrogel with good cylindrical shape. However, volume stability was not examined due to the lack of biological applications of this hydrogel system. Since the precursor solution was viscous due to the viscosity contribution of the high molecular weight HAPA, the system was offered to cooperators using HASH+PEG-diacrylate hydrogels for 3D cultivation of HUVECs but was rejected as this was part of a MD thesis that had already started and a late stage change of the hydrogel system was deemed counterproductive. However, the particular hydrogel properties, namely high initial viscosity, rapid crosslinking, good shape fidelity, low stiffness and high flexibility at already low polymer contents of <1.5 %, were considered favorable for an in-house project of Dr. Blum, C., focusing on the influence of new drugs and drug delivery systems on the invasive behavior of glioblastoma cells in different polymer matrices. Cell spheroids were utilized to match the natural conditions of brain tumor, with cell-cell interactions, and fast gelling hydrogel systems were of great importance to prevent spheroid sedimentation. Thus, the project investigator was demonstrated the respective material handling and subsequently supplied with high molecular weight HASH (380 kDa, 40 %) and HAPA (200-500 kDa, 29 %) for preliminary applicability studies, which were still in progress by the end of this thesis.

2.4.5 HAA

Directly after the successful 8-15 kDa HAA synthesis with different acryl contents, the interest in the crosslinking behavior and properties of hydrogels from pure HAA was raised to identify potential applications. In a quick screening using duplicates different HAA (8-15 kDa, 98 %) concentrations (3, 4, 5, 10 %) in commercial PBS with 0.05 % LAP, the liquid to low viscous precursor solutions were filled in glass cylinders (ID 6 mm) and irradiated with 405 nm flashlight whereas within each duplicate, the samples were exposed to light for either 60 or 120 s. A clear trend of increasing hydrogel stiffness paired with increasing brittle fracture behavior with increasing HAA content was observed while no difference between 60 and 120 s exposure and no swelling of the hydrogels in PBS over 7 days was detected. However, the transparency of the hydrogels decreased slowly with increasing HAA content yielding a slightly turbid hydrogel at 10 % HAA. The stiffness of the hydrogels was much higher, than all other hydrogels produced in this project before, even higher than the HASH+PEG-vinyl sulfone hydrogels for trypanosome fixation (2.4.2, p. 67) and thus was considered a potential alternative for this specific application relying on fast gelling formulations. In the following, the minimum exposure time required was examined by means of 5 % HAA precursor solutions which were irradiated with the identical light source for 10, 20 and 30 s. All exposure times yielded proper crosslinked hydrogels with a very high stiffness and in a non-standardized crosslinking experiment, composed of a precursor solution drop running down a vertical glass surface through the light source beam, the formulation was found to yield a hydrogel within 2 s. Surprised by this extremely fast crosslinking behavior, the formulation was offered to Schwebs, M. for trypanosome fixation and on her request comparative DMA measurements, performed by Oberst, K., between the already utilized HASH+PEG-vinyl sulfone and 5 % HAA hydrogels revealed average Young's moduli of 105 kPa, respectively 330 kPa, which was regarded sufficient for this application. Another potential use for HAA was its application as alternative acrylate component for volumetric printing, a temporary project of Gergely, C. and Galaba, L., focusing on the refinement of the methodology for volumetry printing of GelMA using a rented volumetric printing device from Readily3D[131]. The idea was to first identify crucial printing parameters and resolution based on different resins, dipentaerythritol penta-/hexa-acrylate and subsequently transfer the obtained findings on GelMA. Hence, HAA was offered and demonstrated to the team and first printing trials were conducted with 5 % HAA and 0.05 % LAP. In simultaneous screenings, the

requirements for this specific material were examined with the result that the viscosity had to be adjusted by the addition of a thickener, HA (1-2 MDa), to prevent construct movement while spinning during the printing process and the photoinitiator (LAP) concentration had to be increased for proper curing due to the low intensity of the printers' built-in light source. Printing of larger constructs with the refined formulation of 5 % HAA (8-15 kDa, 98 %), 1 % thickener and 0.1 % LAP was planned but unfortunately could not be completed by the end of this thesis and will be subject of subsequent research. However, casting of tubular structures using this formulation was conducted to demonstrate the materials' potential. Accordingly, a pragmatic approach was chosen in which 2 mL of the formulation were pulled into a 5 mL serological pipette (ID 6 mm) and a spring steel rod (165 x 3 mm) was placed centrally in the solution. After curing with 405 nm visible light for 60 s, the obtained tubular construct with the dimensions of 140 x 6 mm was gently retrieved. Despite a wall thickness of only 1.5 mm, the hollow hydrogel possessed excellent shape fidelity (Figure 58) and was easily perfusable while remaining unaffected by long-term storage (60 days) in PBS. Due to the brittleness of the hydrogel, the flexibility of the construct was reduced along and across the longitudinal axis causing clear fracture in the event. No further experiments using this formulation were performed on account of the near end of this thesis.

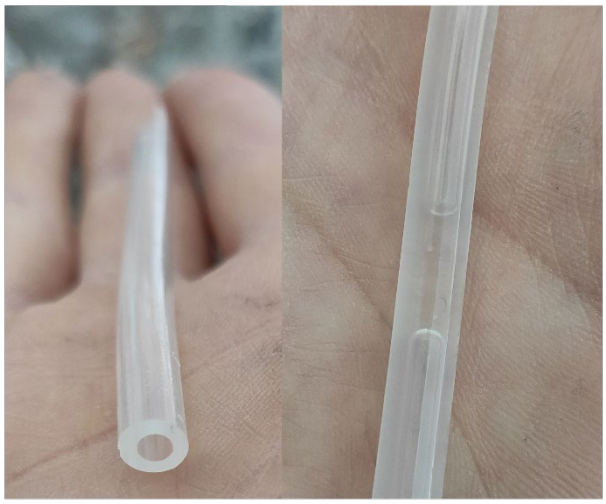

Figure 58: Photography of a casted tubular construct from 5 % HAA (8-15 kDa, 98 %) formulation in profile view of the cross section (left) and top view with meniscus after perfusion with PBS (right).

2.4.6 I2959 vs. LAP

Next to the spontaneous, chemical crosslinking via Michael-addition, UV induced crosslinking is often used for hydrogel preparation via FRP from precursor solutions containing α, β-unsatured carbonyl moieties, or via thiol-ene reaction based on thiols and allyl/vinyl functionalities. Both crosslinking reactions can be triggered without the addition of a photoinitiator as the reactants absorb UV-C radiation. Prominent FRP monomers such as acrylates, acrylamides and methacrylates possess a maximum in the range of 200-260 nm[132-134] whereas thiol-ene reactants require 210-320 nm[135,136] depending on the composition of the formulation. This irradiation with high energetic light is not only severely cell-damaging but also limits the deployable materials for characterization of the hydrogel and its application, as most laboratory inventory is made of plastics and glass, quantitatively absorbing UV light below 260 nm[137,138] and thereby necessitates the application of pricy quartz glass. In order to enable the use of less energetic UV light, photoinitiators were added to the formulation with different chemical und thus physical properties, of which two of the most frequent ones were used in this thesis, I2959 and LAP, and compared in the following. Due to its prominence in the literature and in in-house

projects, I2959 was used in the beginning of this thesis despite several disadvantages, namely its poor water solubility and absorbance maximum at 280 nm[139]. Crosslinking via this initiator was performed with a portable UV lamp, containing two light sources and respective UV filters for light emittance with 254 nm or 365 nm. The emitted light of both modes is non-monochromatic, covering wider ranges of wavelengths with a respective maximum and thereby can trigger the decomposition of I2959[139]. Even though, irradiation with 254 nm (UV-C) is more favorable than 365 nm (UV-A) with regards to quantum yield it was traded for better biological output and applicable material pool at the cost of longer exposure times and first hydrogel and ink developments were conducted using I2959 and 365 nm UV light. The poor water solubility of I2959 was not of importance for this thesis as the developed formulations contained PEG components which were acting as detergents and facilitated the dissolution process of the photoinitiator in the required concentration of 0.05 % while cooperation partners with micelle-forming hydrogel components or emulsion-based applications had severe crosslinking failures as the initiator transitioned to the lipophilic phase. Artificial enhancement of the water solubility was topic of the in-house master thesis of Partholl, L.[140] investigating the effect of POxylation of I2959 on its partition coefficient in water/1-undecanol and initiation efficiency for hydrogel formation. In her thesis, PMeOx was bound to I2959 using copper mediated azide click chemistry (CuAAC) enhancing the water solubility almost by factor 100 and resulted in near quantitative transition into the aqueous phase while the crosslinking efficiency was unfortunately reduced significantly. The multi-step synthesis paired with difficile light exclusion was considered reason for decomposition of the initiator before its application in hydrogel preparation as successful PEGylation of I2959 was demonstrated by Eren *et al*.[141] shortly after thesis submission with minor efficiency loss (0-10 %). Contrary to I2959, LAP represents a highly water-soluble initiator with an absorption maximum in the UV-A region at 370 nm offering several advantages regarding required light source, laboratory material and applicability. The quantum yield of LAP at 365 nm is at its near maximum and promotes very fast crosslinking reaction in all glass materials, whereas the broad range of absorption to up to 420 nm enables crosslinking with cell friendly, visible light through all transparent glass ware and plastics, thus abolishes all limits for application. Identical to I2959, the required LAP concentration was found to be 0.05 %, showing very good cell compatibility and by this replaced I2959 in further hydrogel and bioink systems in which 405 nm visible light was used for triggering the thiol-ene reaction.

2.5 Ink development and characterization

Regarding the development of bioinks, the current literature comprises no clear clues on how to proceed and mostly shows only qualitative final results instead of the development process. On top, the meaning of the terminology "printability" is highly discussed, and each publication has its own definition[142]. In this project, printability was understood as appropriately printable for the 3D bioprinting of hMSCs with the aim to biofabricate human cartilage tissue and matches the generic definition of a recent review from Gillispie *et al*.[142]: "The ability of a material, when subjected to a certain set of printing conditions, to be printed in a way which results in printing outcomes which are desirable for a given application".

2.5.1 HASH + PEG-acrylate + PEG-allyl carbamate

The development of the three component bioink was performed in cooperation with Hauptstein, J. from AG Blunk and consisted of numerous experiments that were conducted in parallel due to a very tight time schedule. The findings of each experiment led either to the termination of currently running experiments, the repetition of all related previous experiments under changed conditions or to the modification of the following series of experiments. Due to the shear amount of setbacks and concurrent non-linear development processes, discussion of each step would complicate the understanding of the bioink development and therefore it is described in summary below by means of the materials from the bioink platform publication[119]. Individual discoveries of the ink development process and subsequent changes will be listed at the end of this recapitulatory section. Data collected from Hauptstein, J. can only be shown partially, as most of it will be contained in her own thesis but will be qualitatively summarized in own words.

Summarized ink development

The targeted dual-stage crosslinking bioink was developed with regards to the application, 3D bioprinting of hMSCs, based on mainly subjective and qualitative evaluation techniques, detached from the recent literature, and the final ink formulation was then characterized objectively and quantitatively in terms of filament classification, printing accuracy and rheology after achievement of 3D bioprinting with the desired biological outcome for comparison with different bioinks and printing conditions of the TRR225. Starting with the first crosslinking stage, Michael-addition, the requirements for gelation, examined previously in chapter 2.4.1, p. 63, were investigated further by means of HASH (230 kDa, 43 %) and 6k-PEG-diacrylate with the focus on minimizing the polymer content for improvement of biological output[143]. For this, the extrudability screening was repeated with a fixed HASH content of 0.5 % and variable acrylate crosslinker concentrations in HEPES (154 mM, pH 7.6) after incubation at 37 °C while a second parameter, the obtained strands, was monitored photographically. An incubation time of 1 h was regarded tolerable for the incorporation of hMSCs according to experiences from preliminary experiments of Hauptstein, J. and hence was chosen for the extrudability screening (Figure 59). The extruded formulations were classified into three categories: drops, smooth strands and grainy strands, which can be correlated to the three states of gelation of Ouyang *et al*.[144]: under-gelation, proper-gelation and over-gelation. Under-gelled formulations were extruded dropwise and deliquesced on the flat surface whereat over-gelled mixtures resulted in grainy strands that exhibited a high shape fidelity but were more likely to break off. Proper-gelled hydrogels were extrudable as continuous smooth strands which kept their shape.

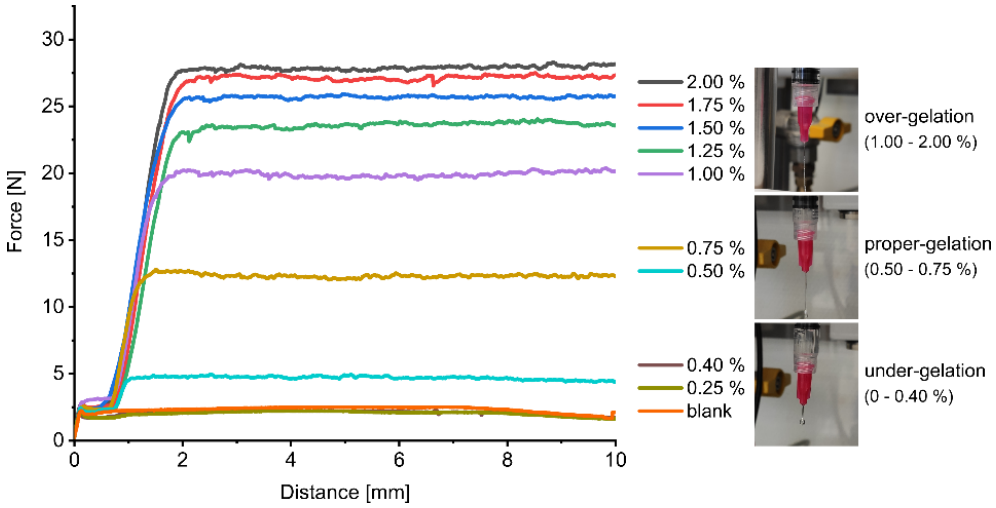

Figure 59: Force-distance diagram from mechanical extrusion of formulations with 0.5 % HASH and different 6k-PEG-diacrylate contents after incubation (1 h, 37 °C) correlated with the gelation status, with permission from Hauptstein *et al*.[119].

In the range of 0-0.4 % PEG-diacrylate no measurable hydrogel was formed within the incubation period and the formulation was extruded dropwise, while 0.5-0.75 % acrylate crosslinker yielded a proper-gelled formulation with the least polymer content forming smooth strands. With increasing crosslinker content, the required force increased initially fast between 0.5-1.0 % and then converged slowly towards 28 N with 2.0 %, which can be related to the saturation of free thiols or the maximal possible crosslinking. Despite the fact, that calculation of the thiol saturation for this specific HASH batch (DS 43 %) revealed 100 % saturation with already 1.60 % PEG-diacrylate, the hydrogel stiffness increased within 1.5-2.0 % which can be attributed to the circumstance that not all acrylates are in reactive proximity to two thiols and slight oversaturation increased the crosslinking chance. Concentrations above 2.0 %, were deemed to result in mono-PEGylation of the thiols instead of crosslinking and consequently reduced hydrogel stiffness. The filaments from the proper-gelled formulations were partially inhomogeneous due to the random nature of the crosslinking mechanism and far away from perfect shape fidelity but were considered comparable with the properties of HASH+P(AGE) hydrogels from a previous publication[143] und thus suitable for the targeted application. First 3D printing experiments, in a two-layer grid pattern, with the proper-gelled formulations were successfully performed by Hauptstein, J. and the results only differed slightly in shape fidelity and spreading of the strands on the flat surface and crossover points. Since air oxidation of the thiols causes the formulation to strengthen over time, the time span from which the formulation becomes printable until the non-printable state was examined and named processing window in the following. The experimental setup was kept simple with only HASH+PEG-diacrylate formulations in different concentrations and 1:1 ratios being incubated at 37 °C while manually monitoring their extrudability and shape fidelity using a displacement pipette (Figure 60) at defined time points: 10, 20, 30, 45, 60, 90, 120, 180, 240, 300 min with the formulation status being recorded accordingly by means of six categories: liquid, viscous, viscous-printable, printable, printable-stiff, stiff.

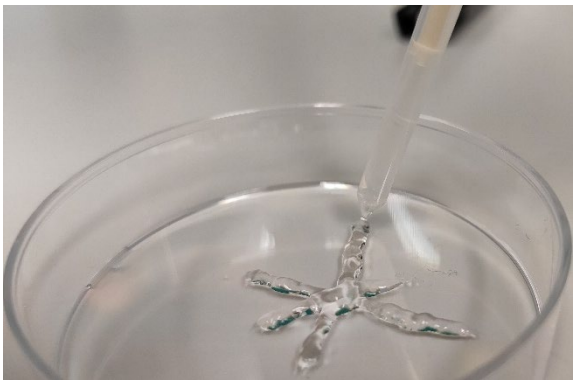

Figure 60: Photography of an exemplary manual extrudability experiment with a 250 µL displacement pipette.

The second crosslinking stage, the thiol-ene reaction between the remaining thiols and PEG-diallyl, was investigated by means of HASH (230 kDa, 44 %), 6k-PEG-diacrylate and 6k-PEG-diallyl carbamate. Long-term incubation of HASH+PEG-diacrylate hydrogels resulted in shrinkage of the gels accompanied by an increase in stiffness, originating from the disulfide formation of the remaining free thiols via air oxidation and coined the term thiol saturation. The idea was to ensure stable hydrogel properties with respect to stiffness and volume stability after the final crosslinking by saturation of the remaining free thiols with an appropriate amount of PEG-diallyl carbamate. Therefore, a saturation screening was conducted consisting of the preparation of hydrogels under identical conditions with constant HASH/PEG-diacrylate content but different concentrations of thiol-ene crosslinker via the dual-stage crosslinking approach and monitoring the wet weight of the resulting hydrogels under cell culture conditions over 21 d. The HASH/PEG-diacrylate content was set to each 0.5 %, as initiator concentration 0.05 % I2959 was used, and the allyl crosslinker was added in concentrations of 0-2.0 % in 0.25 % steps. A better comparability for the desired 3D bioprinting application without complication of the wet weight analysis was generated by extrusion of the formulation into glass cylinders after pre-crosslinking (1 h, 37 °C) following irradiation (365 nm, 10 min). The actual data is content of the published thesis of Hauptstein, J.[145] and will be shortly described in the following. A clear trend was observed for the volume stability depending on the allyl crosslinker content, showing first decreasing shrinkage of the hydrogels between 0-0.75 % and increasing swelling between 1.25-2.0 % PEG-diallyl carbamate. These findings can be explained by the saturation status, meaning that under-saturation results in shrinkage by disulfide formation while over-saturation yields swelling of the hydrogel due to the excess of bivalent, telechelic PEG UV-crosslinker, bound by only one end and hence withdrawing of water from the surrounding, similar to an occurring PEGylation. Total volume stability was solely obtained from the formulation with 1.0 % UV-crosslinker representing a thiol saturation of 93 %. The residual 7 % did not affect the volume stability and were deemed not being in reactive proximity for disulfide formation. With this experiment, the effect of under- and over-saturation of the thiols was clearly demonstrated, and the obtained findings were transferred onto the ink development using other HASH batches[119].

The final formulation was then used for replication of the 3D printing experiment of grid structures, showing no effect of the added low molecular weight PEG UV-crosslinker on the initial viscosity, the pre-crosslinking and 3D printability while increasing the final stiffness of the construct as intended. A consecutive 3D bioprinting experiment with hMSCs was successful and exhibited very good cell viability over 21 d, which was nearly identical to hMSCs in comparative, casted hydrogels, confirming two aspects of the main hypothesis of this subproject: simple incorporation of the cells into the initially low viscos precursor solution and their protection from shear stress during extrusion by the pre-crosslinked ink. The latter indicated shear thinning behavior of the bioink which was proven afterwards via rheological characterization of three formulations by Nadernezhad, A. (Figure 61b). The

gelation point in these characterization experiments was reached after 40-110 min after which a continuous slow increase was observed which can be attributed to the inevitable disulfide formation of the remaining free thiols over the course of time (Figure 61a). Investigation of the UV crosslinking process in the second stage of this dual-stage approach revealed fast reaction kinetics with decreasing slope after 60 s (Figure 61d) that yielded not only the targeted enhancement of the viscoelastic properties (Figure 61c) but also the intended terminal plateau after the second crosslinking stage. Chondrogenic differentiation of the hMSCs after 3D bioprinting was successful and showed homogenous ECM distribution over the whole construct meaning the mesh size of the final hydrogel was flexible or large enough for macromolecular passage and hence represents a major advancement compared to the preliminary ink system based on HASH+P(AGE) using PCL support structures for 3D bioprinting. The influence of the excreted ECM on the hydrogel stiffness was investigated by DMA measurements at day 1 and 21 and revealed a more than 70-fold increase of the Youngs' modulus in printed constructs using bioinks with HASH of larger molecular weight (≥230 kDa), while constructs from low molecular weight HASH (51 kDa) bioink was too dense for a sufficient ECM distribution and consequently showed nearly no change in overall stiffness after differentiation. These findings were underpinned by diffusion experiments using FITC dextran with different molecular weights[119].

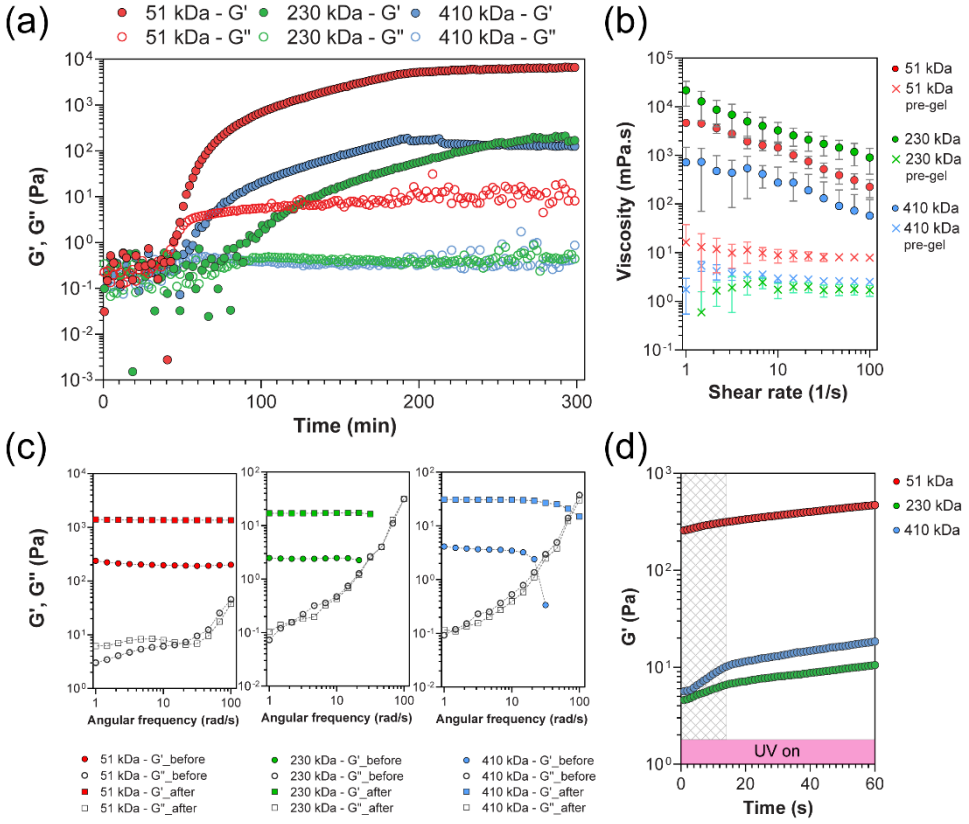

Figure 61: Rheological characterization of three bioinks based on different molecular weights of HASH consisting of a) time sweep of the pre-crosslinking b) shear rate sweep before and after pre-crosslinking c) frequency sweep before and after UV crosslinking d) time sweep of the UV crosslinking process, with permission from Hauptstein *et al.*[119].

Individual findings

During the HASH+PEG-diacrylate hydrogel screening, a 1:1 ratio was used representing 30-33 % thiol saturation for HASH batches with 40-45 % DS whereas formulations with different ratios were also found printable. The main difference between these formulations was the length of the processing window which was the longest with 3 h in the case of 1:1 ratio and became shorter the higher the PEG-diacrylate content was. The processing window was determined by manual extrudability tests of each formulation at defined time points over 5 h, namely 5, 10, 20, 30, 45, 60, 90, 120, 180, 240, 300 min. For this purpose, the formulation was incubated at 37 °C, drawn up a displacement pipette, extruded while its viscosity and obtained strands were evaluated visually by the operator and placed back in the incubator. Progressing oxidation of the thiols led to strengthening of the hydrogel and consequently to gradually decreased water retention capacity of the hydrogel which yielded excretion of the hydrogel media, so called syneresis. This effect was observed for all formulations, independent of their ratios or the utilized buffer, after 3-5 hours of incubation and gradually impeding printability of the formulation (Figure 62).

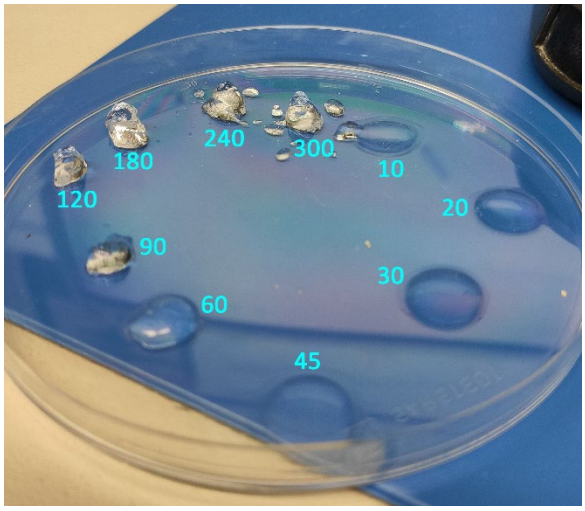

Figure 62: Photography of an exemplary HASH+PEG-diacrylate formulation mechanically extruded at different time points over 300 min of incubation at 37 C, showing the processing window and syneresis. Numbers represent minutes of incubation.

The photography demonstrates the gelation status of the incubated formulation of HASH (230 kDa, 43 %) and 6k-PEG-diacrylate in 0.5/0.5 % ratio over time by the mechanical extrudability experiment. The formulation remains liquid to slightly viscous within the first 45 min that resulted in thin disc-like structures and changed from a broad flat to a narrow tall hydrogel pile between 60-180 min representing the processing window. Afterwards, syneresis progressively occurred indicated by solvent droplets around the extruded hydrogel cf. 240-300 min. Similar to 6k-PEG-diacrylate, the processing window for formulations with 10k- and 20k-PEG-diacrylate was investigated and showed comparable behavior and syneresis during incubation although a larger amount of acrylate crosslinker was required to result in a printable formulation with increasing crosslinker length due to less functionalities per mass of crosslinker[119]. In the next step, the thiol saturation via PEG UV-crosslinker, initially two different geometries and molecular weights were compared with each other, 8-arm-10k-PEG-allyl carbamate and 5k-PEG-diallyl carbamate whereas the linear geometry resulted in more volume stable formulations due to less concentration of functionalities per crosslinker molecule and consequently better distribution. Additionally, the latter was produced from commercial PEG-diamine as the synthesis of PEG-amine was still in progress by this time and replaced, later, by the self-synthesized linear 6kDa variant without changes of the concentration as near identical volume stability observed. This unexpected finding could not be

explained since both crosslinker exhibited quantitative allyl functionalization via identical reaction conditions but might originate from slight oligomerization during the allylation reaction (2.2.5, p. 49) of the 5k variant paired with the only minor difference in molecular weight. Ultimately, the formulation remained unaltered with 0.5/0.5/1.0/0.05 % of HASH/6k-PEG-diacrylate/6k-PEG-diallyl carbamate/I2959 for all HASH batches with M_w 200-500 kDa and DS 40-45 %. The rheological investigation of the processing window by time sweeps was found not matching the observations of manual printability experiments since the gelation point was reached after different time points depending on the concentration of HASH and 6k-PEG-diacrylate and the molecular weight of HASH and could not be fully explained by shear data (Figure 61a, p. 75). However, the hypothesis was formed that this discrepancy originates from the differences in the hydrogel formation in both experiments. While the manual printability evaluation was performed in bulk hydrogels constantly mixed by incubation and extrusion, hydrogels in rheological studies were formed under nearly stationary conditions and feature reduced probability of reactive proximity of the components[119].

2.5.2 HASH + PEG-acrylate + HAPA

During the revision process of the publication on the previous bioink, the expansion of the bioink platform by replacing the 2-arm PEG UV-crosslinker with multi-arm HA vinyl crosslinker, HAPA, was investigated. The underlying hypothesis was based on several aspects. Mainly, the switch from synthetic to natural UV-crosslinker was regarded as more advantageous in terms of biodegradability and the increased content of hyaluronic acid components in the ink was considered to have potentially positive effects on the cell-material interactions. Furthermore, the initial viscosity as well as the final strength of the constructs can be specifically adjusted by the selection of the molecular weight of HAPA, thus enabling application-oriented fine-tuning. Based on the experience from the previous ink developments, a series of HAPA batches with different molecular weights and DS of approx. 30 % were prepared and several experiments were conducted in cooperation with research assistant Oberst, K. to extend the bioink platform, which is described below.

The HASH+PEG-diacrylate concentrations were kept identical to the previous ink at 0.5 % each, corresponding to a thiol saturation of 30 % with respect to the utilized HASH batch (410 kDa, 44 %) while I2959 was replaced by LAP (0.05 %) and visible light (405 nm) was used for triggering the thiol-ene reaction. The required saturation for volume stability was investigated by a screening experiment using HAPA (200-500 kDa, 29 %) similar to the preliminary ink development. Accordingly, hydrogel cylinders (n=3) were prepared via the dual-stage crosslinking approach with different HAPA contents, resulting in calculated thiol saturations of 90, 100 and 110 %, and their swelling behavior was investigated by determining the wet weight deviation over a period of 21 days. The gels were incubated in commercial PBS at 37 °C, the medium was exchanged daily and hydrogels without HAPA were used as reference (Figure 63).

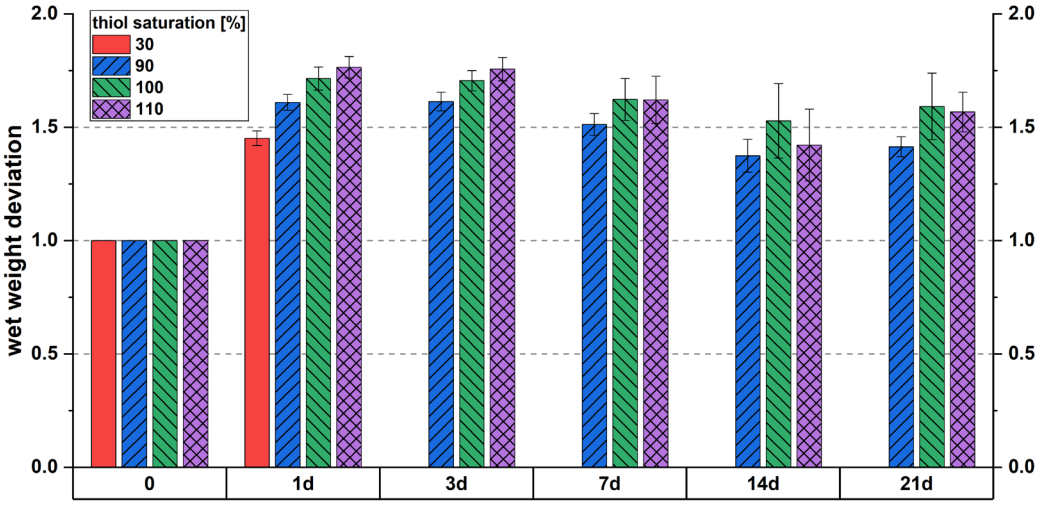

Figure 63: Volume stability of HAPA bioink hydrogels in PBS at 37 °C over 21 days depending on the thiol saturation using HAPA (200-500 kDa, 29 %).

The study showed strong swelling behavior for all hydrogels with HAPA, regardless of the degree of saturation, while the reference gels with 30 % thiol saturation disintegrated after 24 h and could no longer be weighed whereas the weight of the gels with HAPA increased to a maximum of 1.5-1.75x within the first 24 h and continuously converged to lower values of 1.3-1.6x at d21. The swelling of the reference gels to the 1.4-fold until d1 was also observed in the swelling studies with 6k-PEG-diallyl carbamate by Hauptstein, J. Furthermore, the initial viscosity of the precursor solution and the shape fidelity of the hydrogels was increased the higher the HAPA content was and due to the absence of a clear favorite in terms of volume stability, a thiol saturation of 110% with the highest shape fidelity was chosen for subsequent investigation of the influence of the HAPA molecular weight on the swelling behavior under identical conditions. HAPA from all available HA batches except 2.0-2.5 MDa were used with very similar DS of 29-32 % to keep the required HAPA content constant and accordingly ensure comparability. The procedure and conditions were identical to the previous volume stability tests, although this study was limited to 14 days due to time constraints as no trend changes between d14 and d21 were expected. The data obtained revealed a clear trend of increased hydrogel swelling with increasing molecular weight of HAPA and the swelling occurred within the first 24 h after which, the wet weight decreased slightly until d14 (Figure 64). While gels with 1-2 MDa HAPA swelled the most with a factor of 1.9, the weight increase of gels with 8-15 kDa HAPA was only 1.5-fold and thus almost equal to the reference without HAPA. Similar to the swelling behavior, the initial viscosity and the shape fidelity increased the higher the molecular weight of the deployed HAPA, whereas no difference in shape fidelity between 200-500 kDa and 1.0-2.0 MDa HAPA was observed. To exclude swelling from diffusion of unbound HAPA out of the hydrogels, the experiment was repeated using unmodified 200-500 kDa HA instead of HAPA in direct comparison with 200-500 kDa HAPA whereas the HA content was equivalent to the applied HAPA content (Figure 64).

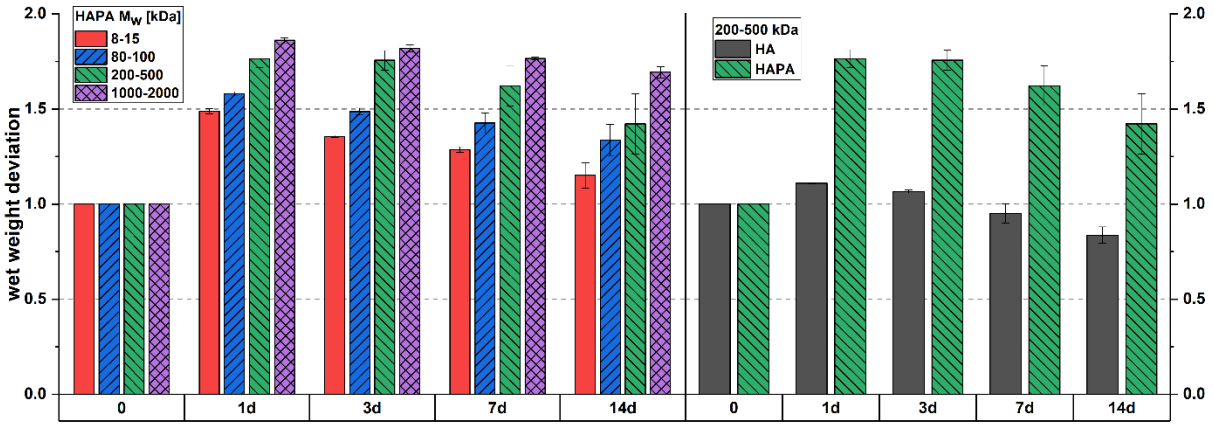

Figure 64: Volume stability of HAPA bioink hydrogels in PBS at 37 °C over 14 days depending on the molecular weight of HAPA (left) and comparison of unmodified HA instead of HAPA with M_w 200-500 kDa (right).

Interestingly, the hydrogels with unmodified HA remained stable over the entire 14 days instead of disintegrating like the reference hydrogels with pure HASH+PEG-diacrylate and swelled only 1.1-fold, significantly less than the HAPA gels with a factor of around 1.75. Based on this, it can be concluded that the unmodified HA does not diffuse or only slightly out of the hydrogel, otherwise the swelling factor at d1 would be significantly higher than for pure HASH+PEG-diacrylate hydrogels. The HA seems to be anchored within the network and not located inside of single meshes, since apparently no or hardly any diffusion takes place which, however, is possible, even for larger macromolecules (ECM), as recently demonstrated by Hauptstein *et al*.[119,143]. Furthermore, crosslinking with HAPA resulted in enhanced swelling depending on its molecular weight. Swelling due to diffusion of low molecular weight components from the HAPA product, such as salts and degradation remnants, can be excluded, since the product does not degrade during synthesis and purification and was dialyzed against MilliQ. Rather, the hypothesis is that the HAPA is partially unbound, drawing additional water due to the associated high degree of freedom, similar to PEGylation. However, testing this hypothesis using HAPA with DS 100 % proved to be complex for several reasons. First, the solubility of HAPA decreases with increasing DS and limits the suitable HAPA batches to a single molecular weight, 8-15 kDa. Second, this very small HAPA exhibits a high density of allyl functionalities, requiring only small amounts to yield 110 % thiol saturation and thus not comparable to the previous experiments. The local concentration of allyl moieties is also highly prone to cause significant differences between calculated and actual thiol saturation as not all reactive thiols are in such close proximity but rather spatially distributed, which favors the formation of disulfides and consequently shrinkage. As a result, the swelling was regarded as inevitable and the ink development continued.

The biocompatibility and ECM distribution of hMSCs after chondrogenic differentiation within the HAPA bioink was subject of the following experiments which were conducted by Hauptstein, J. under identical conditions to the already established bioink. The cells were 3D bioprinted using a bioink composed of HASH (410 kDa, 44 %), 6k-PEG-diacrylate, HAPA (200-500 kDa, 29 %) and LAP in concentrations of 0.5/0.5/0.63/0.05% representing 110 % thiol saturation, differentiated and the biological output was monitored qualitatively and quantitatively over 21 days in comparison with the published bioink based on 6k-PEG-diallyl carbamate. Regarding the biocompatibility after 3D bioprinting, both bioinks exhibited very high cell viability after the printing process proving the protection of the cells from shear stress during printing by the pre-crosslinked bioink (Figure 65) and ECM and DNA quantification revealed no major differences between the ink formulations with each very high ECM production per DNA (Figure 66). Histological staining of ECM components unfortunately showed only mediocre ECM distribution throughout the constructs of the HAPA bioink with more

pronounced pericellular ECM residence compared to the ubiquitous ECM distribution in constructs of the PEG-diallyl carbamate bioink (Figure 67).

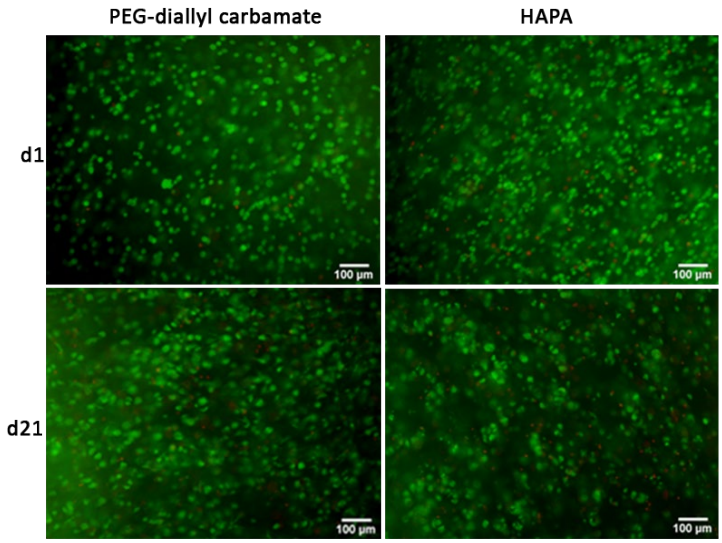

Figure 65: Qualitative cell viability analysis of 3D printed hMSCs in two different bioinks over 21 days via live/dead staining (green/red).

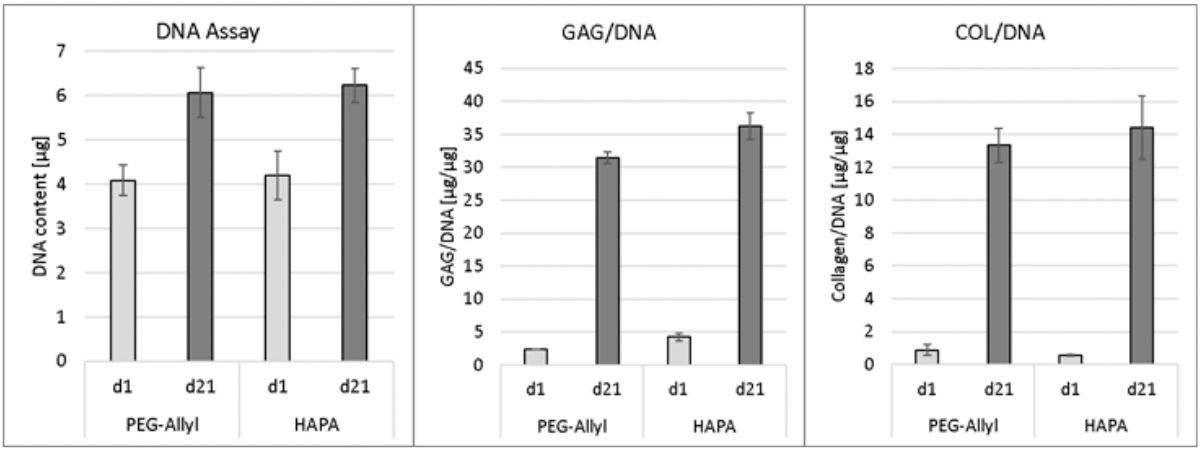

Figure 66: DNA and ECM/DNA quantification analysis of 3D bioprinted constructs from the two different bioinks at d1 and 21.

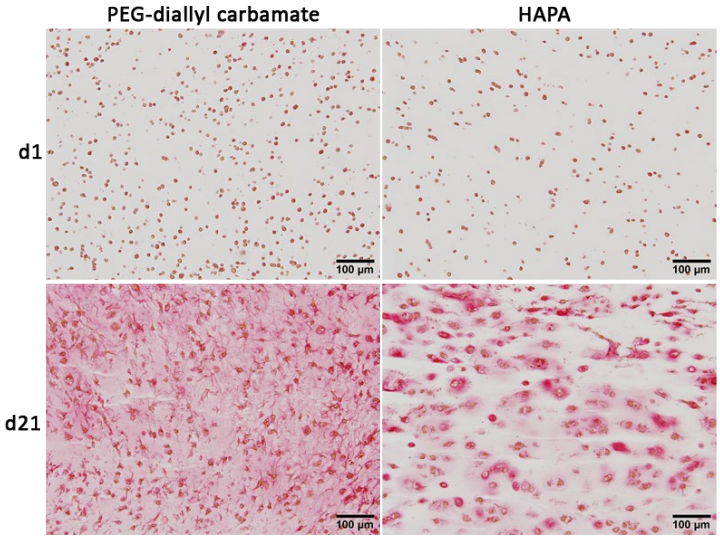

Figure 67: Qualitative histological analysis of ECM distribution in 3D bioprinted constructs from the two different bioinks at d1 and d21 via picrosirius red staining of entire collagens.

The printability assessment and rheological characterization before the investigation of the biological output was omitted as the latter was of highest priority for the ink development. The reduced ECM distribution was regarded as a major drawback with respect to the subprojects' objective application and led to the termination of the ink development in the context within this thesis and will be evaluated in the future. Investigations into the printability and rheological properties of the bioinks were initiated out of interest, but these were not performed in their entirety and only partial documentation of the results is available, which do not meet the scientific requirements of a doctoral thesis and are therefore not shown. In depth investigations of this bioink composition are part of future research. Summarizing the above-mentioned findings, the HAPA bioink exhibits the hypothesized high flexibility in terms of initial viscosity of the precursor solution and final stiffness as well as shape fidelity of the constructs after UV exposure depending on the deployed molecular weight of the HAPA but lacks the required biological output namely ubiquitous ECM distribution. Further investigations with regards to the tunability of ECM distribution by variation of molecular weight and vinyl content of the HAPA were considered potentially worthwhile but could not be conducted by the end of this thesis.

2.5.3 HAA + HA

The observation from the development and characterization of HAA hydrogel formulations towards applications for trypanosome fixation and volumetric printing (2.4.5, p. 69) paired with the call for bioinks of the C03 subproject, investigating 3D models for melanoma cell studies, piqued interest to tailor a suitable HAA bioink for the cooperators. The project was investigating tumor dormancy in different bioink matrices and using by this time 3 % alginate as reference, yielding a stiff hydrogel with a Youngs' Modulus of 80 kPa, according to them. Since unmodified alginate features no inherent cell instructive characteristics[146], highly acrylated hyaluronic acid was deemed to show similar properties and hence possibly match the projects' requirement. However, the hydrogel formulation was not printable and had to be developed towards the applicants' laboratory infrastructure. The general idea was to get shown the cooperators' exact workflow to outline the desired application and to adapt the ink most appropriately but was compromised by the current business trip restriction of the respective institutes and the development had to be performed together in a feedback loop. The loop consisted of the supply with materials plus handling instructions and feedback-based adaptation of the formulation on the A02 site while the cooperators provided the required feedback after evaluation of

the respective 3D (bio-)printing trials (Inkredible+). In the beginning, the necessary hydrogel stiffness was unknown as DMA measurements of the HAA were performed at a later date and a formulation of 10 % HAA (8-15 kDa, 98 %), 4 % HA (1-2 MDa) and 0.05 % LAP was manually tested for printability. The very viscous and transparent, homogeneous solution was easily extrudable and yielded smooth, uniform strands while the strands gradually deliquesced 20 s after deposition, which was tested sufficient for layer wise crosslinking with 405 nm flashlight from a 5 cm distance in a vertical angle. The materials were sent to the cooperators for ink preparation and initial 3D printing trials which were less successful as the dissolution of the thickener in a concentration of 4 % was proved difficult with their laboratory equipment and only inhomogeneous mixtures were obtained. Following, the ink preparation was performed in-house using a benchtop incubator and planetary mixer (Thinky) in 15 mL scale and shipped to the collaborators. The very high viscosity of the ready-to-use ink led to complicated cell incorporation and reduced cell viability after casting as well as printing but showed the targeted dormancy and hence was pursued further. A subsequent viscosity screening with constant HAA and LAP content and thickener concentrations between 1.0-3.0 % in 1 % steps, a viscosity by 2.0 % thickener was required for layer wise crosslinking whereas the printing resolution in all cases was gradually comprised by diffluence the lower the thickener content was. Instead, printing trials with *in situ* crosslinking by the exact 405 nm flashlight used for the manual printing evaluation led to improved printing resolution and counteracted the strand diffluence. A second viscosity screening with 1.0-2.0 % thickener in 0.5 % steps did not reveal new insights as 2.0 % thickener yielded still the best printing resolution of them three. In a further refinement screening, the influence of the photoinitiator concentration on the printing results and cell viability was investigated by means of constant HAA (10 %) and thickener content (2.0 %) whereat discrete LAP concentrations with 0.05, 0.1 and 0.5 % were utilized. Increasing the LAP content to 0.1 and 0.5 % resulted very fast crosslinking and consequently better printing resolution as the strands were nearly instantaneously crosslinked during deposition while the cell viability was slightly (0.1 %) to strongly (0.5 %) reduced compared to the reference with 0.05 % LAP. However, the increased printability of the 0.1 % LAP formulation was found favorable and consequently traded for slightly reduced cell viability. As DMA measurements of 5 % HAA hydrogels for the application as trypanosome fixation hydrogel (2.4.2, p. 67) showed a much higher Youngs' Modulus of 330 kPa compared to the alginate reference with 80 kPa, the 10 % HAA ink formulation was regarded as possibly too stiff for nutrient supply of the cells and subsequently the HAA concentration was reduced in a final screening to 1.0-5.0 % in 1.0 % steps. For reasons of comparability, the HA and LAP concentration was fixed with 2.0 %, respectively 0.1 %. By end of this thesis, these experiments were still in progress.

3 Summary and outlook

The aim of this work was to develop a bioink platform of three-component bioinks based on thiolated hyaluronic acid (HASH), PEG-acrylate and PEG-allyl carbamate tailored for the biofabrication of human mesenchymal stem cells (hMSC). First, the literature-known syntheses of each component were optimized in terms of synthesis parameters and product purification to improve product quality, synthesis reproducibility, and batch size scalability. The synthesis of HASH was carried out in an incubator at 37 °C in buffered media and the formation of an undesired by-product was prevented by the addition of NHS. Dialysis against acidic media with initial addition of TCEP gave the product in the desired quality, whereas the thiol content could be tuned between 1-100 %, but not the molecular weight of the product due to its acid lability and thus random degradation. The choice of starting material enabled molecular weights of up to 577 kDa to be attained, which were determined together with the dispersity via size-exclusion chromatography (SEC MALS). The thiol content was determined by ^{1}H NMR by comparing significant signals of the repeating unit and the thiol-bearing modification. Simultaneously, PEG-acrylates with molecular weights in the range of 1.5-20 kDa and different geometries (linear, 4-armed and 8-armed) were synthesized in a flask or incubator. The quantitative acrylation and the purification of the product were of highest importance for the intended use as ink component and were determined by ^{1}H NMR with the addition of trifluoroacetic anhydride and the molecular weight was investigated by SEC MALS. In the case of linear PEG-acrylates, alcoholysis of acryloyl chloride and recrystallization in EtOH as well as filtration over activated carbon were found to be suitable, while branched PEG-acrylates were better represented via enzymatic transesterification followed by washing. For the synthesis of PEG-allyl carbamate, PEG-amine was first prepared via two different synthetic routes, mesylation followed by amination using aqueous ammonia and via Mitsunobu reaction using phthalimide with subsequent hydrazinolysis. The latter proved to be very sensitive to traces of water and oxygen though prevented oligomerization of the PEG amine and was thus favored. The introduction of the allyl function was realized under alkaline aqueous conditions and addition of allyl chloroformate, while oligomerization of the product was inhibited by cooling the reaction solution to 0 °C.

In addition to the main components of the three-component bioink, other hyaluronic acid derivatives were produced, which were used for the expansion of the bioink platform and for various applications tailored to the requirements of several internal and external cooperators. As an alternative to the introduction of the thiol group via the carboxylic acid function of hyaluronic acid, the thiolation of the C6-alcohol was developed. In the first step, the C6-alcohol was acrylated in a Schotten-Baumann reaction using acrylic anhydride, and a thioester was subsequently introduced using thioacetic acid, which was ultimately hydrolyzed. The degree of thiolation could be selectively adjusted in the range of 30-49 % and the molecular weight of the product (C6-HASH) could be influenced by the choice of starting material. Hyaluronic acid acrylate (HAA) was synthesized by purification after the Schotten-Baumann reaction of the same synthetic route, whereat the use of a different anhydride, pentenoic anhydride, under identical conditions gave another HA ester, hyaluronic acid pentenoate (HAPA). The degree of functionalization (DS) of both hyaluronic acid esters was controlled by the amount of anhydride added, while these products were water-soluble only up to 50 % DS without limitations. The reaction conditions were chosen such mild that the molecular weight of the starting material remained constant throughout the synthesis. While HAPA was synthesized using all available molecular weights of hyaluronic acid batches, HAA was prepared mainly from low molecular weight HA of 8-15 kDa due to the tendency of the product to oligomerize. The purity of the product and the degree of functionalization of C6-HASH and HAA were determined by ^{1}H NMR, whereas HAPA was determined by an in-house developed HPLC assay on account of its increased hydrophobicity with increasing DS. The molecular weight of these three HA derivatives were analyzed by SEC MALS.

In addition to the polymeric products, small organic compounds, DTPH for HASH synthesis and a short non-specific protease-cleavage peptide sequence (APGL) for the improvement of the biodegradability of the bioink, were also prepared in flasks or Schott bottles, which were analyzed via ^{1}H NMR and HRMS. DTPH synthesis was established because of long delivery times and ultimately substandard purity of the commercial product and scaled up to the limit of the laboratory infrastructure, with particular focus on product quality. The peptide synthesis was strategically divided into the preparation of two dipeptides, AP and GL, which were subsequently condensed to form the desired tetrapeptide. The dipeptides were thereby prepared in two steps starting from the Boc-protected amino acids alanine and glycine, which were first converted to the respective NHS ester and then reacted with proline and leucine, respectively. Deprotection of the Boc-GL dipeptide was performed in methanolic HCl to simultaneously generate a methyl ester, which yielded the desired Boc-tetrapeptide by coupling with Boc-AP-NHS and subsequent ester cleavage in methanolic sodium hydroxide solution.

Chapter 2.4 comprises the different hydrogel compositions based on the synthesized HA or PEG derivatives and their respective applications. First, the requirements for gelation via Michael-addition of HASH and PEG-acrylate are presented, which were investigated by several screening experiments based on different batches of the components. By means of one HASH batch, the concentrations of linear PEG-acrylate were varied at a fixed HASH concentration, and the gelation kinetics as well as the hydrogel stiffness were examined manually. Furthermore, the hydrogel properties were mechanically monitored in a specially adapted extrudability test setup from Weichhold, J. of the AG Gbureck and by preliminary rheological experiments. HASH with a thiol content of 40-60 % and PEG-diacrylates with M_n 1.5-20 kDa were shown to be suitable. Multi-arm PEG-acrylates did not show any particular advantage over the linear derivatives because of the increased local density of their functional groups. Depending on the HASH M_w, hydrogels with polymer contents of 1 % or 5 % could be prepared in combination with 6k-PEG-diacrylate, whereas the boundary value of the HASH M_w was between <100 kDa and >200 kDa. The developed hydrogel formulations were given to a variety of collaborators and subsequently tailored to their applications. A formulation with 1.5 % polymer content and 1:1 ratio of HASH to 6k-PEG-diacrylate proved promising in the case of AG Villmann for their investigation on the formation of neuronal networks in 3D cell cultures with ultra-soft matrix, while the collaboration with AG Cicha preferred a hydrogel system with 2 % polymer content with the same ratio of components for 3D cell culture of HUVECs to investigate the embedding of pre- and post-endothelialized networks in tissue-specific hydrogels. In the AG Blunk, low-viscos HASH and 6k-PEG-diacrylate were required for the development of mixing heads for 3D printing of gradient hydrogels. Furthermore, tailored HASH was produced for the existing collaboration with AG Fenz using a HASH/PEG-vinyl sulfone hydrogel system for the fixation of trypanosomes. A molecular weight <15 kDa and a thiol content of 40-45 % were found to be optimal for this application. A composition of high molecular weight HASH and low molecular weight HAA were also investigated without leading to a specific cooperation. It was observed that hydrogel formation of this system occurs within <2 min and, depending on the polymer content, very strong hydrogels can be generated that might be suitable for use as a polymer network in bone replacement composites. In addition, hydrogel systems based on radical thiol-ene crosslinking with the photoinitiator LAP were investigated. Screening experiments for the preparation of HASH/HAPA hydrogels revealed an adjustable high initial viscosity of the precursor solution depending on the choice of HAPA M_w and increased shape fidelity and flexibility while containing a very low polymer content of <1.5 %. The crosslinking in this case occurred under visible light at 405 nm within 60 s and, together with the hydrogel properties, proved to be a potential candidate for the research by Blum, C. in AG Groll focusing on the impact of new drugs and drug delivery systems on the invasive behavior of glioblastoma cells in different polymer matrices. Hydrogels based on pure HAA with and without HA as thickener were developed as an alternative for

the trypanosome fixation via Michael-addition. The mechanical properties (Young's modulus) of both hydrogel systems were analyzed and compared. Hydrogels with pure HAA and a polymer content of 5 % proved to be more than three times as strong as previously used formulations of HASH/PEG-vinyl sulfone with a polymer content of 10 %, with both systems being fully crosslinked in less than 10 s.

In the last subchapter, the development of a bioink platform for the biofabrication of hMSCs is summarized by means of the corresponding publication, and the development of two further bioinks is described. Based on the results of the investigation of HASH/PEG-diacrylate hydrogels, the printability of different formulations was investigated manually and mechanically. With increasing concentration of PEG-diacrylate, the hydrogel stiffness increased until saturation of the free thiols of the deployed HASH. Formulations with 0.5 % HASH (>200 kDa, 40-45 %) and 0.5-0.75 % 6k-PEG-diacrylate were found to be printable for 1-3 h after incubation at 37 °C for 1 h. Subsequent saturation of the remaining thiols using the third component, 6k-PEG-diallyl carbamate, via thiol-ene chemistry with the photoinitiator I2959 was investigated via a swelling study using a printable formulation with 1 % polymer content and 1:1 ratio of HASH/PEG-diacrylate. It was observed that a thiol saturation of about 93 % yielded volume stability over 21 d, while unsaturated and oversaturated formulations either shrank strongly on account of the formation of disulfides by air-oxidation of the remaining thiols or swelled strongly due to PEGylation by the excess of PEG-diallyl carbamate. Finally, by means of three different HASH batches (51 kDa, 230 kDa, 410 kDa) with almost identical thiol content (43-45 %), three bioinks were established and rheologically characterized with the help of Nadernezhad, A. in AG Groll. The polymer content of the formulations containing high molecular weight HASH, 230 kDa and 410 kDa, was 2 %, while the use of HASH with 51 kDa required a higher polymer content of 10 % for biofabrication. The printing experiments and biological studies were performed by Hauptstein, J. in AG Blunk. Long-term cell culture over 21 d of 3D bioprinted hMSCs showed chondrogenic differentiation in all formulations and homogeneous ECM distribution throughout the construct when using 230 kDa and 410 kDa HASH, while only pericellular ECM distribution was observed in the constructs with 51 kDa HASH. Subsequently, an attempt was made to extend the bioink platform by replacing PEG-diallyl carbamate with HAPA. For this purpose, swelling studies were performed over 21 d with a base formulation of HASH/6k-PEG-diacrylate in a 1:1 ratio with 1 % polymer content and HAPA (200-500 kDa, 29 %) as well as LAP, focusing on the influence of different thiol saturations on the volume stability. All formulations swelled strongly, so that no preference could be given. Subsequently, the influence of the HAPA molecular weight on the volume stability was tested at the same thiol saturation (110 %). It was observed that with increasing molecular weight, the hydrogels swelled significantly more. The cause for this could not be identified despite several control studies and the variation of parameters as well as HAPA batches. Long-term cell culture over 21 d of 3D bioprinted hMSCs, performed in AG Blunk, using a formulation with 1.65 % polymer content and 110 % thiol saturation from the first swelling study with HAPA (200-500 kDa, 29 %) showed very good cell viability and improved material properties compared to the previous bioink formulation with 6k-PEG-diallyl carbamate, while the ECM distribution in the constructs was only partially homogeneous with clearly visible pericellular pronouncement and no further development steps were conducted. Moreover, in a collaboration with AG Kengelbach Weigand, a bioink based on HAA with pure HA as thickener and LAP as photoinitiator was developed for their research of tumor dormancy in biofabricated tumor models based on different bioink matrices. The bioink was specially mixed and following steps were performed at AG Weigand, the cell integration, 3D bioprinting and the biological studies. The composition was adapted in such way that cell integration was effortless possible and the desired constructs could be generated by *in situ* crosslinking at 405 nm with simultaneously high cell viability. A composition with 12 % polymer content proved to be feasible, whereas a reduction of the HAA content from 10 % to 5 % is the subject of current development.

In summary, the targeted bioink platform for the biofabrication of hMSCs could be developed via a dual-stage crosslinking mechanism based on modified hyaluronic acid and PEG derivatives, which provided the desired biological effects. The synthesis of the individual components was successfully and reproducibly scaled up to counteract batch-to-batch variations and to meet the material demand of the collaboration partners. In addition, the synthesis of C6-HASH was accomplished for the first time and a protease-cleavable peptide sequence was prepared on a large scale for improving the degradability of the PEG-crosslinkers. Further hydrogel systems and one bioink were successfully developed based on the synthesized portfolio of different HA and PEG derivatives and their characteristics could be adapted to the requirements of a multitude of collaborators. Based on this diverse material repertory, a wide range of hydrogel and ink compositions can be generated in the future, which can be adapted to a variety of applications in the field of biofabrication and tissue regeneration due to their high flexibility in terms of material properties.

Das Ziel dieser Arbeit war es, eine Biotintenplattform aus Drei-Komponenten-Tinten zu entwickeln, basierend auf thiolierter Hyaluronsäure (HASH), PEG-Acrylat und PEG-Allylcarbamat, welche auf die Biofabrikation von humanen mesenchymalen Stromazellen (hMSC) maßgeschneidert ist. Zunächst wurden die literaturbekannten Synthesen der einzelnen Komponenten optimiert hinsichtlich der Syntheseparameter und der Produktaufreinigung zur Verbesserung von Produktqualität, Reproduzierbarkeit der Synthesen und Skalierbarkeit der Batchgrößen. Die Synthese von HASH wurde im Inkubator bei 37 °C in gepuffertem Medium durchgeführt und die Bildung eines unerwünschten Nebenproduktes durch die Zugabe von NHS verhindert. Eine Dialyse gegen saures Medium mit anfänglicher Zugabe von TCEP ergab das Produkt in gewünschter Qualität, wobei der Thiolgehalt zwischen 1-100 % eingestellt werden konnte, nicht aber das Molekulargewicht des Produktes aufgrund dessen Säurelabilität und somit zufälliger Degradation. Durch die Wahl des Ausgangspolymers konnten dabei Molekulargewichte von bis zu 577 kDa erhalten werden, welche zusammen mit der Dispersität über Größenausschlusschromatographie (SEC-MALS) bestimmt wurden. Der Thiolgehalt wurde mittels ^{1}H NMR bestimmt durch den Vergleich der signifikanter Signale der Wiederholungseinheit und der thioltragenden Gruppe. Gleichzeitig wurden PEG-Acrylate mit Molekulargewichten im Bereich von 1.5-20 kDa und den Geometrien linear, 4-armig und 8-armig im Kolben oder Inkubator synthetisiert. Die quantitative Acrylierung und die Aufreinigung des Produktes waren dabei von höchster Bedeutung für die avisierte Verwendung als Tintenkomponente und wurden über ^{1}H NMR unter Zugabe von Trifluoressigsäureanhydrid bestimmt und das Molekulargewicht über SEC-MALS untersucht. Im Falle von linearen PEG-Acrylaten wurde die Alkoholyse von Acrylsäurechlorid und Umkristallisation in EtOH als auch Filtration über Aktivkohle als geeignet befunden während verzweigte PEG-Acrylate besser über enzymatische Umesterung mit anschließender Waschung dargestellt werden konnten. Für die Synthese von PEG-Allylcarbamat wurde zunächst PEG-Amin über zwei verschiedene Syntheserouten hergestellt, Mesylierung mit anschließender Aminierung durch wässrigen Ammoniak sowie mittels Mitsunobu-Reaktion unter Verwendung von Phthalimid und darauffolgender Hydrazinolyse. Letztere erwies sich dabei als sehr sensitiv gegenüber Spuren von Wasser und Sauerstoff verhinderte jedoch die Oligomerisierung des PEG-Amins und wurde somit favorisiert. Die Einführung der Allyl-Funktion wurde im alkalisch wässrigen Milieu durch Zugabe von Chlorkohlensäureallylester realisiert und die Oligomerisierung des Produktes durch Kühlung der Reaktionslösung auf 0 °C verhindert.

Neben den Hauptkomponenten der Drei-Komponenten-Tinte wurden zudem noch weitere Hyaluronsäure-Derivate hergestellt, die zur Erweiterung der Biotintenplattform und in verschiedenen Anwendungen, maßgeschneidert auf die Bedürfnisse mehrerer interner und externer Kooperationspartner, eingesetzt wurden. Als Alternative zur Einbringung der Thiolgruppe über die Carbonsäurefunktion der Hyaluronsäure wurde die Thiolierung des C6-Alkohols entwickelt. Im ersten Schritt wird der C6-Alkohol in einer Schotten-Baumann-Reaktion mittels Acrylsäureanhydrid acryliert und in einem weiteren Schritt mit Thioessigsäure ein Thioester eingebracht, welcher zum Schluss hydrolysiert wird. Der Thiolierungsgrad konnte dabei gezielt im Bereich von 30-49 % eingestellt und das Molekulargewicht des Produktes (C6-HASH) durch die Wahl des Ausgangsmaterials beeinflusst werden. Hyaluronsäure-Acrylat (HAA) wurde synthetisiert durch Aufreinigung nach der Schotten-Baumann-Reaktion derselben Syntheseroute, wobei die Verwendung eines anderen Anhydrids, dem Pentensäureanhydrid, unter identischen Bedingungen einen weiteren HA-Ester, Hyaluronsäure-Pentenoat (HAPA), ergab. Der Funktionalisierungsgrad (DS) beider Hyaluronsäureester wurde über die zugegebene Anhydridmenge kontrolliert eingestellt, wobei diese Polymere lediglich bis 50 % DS ohne Einschränkungen wasserlöslich waren. Die Reaktionsbedingungen wurden so mild gewählt, dass das Molekulargewicht des Ausgangsmaterials über die Synthese unverändert blieb. Während HAPA mit allen verfügbaren Molekulargewichten von Hyaluronsäure-Batches synthetisiert wurde, wurde HAA aufgrund der Neigung des Produktes zur Oligomerisierung hauptsächlich aus niedermolekularer HA mit 8-15 kDa hergestellt. Die Reinheit des Produktes und der

Funktionalisierungsgrad von C6-HASH und HAA wurden über ^{1}H NMR ermittelt, während HAPA wegen der erhöhten Hydrophobizität mit steigendem DS über einen intern-entwickelten HPLC Assay bestimmt wurde. Das Molekulargewicht dieser drei HA-Derivate wurden mittels SEC-MALS untersucht.

Zusätzlich zu den polymeren Produkten wurden in Kolben bzw. Laborflaschen auch kleinere organische Verbindungen hergestellt, DTPH für die HASH-Synthese und eine kurze unspezifische Protease-Spaltsequenz (APGL) zur Verbesserung der Biodegradierbarkeit der Biotinte, welche über ^{1}H NMR und HRMS analysiert wurden. Die DTPH-Synthese wurde aufgrund der langen Lieferzeiten und letztlich minderwertigen Reinheit des kommerziellen Produktes etabliert und bis zum Limit der laboratischen Infrastruktur aufskaliert, wobei die Produktqualität in besonderem Fokus stand. Die Peptidsynthese wurde strategisch unterteilt in die Herstellung zweier Dipeptide, AP und GL, welche anschließend kondensiert wurden, um das gewünschte Tetrapeptid zu bilden. Die Dipeptide wurden dabei in zwei Stufen ausgehend von den Boc-geschützten Aminosäuren Alanin und Glycin hergestellt, welche zunächst in den jeweiligen NHS-ester umgewandelt und anschließend mit Prolin respektive Leucin umgesetzt wurden. Eine Entschützung des Boc-GL Dipeptides wurde in methanolischer HCl praktiziert, um gleichzeitig einen Methylester zu generieren, welcher durch Kupplung mit Boc-AP-NHS und anschließender Esterspaltung durch methanolische Natronlauge das avisierte Boc-Tetrapeptid ergab.

Das Kapitel 2.4 umfasst die verschiedenen Hydrogelkompositionen auf Basis der synthetisierten HA- bzw. PEG-Derivate und deren jeweilige Anwendungen. Zunächst werden die Anforderungen für die Gelierung über Michael-Addition von HASH und PEG-Acrylat dargestellt, die durch mehrere Screeningverfahren auf Basis verschiedener Batches der Komponenten untersucht wurden. Anhand eines HASH-Batches wurden bei fixer HASH-Konzentration die Konzentrationen von linearem PEG-Acrylat variiert und der Gelierungsverlauf sowie die Festigkeiten der erhaltenen Gele manuell untersucht. Des Weiteren wurden in einem eigens adaptierten Extrusionstest von Weichhold, J. aus der AG Gbureck und durch rheologische Vorversuche die Hydrogeleigenschaften maschinell dokumentiert. HASH mit einem Thiolgehalt von 40-60 % und PEG-Diacrylate mit M_n 1.5-20 kDa wurden als tauglich befunden. Mehrarmige PEG-Acrylate wiesen keinen besonderen Vorteil gegenüber den linearen Derivaten auf wegen der erhöhten lokalen Dichte ihrer funktionellen Gruppen. Abhängig vom HASH M_w konnten in Kombination mit 6k-PEG-Diacrylat Hydrogele mit Polymergehalten von 1 % bzw. 5 % hergestellt werden, wobei die Grenze im Bereich von <100 kDa und >200 kDa lag. Die erhaltenen Hydrogelformulierungen wurden an eine Vielzahl von Kooperationspartnern vergeben und anschließend auf deren Anwendungen maßgeschneidert. Eine Formulierung mit 1.5 % Polymergehalt und 1:1 Verhältnis von HASH zu 6k-PEG-Diacrylat erwies sich im Falle der AG Villmann als vielversprechend für deren Untersuchung zur Bildung von neuronalen Netzwerken in 3D Zellkulturen mit ultra-softer Matrix, während die Kooperation mit AG Cicha ein Hydrogelsystem mit 2 % Polymergehalt bei ebenfalls gleichem Verhältnis der Komponenten präferierten für die 3D Zellkultur von HUVECs zur Erforschung der Einbettung von prä- und post-endothelialisierten Netzwerken in gewebespezifischen Hydrogelen. In der AG Blunk wurden niedrigviskose HASH und 6k-PEG-Diacrylat für die Entwicklung von Mischköpfen für den 3D Druck von Gradienten-Hydrogelen benötigt. Des Weiteren wurde passgenaue HASH hergestellt für die bestehende Kooperation mit AG Fenz für deren HASH/PEG-Vinylsulfon Hydrogelsystem zur Fixierung von Trypanosomen. Es konnte festgestellt werden, dass ein Molekulargewicht <15 kDa und ein Thiolgehalt von 40-45 % optimal für diese Anwendung geeignet waren. Eine Komposition aus hochmolekularer HASH und niedermolekularer HAA wurden zudem untersucht, ohne dass sich eine konkrete Kooperation ergab. Es wurde beobachtet, dass die Hydrogelbildung dieses Systems innerhalb von <2 min stattfindet und, abhängig vom Polymergehalt, äußerst feste Hydrogele erzeugt werden können, die für den Einsatz als Polymernetzwerk in Knochenersatz-Kompositen geeignet sein könnten. Zudem wurden Hydrogelsysteme auf Basis von radikalischer Thiol-ene Vernetzung mit dem Photoinitiator LAP untersucht. Screening-Experimente zur Herstellung von HASH/HAPA-Hydrogelen ergaben eine

einstellbar-hohe initiale Viskosität der Präkursorenlösung durch die Wahl des HAPA Molekulargewichts und eine erhöhte Formtreue und Flexibilität bei gleichzeitig sehr geringem Polymergehalt von <1.5 %. Die Vernetzung fand dabei unter sichtbarem Licht mit 405 nm innerhalb von 60 s statt und erwies sich zusammen mit den Hydrogeleigenschaften als potenzieller Kandidat für die Forschung von Blum, C. in der AG Groll mit Schwerpunkt auf dem Einfluss neuer Arzneimittel und Arzneimittelträgersysteme auf das invasive Verhalten von Glioblastomzellen in verschiedenen Polymermatrizen. Als alternatives Hydrogelsystem zur Trypanosomfixierung über Michael-Addition wurden Hydrogele auf Basis reiner HAA mit und ohne HA als Verdicker entwickelt. Die mechanischen Eigenschaften (Young's Modulus) beider Hydrogelsysteme wurden analysiert und verglichen. Hydrogele mit reiner HAA und einem Polymergehalt von 5 % erwiesen sich dabei als mehr als dreifach so fest, wie bereits verwendete Formulierungen aus HASH/PEG-Vinylsulfon mit 10 % Polymergehalt, wobei beide Systeme in weniger als 10 s vollständig vernetzt waren.

Im letzten Teilkapitel wird die Entwicklung einer Biotintenplattform zur Biofabrikation von hMSCs anhand der entsprechenden Veröffentlichung zusammenfassend dargestellt sowie die Entwicklung zweier weiterer Tinten beschrieben. Ausgehend von den Ergebnissen der Untersuchung der HASH/PEG-Diacrylat Hydrogele wurde die Druckbarkeit verschiedener Formulierungen manuell und maschinell untersucht. Mit steigender Konzentration an PEG-Diacrylat stieg dabei die Festigkeit der Hydrogele an bis zur Absättigung der freien Thiole der eingesetzten HASH. Formulierungen mit 0.5 % HASH (>200 kDa, 40-45 %) und 0.5-0.75 % 6k-PEG-Diacrylat erwiesen sich dabei, nach 1 h Inkubation bei 37 °C, als druckbar für 1-3 h. Eine anschließende Sättigung der verbliebenen Thiole mittels der dritten Komponente, 6k-PEG-Diallylcarbamat, über Thiol-ene Chemie unter Verwendung des Photoinitiators I2959 wurde über eine Quellungsstudie anhand einer druckbaren Formulierung mit 1 % Polymergehalt und 1:1 Verhältnis von HASH/PEG-Diacrylat untersucht. Es konnte beobachtet werden, dass eine Thiolsättigung von ca. 93 % eine gute Volumenstabilität über 21 d ergab, während ungesättigte und übersättigte Formulierungen entweder stark schrumpften durch die Bildung von Disulfidbrücken aus den verbliebenen Thiolen oder stark quollen durch die PEGylierung durch den Überschuss an PEG-Diallylcarbamat. Letztlich wurden auf Basis drei verschiedener HASH-Batches (51 kDa, 230 kDa, 410 kDa) mit nahezu gleichem Thiolgehalt (43-45 %) drei Biotinten etabliert und rheologisch mithilfe von Nadernezhad, A. in der AG Groll charakterisiert. Der Polymergehalt der Formulierungen auf Basis beider hochmolekularer HASH, 230 kDa und 410 kDa, lag bei 2 %, während der Einsatz von HASH mit 51 kDa einen höheren Polymergehalt von 10 % benötigte für die Biofabrikation. Die Druckexperimente und biologischen Untersuchungen wurden von Hauptstein, J. in der AG Blunk durchgeführt. Langzeit-Zellkultur über 21 d von 3D biogedruckten hMSCs zeigte eine nachweislich chondrogene Differenzierung in allen Formulierungen und eine homogene ECM-Verteilung über das gesamte Konstrukt unter Verwendung von HASH mit 230 kDa und 410 kDa, während eine lediglich perizelluläre ECM-Verteilung in den Konstrukten mit 51 kDa HASH beobachtet wurde. Anschließend wurde versucht die Tintenplattform zu erweitern durch den Austausch von PEG-Diallylcarbamat mit HAPA. Hierzu wurden Quellungsstudien über 21 d durchgeführt mit einer Basisformulierung von HASH/PEG-Diacrylat im 1:1 Verhältnis mit 1 % Polymergehalt und HAPA (200-500 kDa, 29 %) sowie LAP, wobei der Einfluss verschiedener Thiolsättigungen auf die Volumenstabilität im Fokus stand. Alle Formulierungen quollen dabei sehr, sodass keine Favorisierung erfolgen konnte und im Anschluss der Einfluss des HAPA Molekulargewichts auf die Volumenstabilität bei gleicher Thiolsättigung (110 %) überprüft wurde. Es konnte beobachtet werden, dass mit steigendem Molekulargewicht die Hydrogele deutlich stärker quollen. Der Grund für diesen Sachverhalt konnte trotz mehrerer Kontrollstudien und Variation der Parameter sowie HAPA-Batches nicht gefunden werden. Langzeit-Zellkultur über 21 d von 3D biogedruckten hMSCs, durchgeführt in der AG Blunk, unter Verwendung einer Formulierung mit 1.65 % Polymergehalt und 110 % Thiolsättigung aus der ersten Quellungsstudie mit HAPA (200-500 kDa, 29 %) zeigte zwar eine gute

Zellviabilität und verbesserte Materialeigenschaften im Vergleich zur vorherigen Tintenformulierung mit 6k-PEG-Diallylcarbamat, jedoch war die ECM-Verteilung in den Konstrukten lediglich partiell homogen mit deutlich sichtbarer perizellulärer Ausprägung und es wurde von weiteren Entwicklungsschritten abgesehen. Des Weiteren wurde in einer Kooperation mit AG Kengelbach-Weigand eine Tinte auf Basis von HAA mit reiner HA als Verdicker und LAP als Photoinitiator entwickelt für deren Forschung von Tumor Dormancy in biofabrizierten Tumormodellen auf Basis verschiedener Biotinten-Matrizen. Die Tinte wurde eigens angemischt und anschließend in der AG Weigand die Zellen integriert, verdruckt und die biologischen Untersuchungen durchgeführt. Die Komposition wurde dabei so angepasst, dass die Zellintegration möglichst leicht war und die gewünschten Konstrukte durch *in situ* Vernetzung bei 405 nm mit gleichzeitig hoher Zellviabilität generiert werden konnten. Eine Komposition mit 12 % Polymergehalt erwies sich als dienlich wobei eine Reduktion des HAA-Gehaltes von 10 % auf 5 % Gegenstand der aktuellen Entwicklung ist.

Zusammenfassend konnte die avisierte Biotintenplattform zur Biofabrikation von hMSCs über einen zweistufigen Vernetzungsmechanismus auf Basis modifizierter Hyaluronsäure- und PEG-Derivate entwickelt werden, die die gewünschten biologischen Effekte erzeugte. Die Synthese der einzelnen Komponenten wurde erfolgreich und reproduzierbar aufskaliert, um Batch-to-Batch Variationen entgegenzuwirken und den Materialbedarf der Kooperationspartner zu decken. Zudem wurde erstmal die Synthese von C6-HASH bewerkstelligt und eine protease-spaltbare Peptidsequenz in großem Maßstab hergestellt für die Verbesserung der Degradierbarkeit der PEG-Vernetzer. Weitere Hydrogelsysteme und eine Biotinte wurden erfolgreich auf Basis des synthetisierten Portfolios an verschiedenen HA- und PEG-Derivaten entwickelt und konnten hinsichtlich ihrer Charakteristika auf die Anforderungen einer Vielzahl an Kooperationen angepasst werden. Anhand dieses mannigfaltigen Materialrepertoires können in der Zukunft ein große Bandbreite an Hydrogel- und Tintenkompositionen generiert werden, die durch ihre hohe Flexibilität hinsichtlich der Materialeigenschaften auf eine Vielzahl an Anwendungen im Bereich der Biofabrikation und Geweberegeneration angepasst werden können.

4 Experimental section

4.1 Materials

All chemicals were purchased from Sigma Aldrich (Schnelldorf, Germany) and used without further purification if not stated differently. 1-(3-dimethylaminopropyl)-3-ethylcarbodiimide HCl (EDC; Biosynth Carbosynth, Compton, UK), 1,4-dithiothreitol (DTT; Biosynth Carbosynth, Compton, UK), 2-hydroxy-1-[4-(hydroxyethoxy)-phenyl]-2-methyl-1-propanone (I2959; BASF, Ludwigshafen, Germany), 4-pentenoic acid (TCI, Tokyo, Japan), acrylic anhydride (abcr GmbH, Karlsruhe, Germany), allyl chloroformate (Acros Organics, Fair Lawn, NJ, USA) ammonium hydroxide (28 %; Merck KGaA, Darmstadt, Germany), chloroform-d_1 ($CDCl_3$; Eurisotope, St-Aubin Cedex, France), deuterium oxide (D_2O; Deutero GmbH, Kastellaun, Germany), dialysis tube regenerated cellulose MWCO 1 kDa (Repligen, Waltham, MT, USA), dialysis tube regenerated cellulose MWCO 3.5 kDa (until 2019, Carl Roth, Karlsruhe, Germany), dialysis tube regenerated cellulose MWCO 3.5 kDa (since 2020, Serva Electrophoresis GmbH, Heidelberg, Germany), dichloromethane (DCM; Fisher Scientific, Schwerte, Germany), diethyl ether (DE; Chemobar University of Würzburg, Würzburg, Germany), dimethyl 3,3'-dithiodipropionate (DTP-OMe; TCI Chemical, Tokyo, Japan), dimethyl sulfoxide-d_6 (Deutero GmbH, Kastellaun, Germany), di-potassium hydrogen phosphate (Merck KGaA, Darmstadt, Germany), di-sodium hydrogen phosphate (Merck KGaA, Darmstadt, Germany), Dulbecco's phosphate buffered saline (PBS; Life Technologies, Carlsbad, CA, USA), ethanol (Carl Roth, Karlsruhe, Germany), hyaluronic acid sodium salt (M_w 8-15 kDa; 80-100 kDa; 0.2-0.5 MDa; 0.6-1.0 MDa; 1.0-2.0 MDa; 2.0-2.5 MDa; Biosynth Carbosynth, Compton, UK), hydrochloric acid (32 %; Merck KGaA, Darmstadt, Germany), *iso*-propanol (VWR, Radnor, PA, USA), maleimide (Biosynth Carbosynth, Compton, UK), methanol (Fisher Scientific, Schwerte, Germany), *N*-Boc-alanine (Biosynth Carbosynth, Compton, UK), *N*-Boc-glycine (Biosynth Carbosynth, Compton, UK), *N*,*N*-dimethyl formamide (DMF; Carl Roth, Karlsruhe, Germany), *N*-hydroxysuccinimide (NHS; Biosynth Carbosynth, Compton, UK), phthalimide (Chemobar University of Würzburg, Würzburg, Germany), polydivinylbenzene resin (PAD600; Purolite, King of Prussia, PA, USA), polyethylene glycol 8arm 10 kDa (JenKem Technology USA, Plano, TX, USA), polyethylene glycol vinyl sulfone 8arm 10 kDa (JenKem Technology USA, Plano, TX, USA), polystyrene resin (MN202; Purolite, King of Prussia, PA, USA), potassium dihydrogen phosphate (Merck KGaA, Darmstadt, Germany), sodium chloride (Th. Geyer, Renningen, Germany), sodium hydrogen carbonate (Merck KGaA, Darmstadt, Germany), sodium hydroxide (Merck KGaA, Darmstadt, Germany), sodium nitrate (Grüssing, Filsum, Germany), sodium thiosulfate (ORG Laborchemie, Bunde, Germany), tetrahydrofuran (Fisher Scientific, Schwerte, Germany), toluene (Fisher Scientific, Schwerte, Germany), tris(carboxyethyl)phosphine HCl (TCEP; Biosynth Carbosynth, Compton, UK), vinyl methacrylate (TCI Chemical, Tokyo, Japan).

4.2 Methods

4.2.1 Non-polymer characterization

^{1}H NMR

All non-polymer ^{1}H NMR spectra were measured at a Fourier 300 from Bruker operating at 300.1 MHz at rt with a DUL 5 mm probe head and the data was acquired with 16 scans, recycle delay 5.0 s and sample spinning frequency 20 Hz.

DTPH (25 mg) was dissolved in DMSO-d_6 (0.6 mL, 2.50 ppm) and D_2O (0.6 mL, 4.79 ppm) in which the absence of methyl ester signals of the reactant (DTP-OMe) in both spectra confirmed the success of synthesis.

All peptide derivatives (25 mg) were dissolved in DMSO-d_6 (0.6 mL, 2.50 ppm) and the obtained spectra were compared to the spectra of all reactants of the respective synthesis.

ASAP

All mass spectroscopy analyses were performed by Mahler, C. of the institute of inorganic chemistry of the University Würzburg on a Thermo Scientific Exactive Plus Orbitrap mass spectrometer. In brief, all samples were measured solvent-free using an APCI ion source and hot nitrogen as auxiliary gas. The tip of a melting point capillary was dipped into the sample, wiped with dust-free precision cloths, inserted into the hot nitrogen gas flow via an ASAP mount and the blown off ionized sample was analyzed. The obtained data was plotted in a stack view containing the signal intensity, mass spectra overview, zoomed in peak section of the target molecule ion and a computer generated peak prediction of the target molecule ion.

4.2.2 Polymer characterization

^{1}H NMR

All polymer ^{1}H NMR measurements were performed at a Fourier 300 from Bruker operating at 300.1 MHz at rt with a DUL 5 mm probe head and the data was acquired with 128 scans, recycle delay 7.3 s and sample spinning frequency 20 Hz.

The procedure was identical for all HA derivates independent of the molecular weight of the product. 4-5 mg were dissolved in 0.6 mL D_2O (4.79 ppm) and vortexed at rt until complete dissolution (5-20 min). The integrals were referred to the *N*-Acetyl peak of the repetition unit with an integral of 3. The signal peak of the two anomeric protons served as control, providing it was not covered by the solvent peak and thus could be integrated.

PEG samples were dissolved in 0.7 mL chloroform-d_1 ($CDCl_3$, 7.29 ppm) in different concentrations depending on their molecular weight, measured and then 20 µL of TFAA was added and the samples were measured again. The individual weights were 20 mg (<6 kDa), 30 mg (<10 kDa) and 40 mg (<20 kDa). As control unmodified starting materials were measured the same way and their TFAA spectra were used in overlay views to proof quantitative modification by the absence of TFA esters, formed from unreacted alcohols. Other non-nucleophilic solvents that can be used for this approach are for instance MeCN-d_3, DCM-d_2 and THF-d_8 except for DMSO-d_6 as it reacts with the anhydride and alcohol in an Albright-Goldman oxidation.

SEC MALS

All SEC MALS measurements were conducted on a SEC MALS system (Malvern) using a triple detection consisting of a refractive index detector (VE 3580), a viscometer (270 dual detector), and a multi-angle light scattering detector (SEC-MALS 20).

HA derivates were measured using the A6000M mixed-bed column set (Malvern). 1-2 mL stock solutions in MilliQ with a concentration of 2-4 mg/mL were prepared in 2 mL Eppendorf tubes in a thermostatic mixer over 6 h at rt and diluted with MilliQ to a concentration of 1.0 mg/mL. In case of thiol modified HA, a freshly prepared 0.5 mg/mL TCEP solution was used for dilution. After filtration with a 0.45 µm syringe filter (RC) the measurements were performed within 4 h to prevent falsification of the results by either hydrolytic breakdown or aggregation. For control of column overload and thus peak shifting to smaller molecular weights, each sample was measured twice, once with 100 µL and once with 50 µL injection volume. In case of deviations between both runs, results of the measurements with 50 µL injection volume were used.

PEG derivatives were measured on a A2000-3000 column set (Malvern). For that, 1-2 mL solutions in MilliQ were prepared with a concentration of 4 mg/mL in 2 mL Eppendorf tubes in a thermostatic mixer over 6 h at rt in complete darkness, following a filtration (syringe filter, 0.45 µm, RC). Each sample was measured with two injection volumes (50, 100 µL) and the runs with the lowest injection volume that are still analyzable were used to eliminate possible column overload and thus peak shifting/falsified results.

HPLC

HPLC measurements of HAPA were conducted at a multicomponent HPLC system (Shimadzu) consisting of LC-20AT series type double plunger, SIL-20AC autosampler, RF-20A fluorescence detector, SPD-M20A photodiode array detector, CTO-20AC column oven, CBM-20A system controller, RID-20A refractive index detector, FRC-10A fraction collector and Luna 5 µm C18(2) 100 A LC column using an eluent composed of MilliQ/ACN (85:15) and 854 µL perchloric acid per liter solvent and a flowrate of 1 mL/min. All HAPA samples were measured by Oberst, K. analog to her protocol[80]. In brief, samples of 7.5 mg HAPA were incubated in 5.0 mL 0.02 M NaOH overnight at 37 °C, quenched with 1 mL 2 M acetic acid and filtered (syringe filter, 0.2 µm, RC). 100 µL sample volume were injected into the system and the UV-VIS absorption peak of the hydrolyzed pentenoate at the wave lengths of 205 nm and 210 nm was integrated using a calibration curve based on neat pentenoic acid.

4.2.3 Buffer preparation

Sørensen buffer (0.2 M, pH 5.5)

17.8 g anhydrous Na_2HPO_4 were dissolved in 400 mL MilliQ in a 500 mL graduated flask and then filled up to the 500 mL mark with MilliQ. Likewise, 13.6 g KH_2PO_4 were dissolved. In a 500 mL Schott bottle 450 mL KH_2PO_4 solution was stirred with a pH electrode inside and Na_2HPO_4 solution was added until pH 5.5 was reached (approx. 30 mL).

Dialysis buffer (0.3 mM, pH 5.0)

In a 20 L HDPE screw lid bucket, 5 mL of 10 % HCl, 5 mL of 0.9 M K_2HPO_4 (15.7 g, 100 mL) solution and 1.0 g sodium ascorbate were added to 15 L MilliQ at rt and mixed properly. If required, 1.0 g TCEP was added.

K_2HPO_4 (5 M)

435 g K_2HPO_4 were added to a 500 mL Schott bottle, filled up to the mark with MilliQ and were dissolved using an incubator (rt, 200 rpm).

Phosphate buffer (154 mM, pH 7.6/7.8)

In a 1 L graduated flask 13.06 g K_2HPO_4, 9.00 g NaH_2PO_4 and 0.234 g NaCl were dissolved in 500 mL MilliQ, the pH adjusted respectively with 2 N NaOH (40.0 g, 500mL) and filled up to the mark with MilliQ.

HEPES buffer (154 mM, pH 7.6/7.8)

18.35 g HEPES were dissolved in 250 mL MilliQ in a 500 mL graduated flask at rt. The pH was adjusted accordingly with 2 N NaOH and the solution filled up to the mark with MilliQ.

4.2.4 Hydrogel preparation

Michael-addition

The preparation of hydrogels via Michael-addition from stock solutions followed the general concept of dissolving all HA components in self-made buffers, phosphate or HEPES, and all PEG components in commercial PBS, but was individually adapted according to the deployed components and targeted concentrations. After respective mixing of the component stocks, the precursor solution was incubated at 37 °C until reaching the desired gelation status for the targeted characterization or application. HASH stocks above 2 % were avoided as the stock pH would drop below 7.4 due to the limited buffer capacity of 154 mM and the increased amount of acidic HASH. If more concentrated HASH stocks were required, the initial pH of the HEPES buffer was raised to such value that the stock solution reached at least pH 7.4. PEG component stocks were prepared in concentrations up to 50 % and exhibited only slight increased viscosity. HAPA and HA stocks above 4 % were avoided due to their high viscosity depending on the molecular weight and consequently handling/pipetting challenges.

Thiol-ene Reaction

The stock solutions for hydrogels via thiol-ene reaction were prepared similar to the concept of the hydrogels from Michael-addition. The initiator, I2959 or LAP, was added to the buffer used for stock preparation in the targeted concentration of 0.05 %. Precursor solution using I2959 were irradiated for 10 min at 365 nm UV light from a 6 W hand lamp with UV filters (A. Hartenstein), whereas LAP based formulations were crosslinked with 405 nm visible light from a 3 W 405 nm flashlight (Mastiff). The exposure time and distances depended on the formulation and application and ranged between 60-120 s and 1-6 cm. Usage of other available light sources with different wavelength and intensities was omitted to ensure comparability of the hydrogels/constructs.

Free radical polymerization

Hydrogels for FRP crosslinking were prepared analog to the formulations for thiol-ene reaction. LAP was added to the buffer for stock preparation in concentrations of 0.05-0.1 % and the formulations irradiated for 10-60 s with a 3 W 405 nm flashlight (Mastiff) from a distance of 1-6 cm.

4.2.5 Hydrogel characterization

Hydrogel stiffness

Qualitative hydrogel stiffness analyses were performed using a setup composed of a custom-made syringe mount of Weichhold, J. placed in a Z010 universal testing machine (Zwick Roell) with a 2.5 kN load cell and 3 mL syringe with rubber plunger and Luer lock for connection of 250 µm steel 3D printhead needle (Nordson EFD) were used. Minimum 0.5 mL precursor solution were filled into the syringe and extruded after respective incubation at 37 °C at a constant crosshead displacement rate of 10 mm/min while the required force was monitored.

Mechanical analysis

DMA measurements were conducted at a ElectroForce 5500 (Bose) with a 250 g load cell by Oberst, K. analog to her protocol[80].

4.2.6 Ink development and characterization

Manual printability

Qualitative printability experiments were performed manually using a 250 µL Microman M250 displacement pipette (Gilson). The sample was taken up, extruded on a flat surface, petri dish bottom, to evaluate its viscosity and shape fidelity and placed back into its container for further investigations.

Extrudability

Evaluation of the extrudability of bioink formulations was conducted identically to the hydrogel stiffness experiments whereat, next to the required force, the obtained strands were concurrently monitored via photography.

Rheology

Rheological characterization was conducted by Nadernezhad, A. at a MCR 702 rheometer (Anton Paar) using a solvent trap and 25 mm parallel plate geometry according to the published protocol[119].

4.3 Synthesis of non-polymeric products

4.3.1 3,3'-Dithiobis(propanoic dihydrazide) (DTPH)

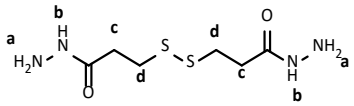

The synthesis was performed according to Vercruysse *et al.*[64] with slight modifications to enable upscaling. Dimethyl 3,3'-dithiodipropionate (82.0 mL, 1.0 eq.) was dissolved in MeOH (1000 mL) in a 2 L Schott-bottle at rt to form a clear, colorless solution and then was cooled to 0 °C by an ice bath. After addition of an excess of hydrazine monohydrate (163 mL, 4.0 eq.), the clear, yellowish reaction solution was stirred for 1 h at 0 °C and then stirred overnight at rt. The obtained shiny, yellowish suspension was transferred into a LC column (Ø9 cm, POR4) and the reaction media was pumped out. The filter cake was washed with MeOH/DE (1:1, 1000 mL) consisting of resuspension and solvent removal until discoloration of the washing suds. MeOH residues were removed by washing with pure DE (5x 500 mL) and the final filter cake was dried *in vacuo* at rt to give a shiny, white powder. In case of lump formation, the product was redissolved in MilliQ (1000 mL) at 50 °C and subsequently freeze dried to form the desired fine, shiny, white powder.

^{1}H NMR (300 MHz, d_6-DMSO): δ= 9.06 (s, 2 H, *H*-**b**), 4.20 (s, 4 H, *H*-**a**), 2.89 (t, 4 H, *H*-**d**), 2.41 (t, 4 H, *H*-**c**) ppm.

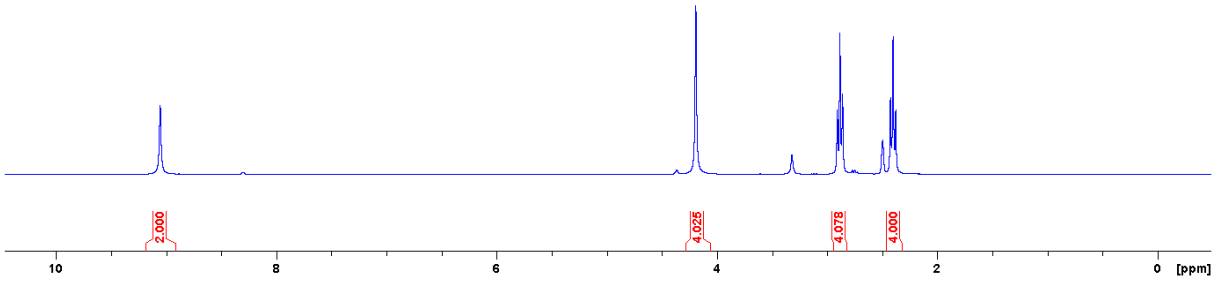

Figure 68: Representative ^{1}H NMR spectra of DTPH in d_6-DMSO.

4.3.2 Leu-Gly-Pro-Ala peptide sequence

Boc-ala-NHS ester

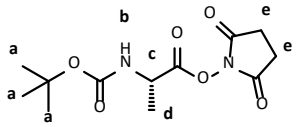

Boc-ala-OH (50.0 g, 1.0 eq.) and NHS (36.5 g, 1.2 eq.) were suspended in DCM (900 mL) in a 1 L round-bottom flask at rt and EDC (55.7 g, 1.1 eq.) was added portion wise over 15 min. The clear, yellowish solution was stirred for 4 h at rt, washed first with MilliQ (5x 400 mL) and then with brine (2x 200 mL). Solvents were removed (roti, 50 °C) and the obtained colorless oil dried *in vacuo* at rt to form a white solid.

^{1}H NMR (300 MHz, d_6-DMSO): δ = 7.13-7.55 (m, 1 H, *H*-**b**), 4.22-4.52 (m, 1 H, *H*-**c**), 2.80 (s, 4 H, *H*-**e**), 1.41 (s, 3 H, *H*-**d**), 1.39 (s, 9 H, *H*-**a**) ppm.

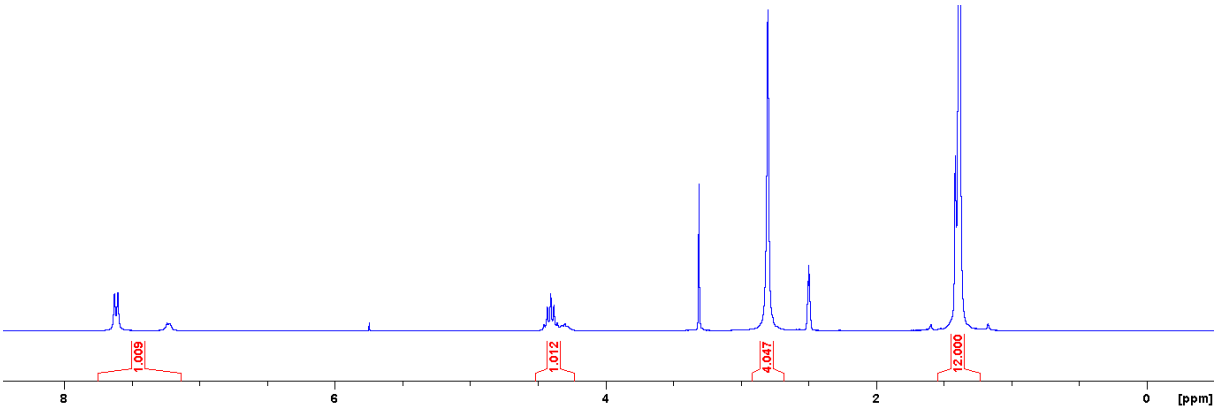

Figure 69: Representative ^{1}H NMR spectra of Boc-ala-NHS ester in d_6-DMSO.

Boc-ala-pro-OH

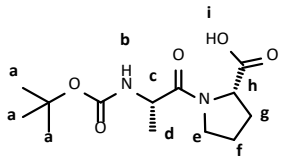

Boc-ala-NHS ester (80.0 g, 1.0 eq.) was dissolved in ACN (1000 mL) in a 2 L Schott bottle at rt. L-proline (35.4 g, 1.1 eq.) was dissolved in MilliQ (400 mL) in a 500 mL Schott bottle at 50 °C and both clear, colorless solutions were combined and cooled to 0 °C by an ice bath. After the addition of TEA (58.1 mL, 1.5 eq.), the clear, yellowish reaction solution was stirred for 1 h at 0 °C, then for 3 h at 40 °C. ACN was removed (roti, 50 °C), the pH decreased to <3 with 10 % HCl and the white suspension centrifuged (5 min, 4500 rpm, rt). The isolated white sediment was redissolved by raising the pH to >8 with 2 N NaOH, washed with DE (5x 200 mL), reprecipitated by lowering the pH to <3 with 10 % HCl and centrifuged (5 min, 4500 rpm, rt). The precipitation procedure was repeated twice more, the final sediment resuspended in MilliQ and freeze dried to form a white solid.

^{1}H NMR (300 MHz, d_6-DMSO): δ = 12.46 (s, 1 H, *H*-**i**), 7.18-6.36 (m, 1 H, *H*-**b**), 4.35-3.99 (m, 2 H, *H*-**c**,**h**), 3.76-3.43 (m, 2 H, *H*-**e**), 2.25-1.73 (m, 4 H, *H*-**f**,**g**), 1.35 (s, 9 H, *H*-**a**), 1.14 (m, 3 H, *H*-**d**) ppm.

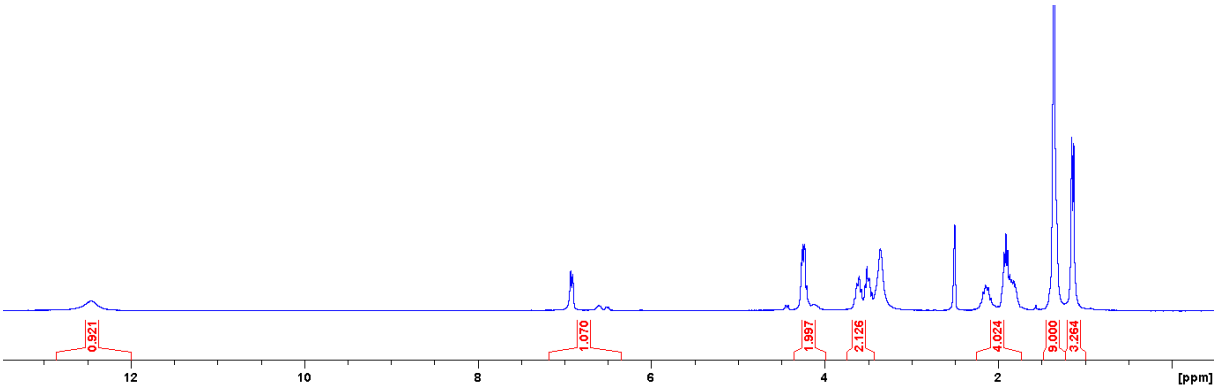

Figure 70: Representative ^{1}H NMR spectra of Boc-ala-proline in d_6-DMSO.

Boc-ala-pro-NHS ester

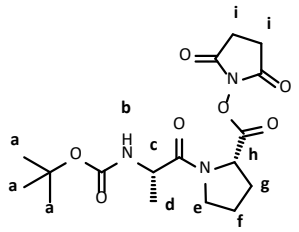

Boc-ala-pro-OH (44.0 g, 1.0 eq.) and NHS (21.2 g, 1.2 eq.) were suspended in DCM (900 mL) in a 1 L round-bottom flask at rt and EDC (55.7 g, 1.1 eq.) was added portion wise over 15 min. The turbid, colorless solution was stirred for 4 h at rt, washed with MilliQ (4x 400 mL) and the solvents removed (roti, 50 °C) to form a colorless oil. The product was obtained as white solid by drying *in vacuo* at rt.

^{1}H NMR (300 MHz, d_6-DMSO): δ = 7.20-6.58 (m, 1 H, *H*-**b**), 4.73 (m, 1 H, *H*-**h**), 4.25 (m, 1 H, *H*-**c**), 3.77-3.94 (m, 2 H, *H*-**e**), 2.80 (m, 4 H, *H*-**i**), 2.45-1.86 (m, 4 H, *H*-**f**,**g**), 1.37 (s, 9 H, *H*-**a**), 1.15 (d, 3 H, *H*-**d**) ppm.

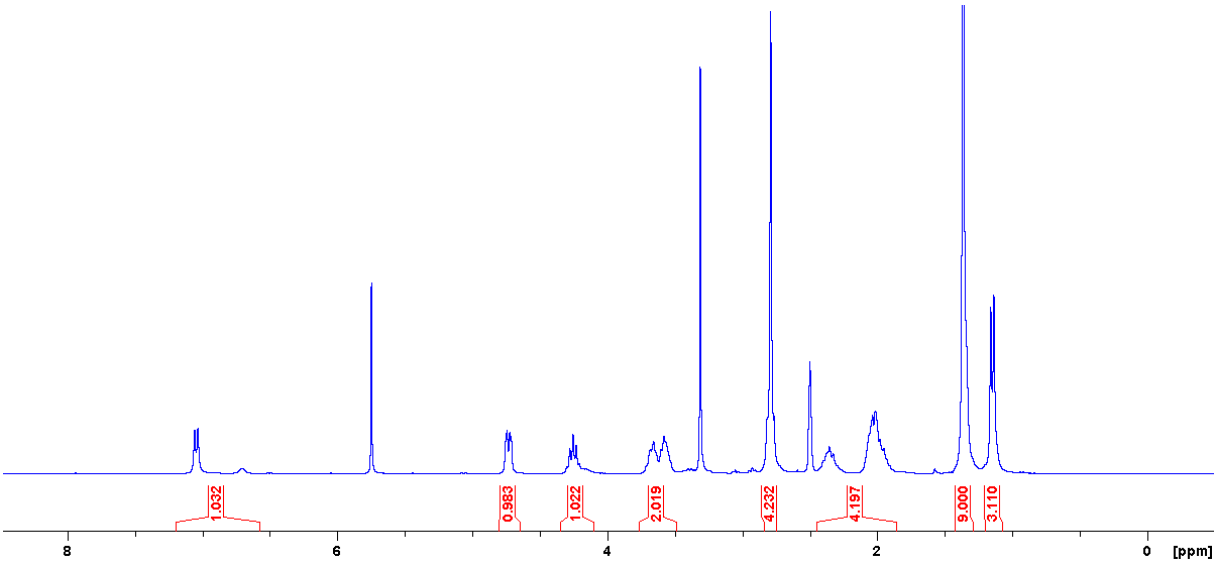

Figure 71: Representative ^{1}H NMR spectra of Boc-ala-pro-NHS ester in d_6-DMSO.

Boc-gly-NHS ester

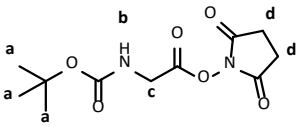

Boc-gly-OH (50.0 g, 1.0 eq.) and NHS (39.4 g, 1.2 eq.) were suspended in DCM (900 mL) in a 1 L round-bottom flask at rt and EDC (60.2 g, 1.1 eq.) was added portion wise over 15 min. The clear, yellowish solution was stirred overnight at rt to form a yellowish suspension. After heating the reaction solution to 30 °C (water bath), the now clear, yellowish solution was washed with warm MilliQ (40 °C, 5x 400 mL) and the layer separated while being warm. Solvents of the final clear, colorless solution were removed (roti, 50 °C) and the obtained colorless oil dried *in vacuo* at rt to form a white solid.

^{1}H NMR (300 MHz, d_6-DMSO): δ = 7.16-6.97 (m, 1 H, *H*-**b**), 4.20-3.93 (m, 2 H, *H*-**c**), 2.81 (s, 4 H, *H*-**d**), 1.39 (s, 9 H, *H*-**a**) ppm.

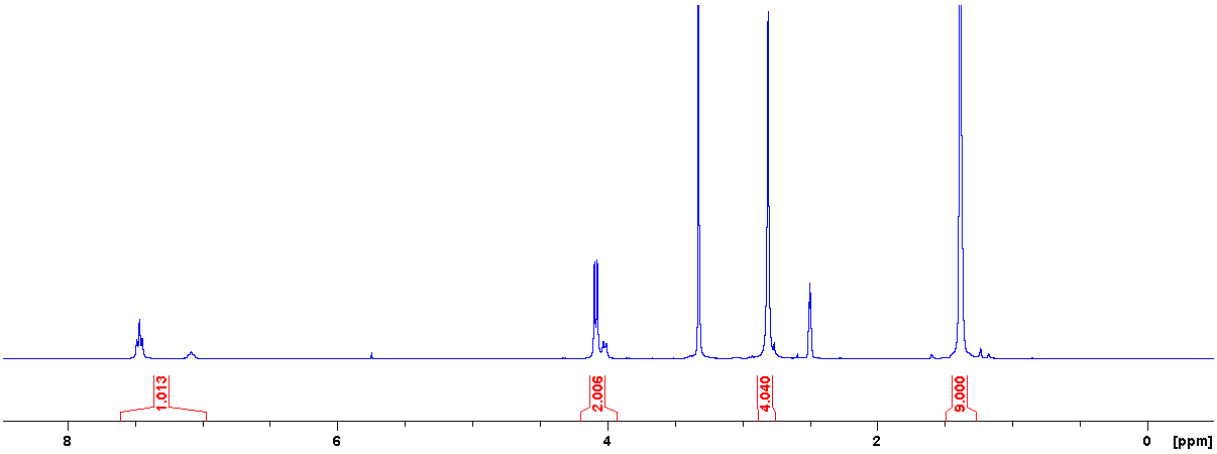

Figure 72: Representative ^{1}H NMR spectra of Boc-gly-NHS ester in d_6-DMSO.

Boc-gly-leu-OH

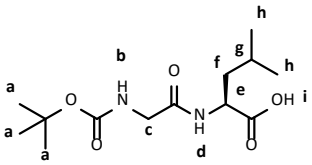

Boc-gly-NHS ester (78.0 g, 1.0 eq.) was dissolved in ACN (1000 mL) in a 2 L Schott bottle at rt. L-leucine (41.3 g, 1.1 eq.) was suspended in MilliQ (400 mL) in a 500 mL Schott bottle at rt and poured to the clear, colorless NHS solution at 0 °C. After the addition of TEA (47.7 mL, 1.2 eq.), the yellowish suspension was stirred for 1 h at 0 °C, then for 4 h at 40 °C. Residual L-leucine flakes were filtered off, ACN was removed (roti, 50 °C) and the pH lowered to <3 with 10 % HCl. The yellowish suspension was centrifuged (5 min, 4500 rpm, rt), the supernatant discarded and the off-white sediment redissolved by raising the pH to >8 with 2 N NaOH. The precipitation procedure was repeated twice more, the final white sediment resuspended in MilliQ and freeze dried to form a white solid.

^{1}H NMR (300 MHz, d_6-DMSO): δ = 13.29-11.53 (s, 1 H, *H*-**i**), 7.94 (d, 1 H, *H*-**d**), 7.03-6.41 (m, 1 H, *H*-**b**), 4.23 (m, 1 H, *H*-**e**), 3.61-3.47 (m, 2 H, *H*-**c**), 1.69-1.45 (m, 3 H, *H*-**f**,**g**), 1.37 (s, 9 H, *H*-**a**), 0.86 (dd, 6 H, *H*-**h**) ppm.

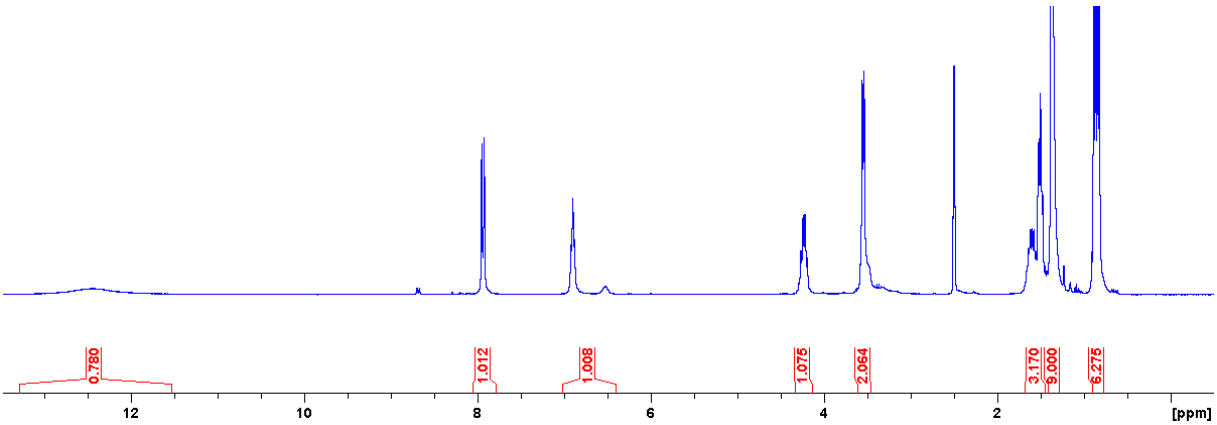

Figure 73: Representative ^{1}H NMR spectra of Boc-gly-leucine in d_6-DMSO.

Gly-leu-OH

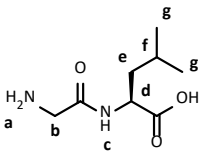

Boc-gly-Leu-OH (10.0 g, 1.0 eq.) was suspended in neat TFA (13.4 mL, 5.0 eq.) in a 50 mL round-bottom flask at 0 °C (ice bath), the bubbling white suspension stirred for 1 h at 0 °C and then for 1 h at rt. The turbid white suspension was poured into cold DE (5x volume), cooled to -20 °C (freezer, 4 h) and centrifuged (15 min, 4500 rpm, 5 °C). The supernatant was discarded, the sediment resuspended in cold DE, centrifuged (15 min, 4500 rpm, 5 °C) and this procedure was repeated twice more. The final white sediment was dried *in vacuo* to give a white powder.

^{1}H NMR (300 MHz, d_6-DMSO): δ = 8.67 (d, 1 H, *H*-**c**), 8.11 (s, 2 H, *H*-**a**), 4.29 (q, 1 H, *H*-**d**), 3.59 (t, 2 H, *H*-**b**), 1.76-1.44 (m, 3 H, *H*-**e**,**f**), 0.88 (dd, 6 H, *H*-**g**) ppm.

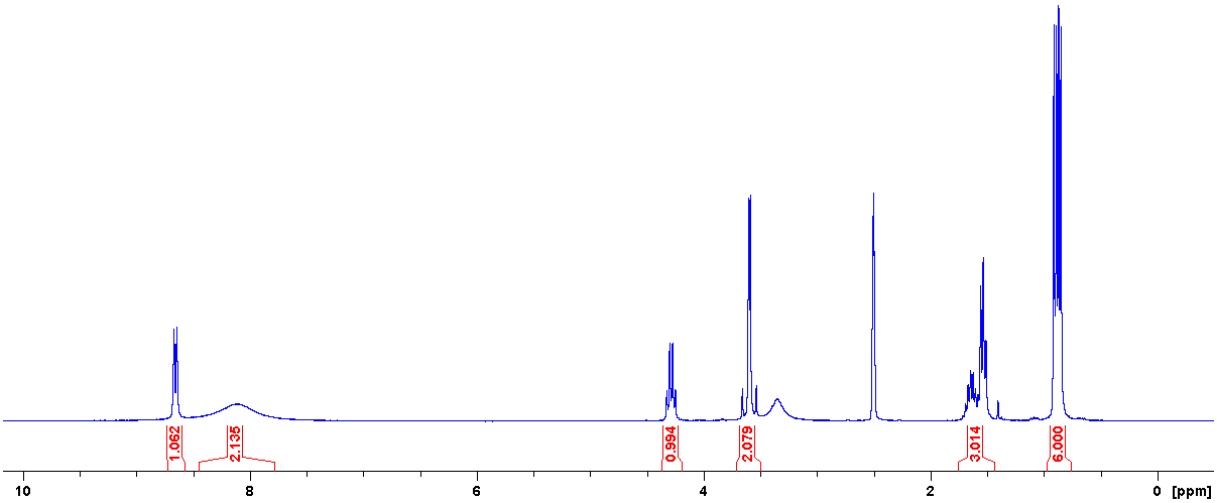

Figure 74: Representative ^{1}H NMR spectra of gly-leucine in d_6-DMSO.

Gly-leu-OMe

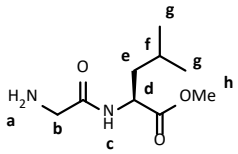

Acetyl chloride (37.0 mL, 2.5 eq.) were added to pre-cooled MeOH (0 °C, 350 mL) in a 500 mL round-bottom flask and Boc-gly-leu-OH (60.0 g, 1.0 eq.) was added at once to the clear, colorless solution. The turbid, colorless suspension was stirred for 1 h at rt, then for 1 h at 50 °C (water bath) to form a turbid, yellowish solution and subsequently filtered (paper filter). Solvents were removed (roti, 50 °C), the white solids dried *in vacuo* at rt and neutralized with 2 N NaOH. After freeze drying the turbid, yellowish solution the product was obtained as off-white powder.

^{1}H NMR (300 MHz, d_6-DMSO): δ = 8.94 (d, 1 H, *H*-**c**), 8.25 (s, 3 H, *H*-**a**), 4.47-4.20 (m, 1 H, *H*-**d**), 3.71-3.42 (m, 5 H, *H*-**b**,**h**), 1.79-1.40 (m, 3 H, *H*-**e**,**f**), 0.86 (q, 6 H, *H*-**g**) ppm.

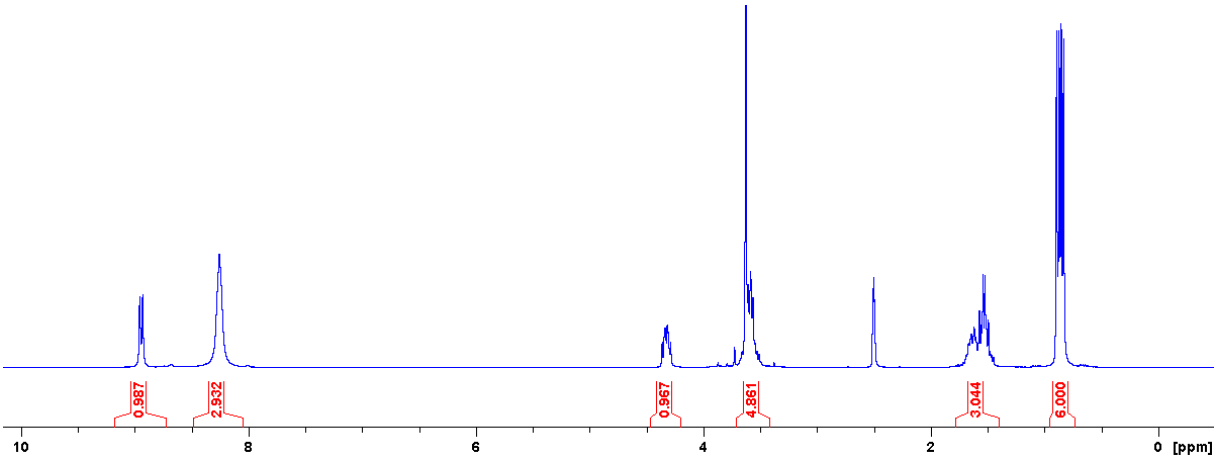

Figure 75: Representative ^{1}H NMR spectra of Boc-gly-leu-OMe in d_6-DMSO.

Boc-ala-pro-gly-leu-OMe

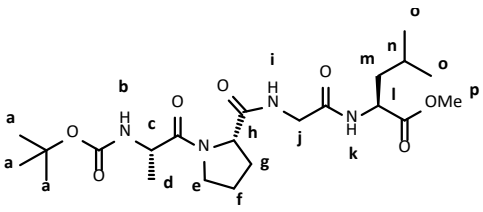

Boc-ala-pro-NHS ester (25.0 g, 1.0 eq.) was dissolved in ACN (350 mL) in a 1 L Schott bottle at rt a mix of gly-leu-OMe (15.8 g, 1.2 eq.) and TEA (10.8 mL, 1.2 eq.) in MilliQ (150 mL) were added at 0 °C (ice bath). The clear, colorless solution was stirred for 1 h at 0 °C, then for 3 h at 50 °C (water bath) and organic solvents were removed (roti, 50 °C). The yellowish suspension was mixed with DCM (500 mL), the clear, yellowish DCM layer washed with dilute HCl (<0.5 %, 3x 200 mL) and NaOH (2 N, 3x 100 mL). The now colorless organic layer was dried ($MgSO_4$), filtered (paper filter) and the solvents removed (roti, 50 °C). The white solids were dried *in vacuo* at rt to form a white powder.

^{1}H NMR (300 MHz, d_6-DMSO): δ = 8.18 (t, 1 H, *H*-**i**), 7.94 (d, 1 H, *H*-**k**), 6.97-6.46 (m, 1 H, *H*-**b**), 4.44-3.98 (m, 3 H, *H*-**c**,**h**,**l**), 3.83-3.39 (m, 7 H, *H*-**e**,**j**,**p**), 2.16-1.45 (m, 7 H, *H*-**f**,**g**,**m**,**n**), 1.36 (s, 9 H, *H*-**a**), 1.15 (d, 3 H, *H*-**d**), 0.86 (dd, 6 H, *H*-**o**) ppm.

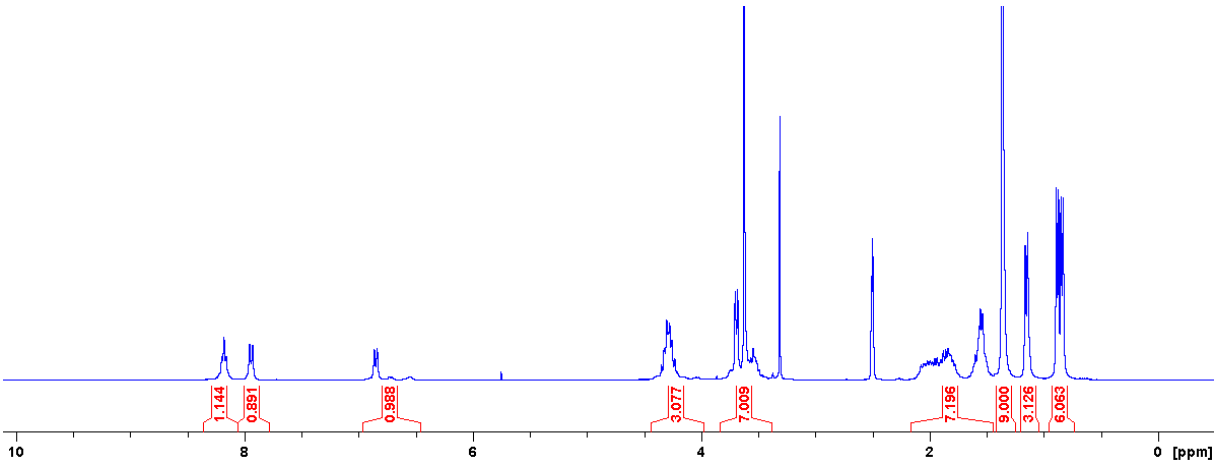

Figure 76: Representative ^{1}H NMR spectra of Boc-ala-pro-gly-leu-OMe in d_6-DMSO.

Boc-ala-pro-gly-leu-OH

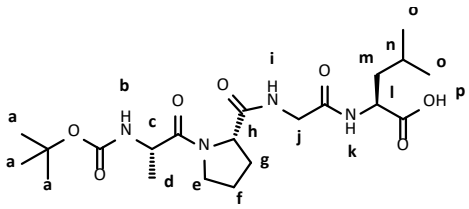

Boc-ala-pro-NHS ester (15.0 g, 1.0 eq.) was dissolved in ACN (300 mL) in a 500 mL Schott bottle at rt and pyridine (7.88 mL, 2.5 eq.) was added at once. gly-leu-OH TFA salt was dissolved in MilliQ (75 mL) at rt and both clear, colorless solutions were combined at 0°C (ice bath). The turbid, colorless reaction solution was stirred for 1 h at 0 °C, then 3 h at 50 °C and solvents were removed (roti, 50 °C). MilliQ (50 mL) was added to the clear yellowish solution, the pH was decreased to <3 with 10 % HCl and the obtained white suspension centrifuged (5 min, 4500 rpm, rt). The supernatant was discarded, the sediment redissolved by raising the pH with 2 N NaOH and the precipitation procedure was repeated twice more. The final white sediment was resuspended in MilliQ and freeze dried to form a white powder. Residues Boc-Ala-Pro-OH remained inseparable by physical or chemical purification methods which ultimately meant the failure of the synthesis.

Boc-ala-pro-gly-leu-OMe (20.0 g, 1.0 eq.) was dissolved in MeOH (200 mL) in a 500 mL Schott bottle at rt, NaOH (2 N, 46.8 mL, 2.2 eq.) was added at once and the clear, colorless reaction solution was stirred for 1 h at rt. After the addition of MilliQ (100 mL), the solution was neutralized with 10 % HCl, MeOH was removed (roti, 50 °C) and the product precipitated by decreasing the pH to <3 with 10 % HCl. The white suspension was centrifuged (5 min, 4500 rpm, rt), the supernatant discarded and white sediment washed with dilute HCl (<0.5 %) twice consisting of resuspension and centrifugation. The final white sediment was resuspended in MilliQ, freeze dried and the product obtained as white powder.

^{1}H NMR (300 MHz, d_6-DMSO): δ = 12.56 (s, 1 H, *H*-**p**), 8.16 (t, 1 H, *H*-**i**), 8.10-7.71 (m, 1 H, *H*-**k**), 6.99-6.44 (m, 1 H, *H*-**b**), 4.45-3.98 (m, 3 H, *H*-**c**,**h**,**l**), 3.82-3.42 (m, 4 H, *H*-**e**,**j**), 2.16-1.45 (m, 7 H, *H*-**f**,**g**,**m**,**n**), 1.36 (s, 9 H, *H*-**a**), 1.15 (d, 3 H, *H*-**d**), 0.86 (dd, 6 H, *H*-**o**) ppm.

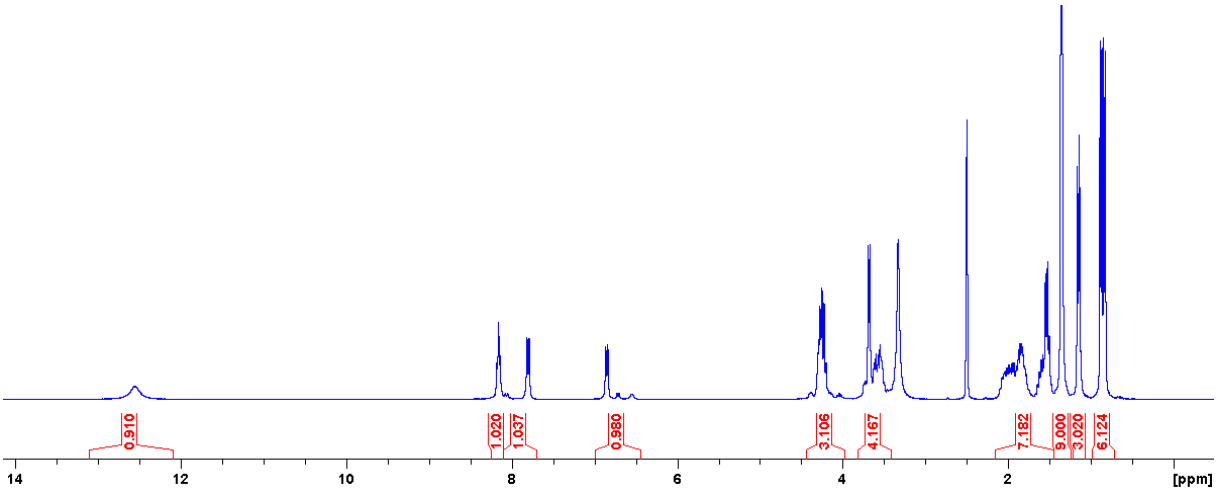

Figure 77: Representative ^{1}H NMR spectra of Boc-ala-pro-gly-leucine in d_6-DMSO.

4.4 Modification of hyaluronic acid (HA) derivates

4.4.1 Thiolated hyaluronic acid (HASH & C6-HASH)

HASH

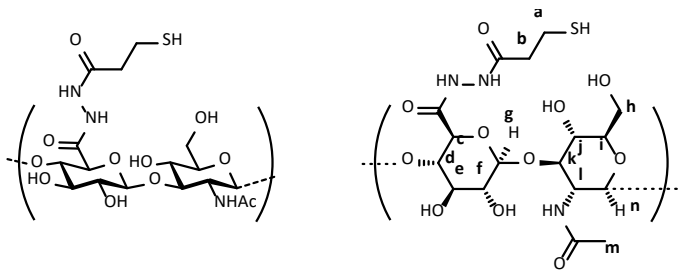

HASH was prepared pursuant to Stichler *et.al.*[35] with several modifications. HA (3.00 g, 1.0 eq.) was dissolved in MilliQ (350 mL) in a 1000 mL Schott bottle in a benchtop incubator at 50 °C (250 rpm, 6 h) and simultaneously DTP (7.13 g, 4.0 eq.) and NHS (3.44 g, 4.0 eq.) were dissolved in Sørensen buffer (0.2 M, pH 5.5, 350 mL) in a 500 mL Schott bottle at 50 °C (1 h, incubator). Both clear, colorless solutions were combined, EDC (10.7 g, 7.5 eq.) was added and dissolved and the pH was adjusted to 4.0 by addition of HCl (10 %, 11.5 mL). After 1 h of incubation at 37 °C (250 rpm), the obtained jelly was alkalified to pH >8.0 with NaOH (2 N, 50 mL), DTT (5.77 g, 5.0 eq.) was added and the mixture incubated at 37 °C (250 rpm, overnight). The pH of the brownish solution was acidified to 3.0 with HCl (10 %, 28 mL) and dialyzed (MWCO 3.5 kDa, RC) against dialysis buffer (0.3 mM, pH 5.0, K_2HPO_4/HCl) with added sodium ascorbate and TCEP (each 1 g / 15 L) for 3 d at rt with 5 media replacements per day, then against dialysis buffer without TCEP for 2 d at rt with identical replacement rate. The final colorless solution was freeze dried to form a white, foamy solid.

^{1}H NMR (300 MHz, D_2O): δ = 4.68-4.46 (s, 2 H, **g**,**n**), 4.19-3.24 (m, 10 H, **c**,**d**,**e**,**f**,**h**,**i**,**j**,**k**,**l**), 2.99-2.60 (m, 4 H, **a**,**b**), 2.16-1.86 (s, 3 H, **m**) ppm.

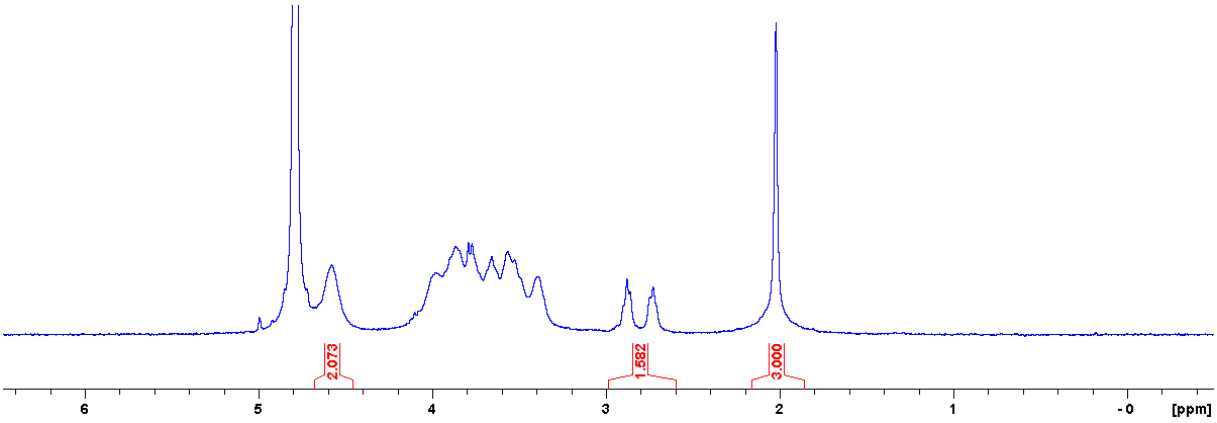

Figure 78: Representative ^{1}H NMR spectra of thiolated hyaluronic acid (HASH) in D_2O.

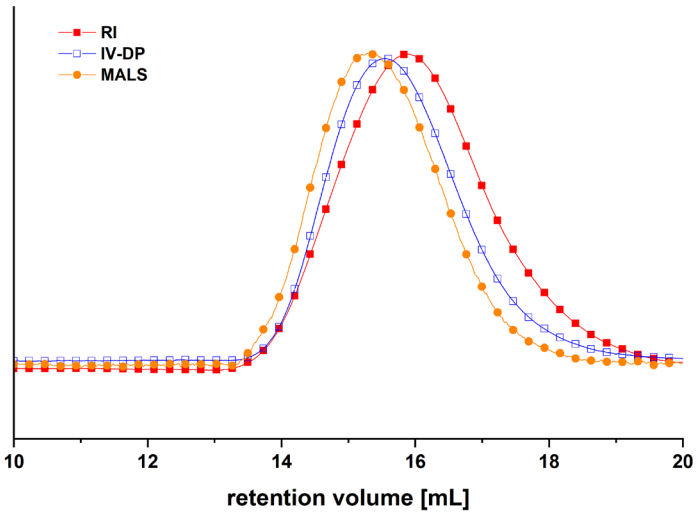

Figure 79: Representative SEC elugram of thiolated hyaluronic acid (HASH) measured in H_2O.

C-6-HASH

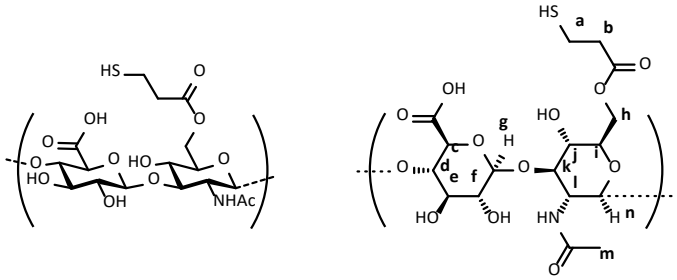

HA (0.2-0.5 MDa, 1.00 g, 1.0 eq.) was dissolved in MilliQ/DMF (50 mL / 33 mL) in a 250 mL Schott bottle in a benchtop incubator at 37 °C (250 rpm, overnight) and cooled to 0 °C (ice bath). Acrylic anhydride (0.504 mL, 1.75 eq.) was added and NaOH (1 N, 4.36 mL, 1.75 eq.) was added in 10 portions every 2.5 min. After stirring the turbid, colorless reaction mixture overnight at 0 °C in complete darkness, a mixture of AcSH (0.321 mL, 5.25 eq.) in DMF (10 mL) was added to the ice-cold solution and stirred for 1 h at 0 °C, then for 3 h at rt under light exclusion. K_2HPO_4 (5 M, 5.00 mL) and DTT (4.04 g, 5.25 eq.) were added and the turbid solution incubated overnight (37 °C, 200 rpm). The solution was acidified to pH 4-5 with 10 % HCl (8 mL), first dialyzed (MWCO 3.5 kDa, RC) against dialysis buffer (0.3 mM, pH 5.0, K_2HPO_4/HCl) with added sodium ascorbate and TCEP (each 1 g / 15 L) for 5 d at rt with 4 media replacements per day, then against dialysis buffer without TCEP for 3 d at rt with identical replacement rate and freeze dried. The product appeared as white, foamy solid.

^{1}H NMR (300 MHz, D_2O): δ = 4.69-4.45 (s, 2 H, **g**,**n**), 4.19-3.24 (m, 10 H, **c**,**d**,**e**,**f**,**h**,**i**,**j**,**k**,**l**), 2.98-2.63 (m, 4 H, **a**,**b**), 2.17-1.81 (s, 3 H, **m**) ppm.

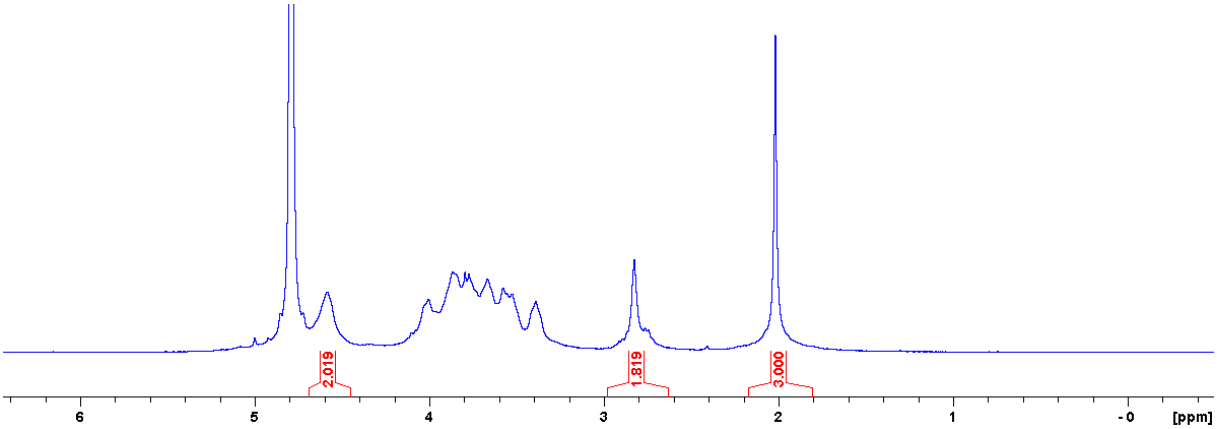

Figure 80: Representative ^{1}H NMR spectra of C6-thiolated hyaluronic acid (C6-HASH) in D_2O.

4.4.2 Hyaluronic pentenoate (HAPA)

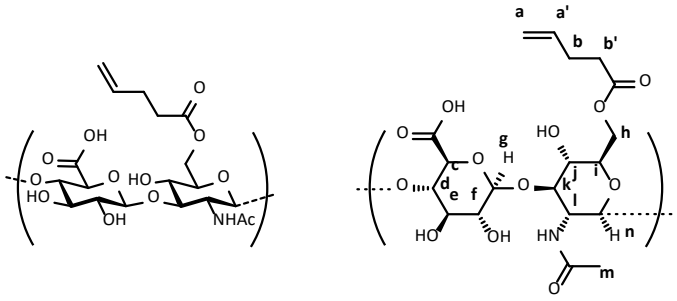

low molecular weight HAPA (M_w [kDa]: 8-15; 80-100; 200-500)

HA (3.00 g, 1.0 eq.) was dissolved in MilliQ/DMF (150 mL / 100 mL) in a 500 mL Schott bottle in a benchtop incubator at 37 °C (250 rpm, overnight) and cooled to 0 °C (ice bath). Pentenoic anhydride (4.51 mL, 3.3 eq.) was added to the clear, colorless solution, NaOH (1 N, 24.7 mL, 3.3 eq.) was added in 6 portions every 5 min and the turbid, colorless reaction mixture was stirred overnight at 0 °C. After dialysis against MilliQ (MWCO 3.5 kDa, RC) at rt for 5 d with 4 media replacements per day, the clear, colorless solution was freeze dried and the product obtained as white, foamy solid. When modifying 8-15 kDa HA, the dialysis was carried out with MWCO 1 kDa RC tubing to prevent greater yield loss.

high molecular weight HAPA (M_w [MDa]: 0.6-1.0; 1.0-2.0; 2.0-2.5)

HA (1.00 g, 1.0 eq.) was dissolved in MilliQ/DMF (100 mL / 66 mL) in a 250 mL Schott bottle in a benchtop incubator at 37 °C (250 rpm, overnight) and cooled to 0 °C (ice bath). Pentenoic anhydride (2.80 mL, 6.15 eq.) was added to the clear, colorless solution, NaOH (1 N, 15.3 mL, 6.15 eq.) was added in 6 portions every 5 min and the turbid, colorless reaction mixture was stirred overnight at 0 °C. After dialysis against MilliQ (MWCO 3.5 kDa, RC) at rt for 5 d with 4 media replacements per day, the clear, colorless solution was freeze dried and the product obtained as white, foamy solid.

^{1}H NMR (300 MHz, D_2O): δ = 5.91 (m, 1 H, **a'**), 5.25-4.94 (m, 2 H, **a**), 4.66-4.36 (s, 2 H, **g**,**n**), 4.17-3.09 (m, 10 H, **c**,**d**,**e**,**f**,**h**,**i**,**j**,**k**,**l**), 2.79-2.19 (m, 4 H, **b**,**b'**), 2.17-1.83 (s, 3 H, **m**) ppm.

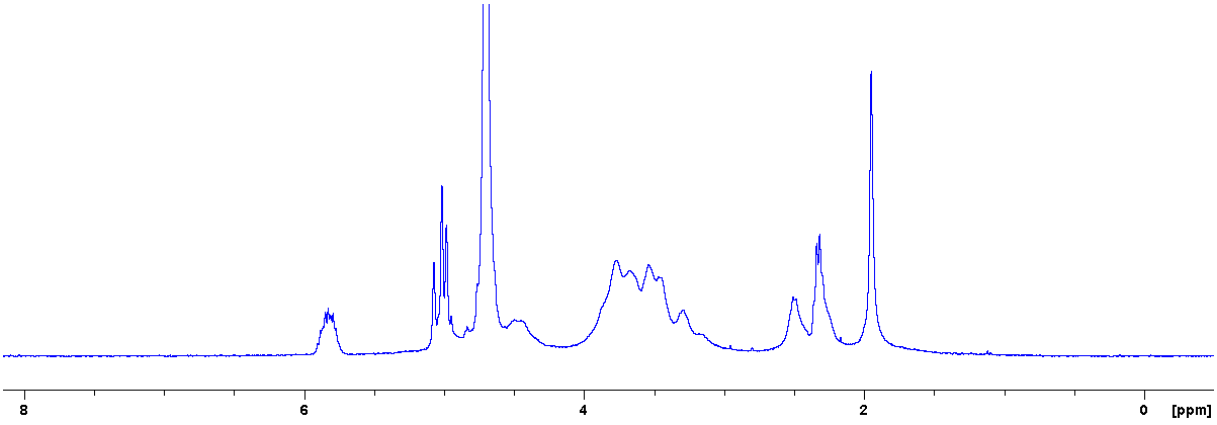

Figure 81: Representative ^{1}H NMR spectra of hyaluronic pentenoate (HAPA) in D_2O.

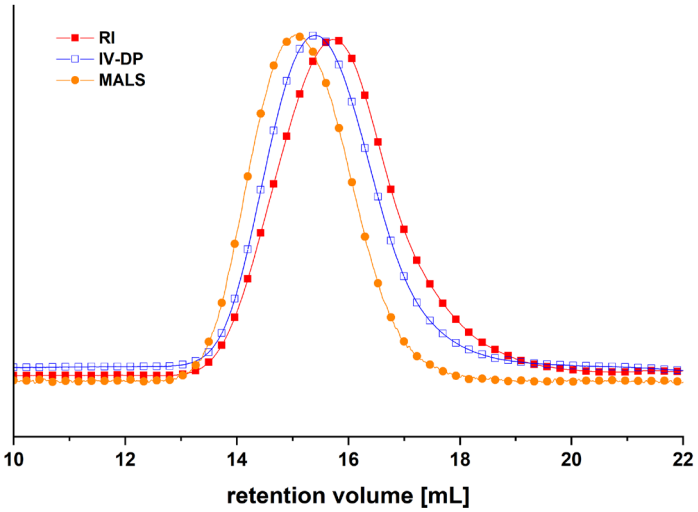

Figure 82: Representative SEC elugram of hyaluronic pentenoate (HAPA) measured in H_2O.

4.4.3 Hyaluronic acrylate (HAA)

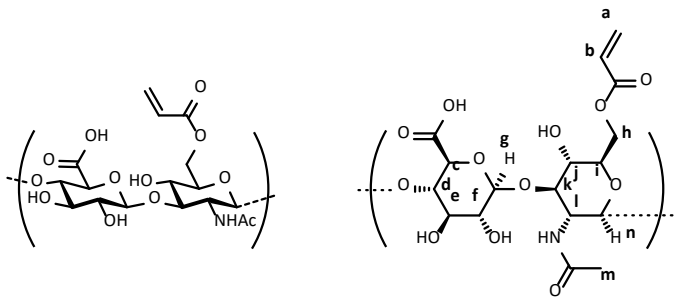

HA (8-15 kDa, 20.0 g, 1.0 eq.) was dissolved in MilliQ (250 mL) in a 500 mL Schott bottle with a benchtop incubator at 50 °C (250 rpm, 1 h) and DMF (167 mL) was added. The clear, colorless solution was cooled to 0 °C (ice bath), acrylic anhydride (8.65 mL, 1.5 eq.) added at once and NaOH (1 N, 74.8 mL, 1.5 eq.) added in 10 portions every 2.5 min. The turbid, colorless reaction mixture was stirred overnight at 0 °C in complete darkness and the obtained clear, colorless solution was precipitated by addition of ice-cold acetone (3500 mL). After 1 h rest, the supernatant was discarded,

the sediment resuspended in ice-cold acetone/MilliQ (9:1, 500 mL) and centrifuged (5 min, 4500 rpm, 5 °C). The sediment was washed with pure ice-cold acetone (5x 300 mL), filtered (paper filter) and dried *in vacuo* at rt to give a fine white powder. In case of remaining DMF traces, the powder was washed again with acetone three more times, filtered and dried.

^{1}H NMR (300 MHz, D_2O): δ = 6.64-5.92 (m, 3 H, **a**,**b**), 4.69-4.41 (s, 2 H, **g**,**n**), 4.19-3.17 (m, 10 H, **c**,**d**,**e**,**f**,**h**,**i**,**j**,**k**,**l**), 2.30-1.73 (s, 3 H, **m**) ppm.

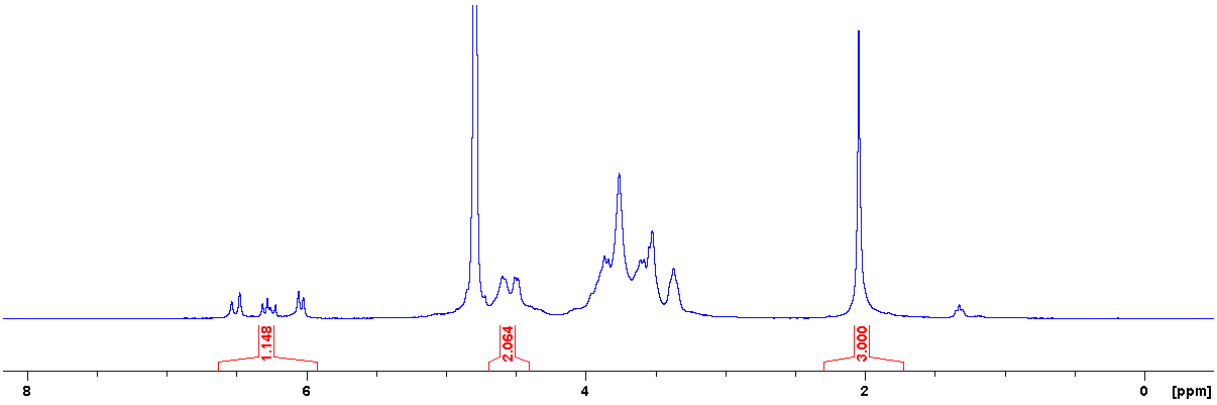

Figure 83: Representative ^{1}H NMR spectra of hyaluronic acrylate (HAA) in D_2O.

4.5 Modification of polyethylene glycol (PEG) derivates

4.5.1 PEG-acrylates

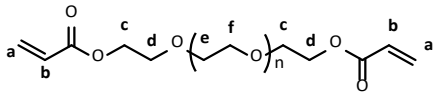

chemical synthesis with recrystallization

PEG (linear 6 kDa, 100 g, 1.0 eq.) was molten at 100 °C in a 1000 mL Schlenk flask, HV applied until end of bubbling, toluene (200 mL) added and the solvents removed azeotropic by distillation. Argon was applied, toluene added (900 mL) and the clear, colorless solution cooled to rt. TEA (13.9 mL, 3.0 eq.) and freshly distilled acryloyl chloride (8.08 mL, 3.0 eq.) were added and the reaction solution was stirred overnight at rt. The formed solids were removed by centrifugation (15 min, 4500 rpm, rt) following a precipitation in ice-cold DE (2000 mL). After a 1 h rest, the supernatant was decanted, the remaining suspension centrifuged (5 min, 4500 rpm, 5 °C) and the supernatant discarded. The orangish sediment was recrystallized in EtOH until complete discoloration of the supernatant, the sediment redissolved in EtOH and precipitated in ice-cold DE (1000 mL). The supernatant was decanted, the remaining suspension centrifuged (5 min, 4500 rpm, 5 °C) and the final sediment dried *in vacuo* at rt to give a white, bulky powder.

chemical synthesis with activated charcoal

PEG (linear 6 kDa, 50.0 g, 1.0 eq.) was molten at 100 °C in a 1000 mL Schlenk flask, HV applied until end of bubble formation, argon applied and cooled to rt. The white solid was dissolved in DCM (500 mL), cooled to 0 °C, pyridine (2.69 mL, 2.0 eq.) and acrylic anhydride (3.84 mL, 2.0 eq.) were added. The clear, colorless reaction solution was stirred for 1 h at 0 °C (ice bath), then for 3 h at rt and the solvents reduced (roti, 50 °C, darkness). Precipitation was conducted by addition of ice-cold DE (1000 mL), the supernatant decanted and the sediment dried *in vacuo* at rt. The yellowish solid was redissolved in MilliQ (500 mL), activated charcoal (60 g) was added and the suspension incubated overnight (rt, 200 rpm, darkness). After 1 d rest, the supernatant was decanted into a paper filter and the filtrate again filtered using a bottle top 0.45 µm sterile filter. The clear, colorless solution was freeze dried and the product obtained as white, bulky solid.

^{1}H NMR (300 MHz, $CDCl_3$): δ = 6.45-5.70 (m, 3 H, **a**,**b**), 4.39-4.16 (m, 2 H, **c**), 3.96-3.24 (m, **d**,**e**,**f**) ppm.

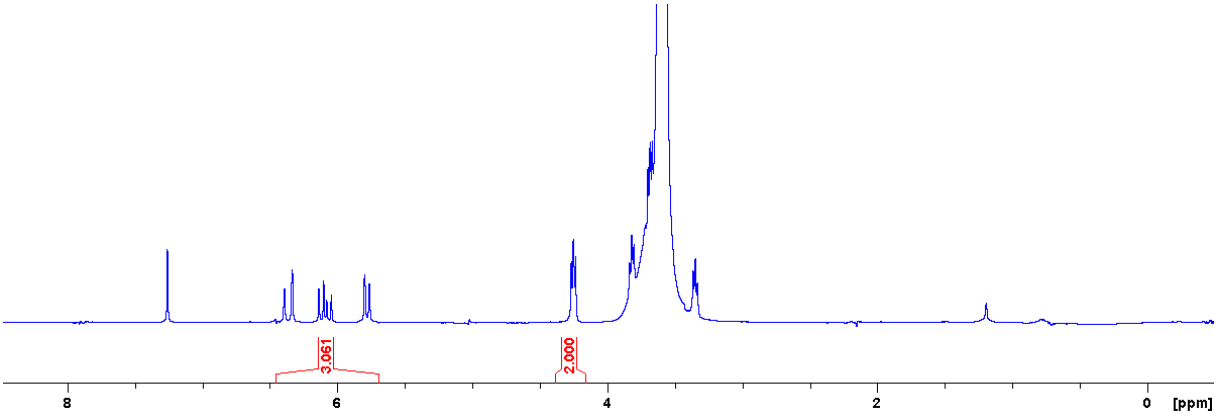

Figure 84: Representative ^{1}H NMR spectra of 6k-PEG-diacrylate in $CDCl_3$.

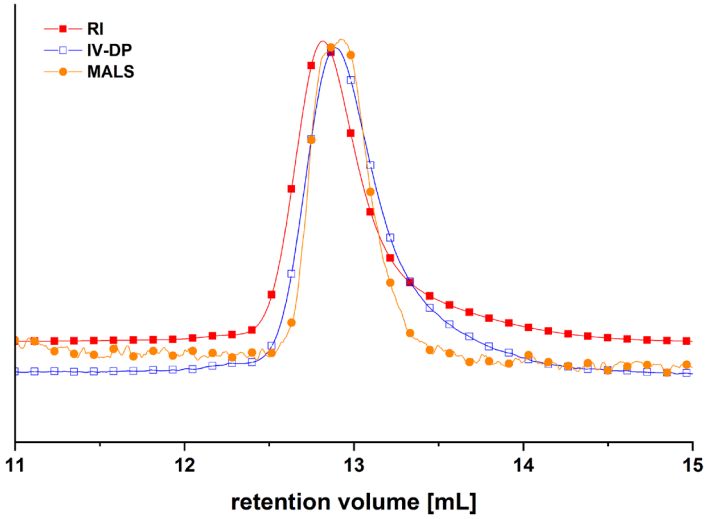

Figure 85: Representative SEC elugram of 6k-PEG-diacrylate measured in H_2O.

enzymatic synthesis

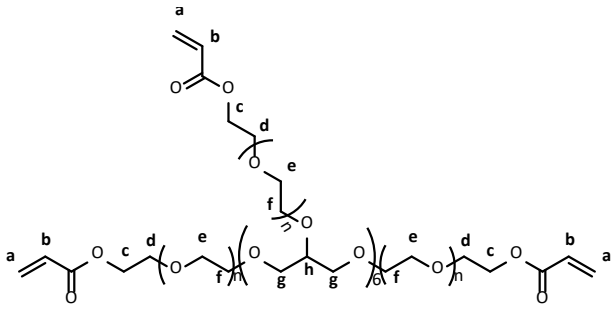

PEG (8-arm 10 kDa, 5.00 g, 1.0 eq.) was molten at 100 °C in a 100 mL round-bottom flask, HV applied until bubbling ended and the hot melt dissolved in toluene (50 mL). The clear, colorless solution was allowed to cool to rt, lipase (Novozyme 435, 0.050 g) and vinyl acrylate (1.24 mL, 3.0 eq.) were added, and the reaction mixture was incubated for 3 d (50 °C, 250 rpm). After filtration (paper filter) and precipitation in ice-cold DE (400 mL), the white suspension was centrifuged (5 min, 4500 rpm, 5 °C), and was washed with DE (3x 100 mL each time), consisting of resuspension in DE, centrifugation and sediment separation. The final white sediment was dried *in vacuo* to give a white, bulky powder.

^{1}H NMR (300 MHz, $CDCl_3$): δ = 6.52-5.76 (m, 3 H, **a**,**b**), 4.37-4.25 (m, 2 H, **c**), 3.96-3.33 (m, **d**,**e**,**f**,**g**,**h**) ppm.

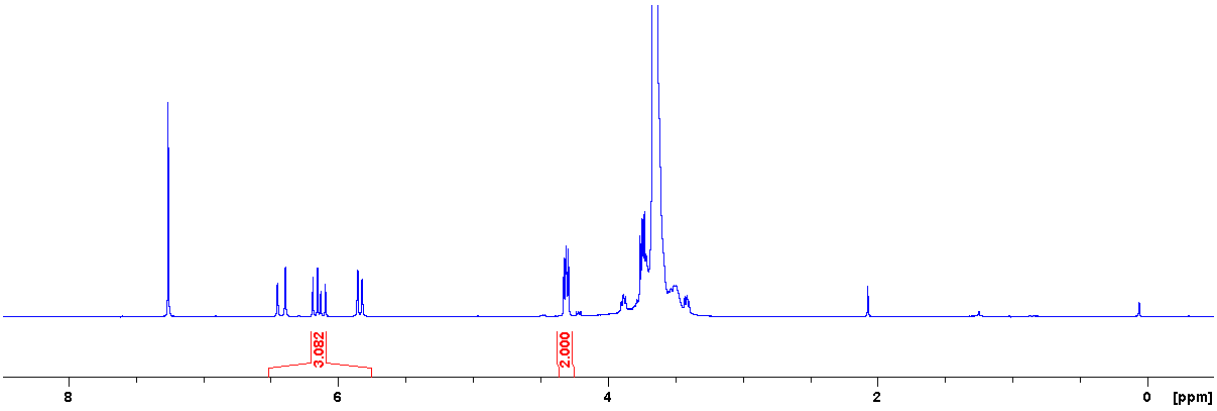

Figure 86: Representative ^{1}H NMR spectra of 8arm-10k-PEG-acrylate in $CDCl_3$.

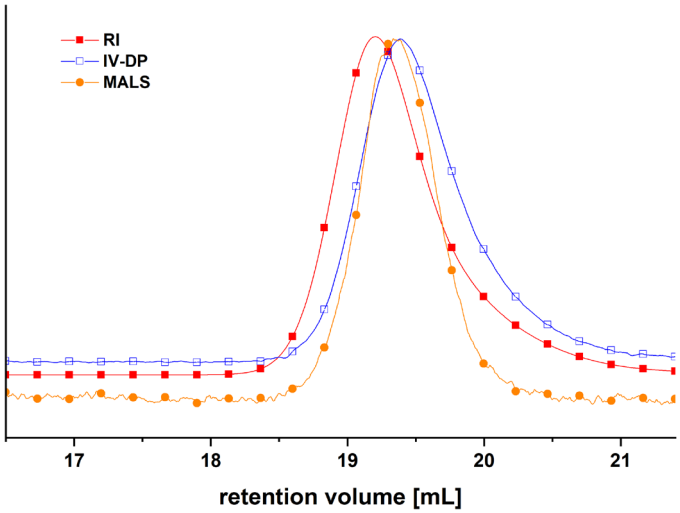

Figure 87: Representative SEC elugram of 8arm-10k-PEG-acrylate measured in H_2O.

4.5.2 PEG-methacrylates

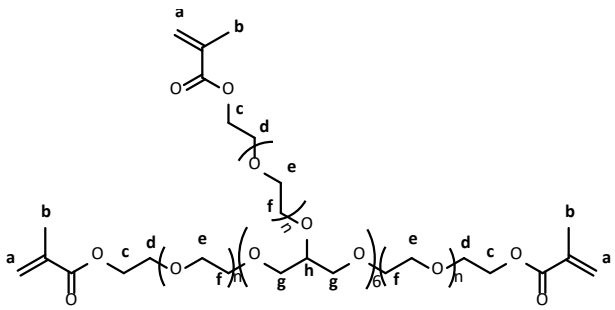

PEG (8-arm 10 kDa, 1.00 g, 1.0 eq.) was dissolved in toluene (25 mL) in a 100 mL Schott bottle at 50 °C, cooled to rt, lipase (Novozyme 435, 0.050 g) and vinyl methacrylate (0.288 mL, 3.0 eq.) were added. After 72 h of incubation (37 °C, 200 rpm) and filtration (paper filter), the polymer was precipitated in ice-cold DE (200 mL), filtered (paper filter) and washed with DE (2x 100 mL). The white filter cake was dried *in vacuo* at rt to form a white, bulky solid.

^{1}H NMR (300 MHz, $CDCl_3$): δ = 6.13 (m, 1 H, **a**), 5.59 (m, 1 H, **a**), 4.38-4.23 (m, 2 H, **c**), 3.97-3.33 (m, **d**,**e**,**f**,**g**,**h**), 1.94 (s, 3 H, **b**) ppm.

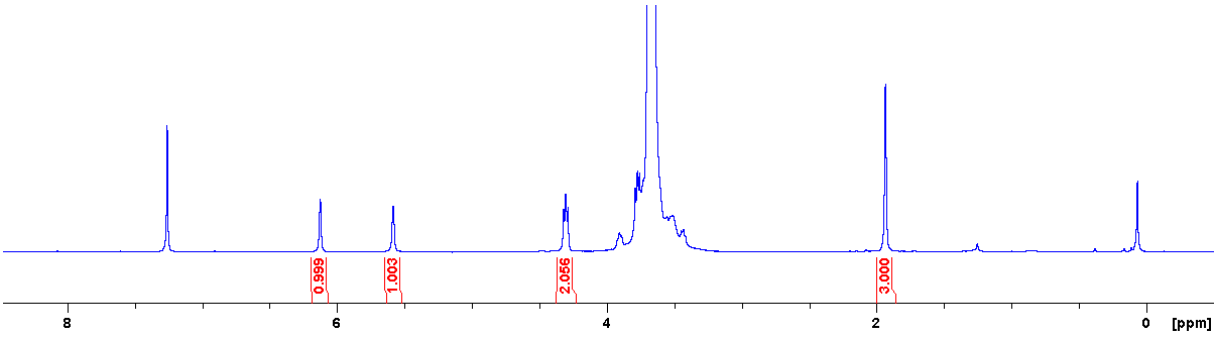

Figure 88: Representative ^{1}H NMR spectra of 8arm-10k-PEG-methacrylate in $CDCl_3$.

4.5.3 PEG-allyl carbonates

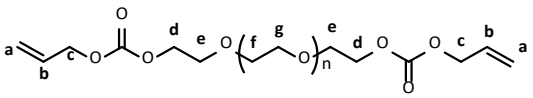

PEG (linear 6 kDa, 1.00 g, 1.0 eq.) was molten at 100 °C in a 50 mL Schlenk flask, HV applied until end of bubbling and cooled to rt. Argon was applied, the cooled melt dissolved in dry DCM (10 mL), DBU (0.149 mL, 3.0 eq.) added and the clear solution was cooled to 0 °C (ice bath). Allyl chloroformate (0.107 mL, 3.0 eq.) was added and the reaction solution stirred for 1 h at 0 °C, then overnight at rt. The polymer was precipitated by addition of ice-cold DE (250 mL), centrifuged (5 min, 4500 rpm, 5 °C) and the sediment dried in vacuo. The obtained white solid was redissolved in MilliQ (50 mL), dialyzed (MWCO 1 kDa, RC) against dialysis buffer (0.3 mM, pH 5.0, K_2HPO_4/HCl) for 5 d at rt with 3 media replacements per day, then dialyzed against MilliQ for 3 d at rt with same replacement rate and freeze dried. The product appeared as white, bulky solid.

^{1}H NMR (300 MHz, $CDCl_3$): δ = 6.00-5.83 (m, 1 H, **b**), 5.40-5.20 (m, 2 H, **a**), 4.67-4.54 (m, 2 H, **c**), 4.34-4.21 (m, 2 H, **d**), 3.92-3.35 (m, **e**,**f**,**g**) ppm.

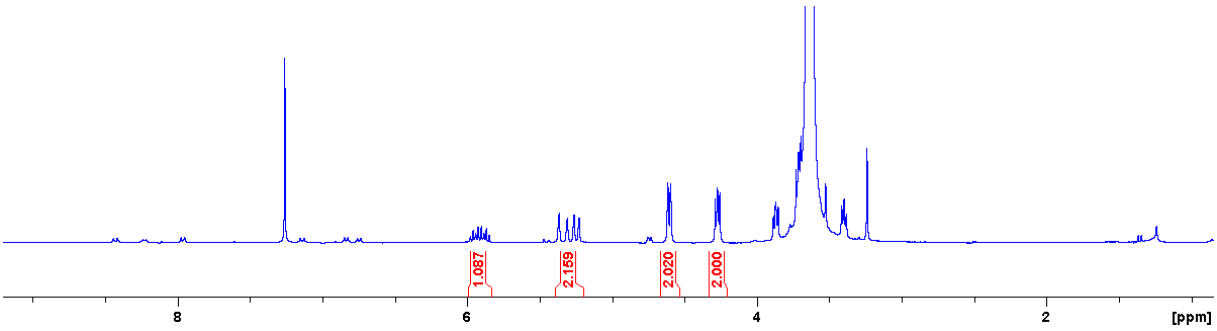

Figure 89: Representative ^{1}H NMR spectra of raw 6k-PEG-diallyl carbonate in $CDCl_3$.

4.5.4 PEG-amines

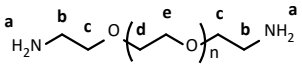

Amino-PEG was synthesized pursuant to Iijima *et.al.*[109] with modifications. PEG (linear 6 kDa, 50.0 g, 1.0 eq.) was molten at 110 °C in a 1 L round-bottom flask and HV applied until formation of bubbles ended while stirring (<2 h). Argon was applied, the melt was cooled to rt and dissolved in dry DCM (400 mL). The clear, colorless solution was cooled to 0 °C (ice bath), TEA (5.78 mL, 2.5 eq.) and MesCl (3.22 mL, 2.5 eq.) were added and the reaction solution was stirred for 1 h at 0 °C, then stirred overnight at rt. Solvents were removed (roti, 50°C), the yellow solid residue redissolved in MilliQ and HV applied until clarification of the solution. (100 mL). After the addition of ammonium hydroxide (28-30 %, 500 mL), the clear, yellowish reaction solution was stirred for 3 d at rt and ammonia was evaporated over 2 d in the fume hood while keeping the pH constant >10 with 2 N NaOH. The clear, yellow solution was extracted with DCM (500 mL, 400 mL, 2x 200 mL), the solvents of the combined DCM layer reduced (roti, 50 °C) and the polymer precipitated by addition of ice-cold DE (1000 mL). The supernatant was decanted, the remaining suspension centrifuged (5 min, 450 rpm, 5 °C) and the supernatant discarded. The white sediment was dried *in vacuo* at rt to give a white, bulky powder.

^{1}H NMR (300 MHz, $CDCl_3$): δ = 4.13-3.29 (m, **c**,**d**,**e**), 3.27-2.48 (m, 4 H, **a**,**b**) ppm.

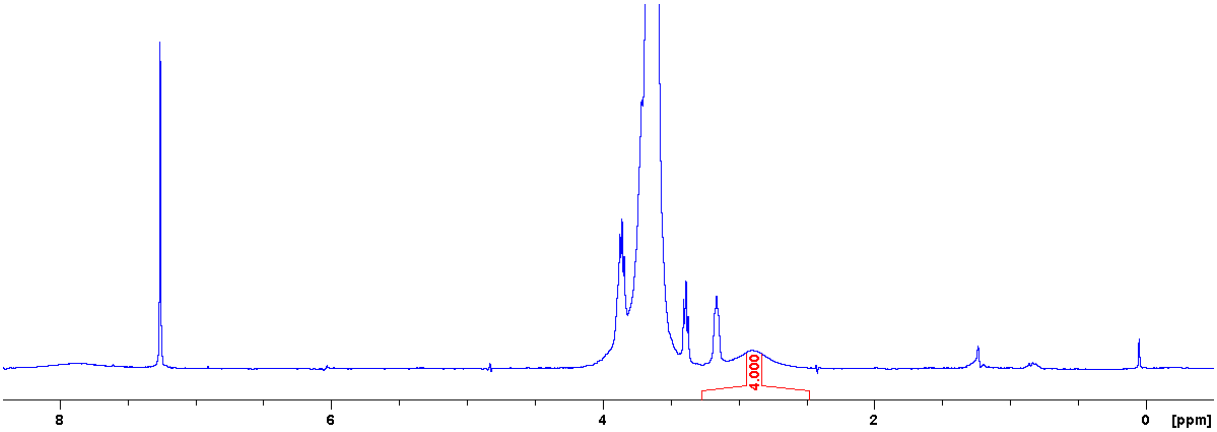

Figure 90: Representative ^{1}H NMR spectra of 6k-PEG-diamine in $CDCl_3$.

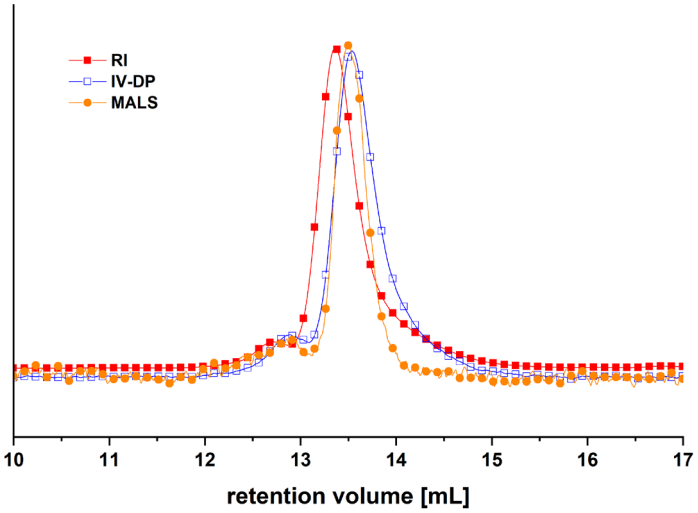

Figure 91: Representative SEC elugram of 6k-PEG-diamine measured in H_2O.

4.5.5 PEG-allyl carbamates

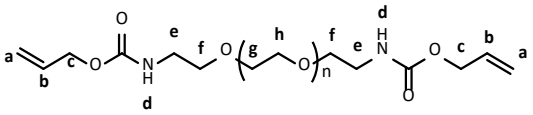

For the allyl carbamate-PEG synthesis, the reaction conditions from Barthel *et. al.*[112] (alloc-alanine synthesis) were transferred on PEG-amines. Amino-PEG (linear 6 kDa, 10.0 g, 1.0 eq.) was dissolved in MilliQ (100 mL) in a 250 mL round-bottom flask at rt, NaOH (2 N, 8.67 mL, 2.0 eq.) added and the solution cooled to 0 °C by an ice bath. Allyl chloroformate (0.569 mL , 1.6 eq.) was added at once, the two-layer system stirred intensively for 3 h at 0 °C and then overnight at rt. The clear, yellowish solution was washed with DE (2x 100 mL), extracted with DCM (5x 75 mL) with addition of brine (50 mL). The combined DCM layer was dried ($MgSO_4$), filtered (paper filter) and the solvents were reduced (roti, 50 °C). The yellowish oil was precipitated in ice-cold DE (1000 mL), centrifuged (15 min, 4500 rpm, 5 °C) and the isolated sediment dried *in vacuo* at rt to form a white, bulky powder.

^{1}H NMR (300 MHz, $CDCl_3$): δ = 6.00-5.81 (m, 1 H, **b**), 5.50-5.12 (m, 3 H, **a**,**d**), 4.63-4.51 (m, 2 H, **e**), 3.94-3.26 (m, **f**,**g**,**h**) ppm.

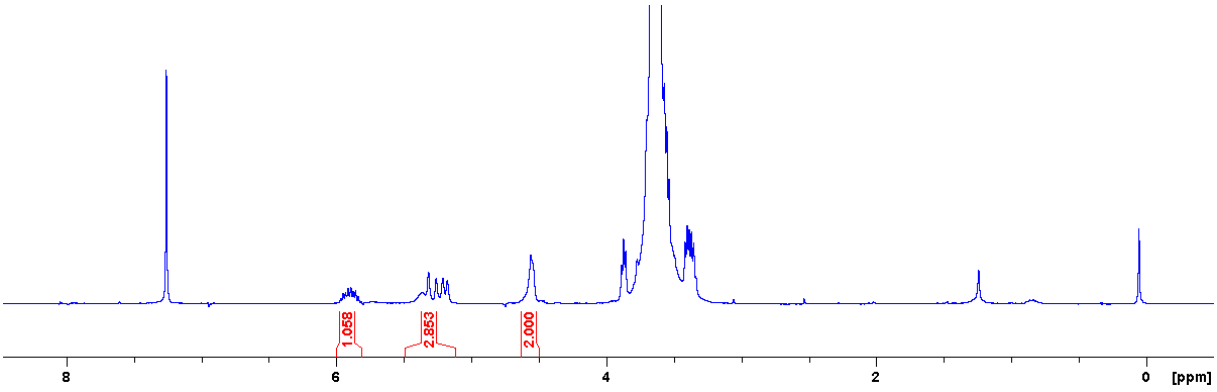

Figure 92: Representative ^{1}H NMR spectra of 6k-PEG-diallyl carbamate in $CDCl_3$.

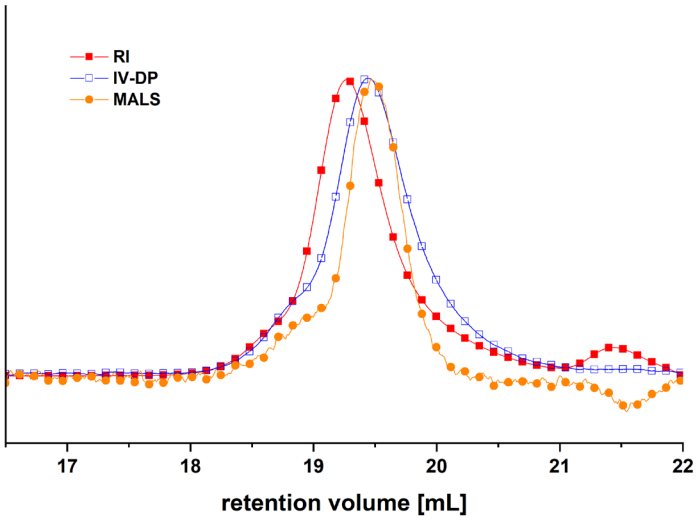

Figure 93: Representative SEC elugram of 6k-PEG-diallyl carbamate measured in H_2O.

4.5.6 PEG-maleimides

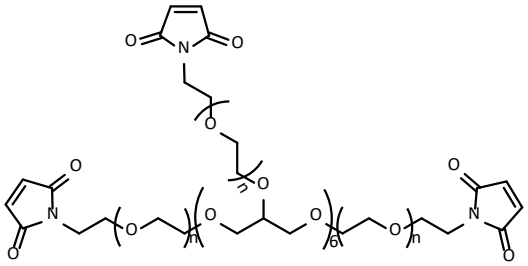

PEG-Maleimide was prepared in according to Mongondry *et.al.*[42] with slight modifications for maleimide introduction. PEG (8-arm 10kDa, 5.00 g, 1.0 eq.) was molten at 100 °C in a 250 mL Schlenk flask, HV applied until bubble formation ended, argon applied and cooled to rt. The colorless melt was dissolved in THF (150 mL) at 40 °C (water bath), cooled to rt and maleimide (0.466 g, 1.2 eq.) was added. After the addition of PPh_3 (1.26 g, 1.2 eq.), a solution of DIAD (0.945 mL, 1.2 eq.) in THF (10 mL) was added dropwise over 30 min and the clear, orange solution was stirred for 3 d at rt. Solvents were removed (roti, 40 °C), MilliQ (100 mL) added to the red-brown oil and the obtained red-brown suspension centrifuged (15 min, 4500 rpm, 5 °C). The supernatant was filtered (paper filter), washed with DE (2x 250 mL) and freeze dried to give a brown-grey, bulky solid.

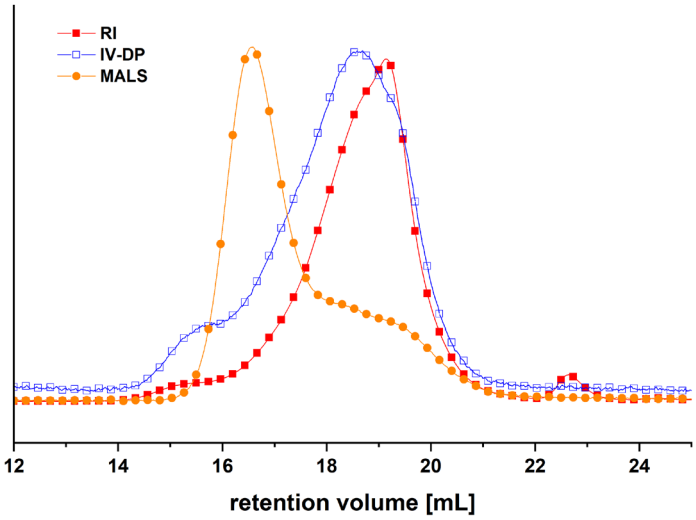

Figure 94: Representative SEC elugram of 8arm-10k-PEG-maleimide measured in H_2O.

5 References

[1] W. Sun, B. Starly, A. C. Daly, J. A. Burdick, J. Groll, G. Skeldon, W. M. Shu, Y. Sakai, M. Shinohara, M. Nishikawa, J. Jang, D. W. Cho, M. H. Nie, S. Takeuchi, S. Ostrovidov, A. Khademhosseini, R. D. Kamm, V. Mironov, L. Moroni, I. T. Ozbolat, *Biofabrication* **2020**, *12*.

[2] V. Mironov, N. Reis, B. Derby, *Tissue Eng* **2006**, *12*, 631-634.

[3] A. B. Dababneh, I. T. Ozbolat, *J Manuf Sci E-T Asme* **2014**, *136*.

[4] Y. J. Seol, H. W. Kang, S. J. Lee, A. Atala, J. J. Yoo, *Eur J Cardiothorac Surg* **2014**, *46*, 342-348.

[5] I. T. Ozbolat, *3D Bioprinting*, Academic Press, **2016**.

[6] E. Lepowsky, M. Muradoglu, S. Tasoglu, *Bioprinting* **2018**, *11*.

[7] S. Vanaei, M. S. Parizi, S. Vanaei, F. Salemizadeh Parizi, H. R. Vanaei, *Eng Regener* **2021**, *2*, 1-18.

[8] G. Decante, J. B. Costa, J. Silva-Correia, M. N. Collins, R. L. Reis, J. M. Oliveira, *Biofabrication* **2021**, *13*.

[9] D. Chimene, K. K. Lennox, R. R. Kaunas, A. K. Gaharwar, *Ann Biomed Eng* **2016**, *44*, 2090-2102.

[10] M. Hospodiuk, M. Dey, D. Sosnoski, I. T. Ozbolat, *Biotechnol Adv* **2017**, *35*, 217-239.

[11] P. S. Gungor-Ozkerim, I. Inci, Y. S. Zhang, A. Khademhosseini, M. R. Dokmeci, *Biomater Sci-Uk* **2018**, *6*, 915-946.

[12] J. Malda, J. Visser, F. P. Melchels, T. Jungst, W. E. Hennink, W. J. Dhert, J. Groll, D. W. Hutmacher, *Adv Mater* **2013**, *25*, 5011-5028.

[13] N. A. Peppas, A. S. Hoffman, in *Biomaterials Science* Academic Press, **2020**, pp. 153-166.

[14] R. Langer, J. P. Vacanti, *Science* **1993**, *260*, 920-926.

[15] W. Tomal, J. Ortyl, *Polymers-Basel* **2020**, *12*.

[16] K. S. Lim, B. J. Klotz, G. C. J. Lindberg, F. P. W. Melchels, G. J. Hooper, J. Malda, D. Gawlitta, T. B. F. Woodfield, *Macromol Biosci* **2019**, *19*, e1900098.

[17] L. Ouyang, J. P. K. Armstrong, Y. Lin, J. P. Wojciechowski, C. Lee-Reeves, D. Hachim, K. Zhou, J. A. Burdick, M. M. Stevens, *Sci Adv* **2020**, *6*.

[18] B. H. Northrop, R. N. Coffey, *J Am Chem Soc* **2012**, *134*, 13804-13817.

[19] V. Findik, I. Degirmenci, S. Catak, V. Aviyente, *Eur Polym J* **2019**, *110*, 211-220.

[20] G. Gil Alvaradejo, M. Glassner, R. Hoogenboom, G. Delaittre, *Rsc Adv* **2018**, *8*, 9471-9479.

[21] Y. Oz, A. Sanyal, *Chem Rec* **2018**, *18*, 570-586.

[22] A. Gandini, *Prog Polym Sci* **2013**, *38*, 1-29.

[23] D. P. Nair, M. Podgorski, S. Chatani, T. Gong, W. X. Xi, C. R. Fenoli, C. N. Bowman, *Chem Mater* **2014**, *26*, 724-744.

[24] J. T. Oliveira, R. L. Reis, *J Tissue Eng Regen Med* **2011**, *5*, 421-436.

[25] J. Necas, L. Bartosikova, P. Brauner, J. Kolar, *Vet Med-Czech* **2008**, *53*, 397-411.

[26] K. Meyer, J. W. Palmer, *J. Biol. Chem.* **1934**, *107*, 629-634.

[27] K. Meyer, J. W. Palmer, *J. Biol. Chem.* **1936**, *114*, 689-703.

[28] M. K. Cowman, S. Matsuoka, *Carbohyd Res* **2005**, *340*, 791-809.

[29] P. Saranraj, M. A. Naidu, *Int J Pharm Biol Sci Arch* **2013**, *4*, 853-859.

[30] L. Lapcik, Jr., L. Lapcik, S. De Smedt, J. Demeester, P. Chabrecek, *Chem Rev* **1998**, *98*, 2663-2684.

[31] A. Zakeri, M. J. Rasaee, N. Pourzardosht, *Biotechnol Rep (Amst)* **2017**, *16*, 65-70.

[32] J. Gaffney, S. Matou-Nasri, M. Grau-Olivares, M. Slevin, *Mol Biosyst* **2010**, *6*, 437-443.

[33] G. D. Prestwich, D. M. Marecak, J. F. Marecek, K. P. Vercruysse, M. R. Ziebell, *J Control Release* **1998**, *53*, 93-103.

[34] W. M. Gramlich, I. L. Kim, J. A. Burdick, *Biomaterials* **2013**, *34*, 9803-9811.

[35] S. Stichler, T. Jungst, M. Schamel, I. Zilkowski, M. Kuhlmann, T. Bock, T. Blunk, J. Tessmar, J. Groll, *Ann Biomed Eng* **2017**, *45*, 273-285.

[36] S. Khetan, M. Guvendiren, W. R. Legant, D. M. Cohen, C. S. Chen, J. A. Burdick, *Nat Mater* **2013**, *12*, 458-465.

[37] S. L. Vega, M. Y. Kwon, K. H. Song, C. Wang, R. L. Mauck, L. Han, J. A. Burdick, *Nat Commun* **2018**, *9*, 614.

[38] J. D. Friedl, V. Nele, G. De Rosa, A. Bernkop-Schnurch, *Adv Funct Mater* **2021**, *31*.
[39] J. K. Tessmar, A. M. Gopferich, *Macromol Biosci* **2007**, *7*, 23-39.
[40] S. Herman, J. Loccufier, E. Schacht, *Macromol Chem Phys* **1994**, *195*, 203-209.
[41] P. D. Drumheller, J. A. Hubbell, *J. Biomed. Mater. Res.* **1995**, *29*, 207-215.
[42] P. Mongondry, C. Bonnans-Plaisance, M. Jean, J. F. Tassin, *Macromol Rapid Comm* **2003**, *24*, 681-685.
[43] J. K. Tessmar, A. G. Mikos, A. Gopferich, *Biomacromolecules* **2002**, *3*, 194-200.
[44] TRR225, Würzburg, **2018**.
[45] X. Z. Shu, Y. C. Liu, Y. Luo, M. C. Roberts, G. D. Prestwich, *Biomacromolecules* **2002**, *3*, 1304-1311.
[46] X. Z. Shu, S. Ahmad, Y. C. Liu, G. D. Prestwich, *J Biomed Mater Res A* **2006**, *79a*, 902-912.
[47] E. M. Horn, M. Beaumont, X. Z. Shu, A. Harvey, G. D. Prestwich, K. M. Horn, A. R. Gibson, M. C. Preul, A. Panitch, *J Neurosurg-Spine* **2007**, *6*, 133-140.
[48] J. M. Heffernan, D. J. Overstreet, L. D. Le, B. L. Vernon, R. W. Sirianni, *Ann Biomed Eng* **2015**, *43*, 1965-1977.
[49] Y. Hao, A. B. Zerdoum, A. J. Stuffer, A. K. Rajasekaran, X. Q. Jia, *Biomacromolecules* **2016**, *17*, 3750-3760.
[50] X. D. Bi, A. Y. Liang, Y. Tan, P. Maturavongsadit, A. Higginbothem, T. Gado, A. Gramling, H. N. Bahn, Q. Wang, *J Biomat Sci-Polym E* **2016**, *27*, 743-757.
[51] T. I. Zarembinski, N. J. Doty, I. E. Erickson, R. Srinivas, B. M. Wirostko, W. P. Tew, *Acta Biomater* **2014**, *10*, 94-103.
[52] T. Bock, V. Schill, M. Krahnke, A. F. Steinert, J. Tessmar, T. Blunk, J. Groll, *Macromol Biosci* **2018**, *18*, e1700390.
[53] X. Zhang, P. C. Sun, L. Z. Huangshan, B. H. Hu, P. B. Messersmith, *Chem Commun* **2015**, *51*, 9662-9665.
[54] S. Stichler, T. Bock, N. Paxton, S. Bertlein, R. Levato, V. Schill, W. Smolan, J. Malda, J. Tessmar, T. Blunk, J. Groll, *Biofabrication* **2017**, *9*, 044108.
[55] S. Pongor, M. Brownlee, A. Cerami, *Arch Biochem Biophys* **1985**, *238*, 458-463.
[56] T. Glonek, J. R. Vanwazer, T. C. Myers, *Phosphorus Sulfur* **1977**, *3*, 137-150.
[57] J. W. Kuo, G. D. Prestwich, in *Comprehensive Biomaterials*, Elsevier, Oxford, **2011**, p. 239.
[58] G. E. Likens, R. F. Wright, J. N. Galloway, T. J. Butler, *Sci Am* **1979**, *241*, 43-51.
[59] IUPAC, in *Compendium of Chemical Terminology*, Blackwell Scientific Publications, Oxford, **1997**, p. 598.
[60] W. P. Jencks, J. Carriuolo, *J Am Chem Soc* **1960**, *82*, 1778-1786.
[61] W. P. Jencks, J. Carriuolo, *J Am Chem Soc* **1960**, *82*, 675-681.
[62] N. Nakajima, Y. Ikada, *Bioconjugate Chem* **1995**, *6*, 123-130.
[63] N. Wrobel, M. Schinkinger, V. M. Mirsky, *Anal Biochem* **2002**, *305*, 135-138.
[64] K. P. Vercruysse, D. M. Marecak, J. F. Marecek, G. D. Prestwich, *Bioconjugate Chem* **1997**, *8*, 686-694.
[65] E. J. Oh, K. Park, J. S. Choi, C. K. Joo, S. K. Hahn, *Biomaterials* **2009**, *30*, 6026-6034.
[66] S. G. Mayhew, *Eur J Biochem* **1978**, *85*, 535-547.
[67] W. W. Cleland, *Biochemistry-Us* **1964**, *3*, 480-&.
[68] K. Kafedjiiski, R. K. R. Jetti, F. Foger, H. Hoyer, M. Werle, M. Hoffer, A. Bernkop-Schnurch, *Int J Pharmaceut* **2007**, *343*, 48-58.
[69] C. P. Fu, H. L. Li, N. N. Li, X. W. Miao, M. Q. Xie, W. J. Du, L. M. Zhang, *Carbohyd Polym* **2015**, *128*, 163-170.
[70] A. J. Simpson, G. Woods, O. Mehrzad, *Anal Chem* **2008**, *80*, 186-194.
[71] M. Namazian, H. Heidary, *J Mol Struc-Theochem* **2003**, *620*, 257-263.
[72] Q. Li, J. R. Lancaster, *Nitric Oxide-Biol Ch* **2013**, *35*, 21-34.
[73] M. J. Janssen, in *The Chemistry of Carboxylic Acids and Esters*, John Wiley & Sons Ltd., **1969**, pp. 705-764.
[74] J. Mergy, A. Fournier, E. Hachet, R. Auzely-Velty, *J Polym Sci Pol Chem* **2012**, *50*, 4019-4028.
[75] C. Schotten, *Ber. Dtsch. Chem. Ges.* **1884**, *17*, 2544-2547.

[76] E. Baumann, *Ber. Dtsch. Chem. Ges.* **1886**, *19*, 3218-3222.
[77] J. M. Townsend, B. T. Andrews, Y. Feng, J. X. Wang, R. J. Nudo, E. Van Kampen, S. H. Gehrke, C. J. Berkland, M. S. Detamore, *Acta Biomater* **2018**, *71*, 148-155.
[78] E. A. Kiyotake, A. W. Douglas, E. E. Thomas, S. L. Nimmo, M. S. Detamore, *Acta Biomater* **2019**, *95*, 176-187.
[79] B. Neises, W. Steglich, *Angew Chem Int Edit* **1978**, *17*, 522-524.
[80] K. Oberst, Julius-Maximilians-University (Würzburg), **2020**.
[81] R. J. H. Stenekes, W. E. Hennink, *Polymer* **2000**, *41*, 5563-5569.
[82] D. I. f. N. e. V. (DIN), Beuth Verlag GmbH, Berlin, **2008**.
[83] T. Zorn, Julius-Maximilians-University (Würzburg), **2020**.
[84] F. Bignotti, E. Ranucci, P. Ferruti, *Macromol Rapid Comm* **1994**, *15*, 659-667.
[85] N. R. Richbourg, M. Wancura, A. E. Gilchrist, S. Toubbeh, B. A. C. Harley, E. Cosgriff-Hernandez, N. A. Peppas, *Sci Adv* **2021**, *7*.
[86] D. L. Hern, J. A. Hubbell, *J. Biomed. Mater. Res.* **1997**, *39*, 266-276.
[87] G. M. Cruise, D. S. Scharp, J. A. Hubbell, *Biomaterials* **1998**, *19*, 1287-1294.
[88] D. L. Elbert, J. A. Hubbell, *Biomacromolecules* **2001**, *2*, 430-441.
[89] P. Guntzel, L. Forster, C. Schollmayer, U. Holzgrabe, *Org Prep Proced Int* **2018**, *50*, 512-516.
[90] L. Forster, Julius-Maximilians-University (Würzburg), **2017**.
[91] W. N. Charman, D. P. Christy, E. P. Geunin, D. C. Monkhouse, *Drug Dev Ind Pharm* **1991**, *17*, 271-280.
[92] F. P. Brandl, A. K. Seitz, J. K. V. Tessmar, T. Blunk, A. M. Gopferich, *Biomaterials* **2010**, *31*, 3957-3966.
[93] S. Warwel, G. Steinke, A. Rusch, M. R. Klaas, *Biotechnol Tech* **1996**, *10*, 283-286.
[94] A. A. Shaikh, S. Sivaram, *Chem Rev* **1996**, *96*, 951-976.
[95] Y. Xie, X. Yang, J. Pu, Y. Zhao, Y. Zhang, G. Xie, J. Zheng, H. Yuan, F. Liao, *Spectrochim Acta A Mol Biomol Spectrosc* **2010**, *77*, 869-876.
[96] F. Debaene, L. Mejias, J. L. Harris, N. Winssinger, *Tetrahedron* **2004**, *60*, 8677-8690.
[97] A. Shaginian, M. C. Rosen, B. E. Binkowski, P. L. Belshaw, *Chem-Eur J* **2004**, *10*, 4334-4340.
[98] H. L. Dexter, H. E. L. Williams, W. Lewis, C. J. Moody, *Angew Chem Int Edit* **2017**, *56*, 3069-3073.
[99] S. Cammas, Y. Nagasaki, K. Kataoka, *Bioconjug Chem* **1995**, *6*, 226-230.
[100] O. Mitsunobu, M. Yamada, *B Chem Soc Jpn* **1967**, *40*, 2380-2382.
[101] O. Mitsunobu, *Synthesis* **1981**, *1981*, 1-28.
[102] R. P. McGeary, S. R. Amini, V. W. S. Tang, I. Toth, *J Org Chem* **2004**, *69*, 2727-2730.
[103] H. Staudinger, J. Meyer, *Helv Chim Acta* **1919**, *2*, 635-646.
[104] Y. G. Gololobov, L. F. Kasukhin, *Tetrahedron* **1992**, *48*, 1353-1406.
[105] E. J. Sakellarios, *Helv Chim Acta* **1946**, *29*, 1675-1684.
[106] S. Zhang, D. J., R. Sun, X. Li, D. Yang, S. Zhang, C. Xiong, Y. Peng, *React Funct Polym* **2003**, *56*, 17-25.
[107] M. S. Gibson, R. W. Bradshaw, *Angew Chem Int Edit* **1968**, *7*, 919-&.
[108] K. Yoshimoto, Y. Hoshino, T. Ishii, Y. Nagasaki, *Chem Commun (Camb)* **2008**, 5369-5371.
[109] M. Iijima, D. Ulkoski, S. Sakuma, D. Matsukuma, N. Nishiyama, H. Otsuka, C. Scholz, *Polym Int* **2016**, *65*, 1132-1141.
[110] F. Brandl, M. Henke, S. Rothschenk, R. Gschwind, M. Breunig, T. Blunk, J. Tessmar, A. Gopferich, *Adv Eng Mater* **2007**, *9*, 1141-1149.
[111] H. K. Hall, *J Am Chem Soc* **1957**, *79*, 5441-5444.
[112] B. L. Barthel, D. L. Rudnicki, T. P. Kirby, S. M. Colvin, D. J. Burkhart, T. H. Koch, *J Med Chem* **2012**, *55*, 6595-6607.
[113] L. A. Laplanche, M. T. Rogers, *J Am Chem Soc* **1964**, *86*, 337-&.
[114] R. J. Abraham, L. Griffiths, M. Perez, *Magn Reson Chem* **2013**, *51*, 143-155.
[115] C. R. Santos, R. Capela, C. S. Pereira, E. Valente, L. Gouveia, C. Pannecouque, E. De Clercq, R. Moreira, P. Gomes, *Eur J Med Chem* **2009**, *44*, 2339-2346.
[116] P. K. Revelou, V. Constantinou-Kokotou, *Synthetic Commun* **2019**, *49*, 1708-1712.
[117] A. Züge, Julius-Maximilians-University (Würzburg), **2018**.

[118] D. Janzen, E. Bakirci, J. Faber, M. Andrade Mier, J. Hauptstein, A. Pal, L. Forster, J. Hazur, A. R. Boccaccini, R. Detsch, J. Tessmar, S. Budday, T. Blunk, P. D. Dalton, C. Villmann, *Adv Healthc Mater* **2022**, e2201826.
[119] J. Hauptstein, L. Forster, A. Nadernezhad, H. Horder, P. Stahlhut, J. Groll, T. Blunk, J. Tessmar, *Macromol Biosci* **2021**.
[120] M. P. Lutolf, J. L. Lauer-Fields, H. G. Schmoekel, A. T. Metters, F. E. Weber, G. B. Fields, J. A. Hubbell, *P Natl Acad Sci USA* **2003**, *100*, 5413-5418.
[121] M. P. Lutolf, G. P. Raeber, A. H. Zisch, N. Tirelli, J. A. Hubbell, *Adv Mater* **2003**, *15*, 888-+.
[122] M. Vigen, J. Ceccarelli, A. J. Putnam, *Macromol Biosci* **2014**, *14*, 1368-1379.
[123] J. Wang, R. Youngblood, L. Cassinotti, M. Skoumal, G. Corfas, L. Shea, *J Control Release* **2021**, *330*, 575-586.
[124] M. Glogger, S. Stichler, I. Subota, S. Bertlein, M. C. Spindler, J. Tessmar, J. Groll, M. Engstler, S. F. Fenz, *J Phys D Appl Phys* **2017**, *50*.
[125] M. Glogger, Julius-Maximilians-University (Würzburg), **2018**.
[126] T. Christel, M. Kuhlmann, E. Vorndran, J. Groll, U. Gbureck, *J Mater Sci-Mater M* **2013**, *24*, 573-581.
[127] M. Schamel, J. Groll, U. Gbureck, *Mater Sci Eng C Mater Biol Appl* **2017**, *75*, 471-477.
[128] M. Rodel, J. Tessmar, J. Groll, U. Gbureck, *Acta Biomater* **2018**, *79*, 182-201.
[129] S. V. Dorozhkin, *J Mater Sci* **2008**, *43*, 3028-3057.
[130] V. G. Muir, T. H. Qazi, J. W. Shan, J. Groll, J. A. Burdick, *Acs Biomater Sci Eng* **2021**, *7*, 4269-4281.
[131] L. Galaba, Julius-Maximilians-University, Würzburg, **2021**.
[132] T. Y. Lee, T. M. Roper, E. S. Jonsson, I. Kudyakov, K. Viswanathan, C. Nason, C. A. Guymon, C. E. Hoyle, *Polymer* **2003**, *44*, 2859-2865.
[133] V. Gokmen, H. Z. Senyuva, J. Acar, K. Sarioglu, *J Chromatogr A* **2005**, *1088*, 193-199.
[134] Y. S. Kim, C. S. P. Sung, *J Appl Polym Sci* **1995**, *57*, 363-370.
[135] N. B. Cramer, J. P. Scott, C. N. Bowman, *Macromolecules* **2002**, *35*, 5361-5365.
[136] N. B. Cramer, S. K. Reddy, M. Cole, C. Hoyle, C. N. Bowman, *J Polym Sci Pol Chem* **2004**, *42*, 5817-5826.
[137] T. T. Shih, I. H. Hsu, J. F. Wu, C. H. Lin, Y. C. Sun, *J Chromatogr A* **2013**, *1304*, 101-108.
[138] A. Garcia-Gil, C. Pablos, R. A. Garcia-Munoz, K. G. McGuigan, J. Marugan, *Sci Total Environ* **2020**, *730*.
[139] A. K. Nguyen, P. L. Goering, V. Reipa, R. J. Narayan, *Biointerphases* **2019**, *14*.
[140] L. Partholl, Julius-Maximilians-University (Würzburg), **2021**.
[141] T. N. Eren, N. Kariksiz, G. Demirci, D. Tuncel, N. Okte, H. Y. Acar, D. Avci, *Polym Chem-Uk* **2021**, *12*, 2772-2785.
[142] G. Gillispie, P. Prim, J. Copus, J. Fisher, A. G. Mikos, J. J. Yoo, A. Atala, S. J. Lee, *Biofabrication* **2020**, *12*.
[143] J. Hauptstein, T. Boeck, M. Bartolf-Kopp, L. Forster, P. Stahlhut, A. Nadernezhad, G. Blahetek, A. Zernecke-Madsen, R. Detsch, T. Jungst, J. Groll, J. Tessmar, T. Blunk, *Adv Healthc Mater* **2020**, *9*.
[144] L. L. Ouyang, R. Yao, Y. Zhao, W. Sun, *Biofabrication* **2016**, *8*.
[145] J. Hauptstein, Julius-Maximilians-University (Würzburg), **2022**.
[146] M. M. Capeling, M. Czerwinski, S. Huang, Y. H. Tsai, A. Wu, M. S. Nagy, B. Juliar, N. Sundaram, Y. Song, W. M. Han, S. Takayama, E. Alsberg, A. J. Garcia, M. Helmrath, A. J. Putnam, J. R. Spence, *Stem Cell Rep* **2019**, *12*, 381-394.

6 Appendix

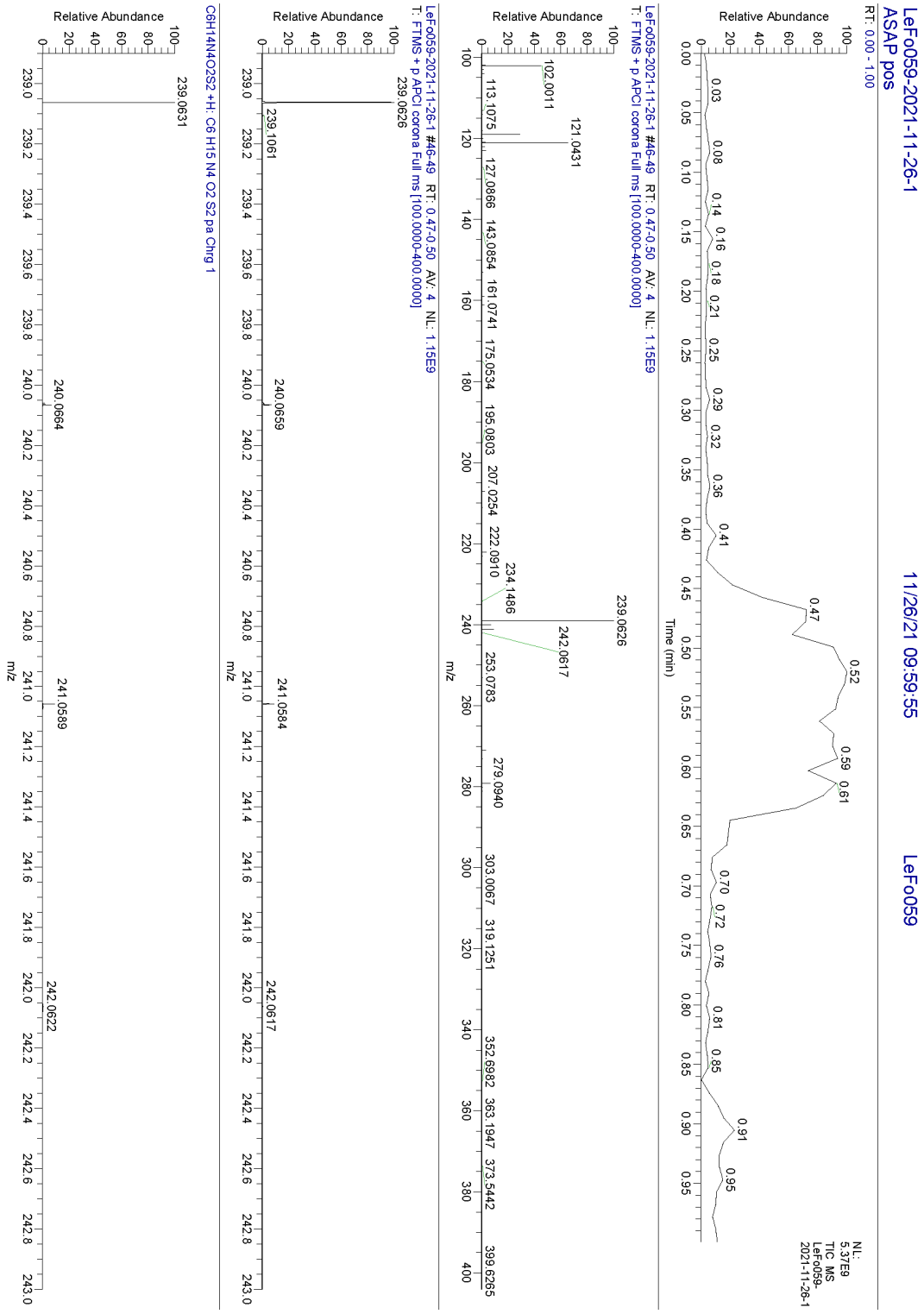

Figure 95: HRMS (ASAP pos) spectrum of DTPH.

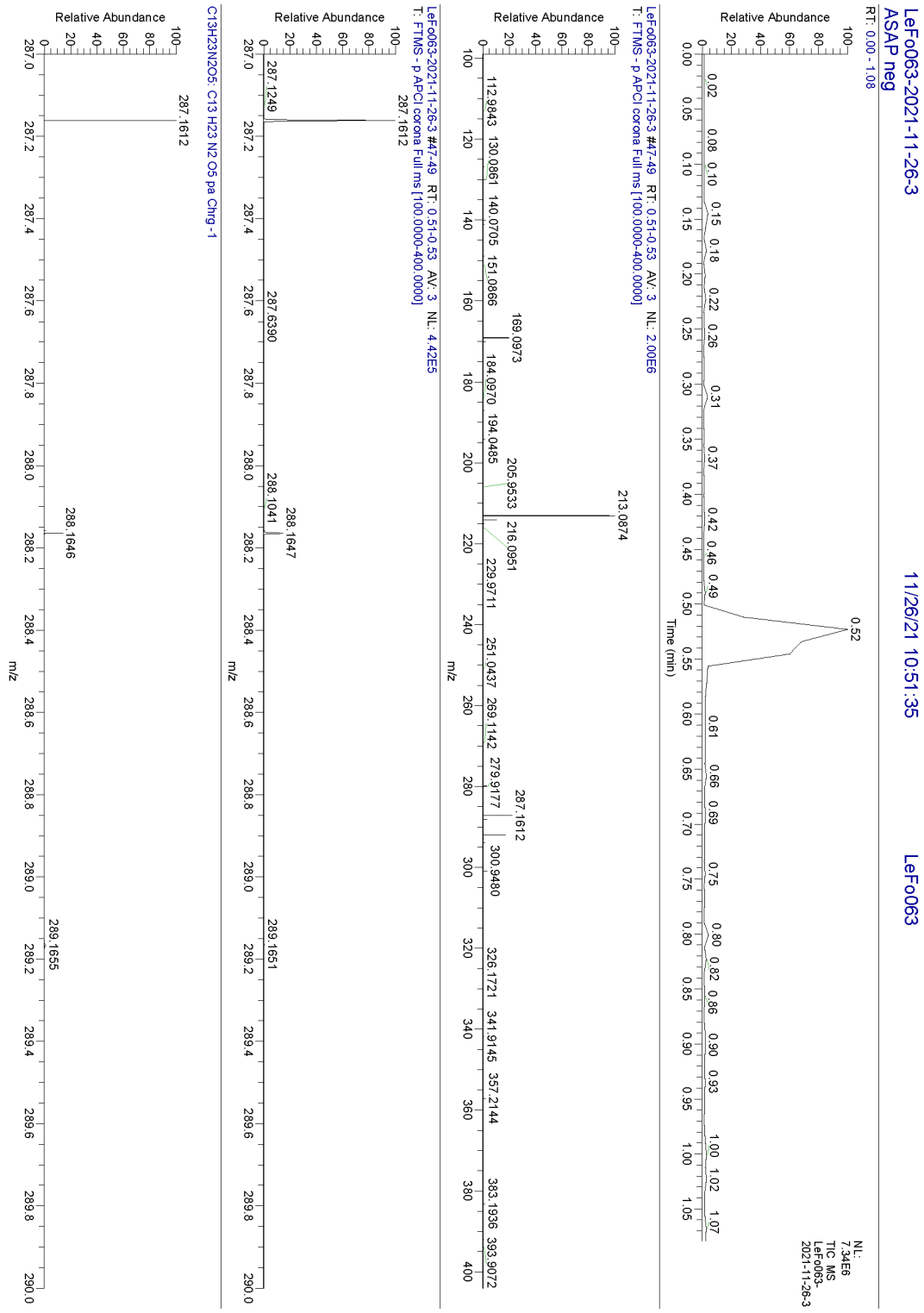

Figure 96: HRMS (ASAP pos) spectrum of Boc-gly-leucine.

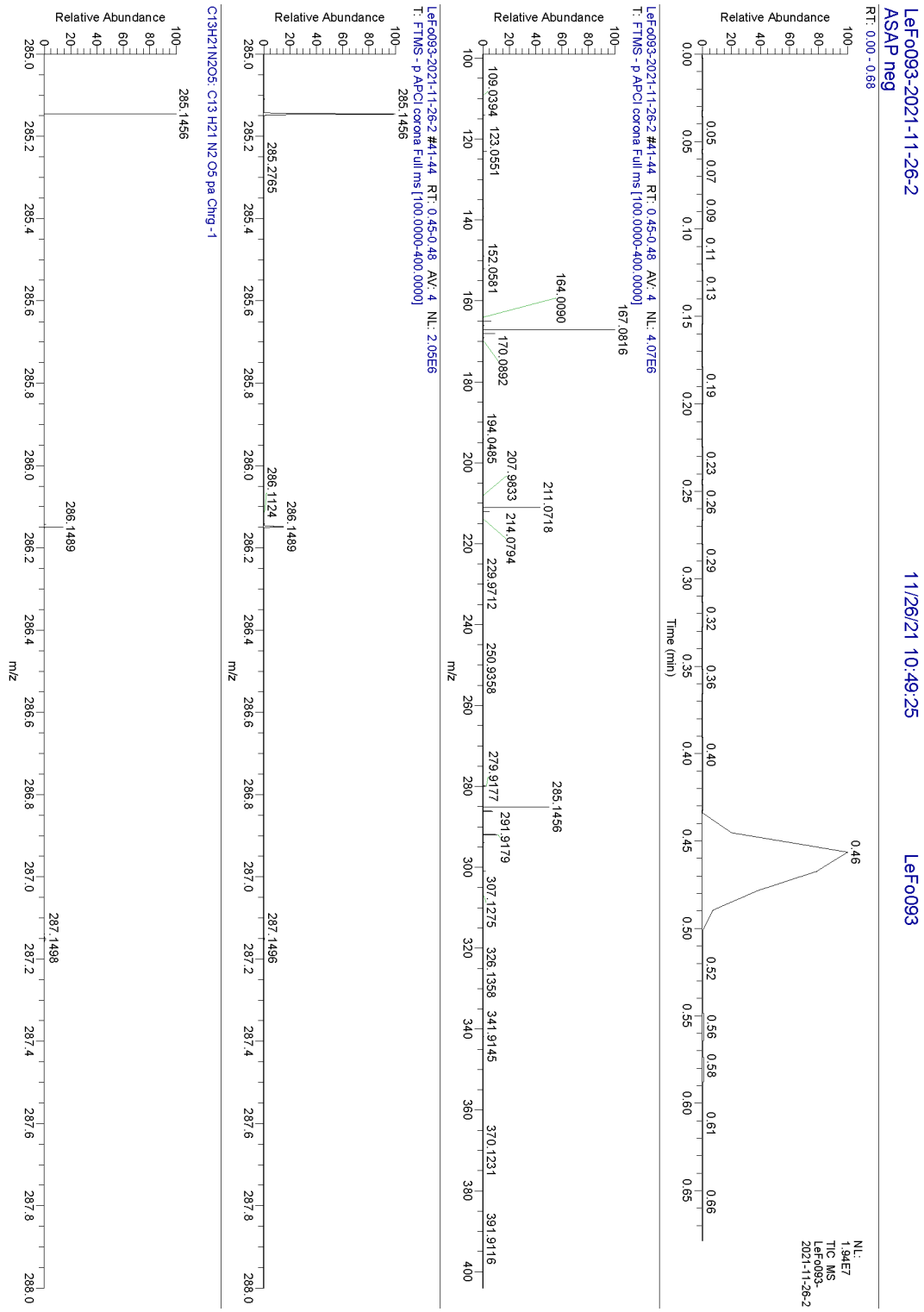

Figure 97: HRMS (ASAP pos) spectrum of Boc-ala-proline.

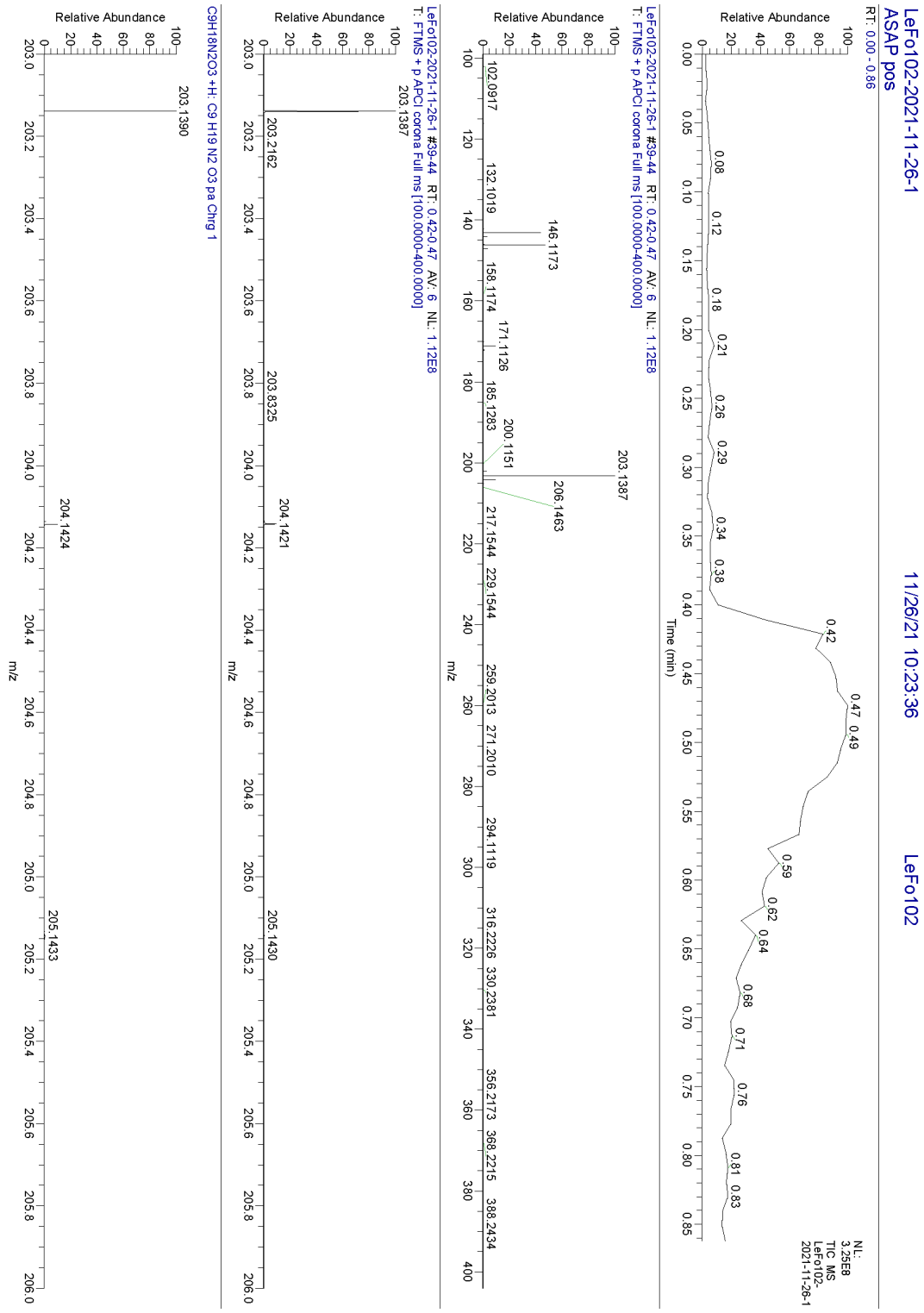

Figure 98: HRMS (ASAP pos) spectrum of gly-leu-OMe.

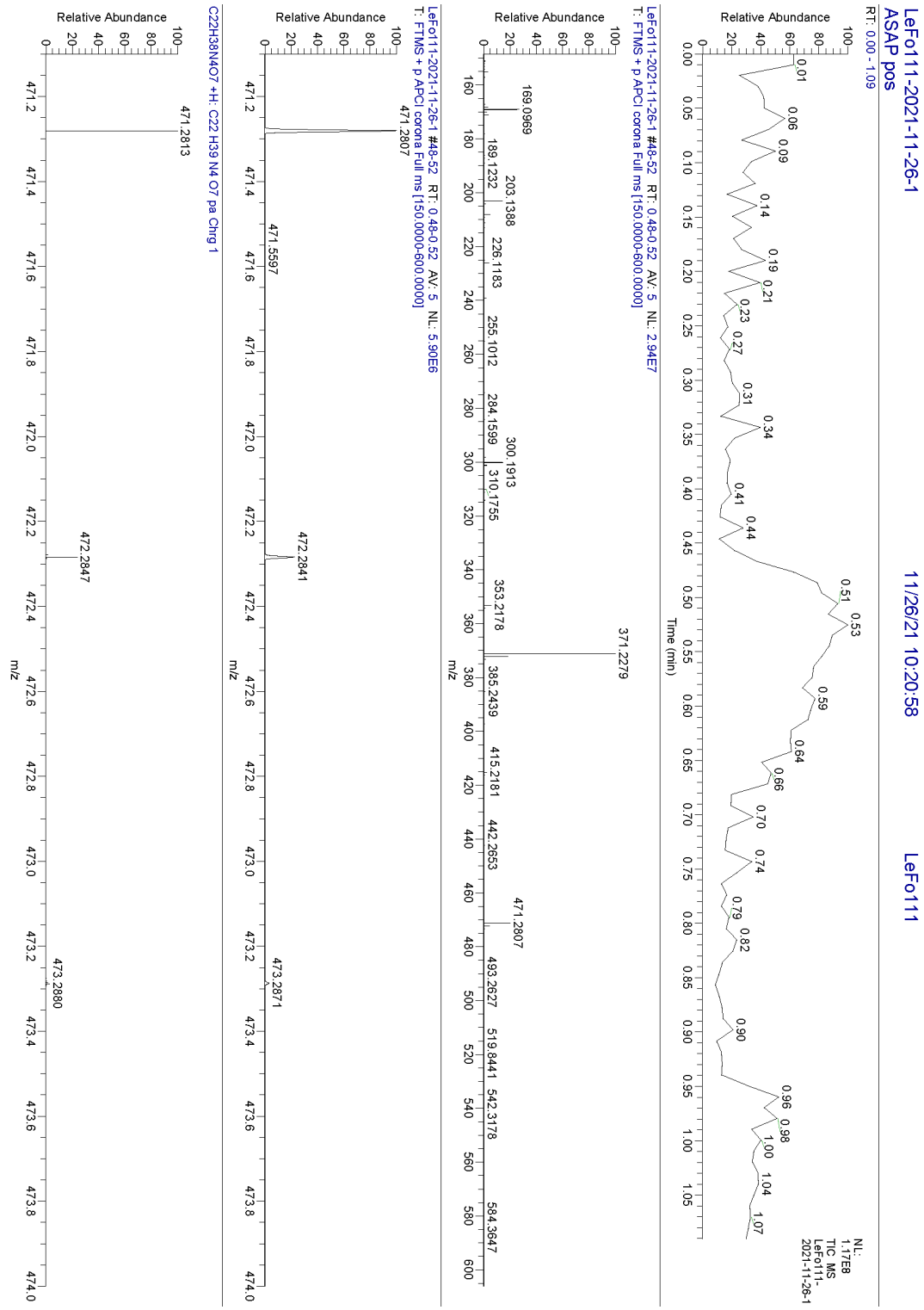

Figure 99: HRMS (ASAP pos) spectrum of Boc-ala-pro-gly-leu-OMe.

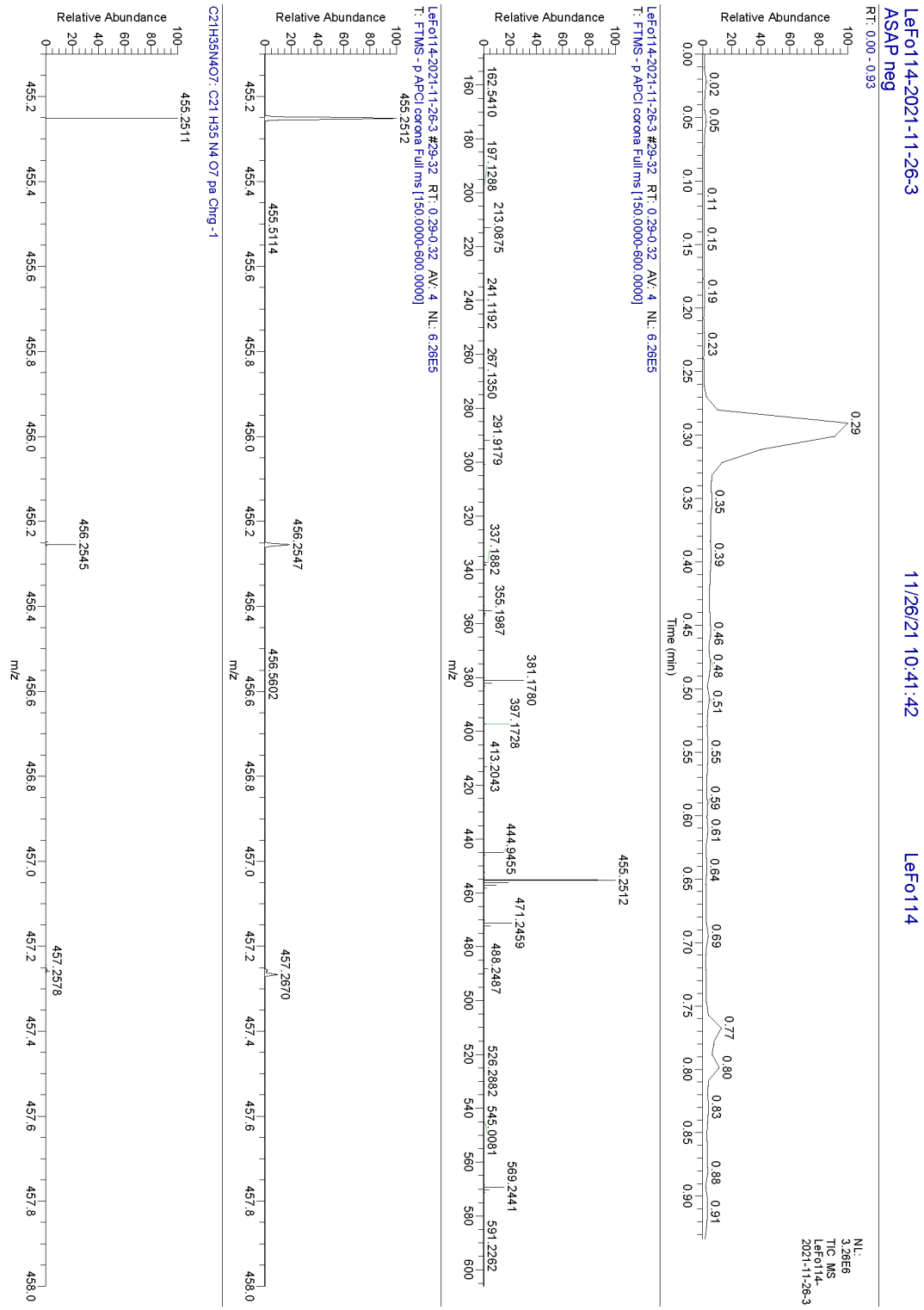

Figure 100: HRMS (ASAP pos) spectrum of Boc-ala-pro-gly-leu-OH.

7 Acknowledgements

Throughout this work, I received a lot of support and help from numerous people in my professional and private life, which I would like to acknowledge here.

I thank the following persons for their contribution to this thesis by assisting with professional advice, with measurements or by performing experiments for me:

I thank my supervisors Dr. Jörg Teßmar, Prof. Torsten Blunk and Dr. Rainer Detsch for their trust and faith in my decisions and work and for the relaxed atmosphere in meetings and on events. Furthermore, I am grateful for the opportunity to gain experience in the field of polymer and material science as well as biofabrication.

Julia Hauptstein (née Martini) has my sincerest gratitude for the uncomplicated and effective cooperation over the whole funding period even in times of disagreement. Your efforts and expertise in 3D (bio)printing and cell biology were crucial for the ink development and your intrepid approach to testing the produced materials was key to the success of this project.

Ali Nadernezhad for the knowledge and performance of rheological characterizations and for sharing his material science perspective. You were relentless when the workload was at its highest and always followed the motto "*through reluctance towards success*"

Katharina Oberst for the HAPA synthesis protocol and the performance of HPLC analyses and 3D printing experiments.

Theresa Zorn and Jun.-Prof. Ann-Christin Pöppler for their constructive ideas and professional advice on NMR measurements and data evaluation.

Christoph Mahler from the Institute of Inorganic Chemistry for his competent support and the fast performance of the mass spectrometric measurements.

I wouldn't have come this far if it weren't for my colleagues at work who supported me anytime I needed advice, who nudged me out of the lab in fits of work mania and who are the main reason for the positive work environment.

I would like to thank Prof. Uwe Gbureck for his active support at all culinary events and gatherings at work as well as for the enjoyable Skat games with Prof. Jürgen Groll at the retreats. Although I was not often the winner, it was always exciting to play with you.

Among my colleagues, I must highlight Jessi, Jun, Jan, Alessandro and Ilona for the after-work activities such as communal dinners, house parties or just relaxing get-together. Ilona deserves special thanks for pleasant company during all the many TRR225 events and the associated obligations as well as during the Spanish course. I wish each of you all the best for your personal and professional future and hope we stay touch.

I thank all my friends from all around the world who have promoted my personal development, who have shared with me memorable moments of wins and fails along with tears and laughter. May you be blessed with happiness and contentment in life.

I thank the group *Unkaputtbar* for including me into your beach volleyball team and spare time activities despite the difference in age. Never have I laughed so much and often due to funny incidences and verbal non-sense that it brought tears to my eyes and my jaws ached the next day. I had great times with you and look forward to the future ones.

Big thanks go to the group *Coole Kidz Connection Wü* for letting me share such wonderful moments with you during our many recreational meetings. It was never boring, never long-winded but always relaxed, fun and entertaining. I must single out Theresa for introducing me to the group and for sharing a memorable time of highs and lows with me even though we have decided to take our own path. I am grateful that we can continue our life journeys as friends.

I thank my sports partners Isabelle and Leonie for the sporty balance to my research work and the distance-defying friendships that developed from it.

Special thanks go to my roommate Lisa for our daily chat and exchange of views on everyday occurrences and the culinary excursions into the world of ayurveda and beyond. There were days when we wished we had each other's traits, and yet taking a different perspective was mostly the solution to any complexity - otherwise it was sweets. As little time we had, as great was your influence on my character and I am grateful for meeting you.

My family has my sincerest gratitude for their unconditional support in every situation during my whole life, when I was near bursting with happiness but also when my body threatened to fail and my mind went astray. You are my anchor even if I am miles away in the deepest rainforest and on the widest mountain plateau.

8 Publication List

List of publication as of 09.11.22

First author:

Hauptstein J*, Forster L*, Nadernezhad A, Horder H, Stahlhut P, Groll J, Blunk T, Teßmar J
Bioink platform utilizing dual-stage crosslinking of hyaluronic acid tailored for chondrogenic differentiation of mesenchymal stromal cells
Macromolecular Bioscience 22(2) (**2021**)

Co-author:

Janzen D, Bakirci E, Faber J, Andrade Mier M, Hauptstein J, Pal A., Forster L, Hazur J, Boccaccini AR, Detsch R, Tessmar J, Budday S, Blunk T, Dalton PD, Villmann C
Reinforced Hyaluronic Acid-Based Matrices Promote 3D Neuronal Network Formation
Advanced Healthcare Materials (2022)

Karakaya E, Bider F, Frank A, Teßmar J, Schöbel L, Forster L, Schrüfer S, Schmidt H-W, Schubert DW, Blaeser A, Boccaccini AR, Detsch R
Targeted printing of cells: evaluation of ADA-PEG bioinks for drop on demand approaches
Gels 8(4) (2022)

Brand JS, Forster L, Bock T, Stahlhut P, Tessmar J, Groll J, Albrecht K
Covalently crosslinked pig gastric mucinhydrogels prepared by radical-based chain-growth and thiol-ene mechanisms
Macromolecular Bioscience 22(4) (**2022**)

Hauptstein J, Forster L, Nadernezhad A, Groll J, Teßmar J, Blunk T
Tethered TGF-β1 in a hyaluronic acid-based bioink for bioprinting cartilaginous tissues
International Journal of Molecular Science 23(2) (2022).

Shan J, Bock T, Keller T, Forster L, Blunk T, Groll J, Tessmar J
TEMPO/TCC as a chemo selective alternative for the oxidation of hyaluronic acid
Molecules 26(19) (2021)

Hauptstein J, Bock T, Bartolf-Kopp M, Forster L, Stahlhut P, Nadernezhad A, Blahetek G, Zernecke-Madsen
A, Detsch R, Jungst T, Groll J, Tessmar J, Blunk T
Hyaluronic acid-based bioink composition enabling 3D bioprinting and improving quality of deposited cartilaginous extracellular matrix
Advanced Healthcare Materials 9(15) (**2020**)

Nadernezhad A, Forster L, Netti F, Adler-Abramovich L, Tessmar J, Groll J
Rheological analysis of the interplay between the molecular weight and concentration of hyaluronic acid in formulations of supramolecular HA/FmocFF hybrid hydrogels
Polymer Journal 52(8) (2020)

Guentzel P, Forster L, Schollmayer C, Holzgrabe U
A Convenient Preparation of Carboxy-pyrone Derivatives: Meconic Acid and Comenic Acid
Organic Preparations and Procedures International, 50(5) 2018